MICROBIAL COMMUNITY COMPOSITION, EXTRACELLULAR ENZYMATIC ACTIVITIES, AND STRUCTURE-FUNCTION RELATIONSHIPS IN THE CENTRAL ARCTIC OCEAN, A HIGH-LATITUDE FJORD, AND THE NORTH ATLANTIC OCEAN

John Paul Piso Balmonte

A dissertation submitted to the faculty at The University of North Carolina at Chapel Hill in partial fulfillment of the requirements for the degree of Doctor of Philosophy in the Department of Marine Sciences in the College of Arts and Sciences.

Chapel Hill
2018

Approved by:

Carol Arnosti

Andreas Teske

Ronnie Glud

Barbara MacGregor

John Bane

ABSTRACT

John Paul Piso Balmonte: Microbial community composition, extracellular enzymatic activities, and structure-function relationships in the central Arctic Ocean, a high-latitude fjord, and the North Atlantic Ocean
(Under the direction of Carol Arnosti and Andreas Teske)

Due to their abundance, diversity, and capabilities to transform and metabolize diverse compounds, microbial communities regulate biogeochemical cycles on micro-, regional, and global scales. The activities of microbial communities affect the flow of matter, energy sources of other organisms, and human health, as well as other aspects of life. Yet, the composition, diversity, and ecological roles of microbes in parts of the global oceans—from the high latitudes to the deep water column—remain underexplored. Drawing from microbiological, oceanographic, and ecological concepts, this dissertation explores several fundamental topics: 1) the manner in which hydrographic conditions influence microbial community composition; 2) the ability of these microbial communities across environmental and depth gradients to hydrolyze organic compounds; and 3) microbial structure-function relationships in different habitats and under altered environmental conditions. In the central Arctic Ocean, the composition and enzymatic function of pelagic, particle associated, and benthic bacterial communities varied with depth and region, in parallel with specific hydrographic features. The microbial structure-function relationship in the pelagic realm indicated functional redundancy, suggesting that bacterial compositional shifts—in response to the changing Arctic—may have complex and less predictable functional consequences than previously anticipated. In Tyrolerfjord-Young Sound, northeast Greenland, microbial enzymatic activity patterns were investigated in rivers and within the fjord. Activity patterns correlated with the composition of bacterial communities and dissolved organic matter in the

same waters, suggesting that factors extrinsic (organic matter supply) and intrinsic (composition) to microbial communities may, in concert, influence their heterotrophic activities. Finally, functional consequences of differences in community composition were further explored in the North Atlantic. Enriched with high molecular weight organic matter, compositionally-distinct microbial communities exhibited convergent and divergent successional patterns. While convergent features were driven by several initially rare taxa, overarching successional differences in microbial community composition and enzymatic profiles provide evidence for the functional significance of community structure. The integration of community compositional analyses and enzymatic activity measurements has provided valuable information on the identity, ecological roles, and environmental sensitivity of microbial communities in previously underexplored oceanic regions and depths. These insights can be used to evaluate the potential for environmental changes to alter marine microbial community structure and function.

To my parents, Thelma and Leonardo,
who taught me that there are no hardships too difficult to overcome.

Maraming, *maraming* salamat, Ma at Pa. Para sa inyo ito.

ACKNOWLEDGEMENTS

I am indebted to so many people for enabling me to carry out my research, be it through research advice, moral support, and/or camaraderie. First and foremost, I am grateful for my two incredibly intelligent and caring mentors, Dr. Carol Arnosti and Dr. Andreas Teske, who nurtured the potential that they saw in me as a prospective student, and provided me with the resources necessary to pursue questions I found most stimulating. Their dedication to helping a student develop into a scientist is unwavering, and their mentorship extended beyond the confines of science. Carol and Andreas, no words can express my deep appreciation for your guidance and generosity over the years. Thank you *so much*. Cheers!

I thank my committee members, Dr. Ronnie Glud, Dr. Barbara MacGregor, and Dr. John Bane, for their insights and thoughtful feedback on my dissertation. I am grateful for Ronnie, whose invitation to join a field campaign in northeast Greenland 2015 enabled me to do fieldwork for one of my chapters. His commitment to being present at every committee meeting, despite the 6 hour time difference, is very much appreciated. I thank Barbara for constantly reminding me to adjust my interpretations in light of methodological limitations, teaching me to be a more thorough scientist. And I want to thank John for always bringing up physical processes when I became too focused on the [micro]biology.

The graduate students in the department are among the brightest, friendliest, and most fun folks with whom I have had the pleasure of working. This cohort of scientists lifted up my spirit during the most challenging parts of graduate school. Several folks deserve special recognition. Dr. Natalie Cohen, the first in our cohort to receive her PhD, has celebrated and commiserated with me through graduate school's ups and downs from day

zero. Our conversations—on science, on the academy, and on inequalities—have inspired me to think critically about many pressing issues. Natalie, thank you for being a wonderful friend and role model. My predecessors in the Teske lab were among my earliest and closest mentors: Dr. Lisa Nigro, Dr. Verena Carvalho, Dr. Luke McKay, Dr. Tingting Yang, and NASA Astronaut, Zena Cardman. I appreciate everything that you all have taught me, as well as your efforts in mitigating the near-disasters that I may (or may not) have caused in the lab. I especially thank Sherif Ghobrial, the Arnosti lab manager, whose efforts in keeping the GPCs running ensured that I have a wealth of data to analyze. Dr. Anna Jalowska played several roles in my life: a deeply-caring friend, a trustworthy colleague and co-instructor, and my North Carolina mom. Anna, you have saved me from crippling stress, and potentially bank-breaking doggy-sitting bills—I am grateful for all with which you've helped. Many other students, in this department and in others, have enriched and elevated the graduate experience, for which I am incredibly grateful. Thank you to (in alphabetical order): Jill Arriola, Jesse Bikman, Sara Coleman, Serena Hackerott, Adrienne Hoarfrost, Andrew Hyde, Ji Hyuk Kim, Rob Lampe, Justin McNabb, Carly Moreno, Kathleen Onorevole, Sertanya Reddy, David Walters, and Barbara Zemskova.

My family provided significant moral support and love. My parents, Thelma and Leonardo, listened to (read: suffered through) all of my explanations on what I had spent a fourth of my life researching. Their enthusiasm for understanding my projects—despite lacking in background—has motivated me to learn how to communicate my science to a broad audience. Their drive to improve their and their children's lives has inspired me to better my own. My brothers—Johnard, Johnathan, Johnaefrey, and John Cris—have been role models in different ways since I entered this world. I will always appreciate their patience in teaching me how to be a better student and an even better person.

Finally, to my future husband, Jake Reardon, and to my dogter, Hallie. Living with the two of you is one of the greatest joys of my life. Thank you for the love and happiness.

TABLE OF CONTENTS

LIST OF TABLES

LIST OF FIGURES

LIST OF ABBREVIATIONS

α-glu	α-glucopyranoside
AAF-Chym	Alanine-Alanine-Phenylalanine-Chymotrypsin
AAPF-Chym	Alanine-Alanine-Proline-Phenylalanine-Chymotrypsin
ADONIS	Analysis of Variance using Distance Matrices
ANOSIM	Analysis of Similarity (ANOSIM)
Ara	Arabinogalactan
β-glu	β-glucopyranoside
BA	Bacterial Abundance
BCC	Bacterial Community Composition
BP	Bacterial Production
CAP	Canonical Analysis of Principal Coordinates
Chn	Chondroitin Sulfate
DCM	Deep Chlorophyl *a* Maximum
DNA	Deoxyribonucleic acid
DOC	Dissolved Organic Carbon
DOM	Dissolved Organic Matter
EEA	Extracellular Enzymatic Activities
ENV	Environmental Conditions
FL	Free-Living
FLA	Fluoresceinamine
FSR-Tryp	Phenylalanine-Serine-Arginine-Trypsin
Fuc	Fucoidan
GEOG	Geographic Distances
GCMS	Gas Chromatography-Mass Spectrometry
GFF	Glass Fiber Filter

LMW	Low Molecular Weight
HMW	High Molecular Weight
Lam	Laminarin
LCMS	Liquid Chromatography-Mass Spectrometry
Ler	Lerbugten
Leu	Leucine
LOI	Loss On Ignition
MCA	Methylcoumarin
MUF	Methylumbelliferyl
NMDS	Non-metric Multidimensional Scaling
OM	Organic Matter
OTU	Operational Taxonomic Unit
PA	Particle-Associated
PCoA	Principal Coordinates Analysis
Pep	Peptide
Poly	Polysaccharide
POM	Particulate Organic Matter
PSU	Practical Salinity Units
Pul	Pullulan
QAR-Tryp	Glutamine-Alanine-Arginine-Trypsin
rRNA	ribosome ribonucleic acid
SFCA	Surfactant-Free Cellulose Acetate
SPMC	Suspended Particulate Matter Concentration
Stn	Station
TCA	Trichoroacetic acid
TCHO	Total Carbohydrate

Temp	Temperature
Tyro	Tyroler
YS	Young Sound
Zac	Zackenberg

CHAPTER 1: DISSERTATION INTRODUCTION

1.1 Background

Microbial communities play a vital role in carbon cycling, altogether processing up to 50% of marine primary production (Azam and Malfatti, 2007). Because a significant fraction of marine organic matter exists as high molecular weight (HMW) compounds, too large to fit through bacterial porins, heterotrophic microbes must secrete extracellular enzymes that hydrolyze organic matter to sizes sufficiently small for uptake (Weiss et al., 1991). The resulting dissolved organic matter (DOM) is either incorporated into biomass or respired to carbon dioxide (Arnosti, 2011). Through biomass incorporation, microbial communities link otherwise biologically unavailable dissolved organic matter to grazing organisms of higher trophic levels (Azam and Malfatti, 2007). The organic matter-degrading capabilities of marine microbial communities therefore determine the quality and quantity of organic carbon that is available to pelagic heterotrophic communities, and which compounds evade degradation, either to fuel benthic heterotrophs, or to be sequestered in sediments (Azam and Malfatti, 2007; Arnosti, 2011). However, the composition, specific heterotrophic activities, and environmental structuring of bacterial communities in various oceanic regions, particularly in the Arctic Ocean, and in the deep water column remain poorly characterized. These limited insights constrain our understanding of microbial structure-function relationships. Thus, the extent to which shifting conditions in much of the world's oceans will alter microbial community composition, and the potential for ecosystem processes to change as a consequence, are poorly understood.

Factors that influence microbial biogeography. Various factors may influence microbial community composition in concert, leading to biogeographical patterns. Spatial

patterns in microbial community composition may vary as a function of physicochemical gradients in the ocean (e.g. sunlight, temperature, salinity, pressure, nutrients, oxygen, etc.) (Crump et al., 2004; DeLong et al., 2006). Thus, strong depth-related, lateral and latitudinal patterns in community composition and diversity have been documented (DeLong et al., 2006; Pommier et al., 2007; Fuhrman and Hagström, 2008; Wietz et al., 2010; Galand et al., 2010). Moreover, particle association can structure communities and create micro-scale heterogeneity (Pedrós-Alió and Brock, 1983; Delong et al., 1993; Polz et al., 2006; Azam and Malfatti, 2007). Particle-associated niches may be largely filled by heterotrophic copiotrophs and organisms that can degrade particulate matter (Datta et al., 2016). Overall, the selection that environmental conditions impose on microbial communities results in communities being dominated by a few abundant phylotypes surrounded by many rare taxa, which altogether comprise only a minor fraction of the total community (Sogin et al., 2006; Pedrós-Alió, 2012)

Due to their small size and dynamic habitat (e.g., due to ocean currents, seasonal mixing, freshwater input into coastal systems, weather-related perturbations, etc.), however, marine microbes may also have high dispersal rates, and consequently have high potential for cosmopolitan distribution in the water column (Martiny et al., 2006). Thus, previous or current geographical barriers to dispersion, spatial isolation and genetic drift, may also shape patterns of community dissimilarity (Martiny et al., 2006; Hanson et al., 2012; Nemergut et al., 2013). Genetic drift—a stochastic community assembly process—is evident from observations of greater community dissimilarity with increasing geographic distance, or a positive distance-decay relationship (Martiny et al., 2006). Evidence suggests that deterministic and stochastic processes can act in concert to influence community assembly processes (Langenheder and Székely, 2011). The tenet “Everything is everywhere, but the environment selects” (Baas Becking, 1934; Martiny et al., 2006) appears to be an

amalgamation of the two community assembly concepts, but instead actually asserts the greater importance of environmental selection (determinism).

Patterns of enzymatic activities. The capabilities of microbial communities to access organic matter depend on the combined contribution of the heterotrophic activities of specific bacterial taxa. While several studies have focused on the role of different bacterial taxa in organic matter degradation—such as *Gramella forsetti* (Bauer et al., 2006; Kabisch et al., 2014), *Alteromonas macleodii* (Ivars-Martinez et al., 2008; Neumann et al., 2015), and *Verrucomicrobia* (Martinez-Garcia et al., 2012; Cardman et al., 2014)—the relationship between the combined enzymatic capabilities and composition of natural microbial communities, arguably more relevant when investigating ecosystem function, is underexplored (Arnosti, 2011). Studies that simultaneously investigated community composition and function have found differences in community composition that parallel variations in enzymatic activity patterns (Davey et al., 2001; Teske et al., 2011; D'Ambrosio et al., 2014). In surface waters, high latitude microbial communities exhibit lower rates and a more limited spectrum of polysaccharide hydrolase activities compared to their temperate counterparts (Arnosti et al., 2011). This latitudinal gradient in polysaccharide hydrolysis parallels decreasing microbial community diversity with increasing latitude (Pommier et al., 2007). In addition, cell-specific enzymatic activities correlate most closely with variations in particle-associated bacterial community composition, when controlling for environmental conditions (Kellogg and Deming, 2014). Whether these patterns extend to under-sampled regions of the Arctic Ocean and to deep waters remains to be determined. Furthermore, insights into the relative importance of factors intrinsic (e.g., composition) or extrinsic (e.g., organic matter supply, environmental conditions) to microbial communities in influencing enzymatic activities are limited.

Structure-function relationships. Integrating investigations of microbial community composition and function sheds light on consequences of community composition for

ecosystem processes. Yet, whether community compositional differences translate to variations in functionality is contingent upon the nature of structure-function relationships (Allison and Martiny, 2008). Communities may be characterized by functional dissimilarity, functional redundancy, or metabolic plasticity (Reed and Martiny, 2007; Allison and Martiny, 2008; Strickland et al., 2009; Comte et al., 2013). Functionally dissimilar communities differ in community composition and function, illustrating that community composition exerts control on ecosystem process rates (Reed and Martiny, 2007 Strickland et al., 2009). In contrast, a weak coupling of structure and function may have different underlying reasons. Functionally redundant communities may differ in composition, but—because the function of interest can be carried out by multiple organisms—do not exhibit functional variations (Langenheder et al., 2005; Allison and Martiny, 2008). Alternatively, metabolically plastic communities are similar in composition, but differ in function in response to differences in environmental conditions (Allison and Martiny, 2008). In the case of functional redundancy and metabolic plasticity, environmental conditions, not community composition, has ultimate control on ecosystem process rates.

Despite the importance of combined compositional and functional biogeography, such investigations—which originate from macroecology (Violle et al., 2014)—are uncommon in marine microbial systems (Green et al., 2008; Brown et al., 2014). A few studies have demonstrated spatial differences in microbial community composition and functional potential, based on metagenomics, which correlate with a range of environmental parameters (Raes et al., 2011; Barberan et al., 2012; Jiang et al., 2012). These studies indicate that the nature of structure-function relationships may be complex, and the relative importance of functional dissimilarity, functional redundancy and metabolic plasticity may be dependent on the ecosystem function of interest (Strickland et al., 2009), as well as environmental conditions (Comte et al., 2013). However, the extent to which these genetic potentials are expressed and influence ecosystem processes can only be revealed through

empirical approaches. Mapping community traits as they relate to contrasting habitats and across physicochemical gradients may provide insights into the functional consequences of ecosystem change (Martiny et al., 2006; Allison and Martiny, 2008).

1.2 Main Questions

The ecological roles of marine microbial communities remain elusive, particularly at high latitudes and in the deep water column, environments less often investigated than temperate and shallow locations. Furthermore, while numerous studies have investigated the manner in which environmental parameters correlate with microbial community composition, the relationship between community composition and function remains underexplored. Identifying the environmental parameters that structure marine microbial communities, their heterotrophic capabilities, and the functional consequences of microbial community composition provides fundamental information on the ecological roles of microbes, particularly in the context of marine carbon cycling. Thus, the questions pursued in this dissertation include the following:

1. How does bacterial community composition vary with region, depth and particle-association in various water masses and regions in the Arctic and in the North Atlantic (Figure 1)? What environmental factors correlate with and explain variations in community dissimilarity? What is the relative importance of measured environmental factors versus geographic distance in shaping community composition? How do changes in physicochemical conditions, in particular due to the enrichment of organic matter, alter community composition?
2. What are the organic matter-degrading capabilities of Arctic and North Atlantic microbial communities, assessed through measurements of extracellular enzymatic activities? Are there observable biogeographic patterns in enzymatic activities? What environmental factors, including hydrographic properties and

organic matter quantity and quality, correlate and potentially influence these heterotrophic activities?

3. What is the nature of microbial structure-function relationships in various oceanic depths and habitats (e.g. water column, particles, sediments)? In particular, do variations in community composition translate to differences in enzymatic activities? Do these patterns indicate that microbial communities are functionally dissimilar, functionally redundant, or metabolically plastic? Could shifts in environmental conditions and in the supply of organic matter, alter these structure-function relationships?

1.3 Study Sites

Central Arctic. The central Arctic Ocean lies above a deep basin surrounded by shallow continental shelves off the coasts of Russia, Alaska, Canada, and Greenland; these continental shelves contain the seven Arctic marginal seas. The deep, central basin is divided by the Lomonosov Ridge into two basins: the Amerasian Basin and the Eurasian basin, further subdivided by the Alpha-Mendeleev Ridge and the Gakkel Ridge, respectively, into the Canada and Makarov Basins on the Canadian side and the Amundsen and Nansen Basins on the Eurasian side (Jakobsson and National Geophysical Data, 2004; Stein and Macdonald, 2004). With mean depths of 3 to 4 km, the four sub-basins create physiographic provinces surrounded by towering ridges that trap water masses and can act as barriers to microbial dispersal (Jakobsson and National Geophysical Data, 2004; Stein and Macdonald, 2004).

Although the Arctic water column is less temperature-stratified than temperate and tropical waters, distinct water masses are still distinguishable with depth. The Polar Mixed Layer occurs in the upper ca.100 meters. Immediately below this water mass is the Atlantic Halocline, which is at its deepest (ca. 300 m) in the Central Arctic (Stein and Macdonald, 2004). Below the Atlantic Halocline is the Atlantic Layer, with a residence time of about 25

years. The Eurasian Basin Deep Water lies beneath the Atlantic layer, and while it has similar water mass characteristics as the water immediately below—the Eurasian Basin Bottom Water—these water masses have distinct hydrographic signatures and residence times of approximately 75 and 290 years, respectively (Stein and Macdonald, 2004).

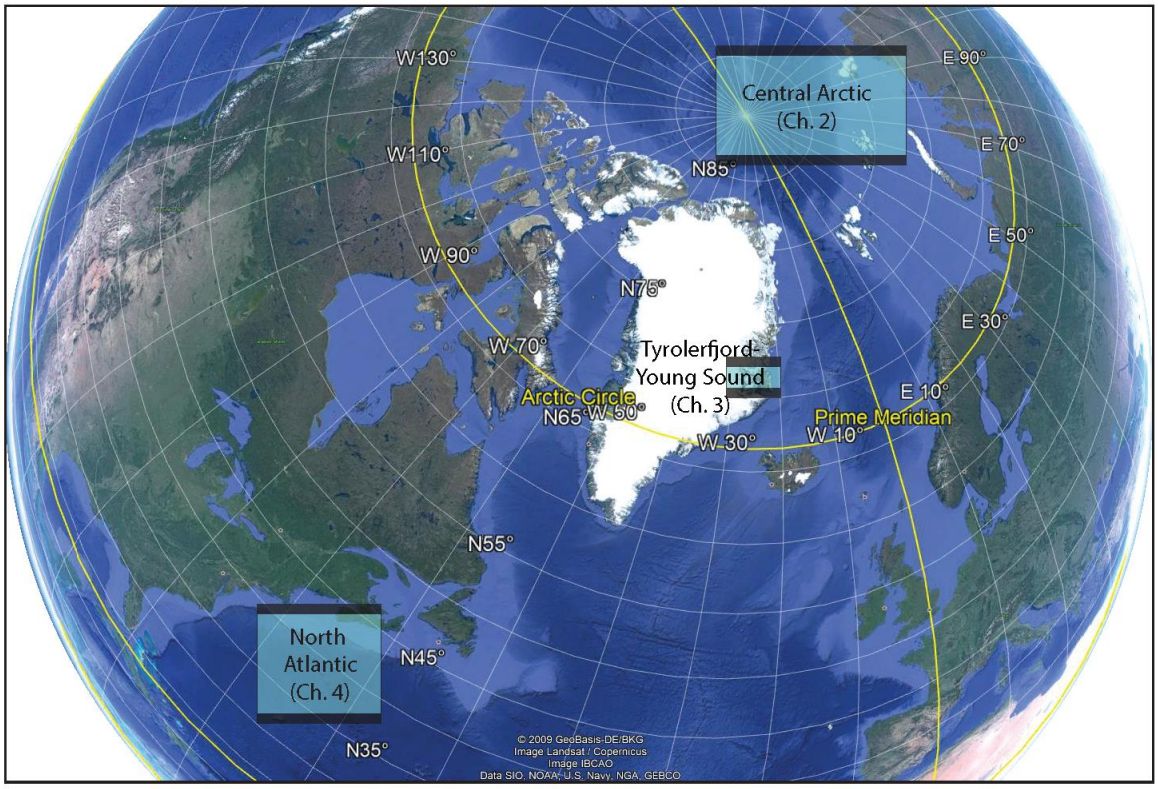

Figure 1-1. Map of field sites. Three regions – Central Arctic Ocean, Tyrolerfjord-Young Sound, and the North Atlantic Ocean—are highlighted. This map was modified from Google Earth.

The predominant Arctic currents circulate surface waters and overlying sea-ice in the Central Arctic and out through the Fram Strait. The Beaufort Gyre circulates surface water and sea-ice clockwise in the Canadian Basin, while the Transpolar Drift runs across the Central Arctic, bringing Pacific Ocean-influenced water from as far as the northern Bering Strait to the Fram Strait (Stein and Macdonald, 2004). Along with surface currents, the Central Arctic downwelling—driven by the formation of cold and salty brine rejected from sea-ice—provides a potential mode of dispersal for microorganisms. Sea-ice is present in

the Central Arctic year-round, but surface waters are seasonally exposed in the lower latitudes—approximately 84°N and below (Stein and Macdonald, 2004).

***Tyrolerfjord-Young Sound, Greenland*.** Located in northeast Greenland, Tyrolerfjord-Young Sound (74°18'N, 20°18'W) is a high-Arctic, deeply-incised fjord that connects parts of the Greenland ice sheet to the Greenland Sea. The fresh- and saltwater influence on Young Sound creates a salinity gradient over tens of kilometers, with salinity values that typically range from around 5 to 33 PSU in the summer (Bendtsen et al., 2014). Young Sound is the seaward portion of the Tyrolerfjord-Young Sound system, and it covers an area of 390 km^2, extending for approximately 90 km in length and up to 7 km in width at its widest (Rysgaard et al., 2003). The average depth throughout the basin is 100 m, but can reach depths of around 360 m (Rysgaard et al., 2003).

Climate data have been recorded at Young Sound since 1958, more recently (since 1999) as part of monitoring efforts by the Zackenberg Ecological Research Operations. In brief, because of its high latitude, Young Sound experiences polar night and midnight sun for 81 and 101 days, respectively (Rysgaard and Nielsen, 2006). Temperatures are below freezing for most of the year, and only from June to August do mean air temperatures reach 4°C (Rysgaard and Nielsen, 2006). Due to the sub-freezing temperatures, sea-ice, which begins to melt around mid-July, covers the system for most of the year. The break-up of sea-ice makes way for phytoplankton blooms—with the deep chlorophyll *a* maximum reaching ca. 15-20 m—which last until August, when nutrients (SiO^4, NO^{3-} and NH^{4+}) become limiting (Rysgaard and Nielsen, 2006; Rysgaard and Glud, 2007).

North Atlantic Ocean. The northwest continental shelf and the deep basin southeast of the shelf break are the North Atlantic regions of focus in this dissertation. The continental shelves in this region of the North Atlantic can be broad, extending up to 200 km from the coastline in the Gulf of Maine, and approximately 150 km from the coast of New York (Townsend et al., 2006). Freshwater discharge from large rivers, including the Hudson

and St. Lawrence Rivers combines with waters from the south-moving, relatively fresh and cold Labrador Current (Chapman and Beardsley, 1989) on the continental shelf, as well as the north-moving warm and higher salinity waters of the Gulf Stream (Townsend et al., 2006). Warm Slope Water, with typical temperature and salinity characteristics of 8-12°C and 34.7-35.5 PSU, flows adjacent to the shelf break, and is of North Atlantic Central Water origin (Gatien, 1976). This confluence of water masses result in sudden salinity and temperature changes across relatively small spatial scales, and may exhibit interannual variability due to changes in wind and climate forcing by the North Atlantic Oscillation (Pershing et al., 2001). Surface waters in the central North Atlantic are largely of Gulf Stream origin. Beneath this water mass lies the North Atlantic Deep Water, sourced from cooled, high salinity waters in the Norwegian, Greenland and Labrador Seas (Morozov et al., 2010).

1.4 Methodological Approaches

Approaches in microbial ecology and geochemistry are combined to investigate the structure and function of marine microbial communities. First, analyses of microbial community composition rely on high throughput sequencing and sequence comparisons of a marker gene: 16S ribosomal RNA (16S rRNA). This marker gene serves as a well-conserved ‘molecular chronometer’ used to infer organismal evolutionary relationships (reviewed in Woese, 1987). Its features include being conserved across domains (bacteria, archaea); in eukarya, its variant, the 18S rRNA, is found. This marker gene is slowly evolving, with independently-evolving units. Thus, the 16S rRNA gene contains highly conserved as well as hypervariable regions (Woese, 1987). Comparison of 16S rRNA gene sequences from cultured and uncultured organisms facilitates the identification of the taxonomic affiliation of organisms. Coupled with polymerase chain reaction (PCR), thousands to millions of copies of 16S rRNA genes can be sequenced. Using state-of-the-art software, these sequences can be efficiently identified and analyzed (Schloss et al.,

2009; Caporaso et al., 2010). Multivariate statistical approaches are subsequently used to identify factors underlying gradients in microbial community composition (Ramette, 2007).

To investigate microbial functionality, two distinct ways of empirically measuring extracellular enzymatic activities are employed (Arnosti, 2011). One approach measures enzymatic activities using low molecular weight substrate analogs labelled with methylcoumarin or methylumbelliferyl fluorogenic molecules. These substrate analogs are typically monomers or oligomers (e.g. leucine, alanine-alanine-proline, α-glucopyranoside), and cannot accurately represent the structural complexity of natural organic matter (Arnosti, 2011). However, these enzymatic assays are efficient, and are conducted over timescales of hours to a few days, and can therefore represent the functional potentials of microbial communities relatively close to the time of sampling. In these assays, enzymatic activities are determined by an enzyme-catalyzed increase in the fluorescence of fluorogenic molecules (Hoppe et al., 1983). The second, complementary approach uses high molecular weight (HMW) algae-derived polysaccharides that are labelled with fluoresceinamine, a constantly-fluorescing molecule (Arnosti, 2003). In contrast to the first approach, enzyme assays using HMW polysaccharides have the advantage of being representative of the structural complexity of natural organic matter. However, due to the incubation length, rate measurements from these enzyme assays may include a wider range of responses from microbial communities unrelated to substrate addition, such as community composition shifts due to ‘bottle effects’ (Stewart et al., 2012). Accordingly, these activities are cautiously interpreted as enzymatic potentials of a community, rather than as *in situ* activities of microbial communities.

Where possible, microbial community composition analyses and enzymatic activity measurements are coupled with other biogeochemical parameters. For example, microbial growth parameters, including bacterial production (Kirchman et al., 1985) and cell counts (Gasol and Del Giorgio, 2000) can be measured. Coupling these parameters with enzymatic

activity measurements illustrates the extent to which variations in enzymatic hydrolysis also parallel substrate uptake and cell growth. Additionally, dissolved organic matter (DOM) is also extracted (Dittmar et al., 2008) and characterized using liquid and gas chromatography mass spectrometry (Hasler-Sheetal et al., 2015). DOM composition can be paired with enzymatic activity measurements to gain insights into whether differences in OM quality co-vary with rates of specific heterotrophic processes.

Structure-function relationships are examined largely through multivariate statistical approaches. In particular, Mantel Tests or Partial Mantel Tests are used to evaluate whether differences in community composition correlate with differences of enzymatic activity profiles, with (Mantel Test) and without (Partial Mantel Test) the effect of environmental conditions on these relationships (Ramette, 2007). A statistically significant correlation between these parameters indicate functional dissimilarity, while the absence of a correlation may be due to functional redundancy and metabolic plasticity—in either case a weak or decoupled structure-function relationship.

1.5 Chapter Divisions

Three independent projects (Chapters 2, 3 and 4) comprise the body of this dissertation. Each project tackles questions pertaining to factors that structure microbial communities, patterns of enzymatic activities across spatial and environmental gradients, and the nature of microbial structure-function relationships. In Chapter 2, the composition and function of pelagic, particle-associated and benthic bacterial communities in the Arctic Ocean are investigated to test the hypothesis that the structure-function relationship varies largely by habitat (e.g., water column, particles, sediments). Chapter 3 tests the hypothesis that the enzymatic strategies employed by microbial communities to hydrolyze organic matter vary in rivers versus within a fjord. A working hypothesis is presented, which postulates that microbial functionality is concertedly influenced by intrinsic factors such as community composition, and extrinsic factors, such as organic matter supply. In Chapter 4,

the compositional and functional succession of distinct microbial assemblages from the North Atlantic in response to HMW particulate organic matter (HMW-POM) addition is characterized. In this chapter, the hypothesis that differences in microbial community composition has consequences for the hydrolysis of HMW-POM is evaluated. Discussions in each chapter include an integration of results into microbial ecological concepts, as well as implications for marine microbial carbon cycling. Key findings from each chapter are recapitulated in Chapter 5 (Synthesis and Conclusions), and are organized to reflect the three overarching themes of this dissertation: 1) factors that shape microbial biogeography; 2) patterns of microbial enzymatic activities across spatial and environmental gradients; 3) the nature of microbial structure and function relationships.

REFERENCES

Allison SD, Martiny JBH. (2008). Resistance, resilience, and redundancy in microbial communities. *Proc Natl Acad Sci USA* **105**: 11512-11519.

Arnosti C. (2003). Fluorescent derivatization of polysaccharides and carbohydrate-containing biopolymers for measurement of enzyme activities in complex media. *J Chromatogr* B **793**: 181-191.

Arnosti C. (2011). Microbial extracellular enzymes and the marine carbon cycle. *Annu Rev Mar Sci* **3**: 401-425.

Azam F, Malfatti F. (2007). Microbial structuring of marine ecosystems. *Nat Rev Microbiol* **5:** 782-791.

Baas Becking, LGM. (1934). *Geobiologie of inleiding tot de milieukunde*. Van Stockum: Den Haag.

Barberan A, Fernandez-Guerra A, Bohannan BJM, Casamayor EO. (2012). Exploration of community traits as ecological markers in microbial metagenomes. *Molec Ecol* **21:** 1909-1917.

Bauer M, Kube M, Teeling H, Richter M, Lombardot T, Allers E *et al.* (2006). Whole genome analysis of the marine Bacteroidetes *'Gramella forsetii*' reveals adaptations to degradation of polymeric organic matter. *Environ Microbiol* **8:** 2201-2213.

Bendtsen J, Mortensen J, Rysgaard S. (2014). Seasonal surface layer dynamics and sensitivity to runoff in a high Arctic fjord (Young Sound/Tyrolerfjord, 74 degrees N). *J Geophys Res Oceans* **119**: 6461-6478.

Brown MV, Ostrowski M, Grzymski JJ, Lauro FM. (2014). A trait based perspective on the biogeography of common and abundant marine bacterioplankton clades. *Mar Genomics* **15:** 17-28.

Caporaso JG, Kuczynski J, Stombaugh J, Bittinger K, Bushman FD, Costello EK. (2010). QIIME allows analysis of high-throughput community sequencing data. *Nat Methods* **7:** 335-336.

Cardman Z, Arnosti C, Durbin A, Ziervogel K, Cox C, Steen AD *et al.* (2014). *Verrucomicrobia* are candidates for polysaccharide-degrading bacterioplankton in an Arctic fjord of Svalbard. *Appl Environ Microbiol* **80:** 3749-3756.

Chapman DC, Beardsley RC. (1989). On the origin of shelf water in the Middle Atlantic Bight. *J Phys Oceanogr* **19**: 384-391.

Comte J, Fauteux L, del Giorgio PA. (2013). Links between metabolic plasticity and functional redundancy in freshwater bacterioplankton communities. *Front Microbiol* **4:** 112.

Crump BC, Hopkinson CS, Sogin ML, Hobbie JE. (2004). Microbial biogeography along an estuarine salinity gradient: Combined influences of bacterial growth and residence time. *Appl Environ Microbiol* **70:** 1494-1505.

D'Ambrosio L, Ziervogel K, MacGregor B, Teske A, Arnosti C. (2014). Composition and enzymatic function of particle-associated and free-living bacteria: a coastal/offshore comparison. *ISME J* **8:** 2167-2179.

Davey KE, Kirby RR, Turley CM, Weightman AJ, Fry JC. (2001). Depth variation of bacterial extracellular enzyme activity and population diversity in the northeastern North Atlantic Ocean. *Deep Sea Res Part II Top Stud Oceanogr* **48:** 1003-1017.

Datta MS, Sliwerska E, Gore J, Polz MF, Cordero OX. (2016). Microbial interactions lead to rapid micro-scale successions on model marine particles *Nat Commun* **7**: 11965.

Delong EF, Franks DG, Alldredge AL. (1993). Phylogenetic diversity of diversity and aggregate-attached vs free-living marine bacterial assemblages. *Limnol Oceanogr* **38:** 924-934.

DeLong EF, Preston CM, Mincer T, Rich V, Hallam SJ, Frigaard NU *et al.* (2006). Community genomics among stratified microbial assemblages in the ocean's interior. *Science* **311:** 496-503.

Dittmar T, Koch B, Hertkorn N, Kattner G. (2008). A simple and efficient method for the solid-phase extraction of dissolved organic matter (SPE-DOM) from seawater. *Limnol Oceanogr Methods* **6:** 230-235.

Fuhrman JA, Hagström Å. (2008) Bacterial and archaeal community structure and its patterns. In *Microbial Ecology of the Oceans*, 2nd Ed. Kirchman, D.L. (ed.). New York, USA: Wiley-Blackwell, pp. 45–90.

Gasol JM, del Giorgio PA. (2000). Using flow cytometry for counting natural planktonic bacteria and understanding the structure of planktonic bacterial communities. *Sci Mar* **64**: 28.

Gatien MG. (1976). A study in the Slope Water region south of Halifax. *J Fish Res Board Can* **33**: 2213-2217.

Green JL, Bohannan BJM, Whitaker RJ. (2008). Microbial biogeography: From taxonomy to traits. *Science* **320:** 1039-1043.

Hanson CA, Fuhrman JA, Horner-Devine MC, Martiny JBH. (2012). Beyond biogeographic patterns: processes shaping the microbial landscape. *Nat Rev Microbiol* **10:** 497-506.

Hasler-Sheetal H, Holmer M. (2015). Sulfide intrusion and detoxification in the seagrass Zostera marina. *PLoS One* **10:** e0129136.

Hoppe, HG. (1993). Use of fluorogenic model substrates for extracellular enzyme activity (EEA) measurement of bacteria, p. 423-431. *In* P. F. Kemp, B. F. Sherr, E. B. Sherr,

and J. J. Cole (ed.), Handbook of methods in aquatic microbial ecology. Lewis Publishers, Boca Raton, FL.

Ivars-Martinez E, Martin-Cuadrado A-B, D'Auria G, Mira A, Ferriera S, Johnson J *et al.* (2008). Comparative genomics of two ecotypes of the marine planktonic copiotroph *Alteromonas macleodii* suggests alternative lifestyles associated with different kinds of particulate organic matter. *ISME J* **2:** 1194-1212.

Jakobsson M and National Geophysical Data, C. (2004) The International bathymetric chart of the Arctic Ocean (IBCAO). In. Boulder, Colo.: National Geophysical Data Center.

Jiang X, Langille MGI, Neches RY, Elliot M, Levin SA, Eisen JA *et al.* (2012). Functional biogeography of ocean microbes revealed through non-negative matrix factorization. *Plos One* **7**. doi: 10.1371/journal.pone.0043866.

Kabisch A, Otto A, Koenig S, Becher D, Albrecht D, Schueler M *et al.* (2014). Functional characterization of polysaccharide utilization loci in the marine Bacteroidetes *'Gramella forsetii*' KT0803. *ISME J* **8:** 1492-1502.

Kellogg CTE, Deming JW. (2014). Particle-associated extracellular enzyme activity and bacterial community composition across the Canadian Arctic Ocean. *FEMS Microbiol Ecol* **89:** 360-375.

Kirchman D, K'Nees E, Hodson R. (1985). Leucine incorporation and its potential as a measure of protein synthesis by bacteria in natural aquatic systems. *Appl Environ Microbiol* **49:** 599-607.

Langenheder S, Lindstrom ES, Tranvik LJ. (2005). Weak coupling between community composition and functioning of aquatic bacteria. *Limnol Oceanogr* **50:** 957-967.

Martinez-Garcia M, Brazel DM, Swan BK, Arnosti C, Chain PSG, Reitenga KG *et al.* (2012). capturing single cell genomes of active polysaccharide degraders: An unexpected contribution of *Verrucomicrobia*. *PLoS One* **7:** 11.

Martiny JBH, Bohannan BJM, Brown JH, Colwell RK, Fuhrman JA, Green JL *et al.* (2006). Microbial biogeography: putting microorganisms on the map. *Nat Rev Microbiol* **4:** 102-112.

Morozov EG. (2010). Abyssal channels in the Atlantic Ocean water structure and flows. Dordrecht: Springer

Nemergut DR, Schmidt SK, Fukami T, O'Neill SP, Bilinski TM, Stanish LF *et al.* (2013). Patterns and Processes of Microbial Community Assembly. *Microbiol Mol Biol Rev* **77:** 342-356.

Neumann AM, Balmonte JP, Berger M, Giebel H-A, Arnosti C, Voget S *et al.* (2015). Different utilization of alginate and other algal polysaccharides by marine *Alteromonas macleodii* ecotypes. *Environ Microbiol* **17**:3857-3868.

Pedrós-Alió C. (2012). The rare bacterial biosphere. *Annu Rev Mar Sci* **4:** 449-466.

Pedrós-Alió C, Brock TD (1983). The importance of attachment to particles for planktonic bacteria. *Archiv fur Hydrobiol* **98:** 354-379.

Pershing AJ, Greene CH, Hannah C, Sameoto D, Head E, Mountain DG *et al*. (2001). Oceanographic responses to climate in the Northwest Atlantic. *Oceanography*, **14**: 76-82.

Polz MF, Hunt DE, Preheim SP, Weinreich DM. (2006). Patterns and mechanisms of genetic and phenotypic differentiation in marine microbes. *Philos Trans R Soc Lond B Biol Sci* **361:** 2009-2021.

Pommier T, Canbäck B, Riemann L, Boström KH, Simu K, Lundberg P *et al.* (2007). Global patterns of diversity and community structure in marine bacterioplankton. *Molec Ecol* **16:** 867-880.

Raes J, Letunic I, Yamada T, Jensen LJ, Bork P. (2011). Toward molecular trait-based ecology through integration of biogeochemical, geographical and metagenomic data. *Mol Syst Biol* **7**:473.

Ramette A. (2007). Multivariate analyses in microbial ecology. *FEMS Microbiol Ecol* **62:** 142-160.

Reed HE, Martiny JBH. (2007). Testing the functional significance of microbial composition in natural communities. *FEMS Microbiol Ecol* **62:** 161-170.

Rysgaard S, Vang T, Stjernholm M, Rasmussen B, Windelin A, Kiilsholm S. (2003). Physical conditions, carbon transport, and climate change impacts in a northeast Greenland fjord. *Arc Antarct Alp Res* **35:** 301-312.

Rysgaard S, Nielsen TG (2006). Carbon cycling in a high-arctic marine ecosystem - Young Sound, NE Greenland. *Prog Oceanogr* **71:** 426-445.

Rysgaard S, Glud RN (Eds.). Carbon cycling in Arctic marine Ecosystems: Caste Study Young Sound. Medd Greenland, Bioscience, 2007.

Schloss PD, Westcott SL, Ryabin T, Hall JR, Hartmann M, Hollister EB. (2009). Introducing MOTHUR Open-Source, platform-independent, community-supported software for describing and comparing microbial communities. *Appl Environ Microbiol* **75:** 7537-7541.

Sogin ML, Morrison HG, Huber JA, Welch DA, Huse SM, Neal PR *et al*. (2006). Microbial diversity in the deep sea and the underexplored “rare biosphere”. *Proc Natl Acad Sci USA* **103**: 12115-12120.

Stein R, Macdonald RW. (2004) *The organic carbon cycle in the Arctic Ocean*. Berlin; New York: Springer.

Stewart FJ, Dalsgaard T, Young CR, Thamdrup B, Revsbech NP, Ulloa O *et al.* (2012). Experimental incubations elicit profound changes in community transcription in OMZ bacterioplankton. *PLoS One* **7:** e37118.

Strickland MS, Lauber C, Fierer N, Bradford MA. (2009). Testing the functional significance of microbial community composition. *Ecology* **90:** 441-451.

Teske A, Durbin A, Ziervogel K, Cox C, Arnosti C. (2011). Microbial community composition and function in permanently cold seawater and sediments from an Arctic fjord of Svalbard. *Appl Environ Microbiol* **77:** 2008-2018.

Townsend DW, Thomas AC, Mayer LM, Thomas M, Quinland J. (2006). Oceanography of the Northwest Atlantic Continental Shelf. pp. 119-168. *In:* Robinson, A.R. and K.H. Brink (eds). *The Sea*, Volume 14, Harvard University Press.

Violle C, Reich PB, Pacala SW, Enquist BJ, Kattge J. (2014). The emergence and promise of functional biogeography. *Proc Natl Acad Sci USA* **111:** 13690-13696.

Weiss MS, Abele U, Weckesser J, Welte W, Schiltz E, Schulz GE. (1991). Molecular architecture and electrostatic properties of a bacterial porin. *Science* **254:** 1627-1630.

Wietz M, Gram L, Jørgensen B, Schramm A. (2010). Latitudinal patterns in the abundance of major marine bacterioplankton groups. *Aquat Microb Ecol* **61:** 179.

Woese CR. (1987). Bacterial evolution. *Microbiol Mol Biol Rev* **51:** 221-271.

CHAPTER 2: STRUCTURE AND FUNCTION OF HIGH ARCTIC PELAGIC, PARTICLE-ASSOCIATED, AND BENTHIC BACTERIAL COMMUNITIES

2.1 Introduction

Microbial communities in the Arctic Ocean are diverse, distinct from lower latitude communities, and structured by a range of features (e.g. Boetius *et al*., 2015). In Arctic marginal seas and the western Arctic Ocean, microbial communities are shaped by spatial variations in physicochemical regimes in the Arctic water column (Galand *et al*., 2010; Kirchman *et al*., 2010; Fu *et al*., 2013; Winter *et al*., 2013; Han *et al*., 2015). Strong temporal fluctuations in environmental conditions result in seasonal changes in community composition in the upper water column (Bano and Hollibaugh, 2002; Alonso-Saez *et al*., 2014). In addition to hydrography, particle association has emerged as a major factor affecting microbial community composition. While particle-associated microbial assemblages are mostly distinct from those of the water column and sediments (DeLong *et al*., 1993; Kellogg and Deming, 2009), recently observed compositional overlap between surface water microbial communities and deep water particle-associated assemblages highlights the role of particle colonization and vertical connectivity in shaping microbial communities (Thiele *et al*., 2015). Hydrographic regimes in overlying water (Hamdan *et al*., 2013; Buttigieg *et al*., 2015) and particle association finally impact benthic microbial community structure, as shown for settling phytodetritus (Bienhold *et al*., 2012; Jacob *et al*., 2013), and sinking sea ice algae aggregates (J. Z. Rapp, unpublished).

Despite low temperatures and a narrow temporal window of primary production in the Arctic (Kirchman *et al*., 2009, Boetius *et al*., 2015), microbial communities in the Arctic Ocean drive biogeochemical cycles of global importance, including photosynthetic carbon

assimilation and heterotrophic carbon degradation. These communities initiate carbon remineralization via the activities of their extracellular enzymes, which determine the quantity and quality of bioavailable substrates (Arnosti, 2011). The rates at which organic substrates are degraded, however, as well as the substrate specificities of microbially produced enzymes, are not well-constrained. Studies from the Arctic marginal seas (Kellogg and Deming 2009; Sala *et al.*, 2010; Tamelander, 2013), fjords (Steen and Arnosti, 2013, Teske *et al*., 2011; Arnosti, 2015), continental shelves (Bienhold *et al*., 2012, Boetius and Damm 1998), and the Canadian Archipelago (Kellogg and Deming 2014), suggest that microbial enzymatic activities are characterized by somewhat lower rates and considerably narrower substrate spectra than those in temperate and tropical latitudes (Arnosti *et al*., 2011). However, beyond pioneering initial surveys (Bano and Hollibaugh, 2002; Galand *et al*., 2010; Kirchman *et al*., 2010; Ghiglione *et al*., 2012), the composition and organic matter degrading capabilities of Arctic microbial communities remain poorly characterized, particularly in sea-ice covered regions and deep waters (Boetius *et al*., 2015).

Whether and to what extent these compositional and functional differences among microbial communities are linked to each other in a predictable manner is a question of considerable interest (Arnosti, 2011). For example, microbial communities and their carbon cycling capabilities may be affected by changes in the Arctic environment, including rising surface water temperatures and declining sea-ice cover (Wassmann, 2011). In coming years, these physical changes may lead to increases in the quantity of dissolved organic carbon routed through the microbial loop (Kirchman *et al*., 2009). Understanding variations in microbial community composition and activities along environmental and depth gradients is a critical step in determining the structure-function relationships of these communities. Consequently, the extent to which microbial communities are functionally dissimilar (i.e. changes in community composition have direct functional consequences) or functionally redundant (i.e. changes in environmental conditions, and not community composition, have

proximate control over microbial functionality) in part determines whether shifts in microbial community composition may result in changes in ecosystem process rates (Reed and Martiny, 2007, Strickland *et al*., 2009).

To investigate this problem, we coupled community composition as determined on the basis of high throughput sequencing of 16S rRNA gene amplicons with empirical measurements of enzymatic activities to characterize the biogeographical distribution and organic matter degrading capabilities of pelagic, particle-associated, and benthic bacterial communities in the central Arctic Ocean. Our aims were to identify the key environmental parameters that affect bacterial community composition and extracellular enzymatic activities along environmental and depth gradients. Using data on community composition and enzymatic activities in the water column, we investigated microbial structure-function relationships, and disentangled the relationships between environmental conditions, bacterial communities, and peptidase activities. This integrated study illuminates surface-to-deep profiles of bacterial community structure and function at a time of rapid changes in the underexplored Arctic Ocean.

2.2 Materials and Methods

Sites and sample collection. Samples were collected from the Eurasian Basin in the high Arctic between August and September 2012, during the ARK-27/3 cruise, and when a historic sea-ice extent minimum occurred (Fig. 1). Seawater from the surface, from the subsurface chlorophyll maximum (SCM; part of the Polar Mixed Layer, which was found at different depths), 500 m (Atlantic Layer), and bathypelagic zone (deep; ≥ 2000 m water; Eurasian Basin Deep Water and Eurasian Basin Bottom Water) were collected via using Niskin bottles mounted on a CTD (Fig. S1). At the SCM and 500 m, bulk seawater was also gravity-filtered through 3 µm pore size filters to separate bulk and ≥ 3 µm particle-associated microbial communities (Table 1). The upper 1 cm of surficial sediments—typically oxic, with the exception of patches of anoxic sediments beneath algal aggregate deposits at Stn. 349

and 360 (Boetius *et al*., 2013)—were collected at each station using a multicorer (MUC), and processed as detailed in the enzymatic activity measurements section. Melt pond and sea-ice aggregates were also collected using Duran bottles from Stn. 349. Environmental data for all ARK-27/3 stations are available in the PANGEA database (Rabe *et al*., 2013).

DNA sampling, extraction, sequencing and analysis*.* For whole community composition analyses, ca. 1 L seawater was filtered using a vacuum pump through a 0.2 µm pore size, 47 mm diameter Millipore filter. An additional ca. 6-8 L of seawater from the SCM and from a depth of 500 m was gravity filtered through a 3 µm pore size, 47 mm Millipore filter for large particle-associated community composition analyses. Aggregates of the diatom *Melosira arctica* were filtered in a similar manner. Samples were stored at -80°C until DNA extraction. DNA was extracted using the PowerSoil DNA Isolation Kit (Qiagen), following the manufacturer's protocol. DNA samples were PCR-amplified and sequenced at the Genomic Sequencing and Analysis Facility at University of Texas at Austin. The V1-V2 hypervariable region of the 16S rRNA gene was amplified with the Hyb8F_rRNA and Hyb338R_rRNA primer set (Supplementary Materials), and sequenced using Illumina MiSeq PE 2x300. QIIME was used to merge paired ends, cluster *de novo* OTUs (97% sequence similarity), and identify the taxonomic affiliation of *de novo* OTUs using the GreenGenes database. Chimeric sequences were identified using Chimera Slayer (Haas et al., 2011) and subsequently removed, along with singletons. Sequences were deposited into the NCBI Sequence Read Archive under the accession number SRP126633.

Non-metric multidimensional scaling (NMDS) ordination with Bray-Curtis dissimilarity index was performed to identify clustering patterns in the sequencing datasets of all sample types using the R package *Phyloseq* (McMurdie and Holmes, 2013). To test for differences in groupings defined according to depth and sample type in the NMDS, we performed an Analysis of Similarity (ANOSIM) using both Bray-Curtis and UniFrac dissimilarities in the R package *vegan* (Oksanen *et al*., 2008). These analyses were also used for pairwise

comparisons of groupings of bacterial communities from different depths, as well as bulk versus particle-associated communities. We used Analysis of Variance using Distance Matrices (ADONIS) with 999 permutations as implemented in *vegan* to investigate the correlation between measured environmental parameters (including temperature, salinity and oxygen) and bacterial community dissimilarity (Bray-Curtis), and to partition the variance that can be explained by each parameter. A partial Mantel test was used to determine the correlation between environmental conditions (temperature, salinity and oxygen) and community dissimilarity, holding for the effect of either geographic distances. We also tested for these correlations on community dissimilarity and geographic distances, holding for the effect of environmental conditions.

Enzymatic activity measurements. Exo- (terminal-unit cleaving) and endo-acting (mid-chain cleaving) peptidase activities were measured using the following substrate analogs, including their constituent single-letter amino acid codes: methylcoumarin (MCA)-labelled leucine (L-MCA), chymotrypsins (AAF-chymotrypsin, AAPF-chymotrypsin), and trypsins (QAR-trypsin, EGR-trypsin). Bulk seawater triplicate incubations were set up in 4 mL cuvettes, and substrates were added to a final concentration of 100 µM (Arnosti, 2015). Autoclaved ambient seawater with the same substrate concentration was used as killed control. Autoclaved and live seawater with no substrate addition were used as blanks. Subsamples were collected from the incubations at 0 h (upon addition of substrate), 24 h, 48 h, and 72 h. Large-particle associated peptidase activities were measured using 1/12th sections of the 3 µm pore-size filters. For each particle-associated incubation, one filter piece was submerged in a 4 mL cuvette containing autoclaved ambient seawater; duplicate live incubations were set up, in addition to a killed control containing autoclaved ambient seawater and a sterile filter piece. These incubations were subsampled at 0 h (addition of substrate), 4 h, 8 h and 12 h. Peptidase activities were measured in sediments using 1:2 (vol:vol) sediment slurries made by adding cooled, autoclaved overlying bottom water to

sediments. Live triplicates and one killed control per substrate were set up for the sediment incubations, and substrates were added to a final concentration of 100 µM. Sediment slurries were subsampled at 0, 1 h, 2 h, and 4 h by taking 2 mL of the incubated slurries, centrifugation, filtration of the supernatant using SFCA-filters, and addition of 1 mL filtered supernatant to 1 mL borate buffer. These procedures followed a previously established protocol (Arnosti, 2015). Fluorescence was converted to concentrations of hydrolyzed substrate by using a standard fluorescence curve of the free fluorophore. All incubations were carried out at 0°C in the dark.

The activities of specific endo-acting polysaccharide hydrolases that cleave their target polysaccharides mid-chain were measured using six fluoresceinamine-labelled (FLA) polysaccharides: pullulan, laminarin, xylan, fucoidan, arabinogalactan, chondroitin (Arnosti, 2003). Enzyme activities for these substrates have previously been measured in marine bacteria, and sequences corresponding to these hydrolytic enzymes have been identified in specific marine bacterial genomes (reviewed in Arnosti, 2011). Bulk seawater incubations were set up for each substrate in triplicates, plus one killed control. Each triplicate and killed control contained 15 mL of live and autoclaved seawater, respectively, to which one substrate per tube was added to a monomer concentration of 3.5 µM (Arnosti, 2003). Incubations were subsampled at 0h, 120 h, 240 h, 360 h, and 600 h. Additionally, large-particle-associated activities were measured on 1/12th sections of 3 µm pore-size filters. Each particle-containing filter piece was submerged in 15 mL of autoclaved ambient seawater amended with a polysaccharide substrate added to a final monomer concentration of 3.5 µM; killed controls were set up in a similar manner, but with 1/12th section of a sterile filter. These incubations were subsampled at the same timepoints as bulk water incubations, and subsampling procedures followed an established protocol (D'Ambrosio *et al*., 2014). Subsamples were processed using gel permeation chromatography and fluorescence detection (Arnosti, 2003). Maximum potential rates, which were measured at different time

points (Fig. S7A,B), are reported. We used ADONIS to test for correlations between enzymatic activities and the environmental parameters of temperature, salinity, and oxygen concentration.

Some methodological limitations for the enzymatic assays have to be considered. Due to the comparatively long timecourse of incubations, measurements with FLA-polysaccharides reflect long-term community potential. These measurements also incorporate a wider range of microbial responses (cellular growth, enzyme induction, and community shifts) than the peptidase activities, which are measured over shorter time courses and likely more closely reflect the microbial community at the time of sampling. However, due to the structural simplicity of the peptide analogs, the peptidase rates only weakly reflect the structural complexity of larger proteins.

Because of likely community shifts in long-term polysaccharide hydrolase enzyme assays, we chose peptidase rates to more directly assess whether differences in community composition are congruent with differences in enzymatic potentials. Thus, the structure-function relationships do not include polysaccharide hydrolase activities. To evaluate the extent of this structure-function relationship, we quantified correlations between community dissimilarity (Bray-Curtis) and peptidase activity dissimilarity (Euclidean distances), using Mantel test, as well as partial Mantel test to remove the effect of environmental conditions. A statistically significant, positive relationship indicates that increasing differences in community composition correlate with those in enzymatic potentials, which suggests functional consequences of community structural differences, or functional dissimilarity. Alternatively, differences in community composition that do not correlate with differences in peptidase potentials signify a functionally redundant or metabolically plastic community, where environmental factors, not community composition, shape functional differences between microbial communities (Reed and Martiny, 2007; Strickland *et al*., 2009).

2.3 Results

Environmental context. With the exception of an open water station in the Laptev Sea, all stations were located in the Eurasian Basin (Figure 1), and spanned a gradient of sea ice conditions ranging from open water at 79°N, to partially ice-covered (first year ice) and fully ice-covered conditions (multi-year ice) at 88°N (Table 1). Water masses targeted include the comparatively low salinity Polar Mixed Layer, the higher salinity Atlantic Layer, and the Eurasian Basin Deep Water and Eurasian Basin Bottom Water (Fig. S1; Stein and Macdonald, 2004).

***Bacterial community composition patterns*.** The dataset contains 1,088,000 sequences, with each sample rarefied to 34,000 sequences, and which represent 4055 unique OTUs at a 97% similarity cutoff. Non-metric multidimensional scaling (NMDS) revealed that bacterial community composition differed by water mass and sample type (Fig. 2). Bacterial communities of the surface water and subsurface chlorophyll maximum (SCM)—bulk as well as particle-associated—clustered close to each other, signifying compositionally similar bacterial communities at these two depths. Bacterial communities from bulk water samples at 500 m and deep waters (≥2000m) formed distinct groups that clustered closely together, but separated from surface and SCM communities. Pairwise comparisons revealed that compositional differences among bulk bacterial communities in the surface and SCM are not significant (ANOSIM, R = -0.076, p = 0.663), while those between 500 m and deep waters are (ANOSIM, R = 0.774, p = 0.001). Particle-associated samples at the SCM formed a tighter cluster than those at 500 m. Sediment bacterial communities formed the tightest grouping (Fig. 2), indicating high compositional similarity across all sites.

Clustering patterns in the ordination space reflect the different relative proportions of taxonomic groups with depth and habitat (Fig. 3). In the sea ice (melt pond and algae aggregate samples) and Polar Mixed Layer water samples (surface, SCM, and SCM

particle-associated samples), members of the class *Alphaproteobacteria* (20-54%), *Flavobacteria* (20-76%), and *Gammaproteobacteria* (18-55%) were well represented. Bulk seawater from the Atlantic Layer and Eurasian Basin Deep Water and Bottom Water were comprised largely of bacterial taxa belonging to *Alphaproteobacteria* (30-50%), *Gammaproteobacteria* (20-48%), *Deltaproteobacteria* (7-18%), and the AB16 clade within the phylum SAR406 (2-9%). Sequences from particles at 500 m primarily correspond to members of the *Gammaproteobacteria* (62-93%), *Alphaproteobacteria* (1-32%), and *Flavobacteria* (1-6%). Bulk water bacterial communities exhibited greater species richness and evenness with increasing depth (Fig. S2). Sediment bacterial communities yielded the highest diversity scores by any measure (Fig. S2); their most relatively abundant groups included *Gammaproteobacteria* (31-46%), *Acidomicrobia* (9-15%), *Alphaproteobacteria*, (12-17%), *Deltaproteobacteria* (6-8%) and *Flavobacteria* (4-8%). The most abundant OTU, most closely related to the Alphaproteobacterium *Pelagibacter ubique* HTCC 1062, comprised 9.2% of the entire dataset. An OTU most closely related to the Flavobacterium *Polaribacter irgensii* was the second most abundant OTU, comprising 5.4% of the dataset. Gammaproteobacterial OTUs related to *Colwellia piezophila*, an uncultured member of the family *Oceanospirillaceae*, and an uncultured member of the OM60 clade represented the third, fourth and fifth most abundant OTUs in the entire dataset, respectively.

***Influences of environmental conditions versus geographic distances*.** We sought to identify environmental factors that correlated with community dissimilarity. Temperature, salinity and oxygen concentrations contributed 29%, 24%, and 21%, respectively, to the variation observed among surface-to-deep pelagic bacterial communities, all with statistical significance (ADONIS, $p = 0.001$); ca. 26% of variances were unaccounted for by the model. As a caveat, however, these correlations were scale-dependent. Taking into account only samples from the Polar Mixed Layer (surface and SCM), bacterial community dissimilarity was only significantly correlated with temperature

(ADONIS, R^2 = 0.42, *p* = 0.003). Because environmental parameters can be spatially structured, we performed partial Mantel tests to measure the relative influence of environmental condition on whole pelagic bacterial community dissimilarity, holding for the effect of geographic distances. We used temperature, salinity, and oxygen to calculate an environmental condition dissimilarity matrix using Euclidean distances. Environmental parameters and bacterial community dissimilarity are strongly correlated (Mantel test, r = 0.78, *p* = 0.001); the relationship between geographic distances and community dissimilarity is not significant (Mantel Test, r = -0.13, *p* = 0.99).

Differentiation and depth-related trends of particle-associated communities. Particle association results in a community distinct from—and with lower species richness and evenness compared to—the bulk water samples both at the SCM (ANOSIM, R = 0.74, *p* = 0.01) and at 500m (ANOSIM, R = 1, *p* = 0.03) (Fig. S2). SCM particle samples included substantial proportions of *Flavobacteria* and *Gammaproteobacteria,* with some contribution of *Alphaproteobacteria* (Fig. 2). Predominantly detected *Flavobacteria* on SCM particles include an OTU closely related to members of an uncultured cluster belonging to the family *Flavobacteraceae*, as well as OTUs closely related to *Polaribacter irgensii* 23-P (Fig. S3). Gammaproteobacteria on SCM particles are largely represented by members of the NOR5/OM60 clade (30-65% of *Gammaproteobacteria*) (Fig. S4A), with some contribution of OTUs closely related to *Colwellia piezophila* and *Colwellia polaris*. In contrast, sequences from the particle-associated samples at 500m were, to a greater degree, dominated by members of *Gammaproteobacteria* (Fig. S4A), primarily consisting of OTUs closely related to *Colwellia piezophila* and *Colwellia polaris* (Fig. S5)—up to 57% and 41%, respectively, of the entire sequence dataset for some samples. Finally, members of the *Alphaproteobacteria* were detected in variable relative proportions on particles, and ranged from ca. 2% at Stn 255 to ca. 35% at Stn 360, both at 500 m (Fig. 2). The large contribution of *Alphaproteobacteria* on 500 m particles at Stn. 360 was composed primarily of members of

Rhodobacteraceae (Fig. S4B), in contrast to members of the *Pelagibacteraceae* (including the SAR 11 group) that predominated in water column samples.

***Sediment bacterial communities*.** Bacterial communities in sediments differed significantly in composition compared to those from deep waters (ANOSIM, R = 1, p = 0.006). Members of the *Gammaproteobacteria*, *Alphaproteobacteria*, *Acidomicrobia*, *Deltaproteobacteria* and *Flavobacteria* were among the most highly represented bacterial classes in sequence datasets from sediments (Fig. 2). Moreover, across the entire dataset, benthic bacterial communities showed the highest α-diversity—based on species richness and evenness (Fig. S2)—and lowest β-diversity, as indicated by the lowest group variance (Table S1). These results are consistent with patterns observed using Bray-Curtis-based community dissimilarities.

Peptidase activities. In order to quantify peptide and protein-cycling capabilities of Arctic microbial communities, we measured exo-acting (leucine aminopeptidase) and endo-acting peptidase activities (chymotrypsins, trypsins) of pelagic, particle-associated and benthic bacterial communities. Peptide hydrolysis was measurable at almost all stations and depths, with the exception of Stn. 224 bottom water (Fig. 4A). Summed peptide hydrolysis rates generally decreased from surface to bottom waters, with rates in surface waters frequently an order of magnitude higher than at 500 m and in bottom waters (Fig. 4A). These trends are driven largely by the substantial contribution of leucine (Leu-MCA) hydrolysis at each station and depth. With the exception of Stn. 360, summed peptide hydrolysis rates were higher in surface waters than at the SCM. Furthermore, summed peptidase rates in surface water were similar at the ice-free and first year ice-covered stations (Stns. 292, 255 and 224, respectively). These stations also showed the highest endopeptidase activities—particularly AAPF-chymotrypsin and/or FSR-trypsin. Summed rates in surface and SCM waters were notably lower at the multi-year ice-covered stations (Stns. 349 and 360), signifying comparatively lower potential for organic matter

remineralization in the upper water column at the two stations with multi-year ice. However, the same stations showed slightly higher activities at depths of 500 m and in bottom water compared to other stations. Peptidase activities in bulk waters correlated weakly with temperature (ADONIS, $R^2 = 0.088$, $p = 0.036$), and strongly with salinity differences (ADONIS, $R^2 = 0.653$, $p = 0.001$).

A broader spectrum of peptidase activities was sometimes measured on particles than in bulk seawater, as evident at Stn 292 SCM and Stn 360 500 m (Fig. 4A, 4B). At many stations and depths, some endopeptidase activities, such as those measured by EGR-trypsin and AAF-chymotrypsin, were only detected on particles. Furthermore, summed particle-associated activities were higher at the SCM than at 500 m, with the exception of Stn 360, where summed particle-associated activities at 500 m were almost double those measured at the SCM (Fig. 4B). Overall, particle-associated peptidase activities accounted for ca. 4-22% and 12-100% of the bulk enzyme activities at the SCM and 500 m, respectively, demonstrating that a greater fraction of peptidase activities at 500 m were likely particle-associated.

Sediment peptidase activities were several orders of magnitude higher than activities in bulk seawater and particle incubations (Fig. 4C). All of the peptide substrates (except EGR-trypsin at Stn 255) were hydrolyzed in sediments. The relative proportions of enzymatic activities in sediments varied little by station. The highest sediment peptidase rates were measured at Stn 292, and were due to the higher AAF-chym (ANOVA, $p < 0.01$) and AAPF-chym hydrolysis (ANOVA, $p < 0.001$) at this station compared to other stations. As in bulk seawater and on particles, L-MCA hydrolysis constituted the largest fraction (ca. 70-80%) of summed peptidase activity.

Polysaccharide hydrolase activities. Of the six polysaccharide substrates, laminarin, pullulan, xylan and chondroitin were hydrolyzed at multiple stations and depths, whereas arabinogalactan and fucoidan were not hydrolyzed at any station or depth (Fig.

5A). Laminarin was hydrolyzed at all sites and depths, and chondroitin was hydrolyzed at depths from the surface to 500 m at Stns. 224, 349 and 360. Pullulan hydrolysis was measured at depths of 500 m and in bottom water, and xylan was hydrolyzed only at few depths and stations, with no evident spatial pattern. Summed polysaccharide hydrolysis rates varied with depth, although the highest summed rates were consistently measured at the SCM or at 500 m (Fig. 5A). Polysaccharide hydrolase activities only significantly correlated with differences in oxygen concentrations (ADONIS, $R^2 = 0.258$, $p = 0.004$).

On a volume-corrected basis, particle-associated polysaccharide hydrolase activities were lower than those for bulk seawater (Fig. 5B). As with bulk seawater, only four of the six substrates were hydrolyzed in particle-associated incubations; arabinogalactan and fucoidan were not measurably hydrolyzed. However, at most depths and locations, the spectrum of substrates hydrolyzed in the particle-associated incubations was greater than for bulk seawater incubations—a trend that parallels some of the observations with peptidase activities. In particular, xylan and pullulan hydrolysis was detected in the particle-associated incubations at depths and stations where it was not measured in the bulk water incubation (Fig. 5B).

***Structure-function relationship*.** Variations in pelagic bacterial community composition weakly correlated with differences in peptidase activities (Mantel test, r = 0.22, p = 0.014). However, removing the influence of environmental conditions (temperature, salinity, and oxygen) to evaluate a direct structure-function link indicates no statistically significant correlation (partial Mantel test, r = 0.02, $p = 0.4$). This analysis illustrates that the structure-function link does not persist independent of environmental variables for peptidase activities.

2.4 Discussion

***Pelagic realm*.** In the central Arctic Ocean, differences in the extent of sea-ice coverage and sea ice melting drive variations in temperature and salinity in surface waters. Seasonal variations in the upper water column, in tandem with the influence of North Atlantic

waters on much of the Eurasian Basin, result in stratified water masses in the central Arctic (Stein and Macdonald, 2004). In our investigation, temperature and salinity correlated most strongly with bacterial community dissimilarity; these environmental parameters have also been correlated with patterns of community composition in global oceans (Zinger *et al*., 2011; Sunagawa *et al*., 2015) and across terrestrial and aquatic habitats (Lozupone and Knight, 2007). Thus, spatial environmental gradients and depth-related hydrographic features differentiate bacterial communities in the central Arctic (Fig. S6), consistent with previous observations in the greater Arctic (Galand *et al*., 2010; Han *et al*., 2015).

The upper water column of the seasonally-productive central Arctic Ocean was populated by organic matter degraders within the bacterial classes *Flavobacteria, Gammaproteobacteria* and *Alphaproteobacteria* (Dang *et al*., 2008; Teeling *et al*., 2012; Williams *et al*., 2013). The large relative contribution of these classes is consistent with trends previously observed in the Arctic (Bano and Hollibaugh, 2002; Boetius *et al*., 2015). Furthermore, variations in relative proportions of specific groups—the comparatively large contribution of *Flavobacteria* especially in the ice-free station—were in accordance with observations of increased flavobacterial proportions in the Canadian Arctic during the 2007 sea-ice minimum (Comeau *et al*., 2011) and in ice-free summer waters off Svalbard (Wilson *et al*., 2017). The absence of several flavobacterial genera in the melt pond and algal aggregate samples in Stn 292 surface and SCM water samples indicates that the large contribution of *Flavobacteria* in these waters are linked to primary productivity rather than bacterial release from the melted sea-ice. Accordingly, net primary productivity was higher at stations with little to no sea-ice at the time of sampling (Fernández-Méndez *et al*., 2015).

Our analyses of bacterial communities extend into previously unexplored deep-water masses, including the European Basin Deep and Bottom Waters. At the mesopelagic (Galand *et al*., 2010) and extending down into the bathypelagic realm, a greater range of bacterial classes, most notably including the *Deltaproteobacteria*, SAR 202 (phylum

Chloroflexi), and AB16 (within phylum *Marinimicrobia*), were detected. While many of the same bacterial groups—on a broad taxonomic level—were detected in the mesopelagic and bathypelagic, OTU-level analyses demonstrated significant community differences at 500 m and deep waters. The depth-related heterogeneity and increase in phylogenetic diversity of pelagic bacterial communities parallels observations from global oceans (Jing *et al*., 2013; Sunagawa *et al*., 2015; Wilson *et al*., 2017).

Depth profiles of microbial activity, including the first empirical measurements of microbial enzyme activities in the Eurasian Basin Deep and Bottom waters, showed opposite trends for peptidases and polysaccharide hydrolase activities (Fig. 6). In the upper water column, summed peptidase activities were higher in the seasonally ice-free and partially ice-covered areas, and lower in the fully ice-covered stations, likely related to differences in primary production along a gradient of sea-ice regimes. Bulk peptidase activities substantially decreased below the SCM—a trend observed at all stations. In contrast, the highest summed rates and the broadest spectrum of polysaccharide hydrolase activities were measured at either the SCM or at 500 m. These depth-related patterns are consistent with the hypothesis that organic nitrogen-containing substrates are preferentially removed from particles as they sink in the water column (Lee *et al*., 2000; Tamelander, 2013). Nevertheless, peptidase activities remain detectable in bottom waters (down to ca. 4350 m) at reduced rates, and with a narrower spectrum of enzyme activities. The relatively constant polysaccharide hydrolase activities throughout the water column at some stations (eg. Stn 292, 349, 360) suggest that carbohydrates may fuel microbial metabolism in surface as well as deep waters, although substrate utilization patterns varied with depth.

While community composition and peptidase activities correlated with environmental conditions and therefore co-varied, the lack of correlation between community structure and peptidase activities by themselves suggests that protein degradation is characterized by functional redundancy. Functional redundancy refers to the ability of different taxa to carry

out the same or closely related functions (Reed and Martiny, 2007; Strickland *et al*., 2009). In such a case, environmental conditions, rather than community composition, ultimately control rates of specific ecosystem processes, as our results suggest. We also note that community plasticity, the physiological or metabolic flexibility of community members under varying environmental conditions (Comte *et al*., 2013), may further confound efforts to identify structure-function relationships. These results suggest that, in the water column, the ability to utilize proteinaceous compounds may be too phylogenetically widespread and non-specific to identify a strong structure-function relationship.

Particle-associated fraction. Particle association contributed significantly to community dissimilarity, although these effects were stronger in the mesopelagic than at the SCM. This observation may be indicative of population maintenance strategies. Particle-associated microbial taxa must maintain a free-living population to colonize newly formed particles in the upper water column, in order not to sink permanently from the photic zone as particles are exported to the seafloor (Pedrós-Alió and Brock, 1983). Under this scenario, particle-associated communities exchange with the free-living bacterial community. Alternatively, only a subset of the population attaches to the particles. In both scenarios, development of a distinct bacterial community on particles is limited. In the mesopelagic, where new particle production is less likely, continuous exchange with a free-living population is no longer needed; thus, particle-associated communities become more distinct from the whole community. Within-particle bacterial community changes during sinking, in addition to decolonization or detachment, may further enhance the development of a distinct particle-associated community (Thiele *et al*., 2015). Both explanations are congruent with observations that taxa attached to deepwater particles are phylogenetically distinct from those of free-living assemblages (Eloe *et al*., 2011; Salazar *et al*., 2015).

The particle-associated niche was largely occupied by members of the class *Flavobacteria* (dominant on SCM particles), *Gammaproteobacteria* (dominant on 500 m

particles) and *Alphaproteobacteria*, providing evidence for a distinct phylogenetic signal of that became more prominent at depth. Taxa within these classes have been classified as particle-associated in other oceanic regions (Salazar *et al*., 2015; Thiele *et al*., 2015), and are among the most ubiquitous surface colonizers (Buchan *et al*., 2014; Dang and Lovell, 2016). Moreover, *Colwellia*-related OTUs—detected in moderate proportions on SCM particles—were proportionally dominant on particles at 500 m, highlighting the influence of epipelagic particle colonization to mesopelagic particle-associated communities (Tamelander, 2013; Thiele *et al*., 2015).

Irrespective of phylogenetically distinct particle-associated communities at the SCM and 500 m, however, polysaccharide hydrolase activities at the two depths overlapped. Such functional redundancy could be essential to initiate remineralization of structurally-diverse high molecular weight compounds within suspended and sinking particulate matter (D'Ambrosio *et al*., 2014). Functional redundancy among surface-associated microbes has also been observed between phylogenetically dissimilar algae-associated bacterial communities that share a core set of functional genes (Burke *et al*., 2011). However, the similarities in particle-associated enzymatic activity may also be attributed to the overlap of particle-associated taxa at the SCM and 500 m. In particular, members of the genus *Colwellia* have wide-ranging organic substrate utilization abilities (Bowman, 2014), and are detected in substantial proportions on particles at the SCM and 500 m.

Particle-associated communities additionally demonstrated a consistently broader range of polysaccharide hydrolase activities than the bulk water community. This trend could in part be due to differences in volumes sampled for our particle-associated (ca. 6-8 L) versus bulk seawater (50 mL) analyses. These results may nevertheless reflect contrasting abilities of particle-associated versus free-living taxa to utilize polysaccharides. Such differences have been documented, for example, among ecotypes of *Polaribacter irgensii*: the putatively algae-associated strain contained a greater range of polysaccharide utilization

genes compared to the planktonic taxon (Xing *et al*., 2015). Furthermore, mechanisms such as quorum sensing on aggregates may lead to production of specific enzymes (Gram *et al*., 2002). Hydrolytic activity originating from particle-associated microbes can then be released as free enzymes to ambient water (Vetter *et al*., 1998; Ziervogel and Arnosti, 2008); however, due to low particle concentrations, the contribution of particle-associated microbes may be too dilute to be detected in bulk seawater measurements. Overall, our findings suggest that the degradation of particulate matter likely requires a broad spectrum of enzymatic 'tools' to access substrates. Consistent with this idea, particle-attached microbes possess a diverse genetic repertoire—compared to their free-living counterparts—necessary to internally transport and utilize substrates from particles (Teeling *et al*., 2012; Smith *et al*., 2013). The abundance of carbon sources on particles enables particle-associated microbes to maintain their copiotrophic lifestyle.

Sediments. Sediment bacterial communities exhibited considerably higher phylogenetic diversity than pelagic or particle-associated communities, in accordance with findings from a global-scale analysis of marine ecosystems (Zinger *et al*., 2011), and diverse terrestrial and aquatic habitats (Lozupone and Knight, 2007). In addition, β-diversity was lower among benthic bacterial communities compared to the bacterial communities of any depth from the water column or particles; nevertheless, subtle variations in community composition were detectable. Hydrographic conditions of overlying water masses may influence benthic bacterial communities (Hamdan *et al*., 2013); the similarity of benthic bacterial communities in the deep central Arctic might reflect in part the influence of relatively homogeneous and stable physical properties of the Eurasian Basin Deep Water and Eurasian Basin Bottom Water across the different stations. Additionally, low productivity regimes impose stronger selective forces than do high productivity ones, which may result in highly similar community composition across oligotrophic sites (Chase, 2010). Therefore, widely similar oligotrophic conditions in Arctic Basin sediments may select for

phylogenetically similar bacterial communities across different sampling locations in this benthic habitat.

Finally, a specific feature of the peptidase activity patterns observed in sediments mirror those detected in the water column and on particles. Leucine aminopeptidase (exo-acting) activities contributed a large majority to the summed peptidase rates, while chymotrypsin and trypsin (endo-acting) activities contributed to a much lesser extent. Our findings of greater exo-acting versus endo-acting peptidase activities contrast with observations from Svalbard fjords (Steen and Arnosti, 2013; Arnosti, 2015) and coastal temperate waters off Japan (Obayashi and Suzuki, 2005; Obayashi and Suzuki, 2008). High leucine aminopeptidase activities have been proposed as microbial adaptations to carbon-poor conditions (Boetius and Lochte, 1996; Polymenakou *et al*., 2008). Accordingly, a succession of proteases, from high endo-acting peptidase activities in unamended coastal temperate seawater to high exo-acting peptidase activity in the 112-day old 'aged' seawater (Bong *et al*., 2013), suggests an association between these hydrolytic enzymes and organic matter quantity and quality; however, the mechanistic basis for this linkage is unclear. Moreover, activities measured as leucine aminopeptidase may instead reflect the collective activity of several high-affinity, but low-specificity aminopeptidases (Steen *et al*., 2015). In any case, the expression of high substrate affinity exo-acting peptidases throughout the Arctic water column and sediments may be linked to ambient organic matter conditions.

Future outlook. Since previous observations (Comte *et al*., 2013) and our own findings indicate that the degree of metabolic plasticity, functional redundancy, and functional dissimilarity exhibited by microbial communities can be highly dependent on environmental conditions, it is imperative that structure-function relationships are evaluated in the context of the environment. Thus, we anticipate changes in bacterial community composition owing to physicochemical alterations in the Arctic (Kirchman *et al*., 2009). Projected shifts in carbon export to Arctic Ocean sediments (Wassmann *et al*., 2011) are

already evident with widespread deposition of large sea-ice algae aggregates in the seafloor (Boetius *et al*., 2013), and can alter the composition of benthic microbial communities over time (Bienhold *et al*., 2012; J. Z. Rapp, unpublished). However, our observation that functional redundancy impacts the microbial structure-function relationship in the water column may complicate efforts to predict the influence of Arctic environmental changes on microbially driven ecosystem processes.

2.5 Acknowledgements

We thank Chief Scientist Prof. Dr. Antje Boetius for her kind invitation to join the cruise on R/V *Polarstern*, and the captain, scientific party and crew of *Polarstern* Expedition PS80 (ARK27/3) for assistance, sampling support and/or scientific discussions. Ship time on R/V *Polarstern* was funded by the Alfred Wegener Institute (AWI) Grant No. AWI_PS80_01. Sherif Ghobrial provided essential help in the lab, and Stephanie O'Daly and Marie English assisted with sample processing. This project was supported by the National Science Foundation awarded to CA (CMG ARC-1025526; OCE 1332881). JPB was additionally funded through the Howard Hughes Medical Institute Teaching Fellowship, and the UNC Dissertation Completion Fellowship.

2.6 Main Figures and Tables

Figure 1. A map of the central Arctic Ocean and marginal seas. The unbroken dark gray line shows the boundaries of the historic minimum in sea-ice extent in 2007, and the dashed line illustrates the historic minimum in sea-ice extent in 2012, around the time of sample collection. Black circles denote the sampling stations, with one in the open ocean (292), two in the ice-margin (224 and 255), and two under full-ice cover (349 and 360). The map was modified from Marcel Nicolaus, Alfred Wegener Institute.

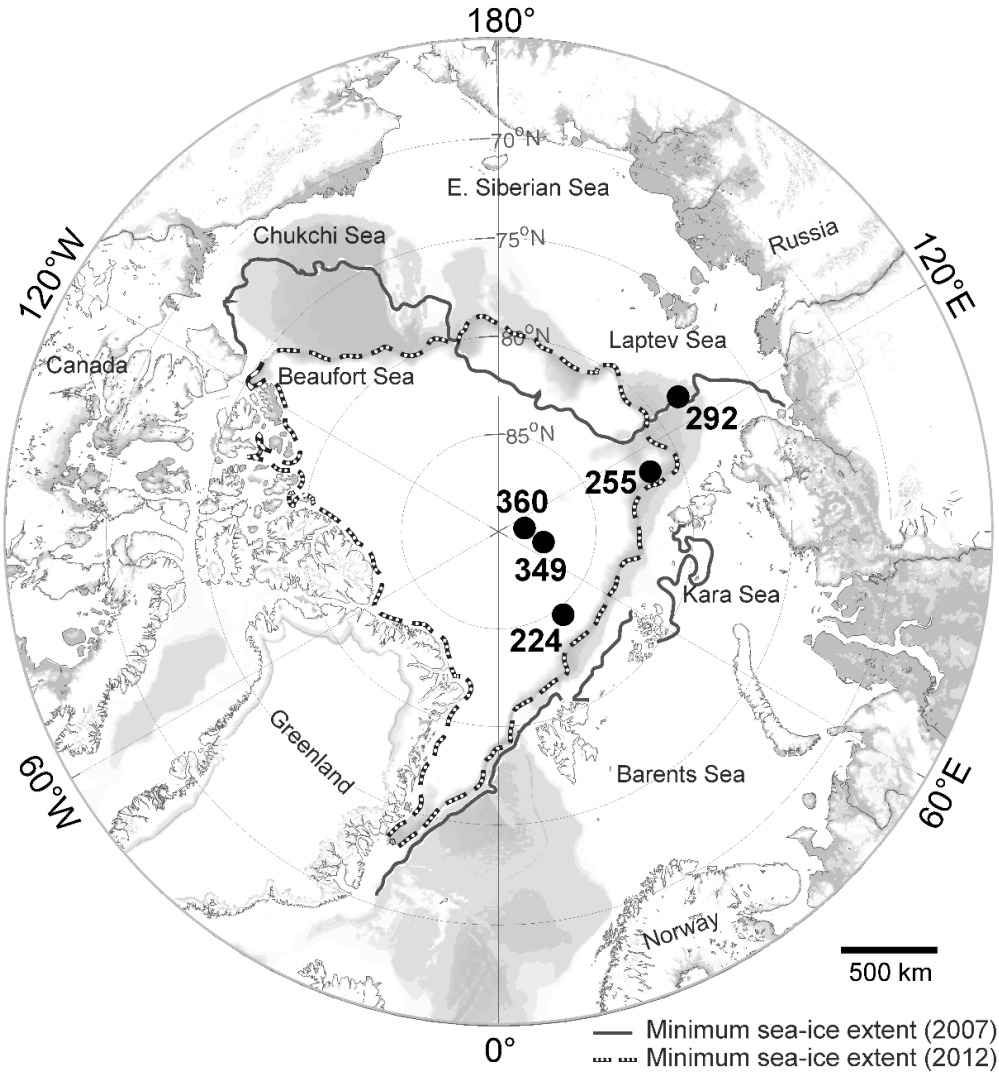

Figure 2. Non-metric multidimensional scaling (NMDS) using Bray-Curtis dissimilarity. Ordinations were conducted based on OTUs identified at 97% sequence similarity. Ellipses correspond to 95% confidence intervals for depth and sample types containing more than three samples. PA indicates particle-associated samples.

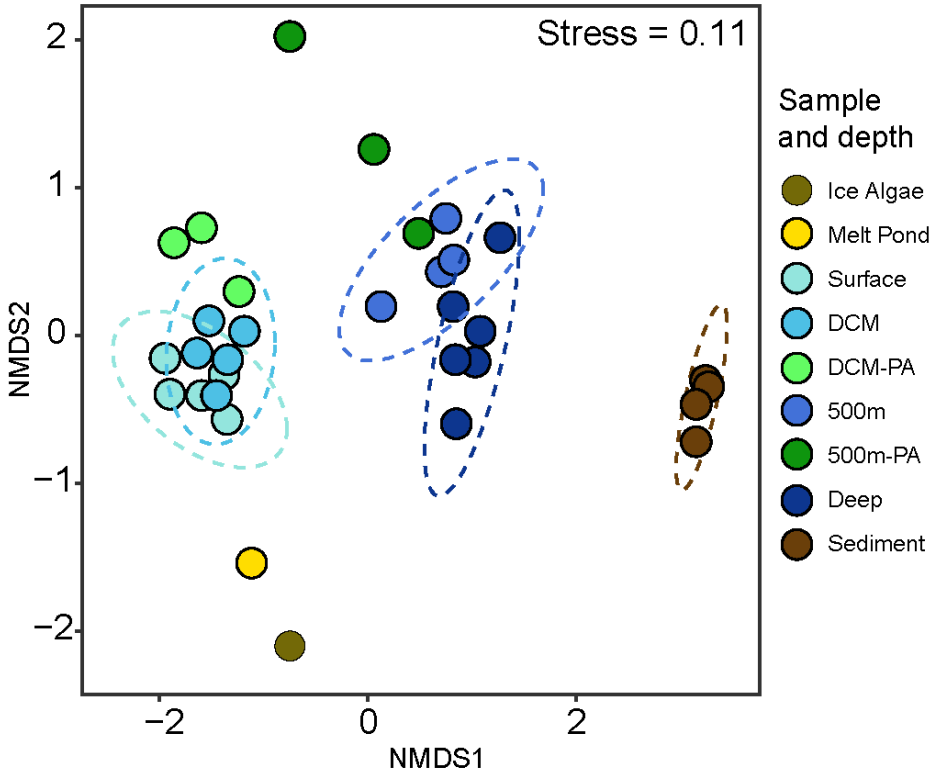

Figure 3. Class-level breakdown of bulk pelagic (A), particle-associated (B), and benthic (C) bacterial communities in the Arctic Ocean. The bar graph only includes classes with relative abundances of ≥ 1% of the entire data set. The sampling depth and sample type are indicated above the bar graphs, and the corresponding water masses for the samples are in bold. PA indicates particle-associated samples. Symbols above the bar graph coincide with those found in Figure 2.

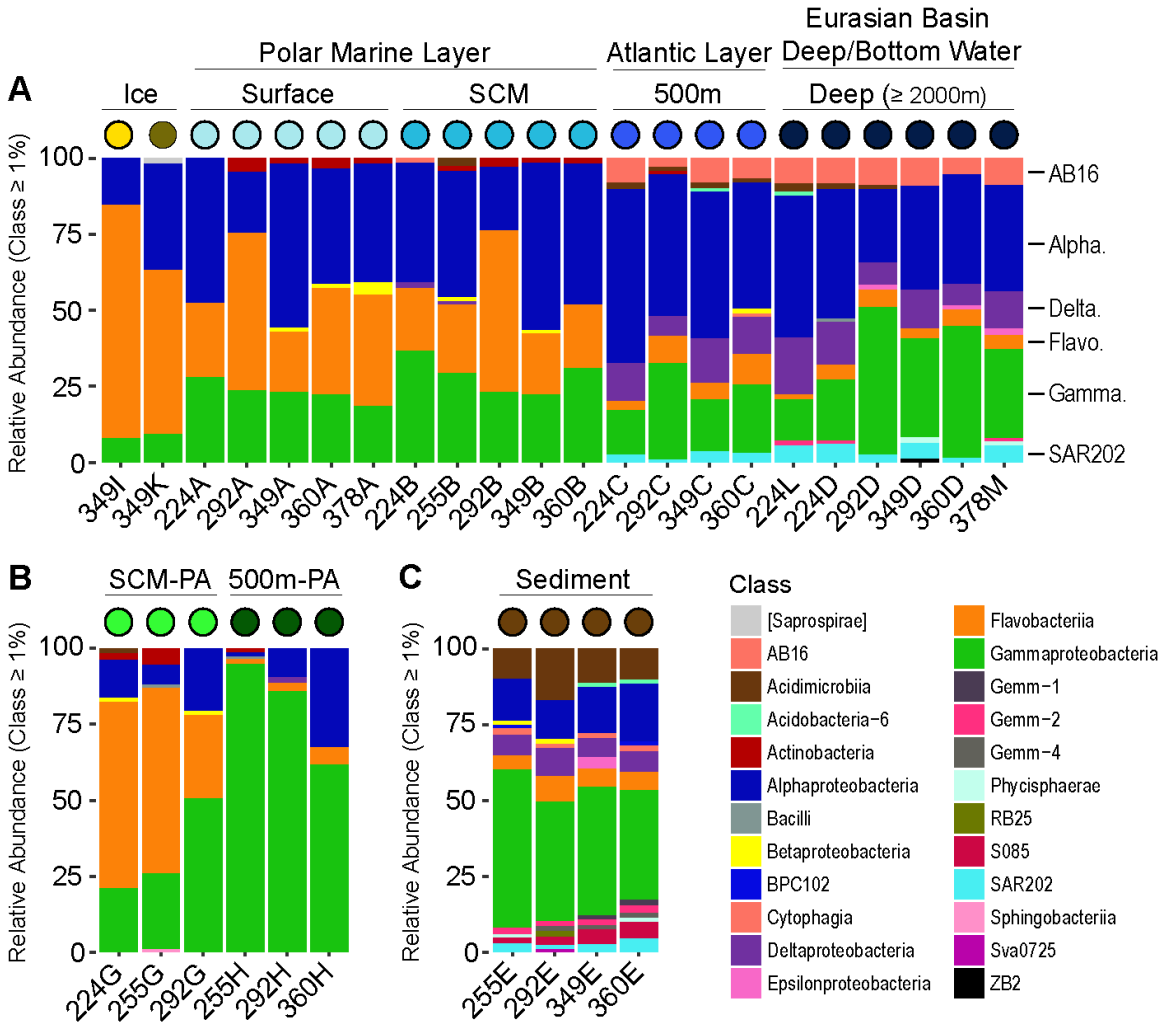

Figure 4. Peptidase hydrolysis rates for (A) bulk seawater samples, (B) ≥3μm particle-associated samples, and (C) surficial sediment samples. For (A) and (B), each stacked bar represents a rate averaged from triplicate incubation across three timepoints; for (C), each stacked bar represents a triplicate-averaged rate only from the first time point (1 h incubation). 'IF', 'FYI', and 'MYI' stand for Ice-Free, First Year ice, and Multi-Year Ice, respectively. Note the differences in scales and units.

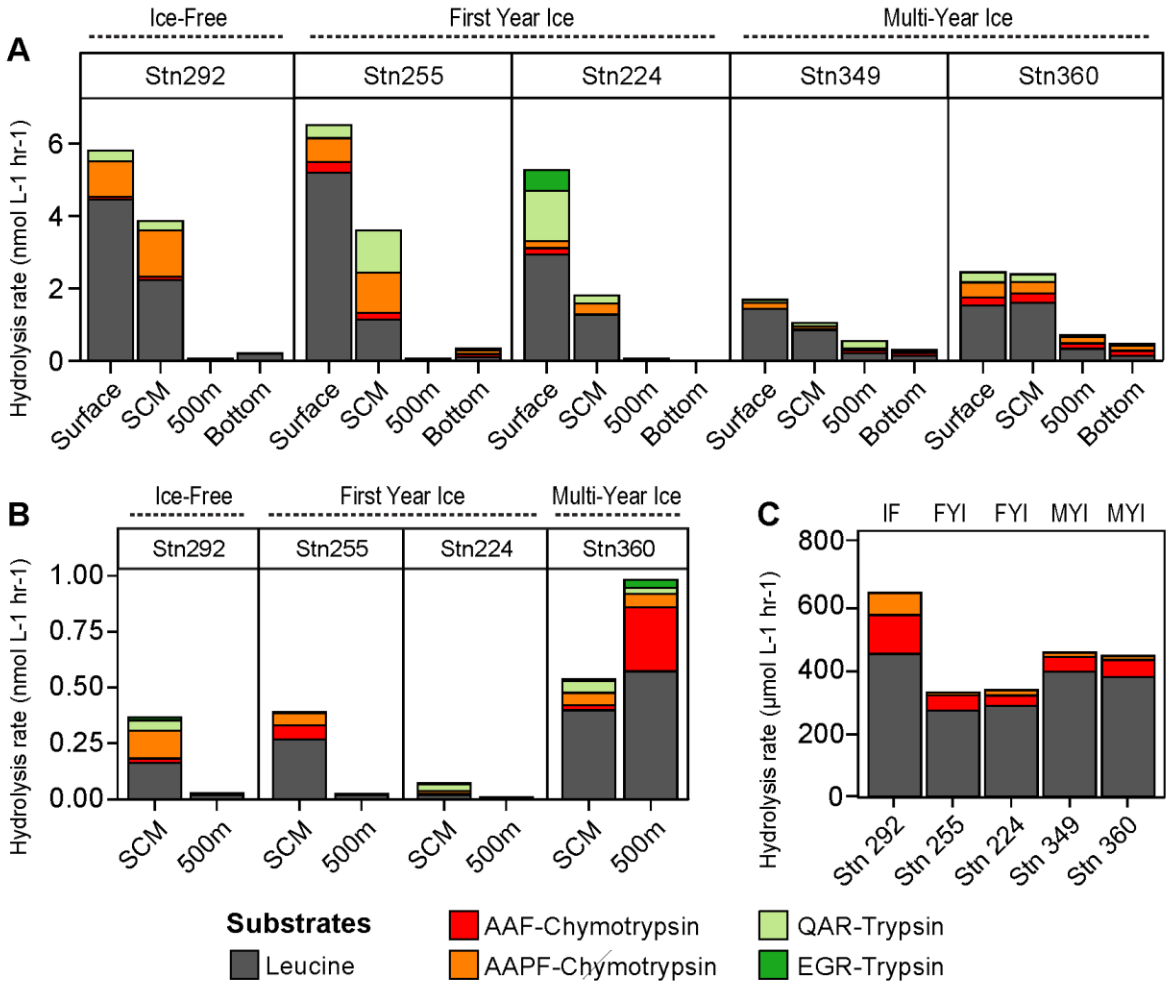

Figure 5. Polysaccharide hydrolase rate potentials for (A) bulk seawater samples, and (B) ≥3µm particle-associated samples. No data for sediment samples are available. Reported rates are the maximum rates calculated throughout the incubation. Note the differences in scale between (A) and (B).

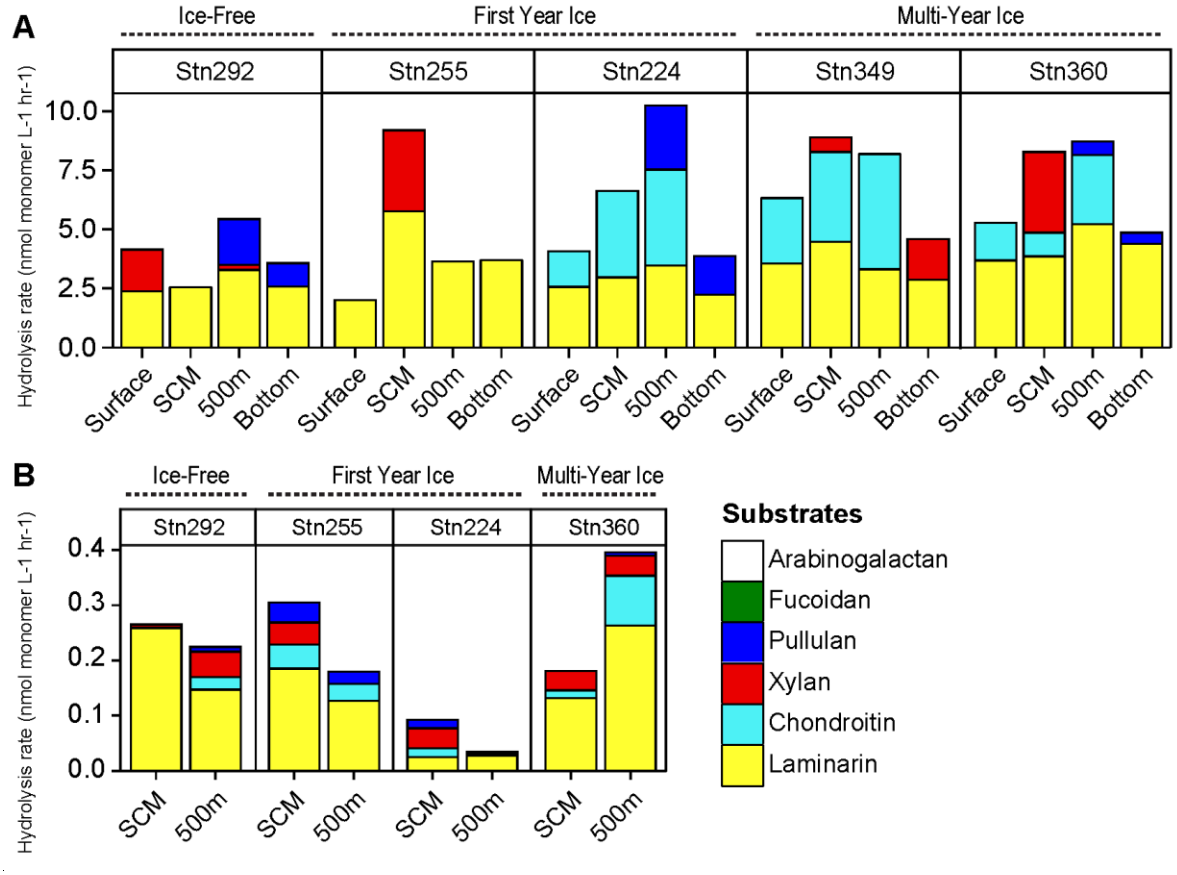

Table 1. List of samples, stations, available data, and physical parameters. BCC is an abbreviation for bacterial community composition; (+) indicates the presence of BCC data for the sample. EEA is an abbreviation for extracellular enzymatic activity; 'pep' indicates peptidase activity measurements, while 'poly' indicates polysaccharide hydrolase rate measurements. DCM-PA and 500m-PA are the particle-associated samples for the DCM and 500 m depths. Temperature, salinity and oxygen values for DCM-PA, 500m-PA and sediments were obtained from the DCM, 500 m, and bottom water values, respectively; bottom water samples are those with 'D' in the Sample column.

Sample name	Latitude (°N)	Longitude (°N)	Sample type	Depth (m)	BCC	EEA	T (°C)	S (PSU)	O2 (µmol/L)
224A	84.02	31.23	Surface	2	+	pep/poly	-1.5	33.4	389.7
224B	84.02	31.23	DCM	50	+	pep/poly	-1.8	34.2	387.9
224G	84.02	31.23	DCM-PA	50	+	pep/poly	-1.8	34.2	387.9
224C	84.02	31.23	500m	500	+	pep/poly	1.2	34.9	315.8
224H	84.02	31.23	500m-PA	500	na	pep/poly	1.2	34.9	315.8
224L	84.02	31.23	Deep	2000	+	na	-0.7	34.9	303.6
224D	84.02	31.23	Deep	3994	+	pep/poly	-0.7	34.9	303.6
224E	84.02	31.23	Sediment	4014	na	poly	-0.7	34.9	303.6
255A	82.71	109.14	Surface	1	na	pep/poly	-1.6	32.8	396.6
255B	82.71	109.14	DCM	23	+	pep/poly	-1.7	33.4	395.3
255G	82.71	109.14	DCM-PA	23	+	pep/poly	-1.7	33.4	395.3
255C	82.71	109.14	500m	500	na	pep/poly	1.1	34.9	316.3
255H	82.71	109.14	500m-PA	500	+	pep/poly	1.1	34.9	316.3
255D	82.71	109.14	Deep	3548	na	pep/poly	-0.7	34.9	303.9
255E	82.71	109.14	Sediment	3569	+	poly	-0.7	34.9	303.9
292A	79.65	130.58	Surface	3	+	pep/poly	0.3	29.9	380.3
292B	79.65	130.58	DCM	18	+	pep/poly	-1.3	31.2	384.3
292G	79.65	130.58	DCM-PA	18	+	pep/poly	-1.3	31.2	384.3
292C	79.65	130.58	500 m	500	+	pep/poly	0.7	34.9	318.9
292H	79.65	130.58	500m-PA	500	+	pep/poly	0.7	34.9	318.9
292D	79.65	130.58	Deep	3365	+	pep/poly	-0.7	34.9	303.7
292E	79.65	130.58	Sediment	3385	+	poly	-0.7	34.9	303.7
349I	87.92	60.94	Melt Pond	Ice	+	na	na	na	na
349K	87.92	60.94	Aggregate*	Ice	+	na	na	na	na
349A	87.92	60.94	Surface	1	+	pep/poly	-1.8	33.1	405.6
349B	87.92	60.94	DCM	14	+	pep/poly	-1.8	33.1	408.1
349C	87.92	60.94	500 m	500	+	pep/poly	0.7	34.9	317.5
349D	87.92	60.94	Deep	4300	+	pep/poly	-0.6	34.9	304.3

349E	87.92	60.94	Sediment	4380	+	poly	-0.6	34.9	304.3
360A	88.81	57.25	Surface	1	+	pep/poly	-1.8	33.0	413.4
360B	88.81	57.25	DCM	20	+	pep/poly	-1.8	33.0	414.0
360G	88.81	57.25	DCM-PA	20	na	pep/poly	-1.8	33.0	414.0
360C	88.81	57.25	500 m	500	+	pep/poly	0.7	34.9	318.0
360H	88.81	57.25	500m-PA	500	+	pep/poly	0.7	34.9	318.0
360D	88.81	57.25	Deep	4350	+	pep/poly	-0.6	34.9	304.7
360E	88.81	57.25	Sediment	4378	+	pep/poly	-0.6	34.9	304.7
378A	86.88	52.29	Surface	3	+	na	-1.8	33.1	400.3
378M	86.88	52.29	Deep	4850	+	na	-0.6	34.9	304.2

2.7 Supplementary Materials

Figure S1. Temperature and salinity plots of the stations with complete or near-complete depth profiles of community composition and enzymatic activities. Water masses are delineated. Details on Arctic Ocean water mass properties can be found in Stein and Macdonald (2004).

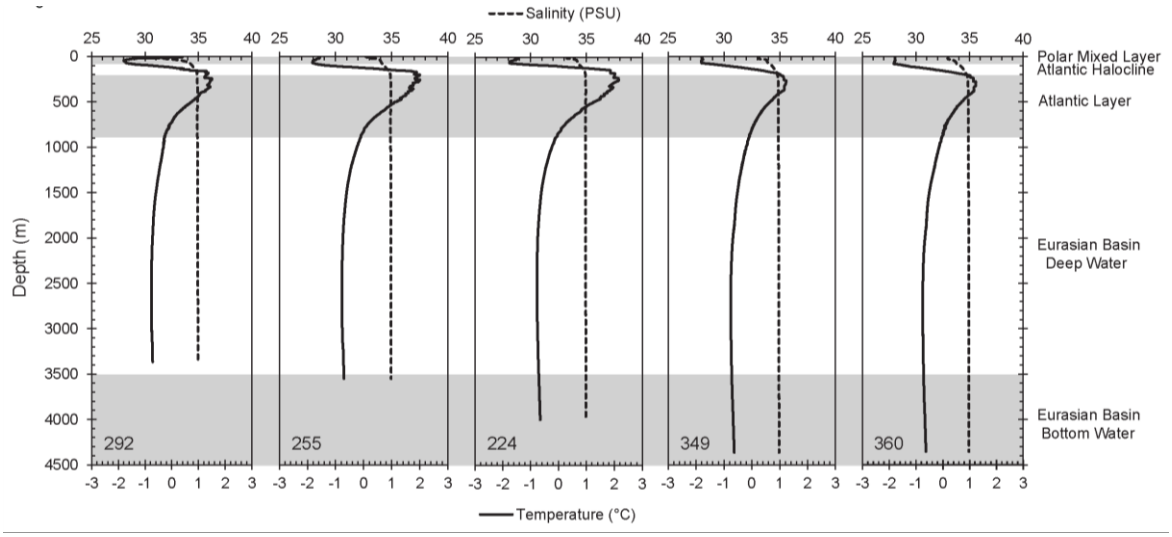

Figure S2. Bacterial community diversity, including (A) OTU richness, (B) Faith's Phylogenetic Diversity, and (C) OTU evenness using Shannon Diversity. Sequence dataset for each sample was rarefied to 22,000 sequences.

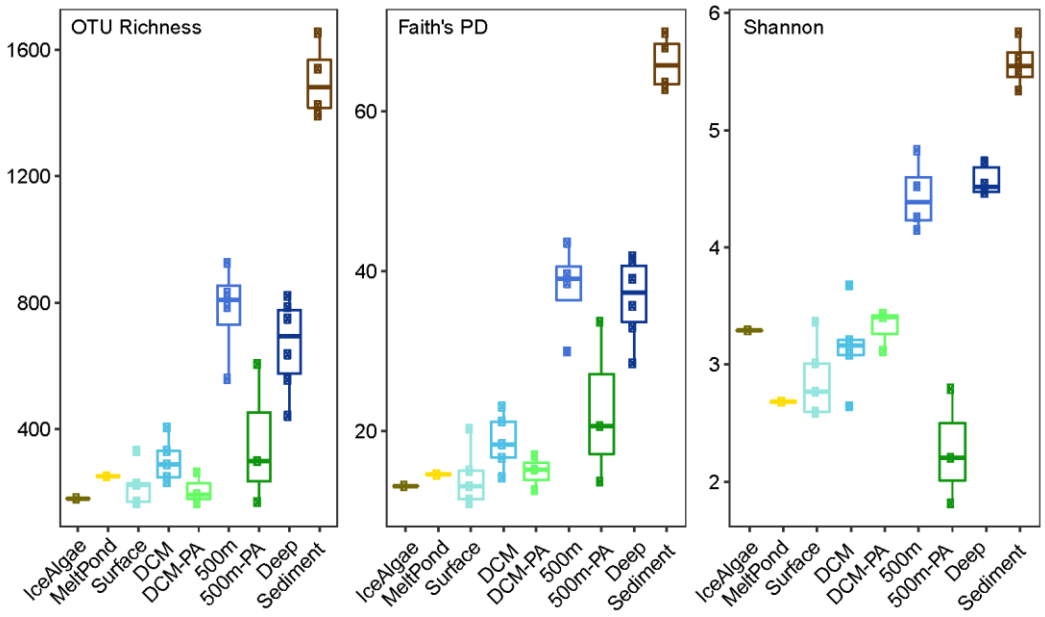

Figure S3. *Polaribacter* Maximum Likelihood phylogenetic tree. Abundant *Polaribacter* OTUs were chosen for phylogenetic analysis using nearly full-length 16S rRNA gene sequences of cultured representatives and clones that are closely related to select OTUs. Phylogenetic trees were inferred using Rapid Analysis Maximum Likelihood (RAxML) on ARB software version 95 (Ludwig *et al*., 2004), implementing the general time-reversible gamma distributed rate variation model (GTRGAMMA) algorithm. Sequences for the select abundant OTUs from this dataset were aligned using SILVA online (Pruesse *et al*., 2007), uploaded into ARB, and inserted into the RAxML tree using the filters that correspond to *E. coli* position 1036-6418. The most abundant sequences found on particles in the SCM are indicated by the light green circles.

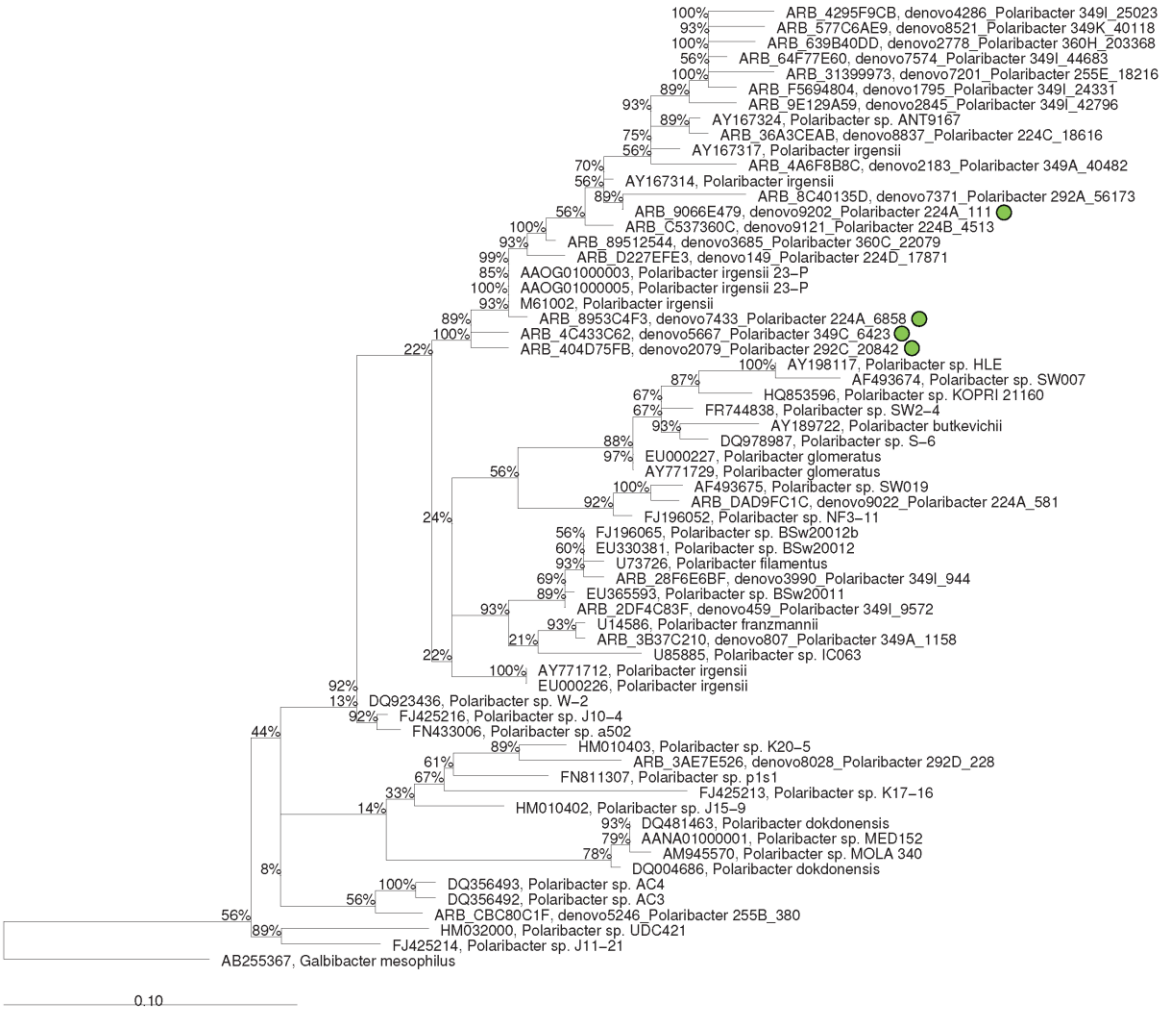

Figure S4. Family-level breakdown of (A) Gammaproteobacteria and (B) Alphaproteobacteria. Only the families with relative proportions of ≥1% are shown in the bar graphs. Square brackets around bacterial class indicate recommended taxonomic nomenclature based on genome trees in the Greengenes database.

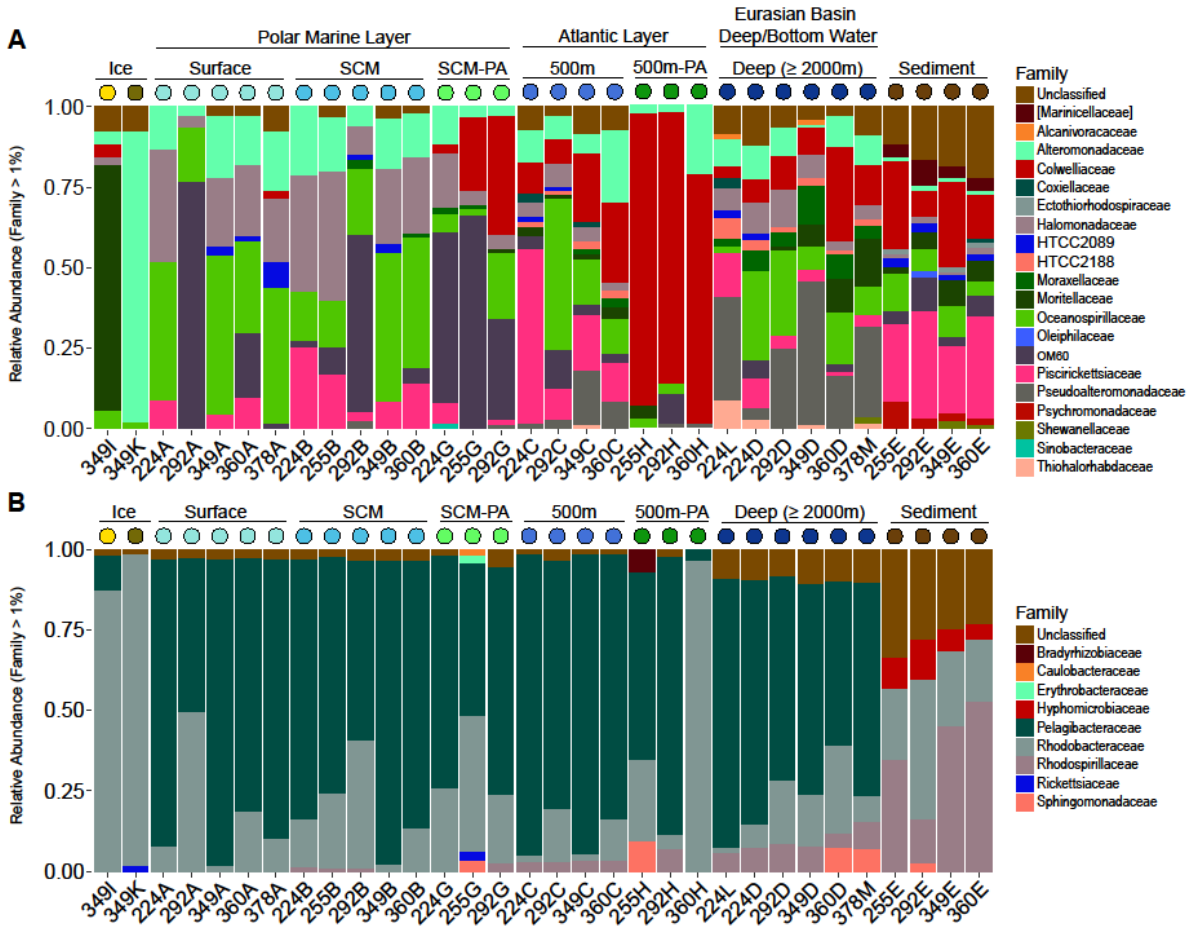

Figure S5. *Colwellia* Maximum Likelihood phylogenetic tree. Abundant *Colwellia* OTUs were chosen for phylogenetic analysis using nearly full-length 16S rRNA gene sequences of cultured representatives and clones that are closely related to select OTUs. Phylogenetic trees were inferred using Rapid Analysis Maximum Likelihood (RAxML) on ARB software version 95 (Ludwig *et al*., 2004), implementing the general time-reversible gamma distributed rate variation model (GTRGAMMA) algorithm. Sequences for the select abundant OTUs from this dataset were aligned using SILVA online (Pruesse *et al*., 2007), uploaded into ARB, and inserted into the RAxML tree using the filters that correspond to *E. coli* position 1036-6418. The most abundant sequences found on particles in at 500 m are indicated by the dark green circles.

[Figure S5 is in the next page]

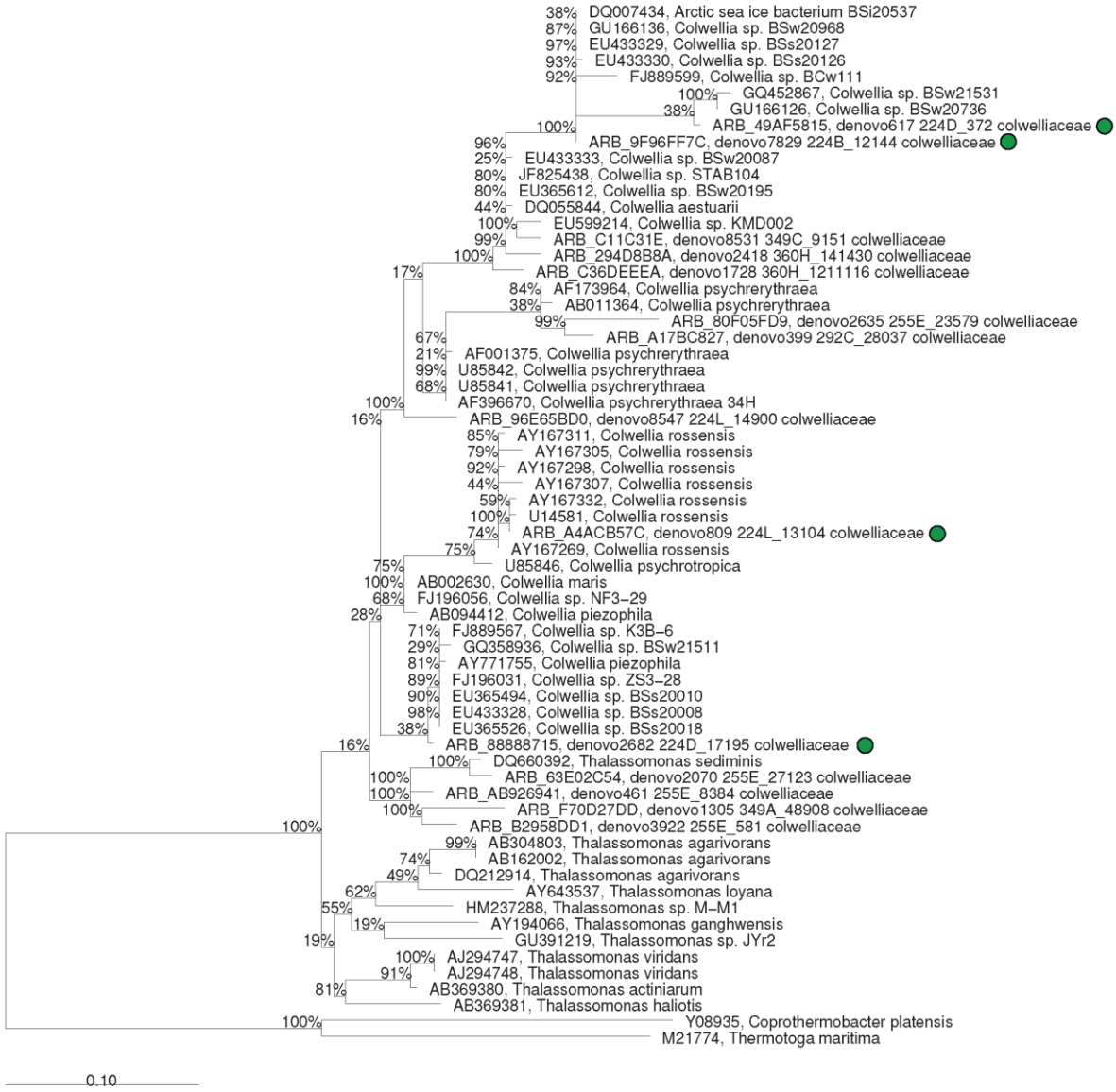
38% DQ007434, Arctic sea ice bacterium BSi20537
87% GU166136, Colwellia sp. BSw20968
97% EU433329, Colwellia sp. BSs20127
93% EU433330, Colwellia sp. BSs20126
92% FJ889599, Colwellia sp. BCw111
100% GQ452867, Colwellia sp. BSw21531
38% GU166126, Colwellia sp. BSw20736
100% ARB_49AF5815, denovo617 224D_372 colwelliaceae
96% ARB_9F96FF7C, denovo7829 224B_12144 colwelliaceae
25% EU433333, Colwellia sp. BSw20087
80% JF825438, Colwellia sp. STAB104
80% EU365612, Colwellia sp. BSw20195
44% DQ055844, Colwellia aestuarii
100% EU599214, Colwellia sp. KMD002
99% ARB_C11C31E, denovo8531 349C_9151 colwelliaceae
100% ARB_294D8B8A, denovo2418 360H_141430 colwelliaceae
17% ARB_C36DEEEA, denovo1728 360H_1211116 colwelliaceae
84% AF173964, Colwellia psychrerythraea
38% AB011364, Colwellia psychrerythraea
99% ARB_80F05FD9, denovo2635 255E_23579 colwelliaceae
67% ARB_A17BC827, denovo399 292C_28037 colwelliaceae
21% AF001375, Colwellia psychrerythraea
99% U85842, Colwellia psychrerythraea
68% U85841, Colwellia psychrerythraea
100% AF396670, Colwellia psychrerythraea 34H
16% ARB_96E65BD0, denovo8547 224L_14900 colwelliaceae
85% AY167311, Colwellia rossensis
79% AY167305, Colwellia rossensis
92% AY167298, Colwellia rossensis
44% AY167307, Colwellia rossensis
59% AY167332, Colwellia rossensis
100% U14581, Colwellia rossensis
74% ARB_A4ACB57C, denovo809 224L_13104 colwelliaceae
75% AY167269, Colwellia rossensis
75% U85846, Colwellia psychrotropica
100% AB002630, Colwellia maris
68% FJ196056, Colwellia sp. NF3−29
28% AB094412, Colwellia piezophila
71% FJ889567, Colwellia sp. K3B−6
29% GQ358936, Colwellia sp. BSw21511
81% AY771755, Colwellia piezophila
89% FJ196031, Colwellia sp. ZS3−28
90% EU365494, Colwellia sp. BSs20010
98% EU433328, Colwellia sp. BSs20008
38% EU365526, Colwellia sp. BSs20018
16% ARB_88888715, denovo2682 224D_17195 colwelliaceae
100% DQ660392, Thalassomonas sediminis
100% ARB_63E02C54, denovo2070 255E_27123 colwelliaceae
100% ARB_AB926941, denovo461 255E_8384 colwelliaceae
100% ARB_F70D27DD, denovo1305 349A_48908 colwelliaceae
100% ARB_B2958DD1, denovo3922 255E_581 colwelliaceae
99% AB304803, Thalassomonas agarivorans
74% AB162002, Thalassomonas agarivorans
49% DQ212914, Thalassomonas agarivorans
62% AY643537, Thalassomonas loyana
55% HM237288, Thalassomonas sp. M−M1
19% AY194066, Thalassomonas ganghwensis
19% GU391219, Thalassomonas sp. JYr2
100% AJ294747, Thalassomonas viridans
91% AJ294748, Thalassomonas viridans
81% AB369380, Thalassomonas actiniarum
AB369381, Thalassomonas haliotis
100% Y08935, Coprothermobacter platensis
M21774, Thermotoga maritima
0.10

Figure S6. Conceptual representation of microbial communities and enzyme activities in the central Arctic Ocean. The three images show the different sea-ice conditions investigated in this study: seasonally ice-free, partially covered with first year ice, and fully covered with multi-year ice; the images were taken during the research expedition. On the left, the Bray-Curtis dissimilarity dendrogram for bacterial communities is colored to indicate the water masses from which the samples within each cluster originate: PML stands for Polar Mixed Layer, Atlantic is for Atlantic Layer. The colored circles in the dendrogram indicate the type(s) of samples found within that cluster; the circles follow the same depth- and sample type-related color code as in Figure 2 and 3. Yellow and red dashed lines qualitatively depict summed bulk water peptidase and polysaccharide hydrolase activities, respectively, for each sea ice condition. Scale differences of several orders of magnitude between summed benthic and bulk water peptidase activities are accommodated by hash marks. The image of the sea-ice algae aggregate trapped in a sediment core was taken at Stn. 360, and is reproduced from Boetius et al., 2013. Depth is not drawn to scale.

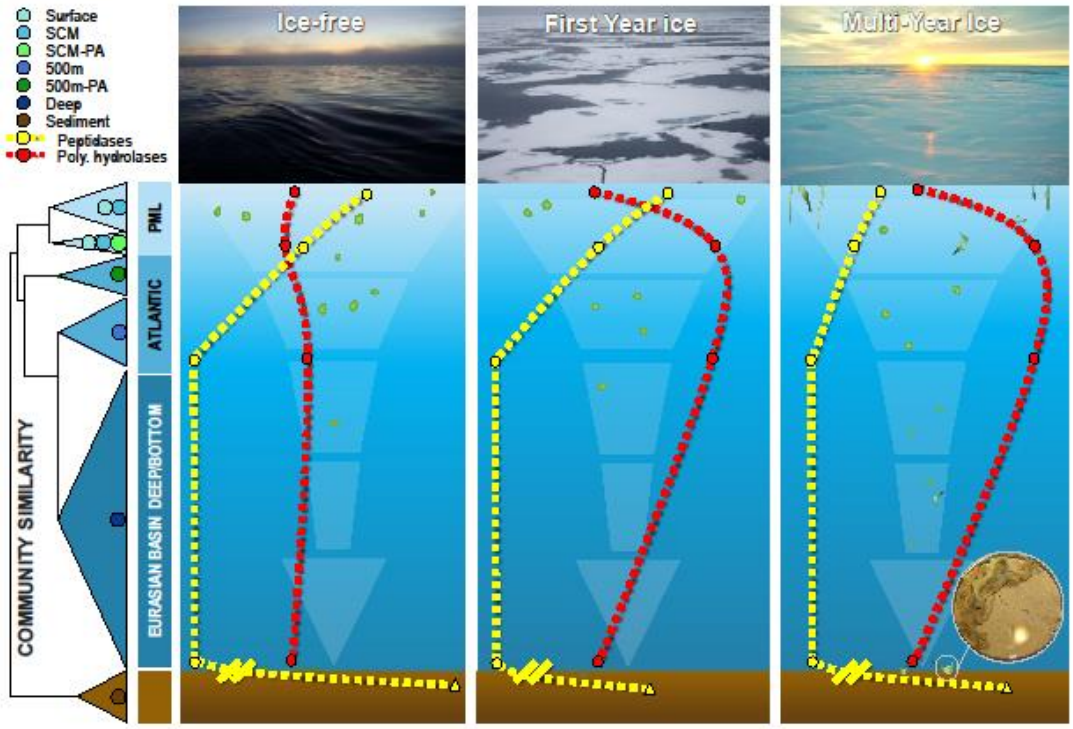

Figure S7. Time course polysaccharide hydrolysis rates for (A) bulk water and (B) particles.

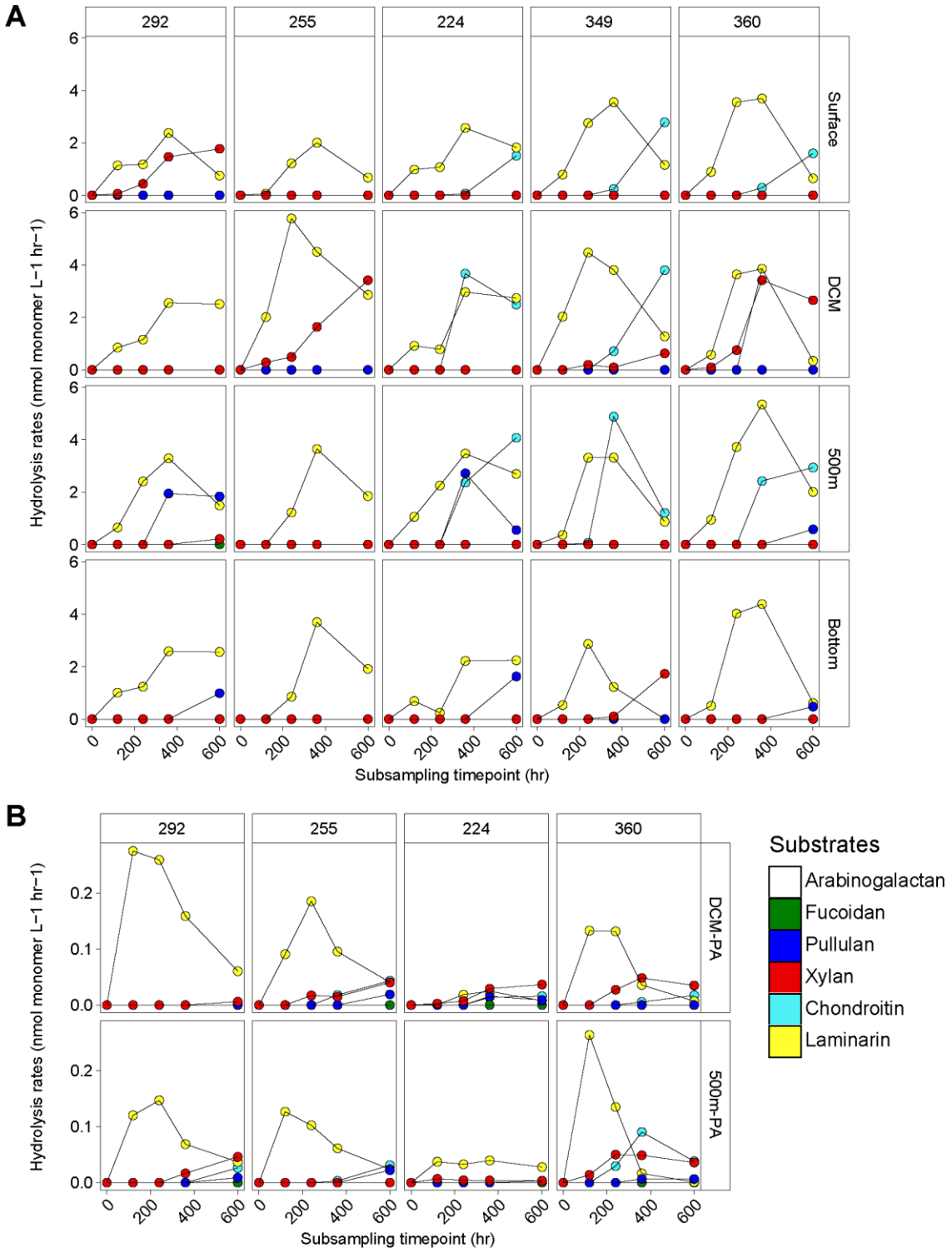

Table S1. Multivariate homogeneity of group dispersions. Samples from the sea-ice (melt pond and algal aggregate) were not included in the analysis. The highest value in is italicized, while the lowest value is bolded.

	Dispersion
Surface	0.265
DCM	0.257
DCM Particles	0.315
500 m	0.25
500 m Particles	*0.338*
Deep	0.278
Sediment	**0.222**

REFERENCES

Alonso-Sáez, L., Zeder, M., Harding, T., Pernthaler, J., Lovejoy, C., Bertilsson, S., *et al.* (2014). Winter bloom of a rare betaproteobacterium in the Arctic Ocean. *Front Microbiol* **5**: 425.

Arnosti, C. (2003). Fluorescent derivatization of polysaccharides and carbohydrate-containing biopolymers for measurement of enzyme activities in complex media. *J Chromatogr B* **793**: 181-191.

Arnosti, C. (2011). Microbial extracellular enzymes and the marine carbon cycle. *Annu Rev Mar Sci* **3**: 401-425.

Arnosti, C., Steen, A.D., Ziervogel, K., Ghobrial, S., Jeffrey, W.H. (2011). Latitudinal gradients in degradation of marine dissolved organic carbon. *PLoS One* **6**: e28900.

Arnosti, C. (2015). Contrasting patterns of peptidase activities in seawater and sediments: An example from Arctic fjords of Svalbard. *Mar Chem* **168**: 151-156.

Bano, N., Hollibaugh, J.T. (2002). Phylogenetic composition of bacterioplankton assemblages from the Arctic Ocean. *Appl Environ Microbiol* **68**: 505-518.

Bienhold, C., Boetius, A., Ramette, A. (2012). The energy-diversity relationship of complex bacterial communities in Arctic deep-sea sediments. *ISME J* **6**: 724-732.

Boetius, A., Lochte, K. (1996). Effect of organic enrichments on hydrolytic potentials and growth of bacteria in deep-sea sediments. *Mar Ecol Prog Ser* **140**: 239-250.

Boetius, A., Damm, E.. (1998). Benthic oxygen uptake, hydrolytic potentials and microbial biomass at the Arctic continental slope. *Deep Sea Res Part I* **45**: 239-275.

Boetius, A., Albrecht, S., Bakker, K., Bienhold, C., Felden, J., Fernandez-Mendez, M. *et al*. (2013). Export of algal biomass from the melting Arctic sea ice. *Science* **339**: 1430-1432.

Boetius, A., Anesio, A.M., Deming, J.W., Mikucki, J.A., Rapp, J.Z. (2015). Microbial ecology of the cryosphere: sea ice and glacial habitats. *Nat Rev Microbiol* **13**: 677-690.

Bong, C.W., Obayashi, Y., Suzuki, S. (2013). Succession of protease activity in seawater and bacterial isolates during starvation in a mesocosm experiment. *Aquat Microb Ecol* **69**: 33-46.

Buchan, A., LeCleir, G.R., Gulvik, C.A., Gonzalez, J.M. (2014). Master recyclers: features and functions of bacteria associated with phytoplankton blooms. *Nat Rev Microbiol* **12**: 686-698.

Buttigieg, P.L., Ramette, A. (2015). Biogeographic patterns of bacterial microdiversity in Arctic deep-sea sediments (HAUSGARTEN, Fram Strait). *Front Microbiol* **5**: 1.

Chase, J.M. (2010). Stochastic community assembly causes higher biodiversity in more productive environments. *Science* **328**: 1388-1391.

Comeau, A.M., Li, W.K.W., Tremblay. J.É., Carmack, E.C., Lovejoy, C. (2011). Arctic Ocean microbial mommunity structure before and after the 2007 record sea ice minimum. *PLoS One* **6**: e27492.

Comte, J., Fauteux, L., del Giorgio, P.A.. (2013). Links between metabolic plasticity and functional redundancy in freshwater bacterioplankton communities. *Front Microbiol* **4**: 112.

D'Ambrosio, L., Ziervogel, K., MacGregor, B., Teske, A., Arnosti, C. (2014). Composition and enzymatic function of particle-associated and free-living bacteria: a coastal/offshore comparison. *ISME J* **8**: 2167-2179.

Dang, H., Li, T., Chen, M., Huang, G. (2008). Cross-ocean distribution of *Rhodobacterales* bacteria as primary surface colonizers in temperate coastal marine waters. *Appl Environ Microbiol* **74**: 52-60.

Dang, H., Lovell, C.R. (2016). Microbial surface colonization and biofilm development in marine environments. *Microbiol Mol Biol Rev* **80**: 91-138.

Delong, E.F., Franks, D.G., Alldredge, A.L. (1993). Phylogenetic diversity of aggregate-attached vs free-living marine bacterial assemblages. *Limnol Oceanogr* **38**: 924-934.

Eloe, E.A., Shulse, C.N., Fadrosh, D.W., Williamson, S.J., Allen, E.E., Bartlett, D.H. (2011). Compositional differences in particle-associated and free-living microbial assemblages from an extreme deep-ocean environment. *Environ Microbiol Rep* **3**: 449-458.

Fernández-Méndez, M., Katlein, C., Rabe, B., Nicolaus, M., Peeken, I., Bakker, K., *et al*. (2015). Photosynthetic production in the central Arctic Ocean during the record sea-ice minimum in 2012. *Biogeosciences* **12**: 3525-3549.

Fu YY, Keats KF, Rivkin RB, Lang AS. (2013). Water mass and depth determine the distribution and diversity of *Rhodobacterales* in an Arctic marine system. *FEMS Microbiol Ecol* **84**: 564-576.

Galand, P.E., Potvin, M., Casamayor, E.O., Lovejoy, C. (2010). Hydrography shapes bacterial biogeography of the deep Arctic Ocean. *ISME J* **4**: 564-576.

Ghiglione, J.F., Galand, P.E., Pommier, T., Pedros-Alio, C., Maas, E.W., Bakker K *et al.* (2012). Pole-to-pole biogeography of surface and deep marine bacterial communities. *Proc ANatl Acad Sci USA* **109**: 17633-17638.

Gram, L., Grossart, H.P., Schlingloff, A., Kiørboe, T. (2002). Possible quorum sensing in marine snow bacteria: Production of acylated homoserine lactones by *Roseobacter* strains isolated from marine snow. *Appl Environ Microbiol* **68**: 4111-4116.

Haas, B.J., Gevers, D., Earl, A.M., Feldgarden, M., Ward, D.V., Giannoukos, G., *et al*., (2011). Chimeric 16S rRNA sequence formation and detection in Sanger and 454-pyrosequenced PCR amplicons. *Genome Res* **21**: 494-504.

Hamdan, L.J., Coffin, R.B., Sikaroodi, M., Greinert, J., Treude, T., Gillevet, P.M. (2013). Ocean currents shape the microbiome of Arctic marine sediments. *ISME J* **7**: 685-696.

Han, D., Ha, H.K., Hwang, C.Y., Lee, B.Y., Hur, H.G., Lee, Y.K. (2015). Bacterial communities along stratified water columns at the Chukchi Borderland in the western Arctic Ocean. *Deep Sea Res Part II* **120**: 52-60.

Jacob, M., Soltwedel, T., Boetius, A., Ramette, A. (2013). Biogeography of deep-sea benthic bacteria at regional scale (LTER HAUSGARTEN, Fram Strait, Arctic). *PLoS One* **8**: e72779.

Jing, H., Xia, X., Suzuki, K., Liu, H. (2013). Vertical profiles of bacteria in the tropical and subarctic oceans revealed by pyrosequencing. *PLoS One* **8**: e79423.

Kellogg, C.T.E., Deming, J.W. (2009). Comparison of free-living, suspended particle, and aggregate-associated bacterial and archaeal communities in the Laptev Sea. *Aquat Microb Ecol* **57**: 1-18.

Kellogg, C.T.E., Deming, J.W. (2014). Particle-associated extracellular enzyme activity and bacterial community composition across the Canadian Arctic Ocean. *FEMS Microbiol Ecol* **89**: 360-375.

Kirchman, D.L., Moran, X.A.G., Ducklow, H. (2009). Microbial growth in the polar oceans - role of temperature and potential impact of climate change. *Nat Rev Microbiol* **7**: 451-459.

Kirchman, D.L., Cottrell, M.T., Lovejoy, C. (2010). The structure of bacterial communities in the western Arctic Ocean as revealed by pyrosequencing of 16S rRNA genes. *Environ Microbiol* **12**: 1132-1143.

Lee, C., Wakeham, S.G., Hedges, J.I. (2000). Composition and flux of particulate amino acids and chloropigments in equatorial Pacific seawater and sediments. *Deep Sea Res Part I* **47**: 1535-1568.

Lozupone, C.A., Knight, R. (2007). Global patterns in bacterial diversity. *Proc Natl Acad Sci USA* **104**: 11436-11440.

Obayashi, Y., Suzuki, S. (2005). Proteolytic enzymes in coastal surface seawater: Significant activity of endopeptidases and exopeptidases. *Limnol Oceanogr* **50**: 722-726.

Obayashi, Y., Suzuki, S. (2008). Occurrence of exo- and endopeptidases in dissolved and particulate fractions of coastal seawater. *Aquat Microb Ecol* **50**: 231-237.

Oksanen, J., Blanchet, F.G., Kindt, R., Legendre, P., Minchin, P.R., O'Hara, *et al*. (2008). vegan: Community Ecology Package. R package version 2.4-3.

McMurdie, P.J., Holmes, S. (2013). phyloseq: An R package for reproducible interactive analysis and graphics of microbiome census data. *PLoS One* **8:** e61217.

Pedrós-Alió, C., Brock, T.D. (1983). The importance of attachment to particles for planktonic bacteria. *Arch Hydrobiol* **98**: 354-379.

Polymenakou, P.N., Lampadariou, N., Tselepides, A. (2008). Exo-enzymatic activities and organic matter properties in deep-sea canyon and slope systems off the southern Cretan margin. *Deep Sea Res Part I* **55**: 1318-1329.

Rabe, B., Wisotzki, A., Rettig, S., Somavilla-Cabrillo, R., Sander, H. (2013). Physical oceanography measured on water bottle samples during POLARSTERN cruise ARK-XXVII/3 (IceArc). *Alfred Wegener Institute, Helmholtz Center for Polar and Marine Research, Bremerhaven,* doi: 10.1594/PANGAEA.819452.

Rapp, J.Z., Fernández-Méndez, M., Bienhold, C., Boetius, A. From sea ice to the deep sea: Effects of ice-algal aggregate export on the connectivity of bacterial core communities in the central Arctic Ocean. *Submitted.*

Reed, H.E., Martiny, J.B.H. (2007). Testing the functional significance of microbial composition in natural communities. *FEMS Microbiol Ecol* **62**: 161-170.

Sala, M.M., Arrieta, J.M., Boras, J.A., Duarte, C.M., Vaqué, D. (2010). The impact of ice melting on bacterioplankton in the Arctic Ocean. *Polar Biol* **33**: 1683-1694.

Salazar, G., Cornejo-Castillo, F.M., Borrull, E., Díez-Vives, C, Lara, E., Vaqué, D., *et al*. (2015). Particle-association lifestyle is a phylogenetically conserved trait in bathypelagic prokaryotes. *Mol Ecol* **24**: 5692-5706.

Smith, M., Zeigler-Allen L., Allen, A., Herfort, L., Simon, H. (2013). Contrasting genomic properties of free-living and particle-attached microbial assemblages within a coastal ecosystem. *Front Microbiol* **4**: 120.

Steen, A.D., Arnosti, C. (2013). Extracellular peptidase and carbohydrate hydrolase activities in an Arctic fjord (Smeerenburgfjord, Svalbard). *Aquat Microb Ecol* **69**: 93-99.

Steen, A.D., Vazin, J.P., Hagen, S.M., Mulligan, K.H., Wilhelm, S.W. (2015). Substrate specificity of aquatic extracellular peptidases assessed by competitive inhibition assays using synthetic substrates. *Aquat Microb Ecol* **75**: 271-281.

Stein, R., Macdonald, R.W. (2004). *The organic carbon cycle in the Arctic Ocean*. Springer: Berlin; New York.

Strickland, M.S., Lauber, C., Fierer, N., Bradford, M.A. (2009). Testing the functional significance of microbial community composition. *Ecology* **90**: 441-451.

Sunagawa, S., Coelho, L.P., Chaffron, S., Kultima, J.R., Labadie, K., Salazar, G., *et al*. (2015). Structure and function of the global ocean microbiome. *Science* **348**: 1261359.

Tamelander, T. (2013). Community composition and extracellular enzyme activity of bacteria associated with suspended and sinking particles in contrasting arctic and sub-arctic marine environments. *Aquat Microb Ecol* **69**: 211-221.

Teeling, H., Fuchs, B.M., Becher, D., Klockow, C., Gardebrecht, A., Bennke, C.M., *et al*. (2012). Substrate-controlled succession of marine bacterioplankton populations induced by a phytoplankton bloom. *Science* **336**: 608-611.

Teske, A., Durbin, A., Ziervogel, K., Cox, C., Arnosti, C. (2011). Microbial community composition and function in permanently cold seawater and sediments from an Arctic fjord of Svalbard. *Appl Environ Microbiol* **77**: 2008-2018.

Thiele, S., Fuchs, B.M., Amann, R., Iversen, M.H. (2015). Colonization in the photic zone and subsequent changes during sinking determine bacterial community composition in marine snow. *Appl Environ Microbiol* **81**: 1463-1471.

Vetter, Y.A., Deming, J.W., Jumars, P.A., Krieger-Brockett, B.B. (1998). A predictive model of bacterial foraging by means of freely released extracellular enzymes. *Microb Ecol* **36**: 75-92.

Wassmann, P. (2011). Arctic marine ecosystems in an era of rapid climate change. *Prog Oceanogr* **90**: 1-17.

Williams, T.J., Wilkins, D., Long, E., Evans, F., DeMaere, M.Z., Raftery, M.J., *et al*. (2013). The role of planktonic *Flavobacteria* in processing algal organic matter in coastal East Antarctica revealed using metagenomics and metaproteomics. *Environ Microbiol* **15**: 1302-1317.

Wilson, B., Müller, O., Nordmann, E.L., Seuthe, L., Bratbak, G., Øvreås, L. (2017). Changes in marine prokaryote composition with season and depth over an Arctic polar year. *Front Mar Sci* **4**: 95.

Winter, C., Matthews, B., Suttle, C.A. (2013). Effects of environmental variation and spatial distance on bacteria, archaea and viruses in sub-polar and arctic waters. *ISME J* **7**: 1507-1518.

Xing, P., Hahnke, R.L., Unfried, F., Markert, S., Huang, S., Barbeyron, T., *et al*. (2015). Niches of two polysaccharide-degrading *Polaribacter* isolates from the North Sea during a spring diatom bloom. *ISME J* **9**: 1410-1422.

Ziervogel, K., Arnosti, C.. (2008). Polysaccharide hydrolysis in aggregates and free enzyme activity in aggregate-free seawater from the north-eastern Gulf of Mexico. *Environ Microbiol* **10**: 289-299.

Zinger, L., Amaral-Zettler, L.A., Fuhrman, J.A., Horner-Devine, M.C., Huse, S.M., Welch, D.B.M., *et al*. (2011). Global patterns of bacterial beta-diversity in seafloor and seawater ecosystems. *PLoS One* **6**: e24570.

CHAPTER 3: INTRINSIC AND EXTRINSIC INFLUENCES ON MICROBIAL HYDROLYSIS OF ORGANIC MATTER ALONG A RIVER-TO-FJORD CONTINUUM IN NE GREENLAND

3.1 Introduction

Coastal microbial communities in high latitudes are exposed to organic matter sourced from autochthonous primary production, coastal water inflow, and glacial and terrestrial runoff (Hood et al. 2009; Fellman et al. 2010; Paulsen et al. 2017). Autochthonous organic matter, especially nitrogen-rich components (Osterholz et al. 2014), can be mineralized rapidly by pelagic microbial communities. In contrast, organic matter from coastal water inflow—sourced from the heavily river-influenced Arctic Ocean—has a strong terrestrial signature (Amon et al. 2003), and is considered to be relatively resistant to microbial remineralization (Paulsen et al. 2017). However, a considerable fraction of relict organic material transported by glacial meltwater is, counterintuitively, efficiently degraded by coastal microbial communities (Hood et al. 2009). The nature and origin of organic matter in the Arctic Ocean thus affect its bioavailability.

In spite of the importance of microbially-driven carbon cycling, the factors that regulate the efficiency of carbon remineralization in fjords, especially at high latitudes, are poorly understood. Differences in organic matter bioavailability along river-to-fjord systems (Fellman et al. 2010; Lawson et al. 2014; Paulsen et al. 2017) suggest that differences in microbial community composition (Crump et al. 1999, Hewson and Fuhrman, 2004) exert controls on microbial carbon cycling. Furthermore, freshwater, estuarine, and marine microbial communities can differentially utilize the same organic matter pool (Fellman et al. 2010), indicating that intrinsic microbial properties may contribute to differences in carbon bioavailability and turnover. However, with few exceptions, the composition of microbial

communities in fjords (Zeng et al. 2009; Teske et al. 2011; Gutiérrez et al. 2015; Paulsen et al. 2017), and the factors that influence community structure (Stibal et al. 2015; Cameron et al. 2017; Dubnick et al. 2017), are not well characterized.

Moreover, little is known regarding the substrate preferences of microbial communities across salinity gradients (Stepanauskas et al. 1999; Eiler et al. 2014), and the extent to which these microbial attributes correlate with the quality of available DOM and community composition (Osterholz et al. 2017). Measurements of extracellular enzymatic activities—the initial step in organic matter breakdown—shed light on the substrate specificity of microbial communities (Arnosti, 2011), but only a limited number of these studies have been carried out in coastal environments, especially in fjords. The few measurements in fjords have shown different rates and range of enzymatic activities between surface versus bottom water microbial communities (Steen and Arnosti, 2013; Arnosti, 2015), which parallel differences in community composition (Teske et al. 2011; Cardman et al. 2014). Furthermore, compared to temperate oceans, microbial communities in high-latitude fjords apparently use a more limited spectrum of enzymatic capabilities based on substrates tested, potentially limiting their access to organic matter (Arnosti and Steen, 2014; Steen and Arnosti, 2014)

The role that organic and inorganic particles play in shaping microbial community composition and carbon remineralization is also understudied in high latitude fjords (Sperling et al. 2013; Osterholz et al. 2014). Particles can host bacterial communities with distinct composition (DeLong et al. 1993; Schmidt et al. 2015) and function (Fernandez-Gomez et al. 2013; D'Ambrosio et al. 2014) compared to their free-living counterparts. Furthermore, the composition of particle-associated bacterial communities differs in freshwater and marine systems (Crump et al. 1999; Ortega-Retuerta et al. 2013; Bižić-Ionescu et al. 2015). Analyses of sinking particulate matter and sediments in fjords show evidence of both terrestrial and marine origins (Rysgaard and Sejr, 2007; Bourgeois et al. 2016; Cui et al.

2017), suggesting that glacial discharge has the potential to shape microbial community structure in fjords through particle transport. High carbon burial rates in Arctic fjords (Glud et al. 1998; Smith et al. 2015; Sørensen et al. 2016) imply that particulate matter evades complete remineralization in surface waters, and ultimately sinks to the bottom of fjords, sustaining benthic heterotrophs. As microbially-mediated particulate matter transformations in the water column greatly affect the quantity and quality of carbon sources available to benthic heterotrophs, determining the identity and organic matter degrading capabilities of particle-attached microbes in these systems is also important.

In this study, we investigated the potential for microbial communities to access a range of organic substrates in Tyrolerfjord-Young Sound, a fjord in northeast Greenland. Increased glacial discharge from the Greenland Ice Sheet, measured over a decade (2003-2015), has resulted in the freshening of subsurface waters in this fjord (Sejr et al. 2017). However, the biogeochemical impacts of recent hydrological changes in this system—and, by extension, in similar fjord systems within the Arctic—remain elusive due to limited information on microbial communities and their activities. We hypothesized that bacterial community composition, enzymatic activity patterns, and DOM composition would vary strongly with salinity, a reflection of the different origins of water mass in these systems: glacial and terrestrial discharge transported to the fjord through rivers versus coastal inflow of Arctic Ocean-derived water. Additionally, we hypothesized that particles discharged from rivers—a relatively unexplored source of microbial diversity in high latitude fjords—would host bacterial communities with distinct composition and range of enzymatic capabilities compared to those on autochthonous particles in the fjord. Investigating microbial communities and their heterotrophic activities in this system elucidates the processes governing carbon turnover in the high Arctic. These insights are necessary as ongoing climatic change in the Arctic will likely affect the quantity and quality of organic carbon supplied to high latitude coastal systems (Hood et al. 2009; Hood et al. 2015; Wassmann,

2015), likely leading to changes in microbially-mediated carbon cycling, and with consequences on organic matter turnover, export, and retention.

3.2 Materials and Methods

Site description and sample collection. Samples were collected during the ice melting season from August 2 to August 17, 2015 in Tylerfjord-Young Sound (Fig. 1). Surface water samples were collected in 20 L carboys from three main rivers that feed into Tyrolerfjord-Young Sound: Tyroler River, Lerbugten River, and Zackenberg River; altogether, these sites will be referred to as 'rivers'. Tyroler River has the greatest glacial influence—with inputs directly from the Greenland Ice Sheet—as well as the largest catchment area (Bendtsen et al. 2014). Lerbugten River is downstream of a small lake, and is influenced by local glaciers. Zackenberg River has the most terrestrial and vegetative influence, receives input from two lakes, and is the largest river of the three investigated in this study (Paulsen et al., 2017). Surface and subsurface water samples were also collected at transition sites where the rivers feed into the fjord (Tyro_01, Zac_30, Ler_30, together referred to as 'river transition sites'). However, only the surface water at the river transition sites has a prominent freshwater signature, as waters at depths of 20 m and below are largely marine based on salinity; thus, the surface waters at the river transition sites will be referred to as 'river plumes'. Surface and subsurface samples were also taken within the fjord, as well as at the mouth of the fjord close to the East Greenland Sea: YS_3.18, YS_3.06, and GH_02, respectively, and altogether referred to as 'fjord sites'. Four of these sites (Tyro_01, YS_3.18, YS_3.06, and GH_02) are part of the Greenland Ecosystem Monitoring (GEM) *MarinBasis* program. Water samples in the river transition sites and in the fjord were collected using Niskin bottles mounted to a CTD aboard the R/V *Aage V. Jensen*, and experiments were conducted at the land-based research station in Daneborg. Frozen samples collected as described below were transported back to, and processed in, the institutional laboratories.

Sample filtration. At all sites and depths, approximately 1 L of water was collected and filtered through a 0.2 µm Nucleopore membrane filter for bulk water (non size-fractionated) bacterial community analyses. Additionally, water samples from the same locations were size-fractionated using gravity filtration through a GF/A filter to capture ≥1.6 µm particles. Gravity-filtered water volumes ranged from approximately 1.02 L in the particle-rich rivers, up to 5.86 L in the subsurface waters of GH_02. Samples were stored at -80°C, both at the research station and once back in the institutional laboratories.

Grain size analysis. Water samples were filtered through 0.45 µm Millipore Cellulose filters, and the retained material was removed from the filters in plastic beakers placed in an ultrasonic bath. The samples were subsequently dispersed using a Bandelin Sonopuls HD2200 Sonifier and particle size distributions were measured using a Malvern Mastersizer E/2000 laser-sizer.

Bacterial production and cell counts. Measurements were made on bulk water and free-living fractions. The free-living fraction was obtained from the filtrate that passed through a GF/A filter by gravity filtration. Bacterial production was measured using ^{3}H-thymidine. Triplicate incubations with ^{3}H-thymidine and either bulk water or filtrate water were set up in 100 mL glass bottles, with additional samples as blanks. ^{3}H-thymidine was added to the live triplicates to a final concentration of 10 nM. Blank samples were fixed with 0.5 mL of 100% trichloroacetic acid (TCA). Samples were incubated at *in situ* temperature on a small plankton wheel to ensure particles remained suspended. After incubation for 6-8 hrs, live samples were fixed with 100% TCA. Live and blank samples were then filtered through 0.2 µm cellulose nitrate filters that were pre-washed with MilliQ, using filtration manifolds that were pre-chilled at -20°C. Glass vials and filtration towers were rinsed with 5% ice cold TCA. Filters were frozen at -20^{o}C in plastic vials and transferred back to the institutional laboratory, where 5 mL of scintillation cocktail was added and the samples were counted on a Perkin Elmer Liquid Scintillation Analyzer (Tri-Carb 2800TR). Results were

converted to bacterial production by assuming production of 2.0 x 10^{18} cells per mole of ^{3}H thymidine fixed.

Samples for bacterial cell counts were fixed in 0.5% glutaraldehyde and stored at 5°C. The cell numbers were quantified by flow cytometry (Attune, Applied Biosystems by Life Technology). Prior to analysis, samples with particles were sonicated 15 s three times to release the particle associated communities, and cells were stained with SYBR Green I (Molecular Probes, Eugene, Oregon, US) following the procedure of Marie et. al (1999). Samples containing high concentrations of inorganic particles were diluted 5-20x to eliminate interference during quantification.

Peptidase and glucosidase activity assays. We measured the activities of five exo- (terminal cleaving) and endo-acting (mid-chain cleaving) peptidases: Leucine-aminopeptidase (Leucine-MCA), AAF-Chymotrypsin (Alanine-Alanine-Phenylalanine-MCA), AAPF-Chymotrypsin (Alanine-Alanine-Proline-Phenylalanine-MCA), FSR-Trypsin (Phenylalanine-Serine-Arginine-MCA), QAR-Trypsin (Glutamine-Alanine-Arginine-MCA) (QAR-Trypsin). We also measured the activities of two glucosidases, α-glucosidase (α-glucopyranoside-MUF), and β-glucosidase (β-glucopyranoside-MUF). All seven low molecular weight substrates were used to measure bulk water and particle-associated (≥1.6 µm) enzymatic activities.

Enzyme activities were measured in triplicate in bulk water by adding 4 mL of water to replicate cuvettes. One cuvette containing autoclaved water (with substrate added after the water had cooled) served as the killed control. This procedure was used for each of the 7 substrates; in addition, for each site and depth, there was one live blank (no substrate added) and one autoclave blank (no substrate, just autoclaved water), resulting in 30 parallel incubations per site/depth. Each cuvette containing either live or autoclaved water was amended with one substrate to a concentration of 100 µM. To measure particle-associated enzyme activities, GF/A filters containing particulate matter were evenly divided

using sterile razor blades into 1/12th pieces. Each piece was submerged in a cuvette containing 4 mL of cooled, autoclaved water from the same station/depth as the live samples. In addition, killed controls consisted of sterile GF/A filters cut into 1/12th pieces. One killed control and duplicate live filter incubations were used for each of the 7 substrates, totaling 21 incubations per site/depth. Bulk water and particle-associated enzyme assays were incubated for up to 24 and 16 hours, respectively; timepoints were taken at specific intervals. Incubations were kept in the dark either at 0°C, 5°C, or 8°C, depending on in situ water temperature at the time of sampling (Table 1-3).

Polysaccharide hydrolase measurements. The activities of polysaccharide hydrolyzing enzymes in bulk water and associated with particles (≥1.6 μm) were measured (Arnosti, 2003) using six structurally distinct polysaccharides: pullulan, laminarin, xylan, fucoidan, arabinogalactan, and chondroitin sulfate. Bulk water incubations were carried out following established procedures (Teske et al. 2011). Briefly, 15 mL of bulk water (in triplicate) and a single 15 ml sample of autoclaved water (as a killed control) were amended with a single substrate at a concentration of 3.5 μM monomer equivalent. Due to its lower fluorescence, the fucoidan was added to a final concentration of 5.0 μM monomer equivalent. A live blank and an autoclave blank were included in each sample set, resulting in 26 incubations per site/depth. For the particle-associated measurements, GF/A filters containing particulate matter was evenly cut using a sterile razor blade into 1/12th pieces. Each filter piece was submerged in 15 mL of cooled, ambient autoclaved water; the live filter incubations were done in duplicates. One sterile GF/A filter bit was used as a single killed control per substrate. In total, 21 particle-associated incubations were made for each site/depth.

Samples were incubated in the dark at near *in situ* temperature (0°C, 5°C, or 8°C), and sub-sampled at specific time intervals—t0 (0h, upon substrate addition), t1 (120 h), t2 (240 h), t3 (360 h) and t4 (600 h). Sub-samples at each timepoint were filtered through 0.2

µM pore size SFCA (surfactant-free cellulose acetate) syringe filters, and the filtrate was collected and frozen at -20°C until processing in the lab. Samples were processed using gel permeation chromatography with fluorescence detection (Arnosti, 2003). To focus on maximum community potential, we report only the maximum rates throughout the incubation in the main text. These maximum rates come from different timepoints; data for all timepoints are in the supplementary materials (Fig. S1A-F).

Bacterial community composition analyses. DNA was extracted from both the 0.2 µm Nucleopore membrane filters and the 1.6 µm GF/A filters for whole and particle-associated bacterial community analyses. The MoBio PowerSoil DNA Extraction kit was used following the manufacturer's protocol. DNA samples were sent to the UNC Core Microbiome Sequencing Facility to sequence 16S rRNA genes using Illumina MiSeq PE 2 x 250, targeting the V1-V2 hypervariable region with the bacterial primers 8F (5'- AGA GTT TGA TCC TGG CTC AG -3') and 338R (5'- GCT GCC TCC CGT AGG AGT -3'). Sequence pairs were merged and OTUs (97% sequence similarity) were picked *de novo* using default parameters on QIIME. Singletons and sequences that were not present in at least two samples were removed, and the Greengenes database was used to classify the remaining OTUs. OTUs detected in the sequencing blank were excluded from further analyses.

The R package *phyloseq* (McMurdie and Holmes, 2013) was used to rarefy the dataset to 85,000 sequences per sample. Principal Coordinates Analysis (PCoA) was conducted on the sequence dataset with the Bray-Curtis dissimilarity index using the R package *vegan* (Oksanen, 2008). Analyses of community dissimilarity (Bray-Curtis) on groupings of bacterial communities were conducted using the function ANOSIM in the package *vegan* with 999 permutations. The relationship between bacterial community dissimilarity (Bray-Curtis) and various environmental parameters was analyzed using Permutational Analysis of Variance (PerMANOVA) implemented on *vegan* with the ADONIS function.

DOM composition analyses. In brief, water samples were initially filtered through GF/F filters to remove larger particles and then processed largely following Dittmar et al. (2008), by acidifying prior to extraction on pre-cleaned (12 mL methanol, MS-grade) PPL cartridges (Agilent Bond Elut PPL, 1g resin, 6 mL volume). The cartridges were rinsed with 0.01 M HCl, and the concentrated DOM was eluted using 12 mL methanol (MS-grade), and stored in muffled 20 ml glass vials. These samples were stored at -80°C until mass spectroscopic analyses.

Samples were analyzed on a 6530-LC-QTOF-MS and a 7200 GC-QTOF-MS (both Agilent Technologies, Santa Clara, US) using chromatographic and mass spectrometric settings, and feature extraction algorithms as previously described (Hasler-Sheetal et al. 2016) with slight modifications. 2 mL of sample was dried in a speed-vac and reconstituted in 100 µl 0.1% formic acid in a methanol:water mix before analysis on LC-QTOF-MS, or derivatized before analysis on GC-QTOF-MS (Hasler-Sheetal et al. 2015). The relative proportions of specific substrates—including glucose, arginine, proline and leucine—were measured in concentrated DOM by GC-QTOF-MS using a previously established method (Hasler-Sheetal et al. 2016). A complete DOM dataset is not available because samples from Tyroler and Lerbugten Rivers were lost during transit.

Differences in DOM composition were analyzed using Canonical Analysis of Principal Coordinates (CAP) based on Bray-Curtis dissimilarities of ranked and square root transformed data. The significance of dissimilarities between groups were evaluated using ANOSIM (Primer 7, PRIMER-E, Plymouth, UK). The relationship between DOM composition and bacterial community (Bray-Curtis) dissimilarities was evaluated using Mantel Test. A similar analysis, conducted on DOM composition dissimilarity calculated using Euclidean distances, yielded similar results. The Partial Mantel Test was used to test this relationship independent of the influence of salinity.

3.3 Results

***Water mass and particle characteristics*.** Rivers in the Tyrolerfjord-Young Sound system contained freshwater with high suspended particulate matter (SPM) concentrations (Table 1), likely due to subglacial and/or terrestrial influence. These SPM concentrations ranged from 234.4 to 552.3 mg/L. The river plumes contained a mixture of fresh and marine waters (12.55 – 15.52 PSU), with SPM concentrations that gradually decreased along the river-fjord transition, reaching values of only 7.8 to 95.3 mg/L. Subsurface waters (20 m) at the river transition sites were largely marine in origin (31.33 – 31.52 PSU), and contained among the lowest SPM concentrations, in the range of 2.0 – 5.8 mg/L (Table 2). Within the fjord, surface waters were mostly marine, as indicated by salinity (27.83 – 29.05 PSU); subsurface waters showed a stronger marine salinity signature (29.48 – 31.23 PSU). SPM concentrations in the fjord were low, in the range of 1.2 – 7.7 mg/L (Table 3). As indicated by loss on ignition (LOI, Table 1), particles in rivers typically contained a lower percentage of organic matter (2.5 – 6.3%) compared to those within the fjord (Table 3). In the river plumes, LOI ranged from 9.2 to 10.1%, while those in subsurface waters of the river transition sites were higher (22.2 – 23.1%). LOI values in surface and subsurface waters within the fjord included the highest values measured, ranging from 12 to 40%. The smallest particles were found in Zackenberg River (5.7 µm), but mean particle size from Lerbugten River (17.8 µm) was comparable to those in the river transition sites (Table 3). In the fjord, particles were even larger, and ranged from 10.4 to 29.6 µm (Table 3).

***Bacterial cell counts and production*.** Bulk bacterial cell counts were lowest on average in rivers (0.15 – 0.51 x 10^6 cells/mL), and highest in the fjord (3.0 – 3.5 x 10^6 cells/mL); this spatial trend was also observed for the free-living and particle-associated communities (Table 1-3). For most stations and depths, particle-associated bacterial cell counts were greater than those for the free-living community. Bacterial production measurements were highly variable and showed no general trend between environments.

However, lowest rates of bulk bacterial production were measured in Tyroler River (0.33 µg C L^{-1} d^{-1}) and in the surface and subsurface waters of Tyro_01 (0.46 and 0.26 µg C L^{-1} d^{-1}, respectively). Highest rates of bulk bacterial production were observed at Lerbugten and Zackenberg Rivers (Table 1).

Peptidase and glucosidase activities. Summed peptidase and glucosidase activities in bulk water were lower in rivers than in river transition sites and in the fjord (Fig. S2A). Among the rivers, the highest summed activity was measured at Zackenberg River, while summed activities at Tyroler River and Lerbugten River were comparable, but with differing spectra of enzyme activities. In river transition sites, the highest summed activities were measured at Zac_30, while the lowest were found in Ler_30. In fjord sites, the highest summed activities were measured at YS_3.18—at the confluence of Zackenberg and Lerbugten River outflow. Summed peptidase and glucosidase activities in bulk waters showed a moderate, but statistically significant positive correlation with cell counts (R^2 = 0.42, p = 0.018) (Fig. S3A).

Bulk water peptidase and glucosidase activities showed contrasting patterns across the salinity gradient. Leucine-aminopeptidase activity was consistently detected at all sites, although activities generally increased with salinity (Fig. 2A). For the two chymotrypsin substrates, AAPF-chymotrypsin showed higher activities; AAF-chymotrypsin activities were not measurable at every site, and were lowest in rivers and higher and comparable at all sites in the fjord. The activities of both types of trypsin enzymes generally increased along the salinity gradient, but QAR-tryp had higher activities overall than FSR-tryp. In contrast to peptidase trends, glucosidase activities tended to decrease with increasing salinity (Fig. 2A). The extent to which enzymatic activities in surface and subsurface waters were similar depended on the substrate. Leucine aminopeptidase, FSR-trypsin, and QAR-trypsin activity patterns were similar at both depths, while the rest of the enzyme activities were not. Notably, cell count-normalized rates showed a decrease in the activities of most peptidases

with increasing salinity (Fig. S4); the exception was QAR-trypsin. Cell-specific glucosidase activities also decreased with salinity, similar to trends observed with non-normalized enzymatic activities.

Particle-associated peptidase and glucosidase activities exhibited some patterns along the salinity gradient that were similar to those in bulk waters, but diverged strongly in other cases. For example, summed particle-associated peptidase and glucosidase activities were higher in the fjord than in the rivers (Fig. S2B), a pattern that was likely driven in part by higher cell counts in the fjord ($R^2 = 0.61$, $p = 0.003$) (Fig. S3B). This pattern was also observed in bulk water (Fig. S2A, S3A); however, in the free-living fraction, the relationship between cell counts and summed peptidase and glucosidase rates was positive, but not statistically significant (Fig. S3C). Some substrate-specific trends were also similar in bulk water and on particles, as evident by leucine aminopeptidase activities (Fig. 2B). In contrast, particle-associated AAPF-chymotrypsin activities had a notably different pattern across the salinity gradient compared to that of bulk water. Furthermore, particle-associated rates (normalized to the volume of water filtered to obtain the particles) were generally lower than rates measured in bulk seawater. This trend is evident for leucine aminopeptidase, FSR-trypsin, QAR-trypsin, α-glucosidase and β-glucosidase (Fig. 2B).

Polysaccharide hydrolase activities. The spectrum and activities of polysaccharide hydrolases in bulk waters showed considerable differences between the rivers versus river transition and fjord sites (Fig. 3A, Fig. S5A). In rivers, only laminarin and xylan were consistently hydrolyzed, although very low rates of pullulan and chondroitin hydrolysis were also detected in Zackenberg River (Fig. 3A). In surface and subsurface waters of river transition sites, only laminarin was hydrolyzed at all sites; xylan, chondroitin and pullulan hydrolysis were also detected in most of the river plume waters. In subsurface waters of river transition sites and both depths in fjord sites, in bulk waters, laminarin, chondroitin, and xylan were consistently hydrolyzed. Pullulan was hydrolyzed at most of

these sites, while fucoidan was only measurably hydrolyzed at YS_3.18. Arabinogalactan was not detectably hydrolyzed in bulk waters. Furthermore, the rate at which xylan and chondroitin were hydrolyzed exhibited robust trends across the salinity gradient. Highest rates of xylan hydrolysis were measured in the rivers (Fig. 3A). In contrast, rates of chondroitin hydrolysis peaked in the fjord, but these rates remained very low or unmeasurable in rivers (Fig. 3A).

A wider spectrum of polysaccharide was hydrolyzed on particles compared to bulk waters (Fig. 3B, Fig. S5B). Laminarin, xylan, chondroitin, and pullulan were consistently hydrolyzed on particles in rivers (Fig. 3B). In river transition sites, laminarin, xylan, and pullulan hydrolysis were consistently measured. Chondroitin was hydrolyzed on particles from all river transition sites, with the exception of the surface water at Ler_30. Particle-associated fucoidan hydrolysis was also detected in most river transition sites; the exceptions were on particles from Ler_30 surface water and Tyro_01 subsurface water. Moreover, in the river transition sites, arabinogalactan hydrolysis was only detected on particles from Tyro_01 surface water and Zac_30 subsurface water. Particle-associated polysaccharide hydrolase activities at the river transition sites were generally lower in subsurface waters compared to surface waters. In the fjord, laminarin, chondroitin and fucoidan were consistently hydrolyzed on particles. Particle-associated xylan and arabinogalactan hydrolysis were detected at almost all fjord sites, with the exception of YS_3.18 subsurface waters. Pullulan hydrolysis was also detected on particles from almost all of the fjord sites, with the exception of YS_3.18 and GH_02 subsurface waters. Across all sites, the highest particle-associated summed rates were detected in rivers (Fig. S5B). Outside of the rivers, summed hydrolysis rates were generally higher in surface compared to subsurface waters.

Spatial patterns in bacterial community composition. Bacterial communities grouped into three clusters with significant compositional differences (ANOSIM, R = 0.997, *p*

= 0.001; Table S1), and which correlated significantly with salinity (PERMANOVA, R^2 = 0.392, p = 0.001) (Fig. 4). Group A included the riverine bulk water communities, with members from a greater diversity of bacterial classes compared to communities in other clusters (Fig. 5). Some of these communities, however, showed surprisingly lower OTU-level diversity (species richness) compared to river-transition and fjord communities (Fig. S6), for which a narrower range of bacterial classes were detected (Fig. 5). Additionally, this freshwater cluster showed low to moderate relative proportions—but high diversity—of *Alphaproteobacteria*. Moderate to large relative abundances of the class *Actinobacteria*, and large contributions of *Betaproteobacteria* also characterized the freshwater group (Fig. 5). Group B contained the Tyroler River particle-associated sample and most of the river transition samples. This group exhibited large relative proportions of *Betaproteobacteria* and *Actinobacteria*, similar to Group A; however, Group B contained greater proportions of *Flavobacteria* and *Alphaproteobacteria*, and lower diversity in bacterial classes. Group C included communities from fjord sites and two river transition sites (surface whole community at Ler_30 and Zac_30). This group was also characterized by large relative contributions of *Flavobacteria, Alphaproteobacteria* and moderate proportions of *Gammaproteobacteria*, but contained among the most species rich bacterial communities (Fig. S6).

The particle-associated versus bulk bacterial community distinction was stronger in the Tyroler River—the only river where this comparison was possible due to very low DNA extraction efficiency—relative to those in the river transition sites and in the fjord (Fig. 4). Furthermore, the Tyroler River particle-associated bacterial community exhibited high compositional similarity with the surface water of the river transition sites, and the bulk surface water community at Tyro_01 (Fig. 5). The observed differences were driven by changes in the relative proportions of specific members of *Alphaproteobacteria* and *Betaproteobacteria* (Fig. 5). Within *Alphaproteobacteria*, members of the family

Rhodobacteraceae were detected in minimal to moderate relative proportions in bulk river communities—at ca. 4-20% of *Alphaproteobacteria*—but dominated the particle-associated community in Tyroler River and river plumes; a similar trend was observed with members of the family *Alcaligenaceae* of the class *Betaproteobacteria*. In contrast, particle-associated communities in Group C were not significantly different compared to the bulk bacterial communities in the same waters (ANOSIM, R = 0.042, p = 0.275; Table S1).

***DOM Composition*.** A total of 15439 metabolite entities were detected in the entire DOM dataset. Canonical Analysis of Principal Coordinates revealed three main pools of DOM: river water, river plume and marine mixture, and purely marine (Fig. 6). Thus, variations in the relative proportions of DOM components (Bray-Curtis dissimilarity) were correlated with salinity. Excluding samples from Zackenberg River—the only freshwater site where samples were available—three separate clusters formed: mid fjord, outer fjord, and coastal (Fig. S7).

DOM, BCC, and EEA relationships. We analyzed correlations between bacterial community composition, enzymatic activities, and DOM composition across the salinity gradient. For the first analysis, only samples containing data for bacterial community composition and DOM composition were included (n = 11). Dissimilarities (Bray-Curtis) in the composition of bacterial community and DOM were significantly correlated (Mantel, r = 0.751, p = 0.004). Salinity differences also correlated with DOM composition (Mantel, r = 0.771, p = 0.01), similar to trends with bacterial community composition. Removing salinity differences from this relationship indicated spatial autocorrelation between bacterial community composition and DOM composition (Partial Mantel Test, r = 0.3867, p = 0.126).

We further evaluated the relationship between activities of specific enzymes and relative concentrations of their putative hydrolysis products across the system. These analyses showed variability in the strength of the correlation between enzyme activities and relative proportions of hydrolysis products. For example, leucine aminopeptidase and

relative concentrations of leucine were only weakly correlated (Fig. 7A). In contrast, the relationship between the combined activities measured using the two trypsin-associated substrate proxies (QAR- and FSR-trypsin) with the relative concentrations of arginine—as well as the relationship between α- and β-glucosidase activities with glucose—were strong and statistically significant (Fig. 7B,C). Because the relative concentrations of phenylalanine—the amino acid produced by the activity of AAPF-chymotrypsin—was unavailable, we correlated AAPF-chymotrypsin activities with relative proportions of proline, the amino acid to which phenylalanine is attached in our substrate analog; this analysis also showed a strong, statistically significant positive relationship (Fig. 7D). Thus, the relative concentrations of specific compounds (Fig. S8) followed the salinity-related trends exhibited by the peptidase and glucosidase activities.

3.4 Discussion

Characterizing the composition and substrate preferences of microbial communities, as well as the organic matter pool with which they interact, provides insights into the fate of organic matter. We show robust differences in the composition of bacterial communities and dissolved organic matter (DOM) that corresponded primarily with their water mass origin (e.g., river water, coastal water inflow, or a mix of the two). These spatial trends in bacterial community composition also paralleled contrasting patterns of microbial enzymatic capabilities. Furthermore, enzymatic activity patterns correlated with the relative concentrations of specific DOM compounds. These results indicate that factors extrinsic (i.e., organic matter quality and supply) as well as intrinsic (i.e., OM degradation potentials) to microbial communities concurrently influence organic matter processing. Thus, increased freshening and changes in organic matter supply in fjords, due to increased glacial discharge (Hood et al., 2015; Sejr et al., 2017), have the potential to change microbial carbon cycling.

As glacial runoff can be comprised of supraglacial, englacial and subglacial fractions, meltwater has the potential to carry and disperse bacterial communities from these layers (Stibal et al. 2012). Along its path to downstream systems, glacial runoff can erode the underlying bedrock and entrain soils, incorporating terrestrially-derived organic matter and microbial cells. Hence, glacial meltwaters largely contains microbial taxa of freshwater origin, with terrestrial signatures (Dubnick et al. 2017; Paulsen et al. 2017). Results from this study similarly demonstrate a freshwater and terrestrial provenance of riverine bacterial communities. Subsequently, river water mixes with saline water within the fjord, and at these river transition sites, the bulk of bacterial communities is composed of typically-marine members. In the middle portion and outer reaches of the fjord, the large relative proportions of *Alphaproteobacteria*, *Flavobacteria*, and low-to-moderate contributions of *Gammaproteobacteria* signal a largely marine microbial community (Gutiérrez et al. 2015). Thus, the influence of glacial meltwater on microbial communities in the fjord diminishes with distance from the rivers, as within-fjord microbial communities increasingly become influenced by Greenland Sea coastal water inflow (Paulsen et al. 2017).

Freshwater runoff from glaciers has a profound influence on the composition of DOM in downstream aquatic ecosystems (Hood and Scott, 2008; Bhatia et al. 2010; Singer et al. 2012). In this study, DOM composition in rivers, river plume water, and within the Tyrolerfjord-Young Sound system exhibit differences that are strongly correlated with salinity and indicative of differences in water mass origins. Varying C:N ratios in river versus fjord waters previously observed in this system further confirm water mass-related differences in DOM quality (Paulsen et al. 2017). This difference in DOM composition in fresh versus marine waters parallels patterns of bacterial community composition across these sites. Moreover, the positive relationship between dissimilarities in DOM composition and bacterial community composition implies that compositionally-distinct freshwater and marine microbial communities interact with organic matter pools that differ as a function of water mass.

However, this relationship should be interpreted with caution, as active microbial members may differ from total community composition (D'Ambrosio et al. 2014; Osterholz et al. 2016).

The heterotrophic capabilities of distinct microbial assemblages along the river-to-fjord continuum determine the fate of allochthonous and autochthonous organic matter. Differences in enzymatic activities across water masses paralleled contrasts in freshwater and marine bacterial cell counts, bacterial production, and the composition of microbial communities and DOM. Salinity is known to strongly structure the composition of aquatic microbial communities (Crump et al. 1999, Hewson and Fuhrman, 2004; Fortunato and Crump, 2015), with consequences for microbial heterotrophic metabolism (Ghai et al. 2011; Eiler et al. 2014). In this study, freshwater communities exhibited higher glucosidase and xylanase activities, compared to their downstream marine counterparts. That highest glucosidase and xylanase activities were measured in rivers is especially notable in light of low bacterial cell counts measured in these waters. Cell-specific glucosidase and xylanase hydrolysis rates, in particular, suggest that freshwater microbial communities, even at low abundances, may have a significant influence on the hydrolysis and fate of specific organic compounds. Furthermore, these patterns in enzyme activities are consistent with genomic content that include high relative abundance of genes encoding glycoside hydrolases and xylose transporters detected in freshwater microbial metagenomes (Eiler et al. 2014). Xylose—the constituent monomer of plant-derived xylan (Opsahl and Benner, 1999)—may have been sourced from supraglacial croyoconite holes (Stibal et al. 2010). Evidence from Alpine glacier-fed, freshwater streams demonstrates that more bioavailable organic matter compounds are nitrogen-free; in contrast, nitrogen-rich peptides and lipids in streams contribute minimally to bioavailability (Singer et al. 2012). Enzyme activities of freshwater microbial communities therefore suggest efficient utilization of microbially- and terrestrially-derived carbohydrates sourced from glacial meltwater and limited vegetation. Findings of high bacterial production rates in these rivers—in this study and by Paulsen et al. (2017)—

further confirm the presence of a highly active freshwater microbial community. That a high fraction of the DOC pool is bioavailable in these rivers also signify the efficiency with which freshwater microbial communities can utilize available organic matter (Paulsen et al. 2017).

Microbial communities in the fjord, in contrast, exhibited higher cell counts and bulk rates of peptidase activities, and possessed polysaccharide hydrolytic capabilities distinct from those of riverine microbes. High leucine aminopeptidase, chymotrypsin, and trypsin activities within the fjord are consistent with suggestions of rapid remineralization of proteinaceous compounds following a phytoplankton bloom in two Svalbard fjords (Osterholz et al. 2014). An overrepresentation of genes for amino acid transporters detected in marine microbial metagenomes (Eiler et al. 2014) may be necessary for efficient uptake of peptide hydrolysis byproducts. Moreover, the ability to rapidly hydrolyze chondroitin sulfate, and occasionally fucoidan and arabinogalactan, sets marine microbial communities apart from their freshwater counterparts; these marine enzymatic activities mirror patterns observed in a Svalbard fjord (Teske et al. 2011). Overall, the differing spectrum of polysaccharide substrates consistently utilized by freshwater versus marine microbial taxa may be an adaptation to varying pools of organic matter in rivers and fjords. Accordingly, contrasting metabolic strategies to utilize allochthonous or autochthonous organic matter have previously been observed along a river-to-ocean gradient (Ghai et al. 2011).

While differences in factors intrinsic to microbial communities (i.e., composition and metabolic potential) parallel substrate utilization, our results indicate that an extrinsic factor—the composition of the organic matter pool—may additionally influence specific carbon processing abilities. In addition, the positive relationship between enzymatic activities and the relative concentrations of putative hydrolysis products links microbial enzymatic hydrolysis to outputs of their activities, and underscores the consequences of microbial heterotrophic processes on the organic matter pool. Moreover, the strength of these relationships are consistent with the known specificity of the substrate analogs used.

For example, the relationship between leucine aminopeptidase and leucine relative concentrations is weak. This result is in accordance with findings that hydrolysis rates measured using the substrate analog Leu-MCA can reflect the combined activities of aminopeptidases beyond just leucine aminopeptidase (Steen et al. 2015), as well as the probability that leucine as a free amino acid is rapidly taken up by the microbial community. Nevertheless, these observations suggest that intrinsic capabilities of microbial communities and external supply of organic compounds concurrently shape heterotrophic activities of freshwater and marine microbial communities in coastal Arctic waters. Varying enzymatic potentials may explain differences in carbon bioavailability between freshwater and marine microbial communities in glacial-fed high latitude systems (Fellman et al., 2010; Paulsen et al. 2017).

Our study also demonstrates that particles shape microbial community composition and activities in this fjord. Riverine particles host a bacterial assemblage distinct from that observed in bulk river waters, and this particle-associated community persists into river transition sites. However, at the river transition sites, bulk community composition resembles that of high-salinity fjord sites. The only exception to this pattern is the bulk bacterial community in the surface Tyroler River plume within the fjord, which also bears high similarity to the particle-associated community and retains a robust freshwater signature. This observation is likely related to the lower salinity of Tyro_01 surface water compared to other river plume surface waters. Thus, particles—carried in glacial meltwater transported from rivers into the fjord—are conduits of bacterial dispersal in these systems, shaping the river-to-fjord microbial metacommunity. Terrestrially-derived particles, in particular, may be a vessel through which soil microbial taxa can be integrated into freshwater microbial communities, as observed in Arctic freshwater systems (Crump et al. 2012). The influence of riverine particles on microbial community composition, however, is limited in the inner and

outer fjord, reflecting the combined effects of particle degradation and possibly vertical particle export in the fjord (Sejr and Rysgaard, 2007).

Additionally, microbial communities on particles, independent of origin, possess distinct capabilities from those in bulk water. Specifically, a broader range of polysaccharide substrates were hydrolyzed on particles compared to the bulk water, regardless of location, as well as particle source and characteristics. Using the same set of substrates and a similar experimental approach, this particle-associated versus bulk polysaccharide hydrolase activity pattern was also observed at various sites and depths in the central Arctic (J. P. Balmonte unpubl.). In contrast, the pattern of broader spectrum of enzymes active on particles versus bulk waters was not observed with the peptidase and glucosidase activities. This trend highlights the contribution of non-particle-associated assemblages to organic matter remineralization; in particular, the activity of AAPF-Chymotrypsin can almost entirely be attributed to the non-particle-associated fraction. These differing enzymatic capabilities suggest that particle-associated microbial taxa, compared to their free-living counterparts, may be equipped with a broader spectrum of hydrolytic enzymes that can hydrolyze high molecular weight components of particles (D'Ambrosio et al. 2014). Concentrating particle-associated taxa thus enabled the detection of polysaccharide substrates that were not detectably hydrolyzed in bulk waters.

3.5 Conclusion

Along a river-to-fjord continuum, microbial community composition, enzymatic activities, and DOM composition varied largely with salinity differences—an indication that glacial meltwater directly influences microbial carbon cycling in fjords. Meltwater discharge carries a community of microbes—of freshwater and terrestrial origins—that efficiently break down microbially- and terrestrially-derived carbohydrates. The meltwater influence on fjord microbial communities is observed primarily at the river transition sites, where the particle-associated communities resemble those detected in rivers. However, bulk bacterial

communities in the fjord are of largely marine origin, and exhibit higher cell abundances. Fjord microbial communities are attuned to breaking down protein-rich compounds, and an array of polysaccharides distinct from those hydrolyzed in rivers. Salinity-related differences in community composition and activities parallel large variations in DOM composition, highlighting the influence of different water masses in Tyrolerfjord-Young Sound. Moreover, the distribution of specific DOM compounds in this system positively correlates with enzymatic activities, indicating that the organic matter-degrading capabilities of freshwater and marine microbial communities reflect their adaptation to organic matter supply. Our findings may be more broadly applicable to other coastal systems in which fresh and marine waters mix. At the very least, within the pan-Arctic these results suggest that projected increases in meltwater discharge into fjords may alter microbial carbon cycling—beside hydrological implications—through changes in the composition of microbial communities and the organic matter pool.

3.6 Acknowledgements

We thank Egon and Charlotte Frandsen, Karl Attard, Johnna Holding, and Achim Randelhoff for their field and lab support, scientific advice, and camaraderie. We additionally thank Sherif Ghobrial and Karylle Abella for their assistance with sample processing. JPB was supported in part by NSF (OCE-1332881 and -1736772 to CA), and was additionally funded by a UNC Dissertation Completion Fellowship. RNG and MM were supported by European Union's Horizon 2020 Research and Innovation Program (Grant agreement No. 669947; HADES-ERC) and the Danish National Research Council (FNU; 0602-02276B). This work was also partially funded by a Diversity Grant from the American Geosciences Institute through the Deep Carbon Observatory awarded to JPB.

3.7 Main Figures and Tables

Figure 1. Map of Tyrolerfjord-Young Sound. Sampling sites in the river (light gray), river transition sites (dark gray) and fjord (black) are denoted. The dashed line represents the basin of Tyrolerfjord-Young Sound. The land-based research station is located in Daneborg.

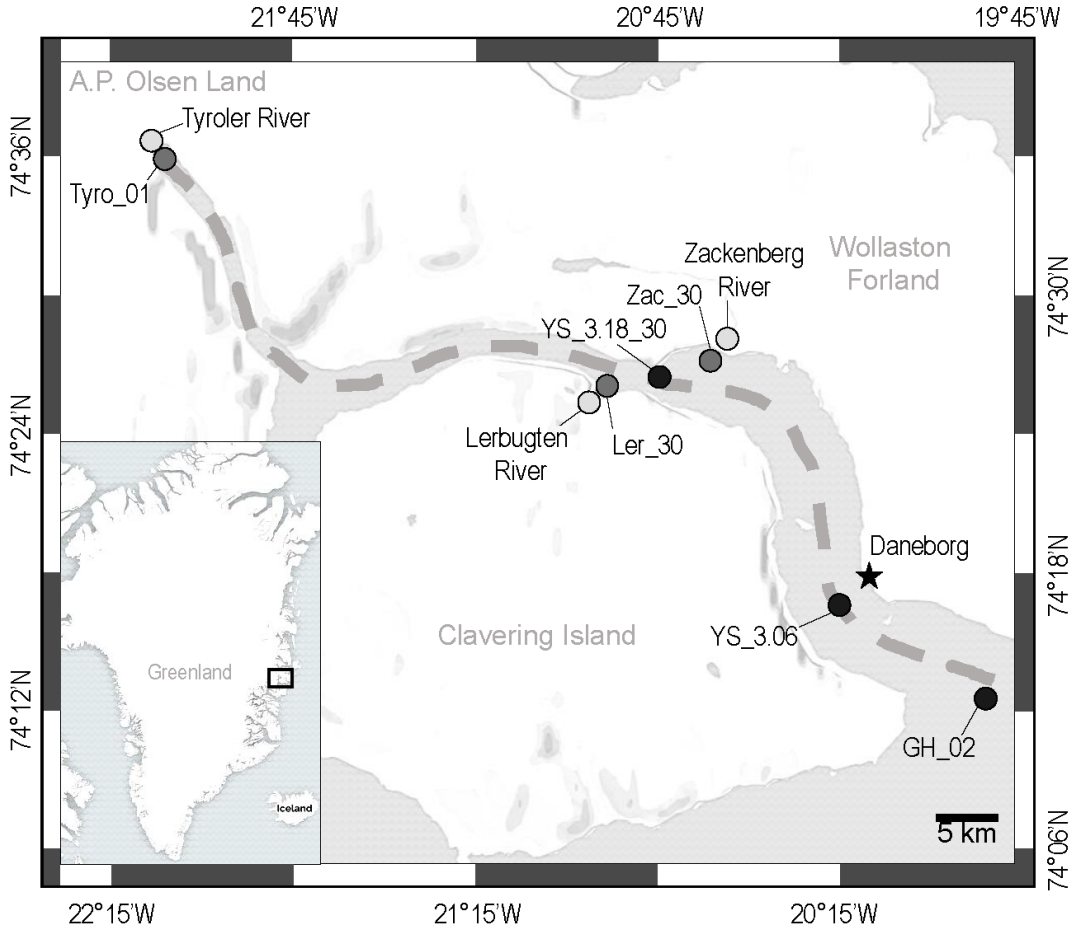

Figure 2. Whole community (A) and particle-associated (B) peptidase and glucosidase activities shown by substrate. The light grey shading in the panels indicates that no subsurface measurements were taken in the rivers. Within each plot, stations are arranged by salinity (increasing to the right), and from the inner to the outer part of the fjord. Note the differences in scale across all plots. Reported rates are averaged from triplicate (whole community) or duplicate (particle-associated) incubations, and measured 12 hrs after the start of incubation.

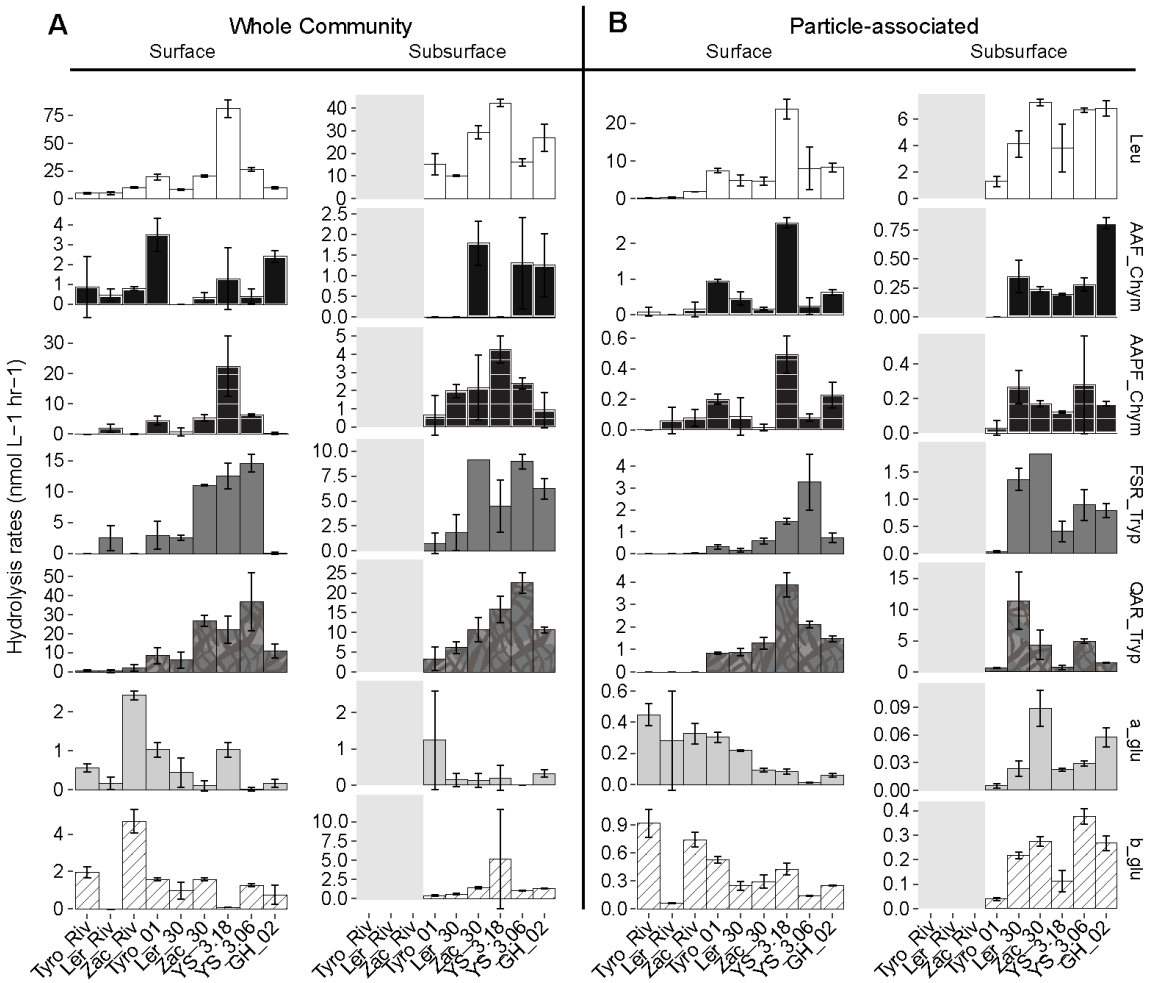

Figure 3. Whole community (A) and particle-associated (B) polysaccharide hydrolase activities shown by substrate. The light grey shading in the panels indicates that no subsurface measurements were taken in the rivers. Within each plot, stations are arranged by salinity (increasing to the right), and from the inner to the outer part of the fjord. Note the scale differences. Reported rates are averaged from triplicate (whole community) or duplicate (particle-associated) incubations, and taken at different timepoints throughout the incubation. See supplementary materials (Fig. S1A-F) for all rates. Pull = pullulan, lam = laminarin, xyl = xylan, fuc = fucoidan, ara = arabinogalactan, chn = chondroitin sulfate.

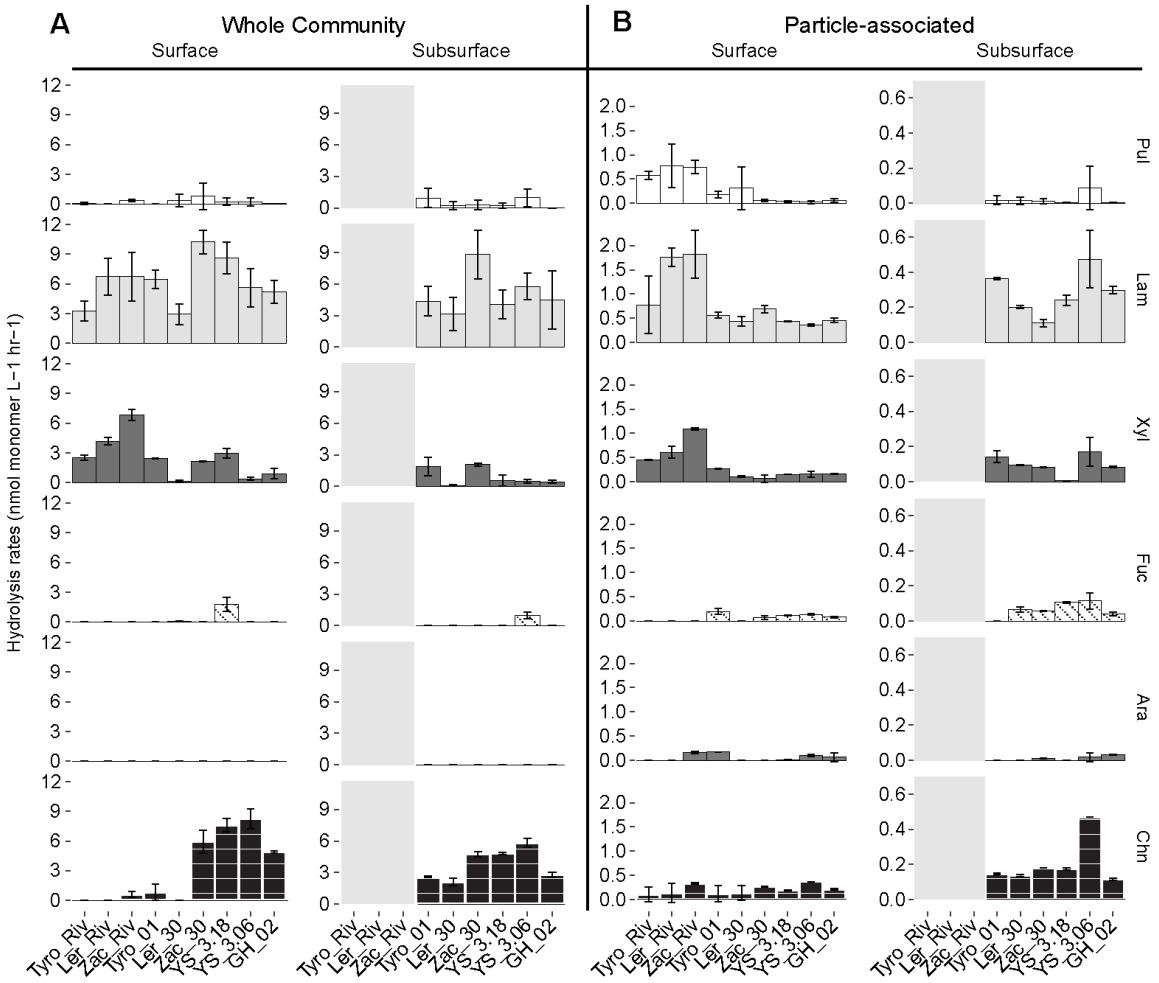

Figure 4. Principal Coordinates Analysis (PCoA) of bacterial community composition using Bray-Curtis dissimilarity index. OTU cutoff was set at 97% sequence similarity, and was picked using *de novo* methods. The groupings are significantly different based on ANOSIM.

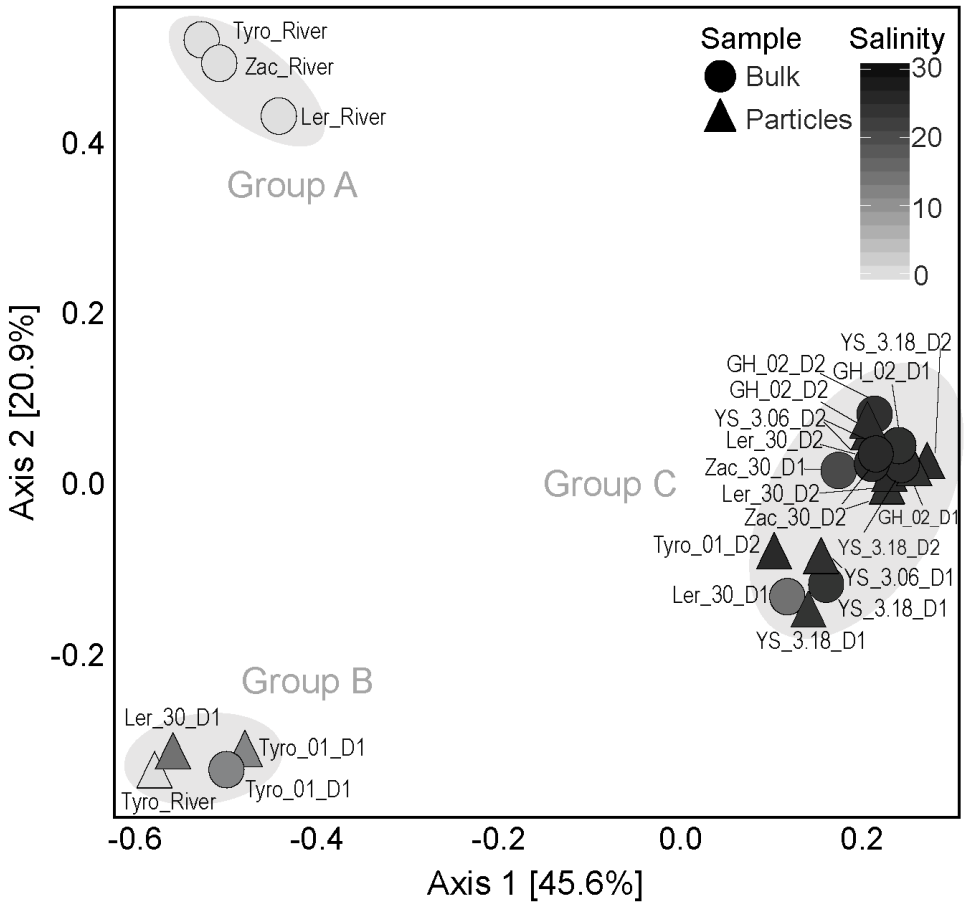

Figure 5. Class-level taxonomic breakdown of bacterial communities, arranged from left to right in order of increasing salinity, and from the head to the mouth of the fjord. Only bacterial classes with relative proportions of ≥1% was visualized to de-convolute the plot. The groups and legends for the symbols above the bar graph, are the same as those in Fig. 4. Square brackets around *Saprospirae* indicate the recommended taxonomic nomenclature based on genome trees in the Greengenes database.

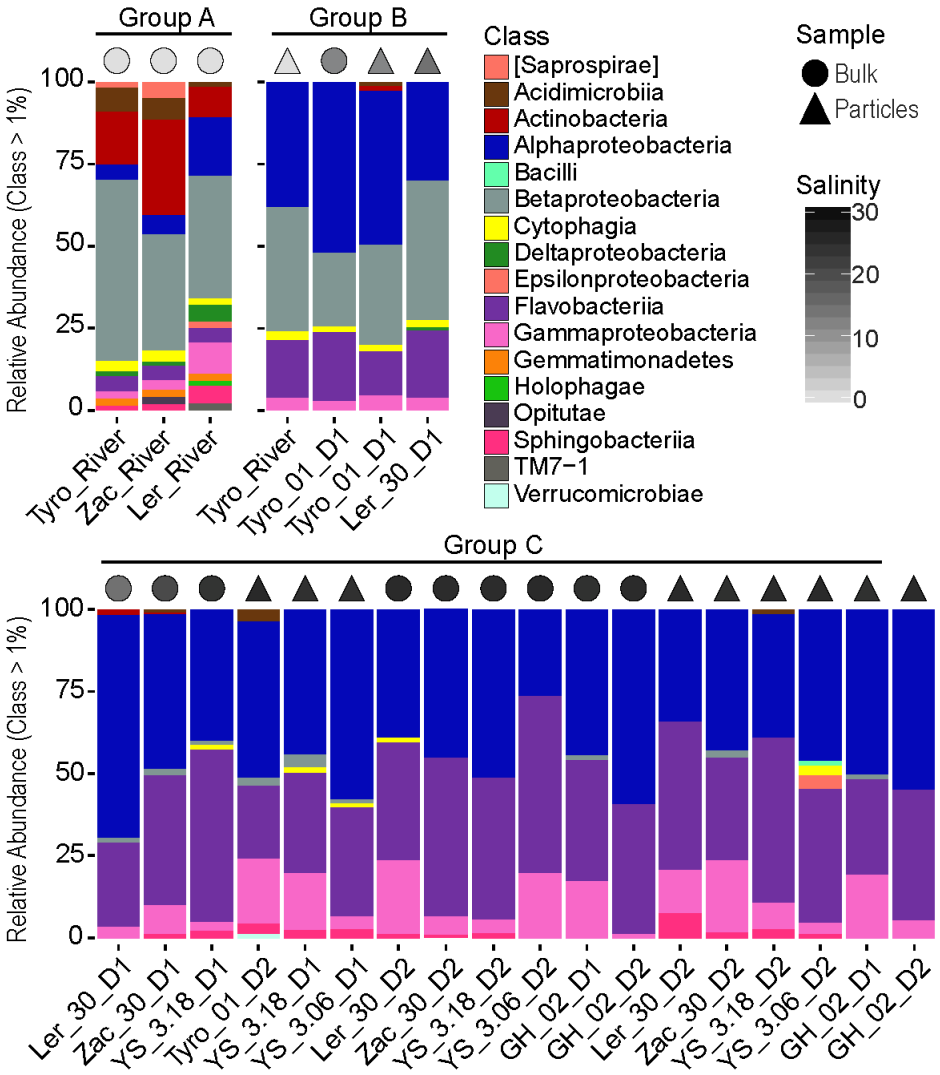

Figure 6. Constrained Analysis of Principal Coordinates of Bray-Curtis based dissimilarities in dissolved organic matter (DOM) composition. Data was square root transformed.

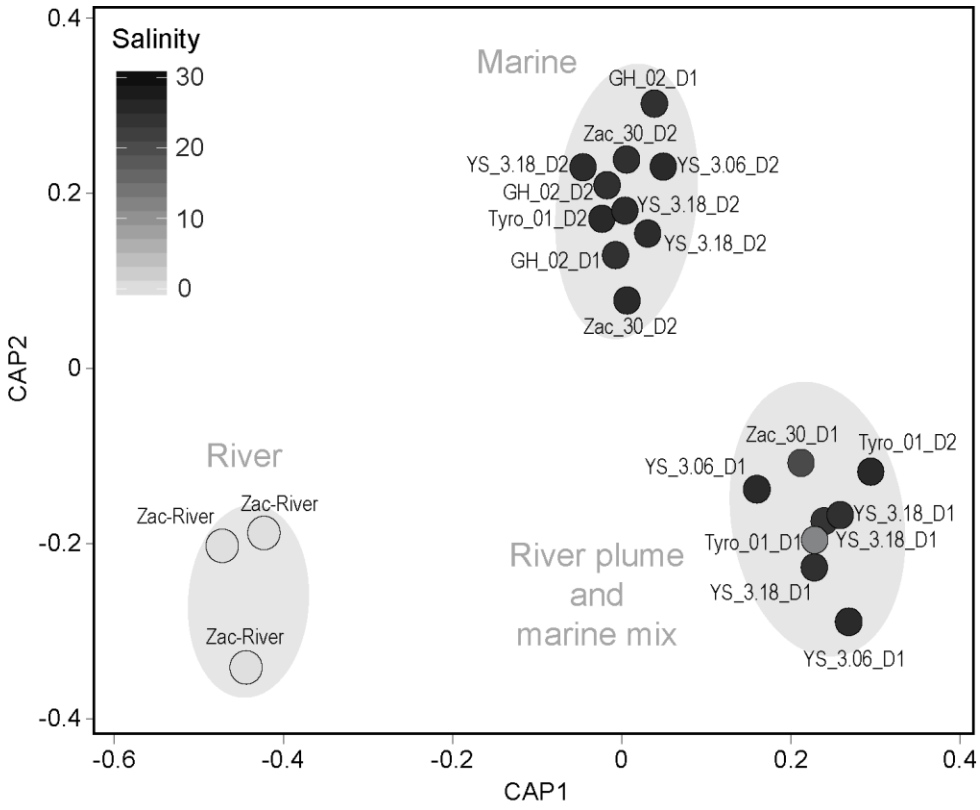

Figure 7. Relationship between specific enzyme activities and the relative proportions of their putative hydrolysis products. The analysis included: (A) leucine aminopeptidase vs. leucine; (B) combined QAR- and FSR-trypsin vs. arginine; (C) combined α- and β-glucosidase vs. glucose; and (D) AAPF-chymotrypsin vs. proline. The gray band corresponds to the 95% confidence interval for predictions from the linear model.

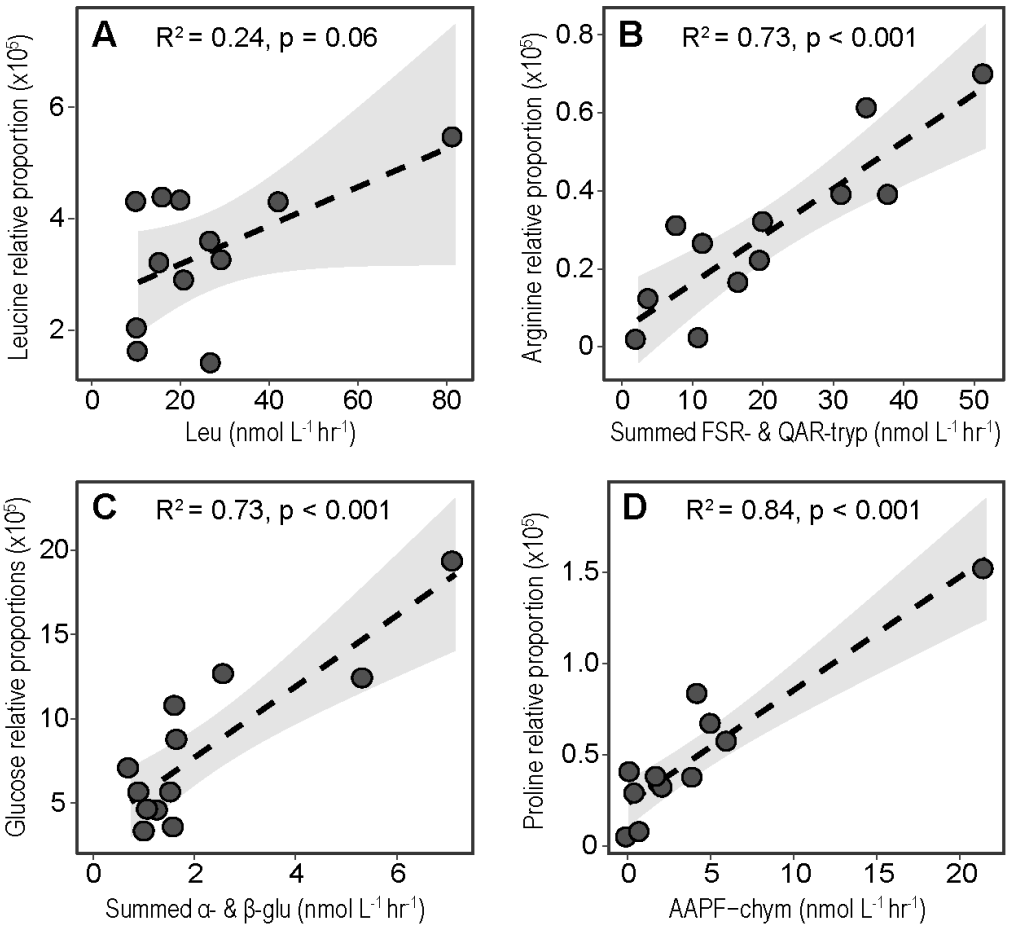

Table 1. Physical, geochemical, and bacterial parameters measured in rivers. SPM = Suspended Particular Matter. LOI = Loss on Ignition. BP = Bacterial Production. PA = Particle-Associated. FL = Free-Living. BA = Bacterial Abundance (cell counts).

	Tyroler River	Lerbugten River	Zackenberg River
Depth (m)	1	1	1
Temperature (°C)	NA	NA	7.9°C
Salinity (PSU)	0	0	0
Turbidity (FTU)	NA	NA	NA
Oxygen (µM)	NA	NA	NA
SPM (mg L^{-1})	316.1	552.3	234.4
LOI (%)	4.8	2.5	6.3
Mean grain size (µm)	8.5	17.8	5.7
BP - Bulk (µg C L^{-1} d^{-1})	0.33 ± .03	3.03 ± 0.42	3.28 ± 0.72
BP - PA (µg C L^{-1} d^{-1})	0.24	0.73	3.11
BP - FL (µg C L^{-1} d^{-1})	0.09 ± 0.01	2.29 ± 0.10	0.16 ± 0.06
BA - Bulk (10^6 cells mL^{-1})	0.29 ± 0.02	0.15 ± 0.03	0.51 ± 0.09
BA - PA (10^6 cells mL^{-1})	0.19	0.08	0.24
BA - FL (10^6 cells mL^{-1})	0.10 ± 0.08	0.07 ± 0.03	0.27 ± 0.01

Table 2. Physical, geochemical, and bacterial parameters measured in river transition sites. SPMC = Suspended Particular Matter. LOI = Loss on Ignition. BP = Bacterial Production. PA = Particle-Associated. FL = Free-Living. BA = Bacterial Abundance (cell counts).

	Tyro-01 Surface	Tyro-01 Subsurface	Ler-30 Surface	Ler-30 Subsurface	Zac-30 Surface	Zac-30 Subsurface
Depth (m)	2	20	2	20	2	20
Temp. (°C)	7.94	-0.27	6.22	0.29	0.2	0.1
Salinity (PSU)	12.55	31.52	15.52	31.33	22.3	29.9
Turbidity (FTU)	34.37	6.4	30.37	7.8	NA	NA
Oxygen (µM)	336.74	403.84	338.33	409.13	NA	NA
SPM (mg L^{-1})	7.8	2	71.5	5.8	95.3	4.4
LOI (%)	9.2	22.2	NA	NA	10.1	23.1
Mean grain size (µm)	9.3	12.1	10.5	NA	15	16.7
BP - Bulk (µg C L^{-1} d^{-1})	0.46 ± 0.10	0.26 ± 0.13	1.99 ± 1.03	2.03 ± 0.82	1.09 ± 0.44	1.20 ± 0.09
BP - PA (µg C L^{-1} d^{-1})	0.06	0	1.44	0.62	0.76	0.96
BP - FL (µg C L^{-1} d^{-1})	0.40 ± 0.10	0.27 ± 0.19	0.55 ± 0.23	1.41 ± 0.30	0.32 ± 0.08	0.23 ± 0.23
BA - Bulk (10^6 cells mL^{-1})	1.10 ± 0.01	0.32 ± 0.07	0.57 ± 0.07	3.90 ± 0.11	2.90 ± 0.58	2.20 ± 0.19
BA - PA (10^6 cells mL^{-1})	0.41	0	0.14	2.50	2.17	1.43
BA - FL (10^6 cells mL^{-1})	0.69 ± 0.05	0.76 ± 0.16	0.43 ± 0.06	1.40 ± 0.41	0.73 ± 0.06	0.77 ± 0.06

Table 3. Physical, geochemical, and bacterial parameters measured in the fjord. SPM = Suspended Particular Matter. LOI = Loss on Ignition. BP = Bacterial Production. PA = Particle-Associated. FL = Free-Living. BA = Bacterial Abundance (cell counts).

	YS 3.18 Surface	YS 3.18 Subsurface	YS 3.06 Surface	YS 3.06 Subsurface	GH02 Surface	GH02 Subsurface
Depth (m)	5	20	5	20	5	20
Temp. (°C)	2.74	0.15	1.14	-0.44	-1.42	-1.5
Salinity (PSU)	27.83	31.13	29.26	31.23	29.05	29.48
Turbidity (FTU)	9.28	1.87	4.07	2.24	8.69	3.29
Oxygen (µM)	361.81	392.55	370.17	381.57	372.7	380.95
SPM (mg L^{-1})	NA	NA	1.2	NA	7.7	2.4
LOI (%)	38	21.3	NA	NA	12	40
Mean grain size (µm)	29.6	10.4	NA	NA	NA	NA
BP - Bulk (µg C L^{-1} d^{-1})	2.36 ± 0.86	1.16 ± 0.17	4.39 ± 0.48	3.45 ± 1.24	NA	NA
BP - PA (µg C L^{-1} d^{-1})	0.57	0.53	2.16	1.01	NA	NA
BP - FL (µg C L^{-1} d^{-1})	1.80 ± 0.26	0.62 ± 0.05	2.24 ± 1.01	2.44 ± 0.87	NA	NA
BA - Bulk (10^6 cells mL^{-1})	NA	NA	3.50 ± 0.09	3.00 ± 0.69	NA	NA
BA - PA (10^6 cells mL^{-1})	NA	NA	2.40	1.90	NA	NA
BA - FL (10^6 cells mL^{-1})	NA	NA	1.10 ± 0.34	1.10 ± 0.19	NA	NA

3.8 Supplementary Figures

Figure S1. Timecourse development for polysaccharide hydrolase activities, including those for: (A) river bulk waters, (B) river particles, (C) transition site bulk waters (D) transition site particles, (E) fjord bulk waters, and (F) fjord particles. Data shown are the average rates and standard deviations across triplicate incubations per substrate. Note the scale differences across different figure panels.

A

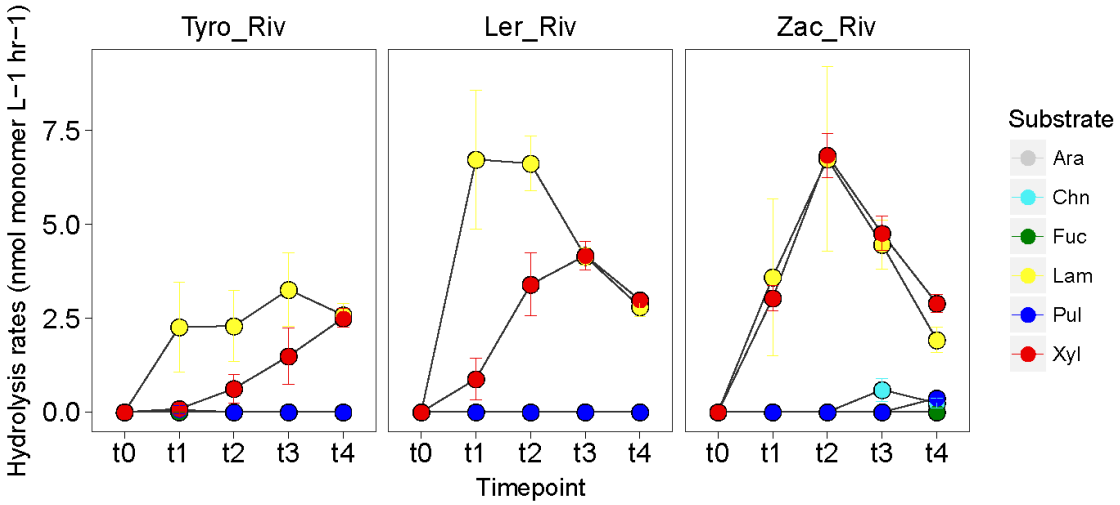

B

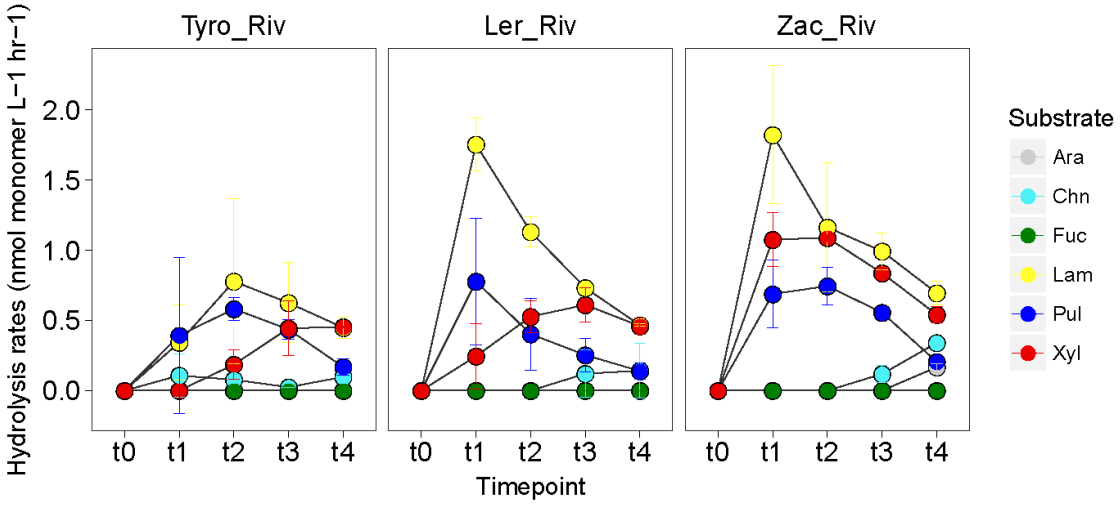

[Figures S1C, S1D, S1E, and S1F are in the next pages]

Figure S1. Timecourse development for polysaccharide hydrolase activities, including those for: (A) river bulk waters, (B) river particles, (C) transition site particles, (D) transition site particles, (E) fjord bulk waters, and (F) fjord particles. Data shown are the average rates and standard deviations across triplicate incubations per substrate. Note the scale differences across different figure panels.

C

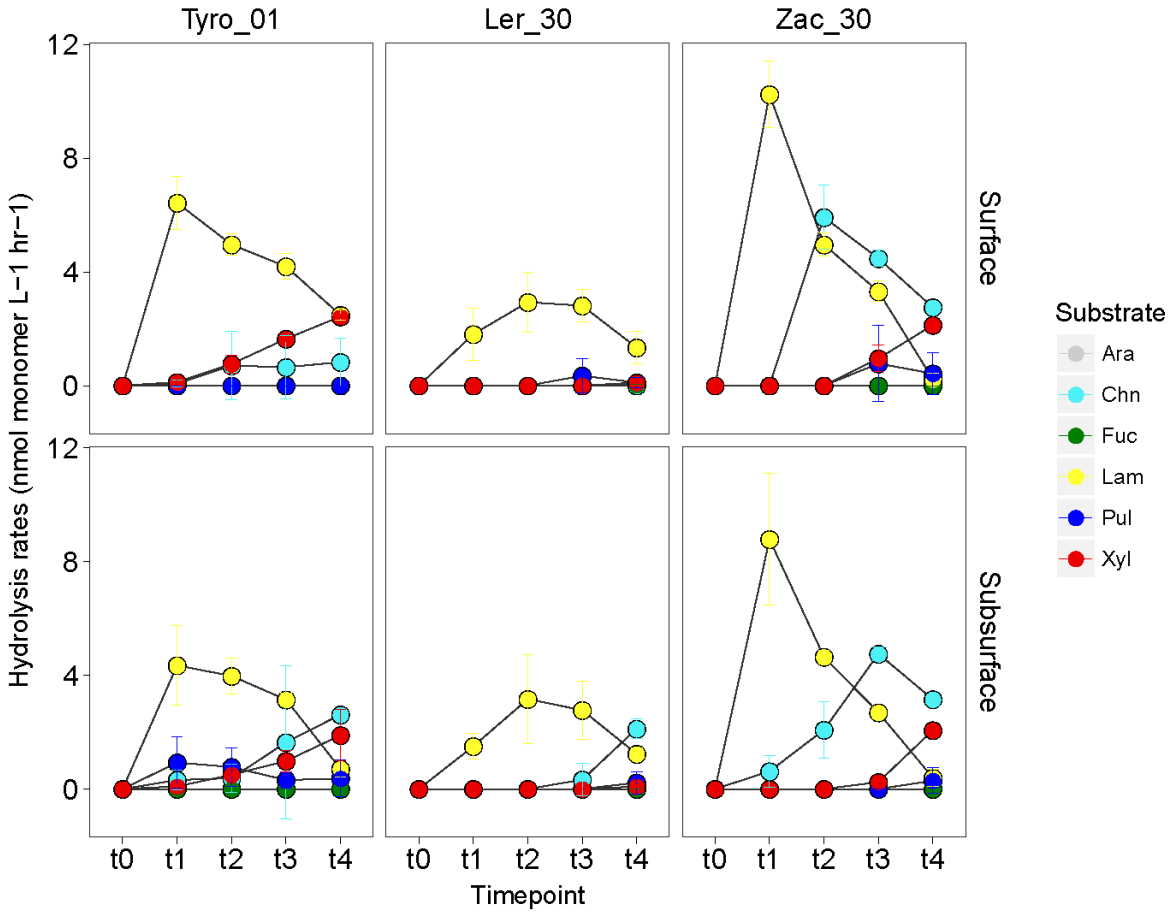

[Figures S1D, S1E, and S1F are in the next pages]

Figure S1. Timecourse development for polysaccharide hydrolase activities, including those for: (A) river bulk waters, (B) river particles, (C) transition site particles, (D) transition site particles, (E) fjord bulk waters, and (F) fjord particles. Data shown are the average rates and standard deviations across triplicate incubations per substrate. Note the scale differences across different figure panels.

D

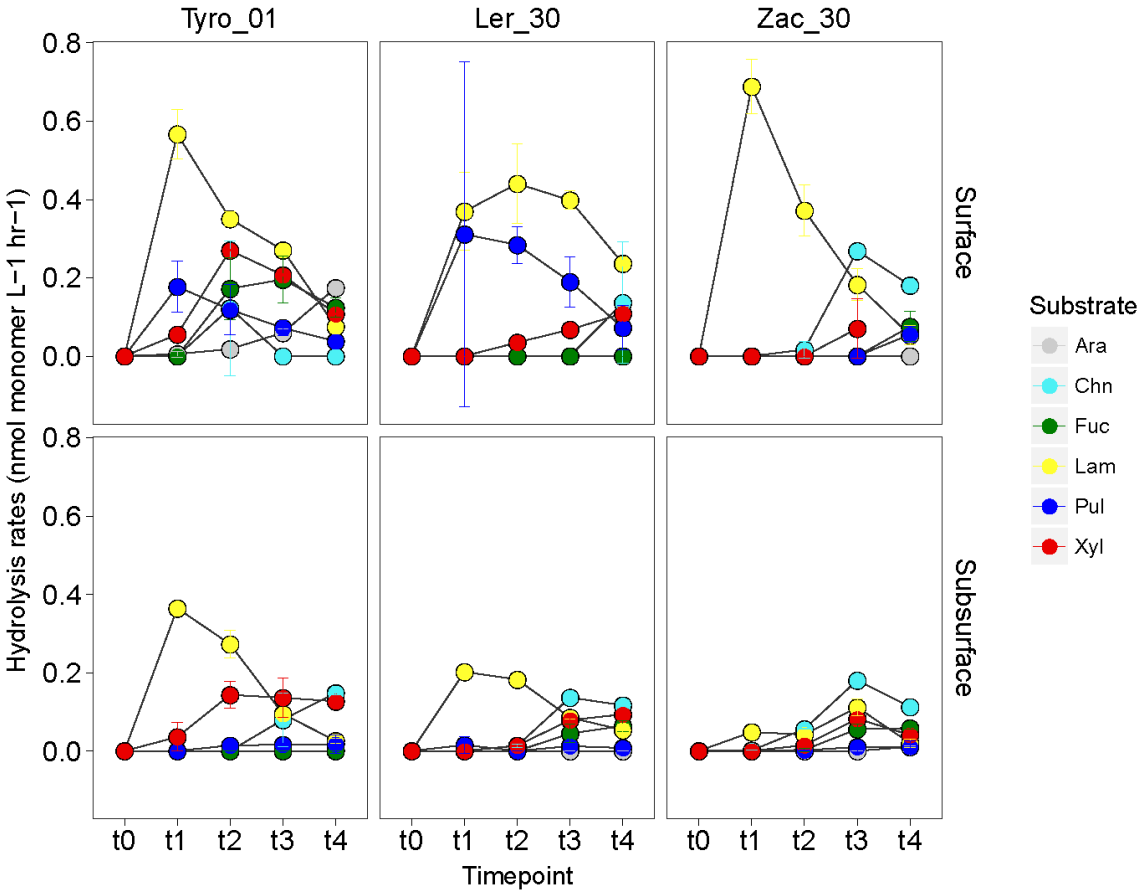

[Figures S1E, and S1F are in the next pages]

Figure S1. Timecourse development for polysaccharide hydrolase activities, including those for: (A) river bulk waters, (B) river particles, (C) transition site particles, (D) transition site particles, (E) fjord bulk waters, and (F) fjord particles. Data shown are the average rates and standard deviations across triplicate incubations per substrate. Note the scale differences across different figure panels.

E

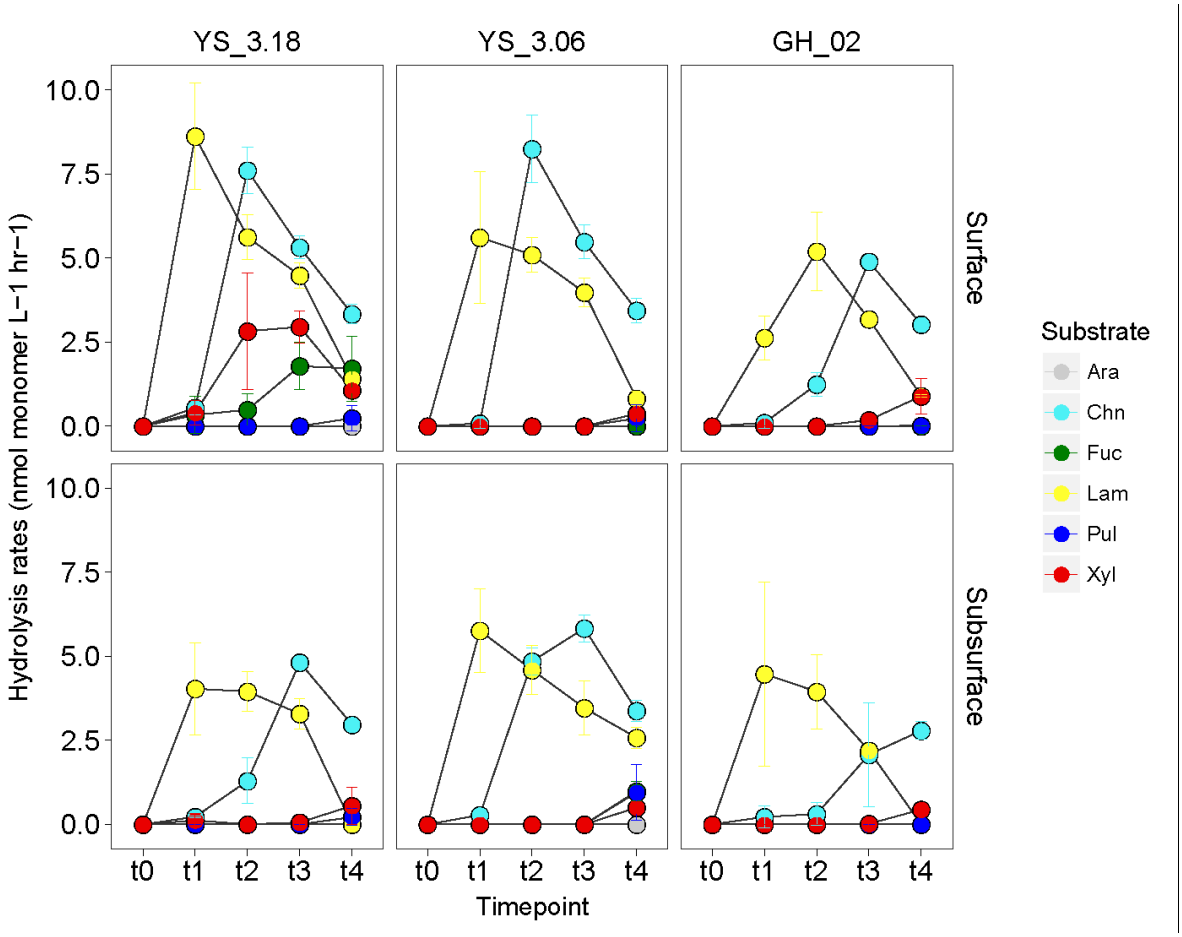

[Figures S1F is in the next page]

Figure S1. Timecourse development for polysaccharide hydrolase activities, including those for: (A) river bulk waters, (B) river particles, (C) transition site particles, (D) transition site particles, (E) fjord bulk waters, and (F) fjord particles. Data shown are the average rates and standard deviations across triplicate incubations per substrate. Note the scale differences across different figure panels.

F

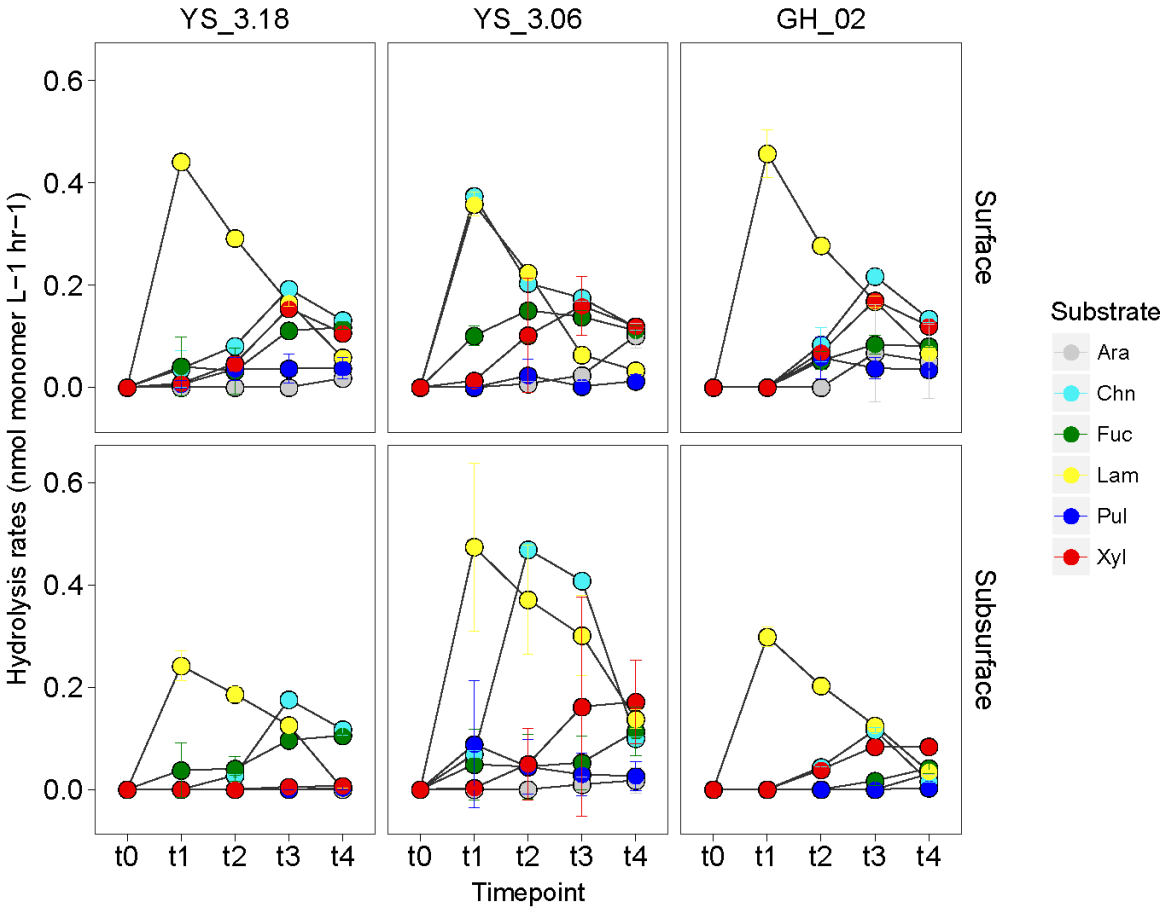

Figure S2. Whole community (A) and particle-associated peptidase and glucosidase activity rates for surface and subsurface waters. The light grey shading in the subsurface panels indicates that no subsurface measurements were taken in the rivers. From left to right within each plot, stations are arranged by salinity and from the inner to the outer part of the fjord. Reported rates are averaged from triplicate (whole community) or duplicate (particle-associated) incubations, and taken 12 hrs after the start of incubation.

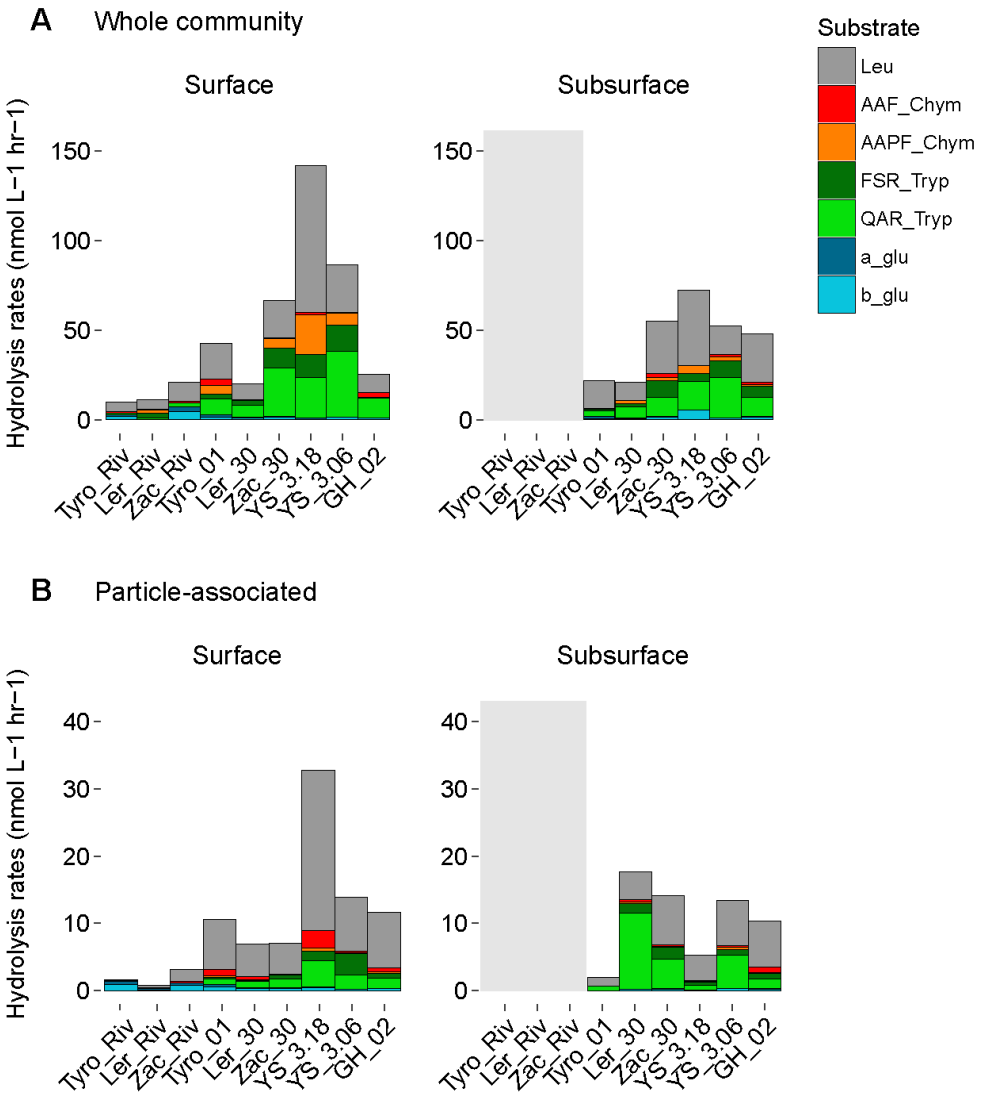

Figure S3. Comparison of bulk summed peptidase and glucosidase rates versus bacterial cell counts in bulk waters (A), on particles (B) and for the free-living fraction (C). Peptidase and glucosidase rates for the free-living fraction were not directly measured. To obtain free-living enzymatic activity rates, particle-associated rates were subtracted from the bulk water rates. Note the differences in scale.

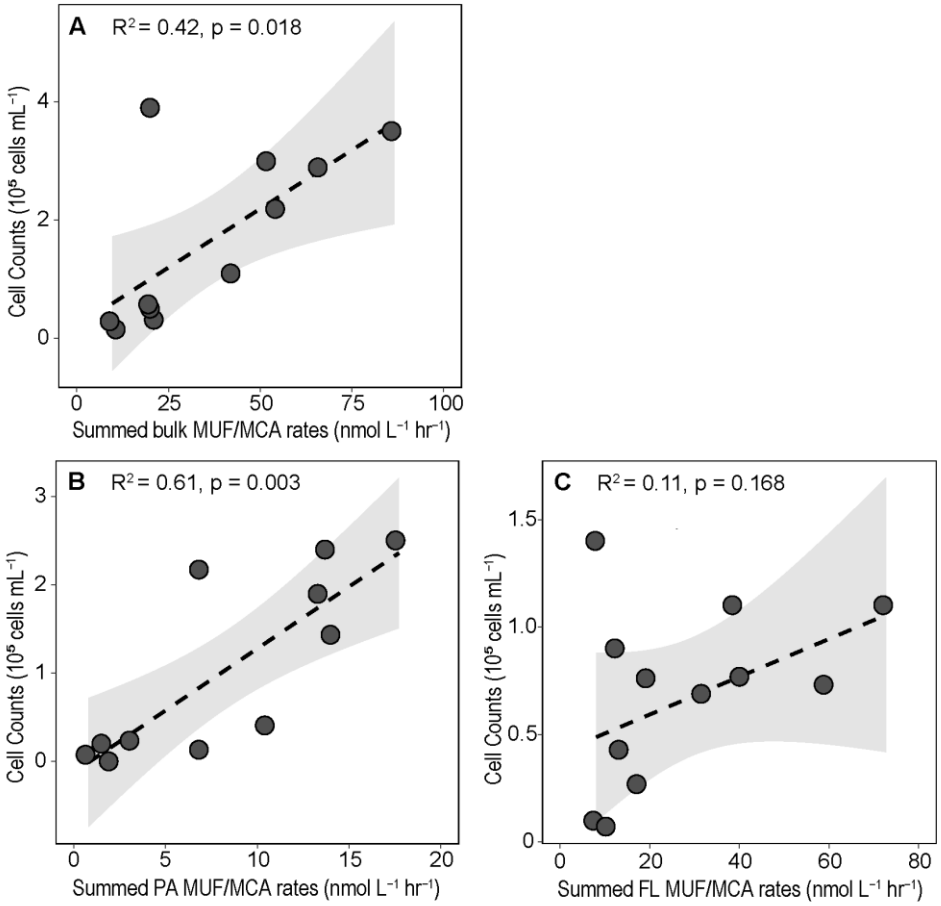

Figure S4. Cell count-normalized peptidase and glucosidase activities in surface and subsurface waters. (A) Leucine-aminopeptidase, (B) AAF-Chymotrypsin, (C) AAPF-Chymotrypsin, (D) FSR-Trypsin, (E) QAR-Trypsin, (F) α-glucosidase, and (G) β-glucosidase. Note the scale differences.

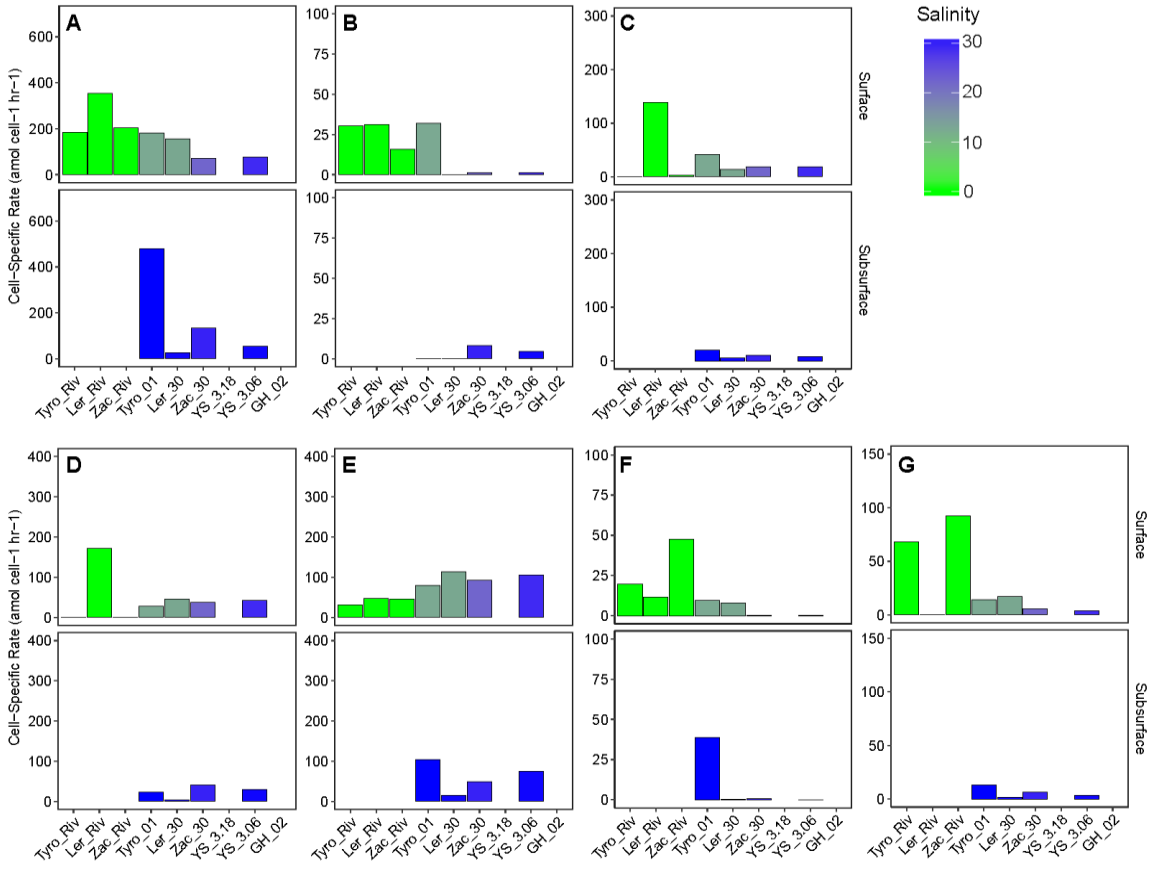

Figure S5. Whole community (A) and particle-associated polysaccharide activity rates for surface and subsurface waters. The light grey shading in the subsurface panels indicates that no subsurface measurements were taken in the rivers. From left to right within each plot, stations are arranged by salinity and from the inner to the outer part of the fjord. Reported rates are averaged from triplicate (whole community) or duplicate (particle-associated) incubations, and taken at varying timepoints throughout the incubation.

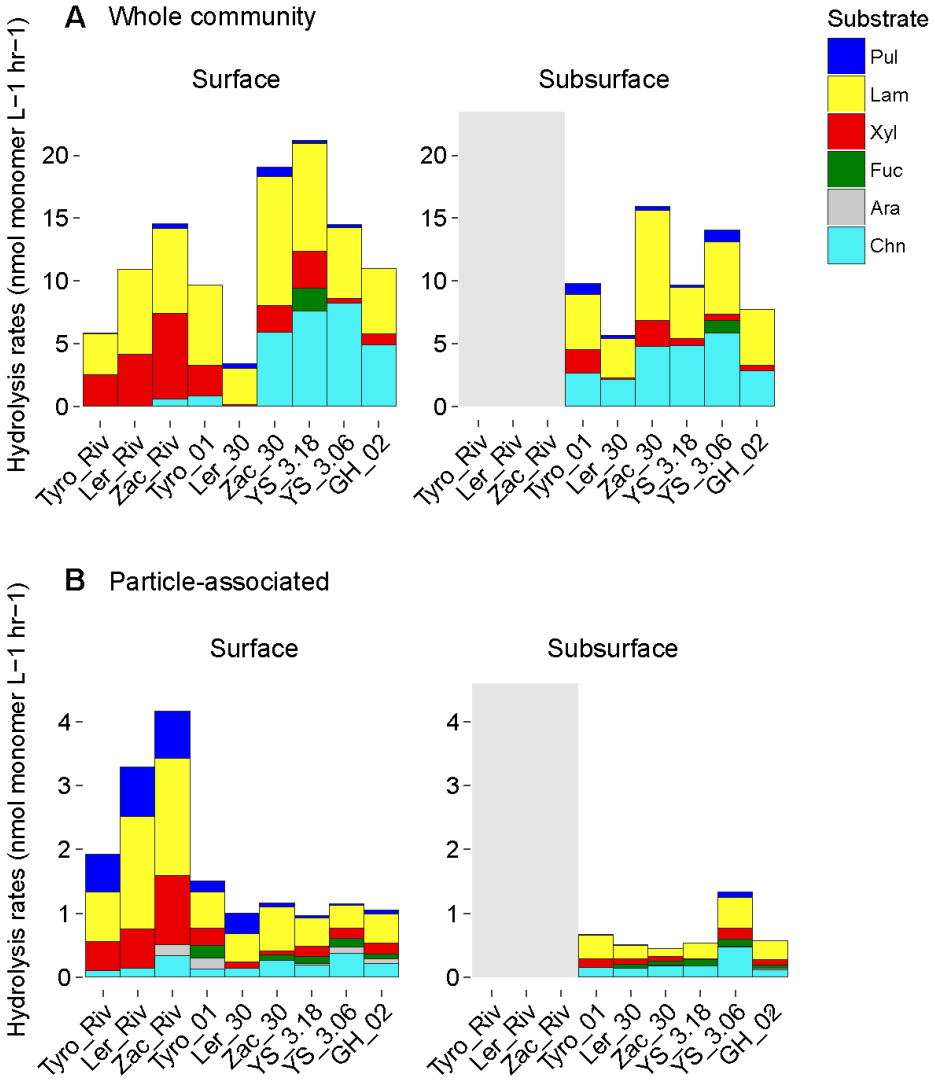

Figure S6. Alpha diversity measures, including observed species richness, Chao1 species richness index, and Shannon index for species evenness. The stations are ordered by increasing average species richness (based on observed species richness) for various sample types (surface, subsurface, bulk, particles) per station.

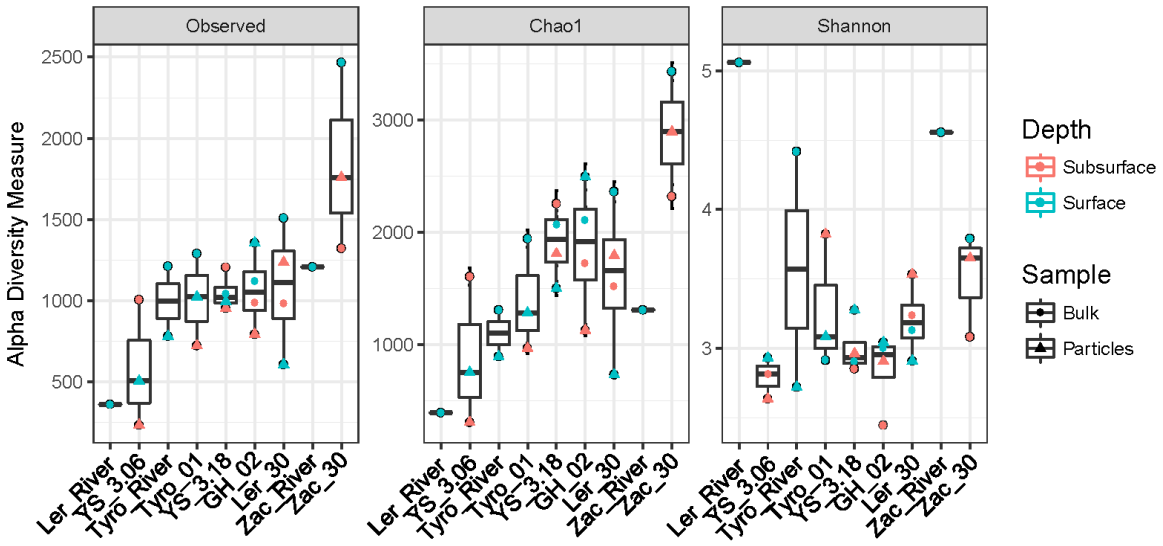

Figure S7. Constrained Analysis of Principal Coordinates of Bray-Curtis based dissimilarities in dissolved organic matter (DOM) composition, excluding river samples. Data was square root transformed.

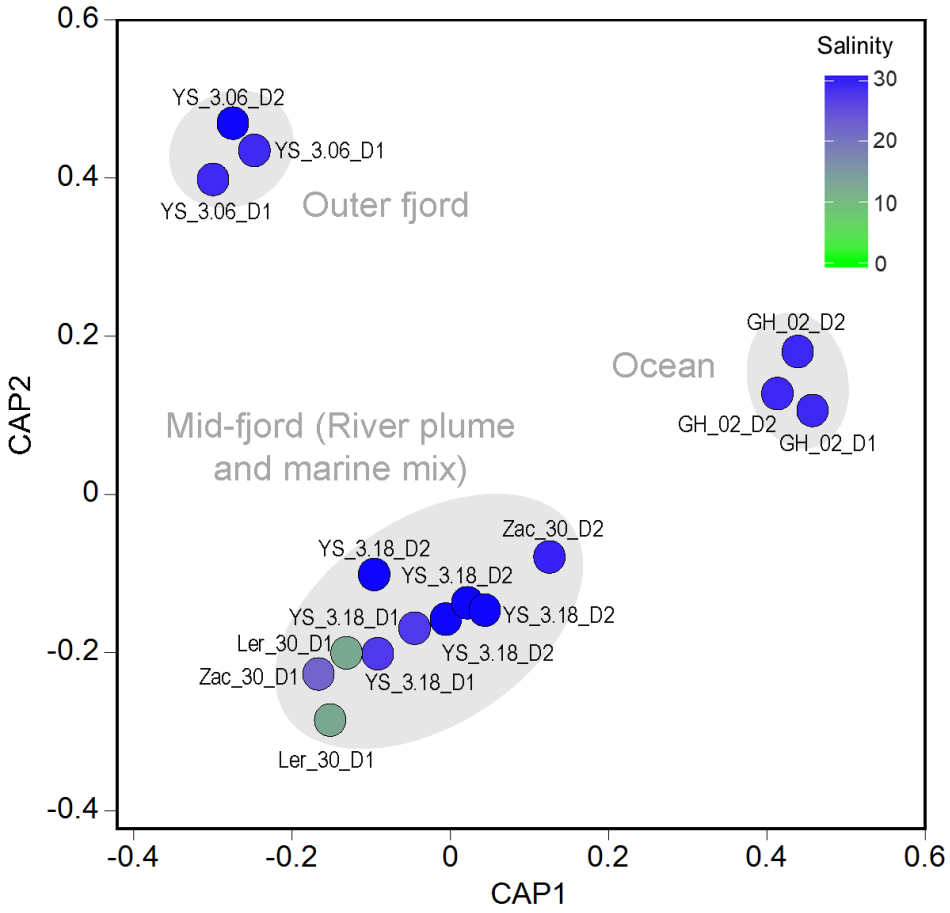

Figure S8. Relative concentrations of specific enzymatic hydrolysis products from the DOM composition dataset, including (A) leucine, (B) proline, (C) arginine, and (D) glucose. No samples were available for stations and/or depths with no data. As these are relative proportions, the values can only be compared across stations for each substrate. However, still note the scale differences.

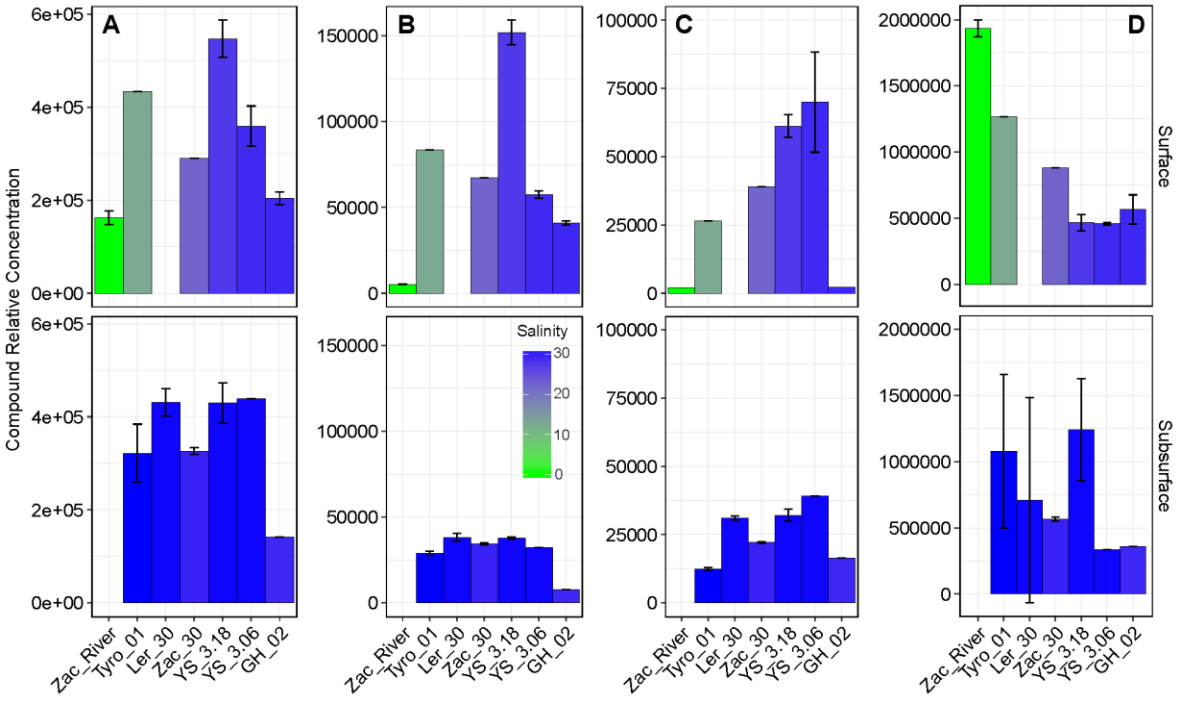

Table S1. Analysis of Similarity comparisons for bacterial community groupings in the Principal Coordinate Analysis (Fig. 4). Bray-Curtis dissimilarity index is used for the analyses. *Pvalues* in bold are considered statistically significant (≤0.05).

ANOSIM comparison	R	p_{val}
All samples (by groups)	0.997	**0.001**
Group A vs Group B	1	**0.026**
Group A vs Group C	1	**0.001**
Group B vs Group C	0.999	**0.002**
Group C (bulk vs. particle-associated)	0.042	0.275

REFERENCES

Amon, R. M. W., G. Budéus, and B. Meon. 2003. Dissolved organic carbon distribution and origin in the Nordic Seas: Exchanges with the Arctic Ocean and the North Atlantic. J. Geophys. Res. **108**: 1-17, doi:10.1029/2002JC001594

Arnosti, C. 2003. Fluorescent derivatization of polysaccharides and carbohydrate-containing biopolymers for measurement of enzyme activities in complex media. J. Chromatogr. B. **793**: 181-191

Arnosti, C. 2011. Microbial extracellular enzymes and the marine carbon cycle. Annu. Rev. Mar. Sci. **3**: 401-425

Arnosti, C. 2015. Contrasting patterns of peptidase activities in seawater and sediments: An example from Arctic fjords of Svalbard. Mar. Chem. **168**: 151-156

Arnosti, C., and A. Steen. 2013. Patterns of extracellular enzyme activities and microbial metabolism in an Arctic fjord of Svalbard and in the northern Gulf of Mexico: contrasts in carbon processing by pelagic microbial communities. Front. Microbiol. **4**: 318. doi:10.3389/fmicb.2013.00318

Bendtsen, J., J. Mortensen, and S. Rysgaard. 2014. Seasonal surface layer dynamics and sensitivity to runoff in a high Arctic fjord (Young Sound/Tyrolerfjord, 74°N). J. Geophys. Res. Ocean. **119**:6461-6478

Bižić-Ionescu, M. and others 2015. Comparison of bacterial communities on limnic versus coastal marine particles reveals profound differences in colonization. Environ. Microbiol. **17**: 3500-3514

Bourgeois, S., P. Kerhervé, M. L. Calleja, G. Many, and N. Morata. 2016. Glacier inputs influence organic matter composition and prokaryotic distribution in a high Arctic fjord (Kongsfjorden, Svalbard). J. Mar. Sys. **164**: 112-127

Cameron, K. A. and others 2015. Diversity and potential sources of microbiota associated with snow on western portions of the Greenland Ice Sheet. Environ. Microbiol. **17**: 594-609

Crump, B. C., L. A. Amaral-Zettler, and G. W. Kling. 2012. Microbial diversity in arctic freshwaters is structured by inoculation of microbes from soils. ISME J. **6**: 1629-1639

Crump, B. C., E. V. Armbrust, and J. A. Baross. 1999. Phylogenetic analysis of particle-attached and free-living bacterial communities in the Columbia river, its estuary, and the adjacent coastal ocean. Appl. Environ. Microbiol. **65**: 3192-3204

Cui, X., T. S. Bianchi, and C. Savage. 2017. Erosion of modern terrestrial organic matter as a major component of sediments in fjords. Geophys. Res. Lett. **44**: 1457-1465

D'Ambrosio, L., K. Ziervogel, B. MacGregor, A. Teske, and C. Arnosti. 2014. Composition and enzymatic function of particle-associated and free-living bacteria: a coastal/offshore comparison. ISME J. **8**: 2167-2179

Delong, E. F., D. G. Franks, and A. L. Alldredge. 1993. Phylogenetic diversity of aggregate-attached vs free-living marine bacterial assemblages. Limnol. Oceanogr. **38**: 924-934

Dittmar, T., B. Koch, N. Hertkorn, and G. Kattner. 2008. A simple and efficient method for the solid-phase extraction of dissolved organic matter (SPE-DOM) from seawater. Limnol. Oceanogr: Methods. **6**: 230-235

Dubnick, A. S. Kazemi, M. Sharp, J. Wadham, J. Hawkings, A. Beaton, and B. Lanoil. 2017. Hydrological controls on glacially exported microbial assemblages. J. Geophys Res. Biogeosci. **122**: 1049-1061.

Eiler, A. and others. 2014. Productivity and salinity structuring of the microplankton revealed by comparative freshwater metagenomics. Environ. Microbiol. **16**: 2682-2698

Fellman, J. B., R. G. M. Spencer, P. J. Hernes, R. T. Edwards, D. V. D'Amore, and E. Hood. 2010. The impact of glacier runoff on the biodegradability and biochemical composition of terrigenous dissolved organic matter in near-shore marine ecosystems. Mar. Chem. **121**: 112-122

Fernandez-Gomez, B. and others. 2013. Ecology of marine Bacteroidetes: a comparative genomics approach. ISME J. **7**: 1026-1037

Fortunato, C. S., and B. C. Crump. 2015. Microbial gene abundance and expression patterns across a river to ocean salinity gradient. PLoS One. **10**: e0140578

Ghai, R. and others. 2011. Metagenomics of the water column in the pristine upper course of the Amazon River. PLoS One. **6**: e23785

Glud, R. N. O. Holby, F. Hofmann, and D. E. Canfield.1998. Benthic mineralization in Arctic sediments (Svalbard). Mar Ecol Prog Ser. **173**:237-251

Gutiérrez, M. H., P. E. Galand, C. Moffat, and S. Pantoja. 2015. Melting glacier impacts community structure of Bacteria, Archaea and Fungi in a Chilean Patagonia fjord. Environ. Microbiol. **17**: 3882-3897.

Hasler-Sheetal, H., M. C. N. Castorani, R. N. Glud, D. E. Canfield, and M. Holmer. 2016. Metabolomics reveals cryptic interactive effects of species interactions and environmental stress on nitrogen and sulfur metabolism in seagrass. Environ. Sci. Tech. **50**: 11602-11609

Hasler-Sheetal, H., L. Fragner, M. Holmer, and W. Weckwerth. 2015. Diurnal effects of anoxia on the metabolome of the seagrass *Zostera marina*. Metabolomics. **11**: 1208

Hewson, I., and J. A. Fuhrman. 2004. Richness and diversity of bacterioplankton species along an estuarine gradient in Moreton Bay, Australia. Appl. Environ. Microbiol. **70**: 3425-3433

Hood, E., and L. Berner. 2009. The effect of changing glacial coverage on the physical and biogeochemical properties of coastal streams in southeastern Alaska. J. Geophys. Res. **114**: G03001

Hood, E. and others 2009. Glaciers as a source of ancient and labile organic matter to the marine environment. Nature. **462**: 1044-1047

Hood, E., and D. Scott. 2008. Riverine organic matter and nutrients in southeast Alaska affected by glacial coverage. Nature Geosci. **1**: 583-587

Lawson, E. C. and others 2014. Greenland Ice Sheet exports labile organic carbon to the Arctic oceans. Biogeosciences. **11**: 4015-4028

Marie, D., C. P. D. Brussaard, R. Thyrhaug, G. Bratbak, and D. Vaulot. 1999. Enumeration of marine viruses in culture and natural samples by flow cytometry. Appl. Environ. Microbiol. **65**: 45-52

McMurdie, P. J., and S. Holmes. 2013. phyloseq: An R Package for Reproducible Interactive Analysis and Graphics of Microbiome Census Data. PLoS One. **8:** e61217

Mernild, S. H., Sigsgaard, C., Rasch, M., Hasholt, B., Hansen, B. U., Stjernholm, M. & Pedersen, D. 2007. Climate, river discharge and suspended sediment transport in the Zackenberg River drainage basin and Young Sound/Tyrolerfjord, Northeast Greenland. In: Rysgaard, S. & Glud, R. N. (Eds.), Carbon cycling in Arctic marine ecosystems: Case study Young Sound. Meddr. Grønland, Bioscience. **58**: 24-43

Oksanen J., and others. 2008. vegan: Community Ecology Package. R package 2.4-3

Opsahl, S., R. Benner, and R. Amon. 1999. Major flux of terrigenous dissolved organic matter through the Arctic Ocean. Limnol. Oceanogr. **44**: 2017-2023

Ortega-Retuerta, E., F. Joux, W. H. Jeffrey, and J. F. Ghiglione. 2013. Spatial variability of particle-attached and free-living bacterial diversity in surface waters from the Mackenzie River to the Beaufort Sea (Canadian Arctic). Biogeosciences. **10**: 2747-2759

Osterholz, H., T. Dittmar, and J. Niggemann. 2014. Molecular evidence for rapid dissolved organic matter turnover in Arctic fjords. Mar. Chem. **160**: 1-10.

Osterholz, H. and others. 2016. Deciphering associations between dissolved organic molecules and bacterial communities in a pelagic marine system. ISME J. **10**: 1717-1730.

Paulsen, M. L. and others 2017. Carbon bioavailability in a high Arctic fjord influenced by glacial meltwater, NE Greenland. Front. Mar. Sci. **4**: 176. doi: 10.3389/fmars.2017.00176

Rysgaard, S. & Sejr, M. K. 2007. Vertical fl ux of particulate organic matter in a High Arctic fjord: Relative importance of terrestrial and marine sources. In: Rysgaard, S. & Glud, R. N. (Eds.), Carbon cycling in Arctic marine ecosystems: Case study Young Sound. Meddr. Grønland, Bioscience. **58**: 110-119

Schmidt, M. L., J. D. White, and V. J. Denef. 2016. Phylogenetic conservation of freshwater lake habitat preference varies between abundant bacterioplankton phyla. Environ. Microbiol. **18**: 1212-1226

Sejr, M. and others. 2017. Evidence of local and regional freshening of Northeast Greenland coastal waters. Sci. Rep. **7**:13183

Smith, R. W., T. S. Bianchi, M. Allison, C. Savage, and V. Galy. 2015. High rates of organic carbon burial in fjord sediments globally. Nature Geosci. **8**: 450-453

Sørensen, H. L. and others. 2015. Seasonal carbon cycling in a Greenlandic fjord: An integrated pelagic benthic study. Mar Ecol Prog Ser. **539**:1-17

Sperling, M. and others 2013. Effect of elevated CO_2 on the dynamics of particle-attached and free-living bacterioplankton communities in an Arctic fjord. Biogeosciences. **10**: 181-191

Steen, A. D., and C. Arnosti. 2013. Extracellular peptidase and carbohydrate hydrolase activities in an Arctic fjord (Smeerenburgfjord, Svalbard). Aquat. Microb. Ecol. **69**: 93-99

Steen, A. D., J. P. Vazin, S. M. Hagen, K. H. Mulligan, and S. W. Wilhelm. 2015. Substrate specificity of aquatic extracellular peptidases assessed by competitive inhibition assays using synthetic substrates. Aquat. Microb. Ecol. **75**: 271-281

Stepanauskas, R., H. Edling, and L. J. Tranvik. 1999. Differential dissolved organic nitrogen availability and bacterial aminopeptidase activity in limnic and marine waters. Microb. Ecol. **38**: 264-272

Stibal, M. and others 2015. Microbial abundance in surface ice on the Greenland Ice Sheet. Front. Microbiol. **6**: 225

Stibal, M., E. C. Lawson, G. P. Lis, K. M. Mak, J. L. Wadham, and A. M. Anesio. 2010. Organic matter content and quality in supraglacial debris across the ablation zone of the Greenland ice sheet. Ann. Glaciol. **51**: 1-8

Stibal, M., M. Sabacka, and J. Zarsky. 2012. Biological processes on glacier and ice sheet surfaces. Nature Geosci. **5**: 771-774

Teske, A., A. Durbin, K. Ziervogel, C. Cox, and C. Arnosti. 2011. Microbial community composition and function in permanently cold seawater and sediments from an Arctic fjord of Svalbard. Appl. Environ. Microbiol. **77**: 2008-2018

Wassmann, P. 2015. Overarching perspectives of contemporary and future ecosystems in the Arctic Ocean. Prog. Oceanogr. **139**: 1-12

Zeng, Y., T. Zheng, and H. Li. 2009. Community composition of the marine bacterioplankton in Kongsfjorden (Spitsbergen) as revealed by 16S rRNA gene analysis. Polar Biol. **32**: 1447-1460

CHAPTER 4: CONSEQUENCES OF COMMUNITY STRUCTURAL DIFFERENCES FOR MICROBIAL RESPONSE TO HIGH MOLECULAR WEIGHT ORGANIC MATTER

4.1 Introduction

Marine microbial communities play a crucial role in global carbon cycling by secreting enzymes that catalyze the initial step of organic matter degradation (Arnosti, 2011). The enzymatic capabilities of microbial communities determine which constituents of organic matter are assimilated into biomass or remineralized, and which fractions evade degradation. Yet, despite the global importance of microbial carbon cycling, factors that control the breakdown of organic matter are poorly constrained. In particular, the extent to which differences in degradation processes parallel variations in environmental factors and microbial community composition remain little understood (Arnosti, 2011). This limitation ultimately hinders our understanding of the functional consequences of community composition for the degradation of organic matter.

Studies provide conflicting evidence on the relative influence of environmental conditions versus bacterial community structure on community function. Observations that microbial communities—shaped by different assembly processes (Martiny et al., 2006, Ramette and Tiedje, 2007; Nemergut et al., 2013)—exert control on community function signify functional dissimilarity (Reed and Martiny, 2007, Strickland et al., 2009). In contrast, findings that specific functions of interest can be carried out by multiple members of the community indicate functional redundancy (Burke et al., 2011; Frossard et al., 2012, D'Ambrosio et al., 2014). These findings suggest that environmental conditions, in certain instances, may govern the functioning of microbial communities, resulting in little to no

functional variation despite community differences (Langenheder et al., 2006, Allison and Martiny, 2008; Frossard et al., 2012).

The degree of functional redundancy within communities is determined in part by the phylogenetic breadth of specific traits of interest. For example, rates of broad-scale processes that are phylogenetically widespread, such as carbon remineralization or respiration, are invariant even with differences in community composition (Balser and Firestone, 2005, Langenheder et al., 2006). In contrast, functions that are phylogenetically less widespread, such as nitrogen fixation (Bell et al., 2005) and specific enzymatic activities, show variations in process rates with differences in community structure (Langenheder et al., 2006). For carbon utilization, the ability to utilize low molecular weight organic matter is more phylogenetically widespread than that for high molecular weight compounds (Logue et al., 2016). As trait complexity—which increases with the number of genes involved in the function—and phylogenetic distribution may be inversely correlated (Martiny et al., 2013), the taxonomic breadth of traits of interest should be considered in investigations of structure-function relationships (Comte et al., 2013; Knelman and Nemergut, 2014).

The balance between functional dissimilarity and functional redundancy within a community determines whether microbial responses to natural environmental fluctuations or disturbances have functional implications (Allison and Martiny, 2008). However, whether community shifts following perturbations result in an enhanced or decreased community function depends on the relationship between ‘response traits’ and measured ‘effect traits’ (Knelman and Nemergut, 2014). Response traits directly interact with environmental changes and shape the distribution of members of a community (e.g., tolerance to increased salinity, ability to associate with organic particles), whereas effect traits partially determine their functional role (e.g., carbon fixation or remineralization). If communities are shaped primarily by niche-based (deterministic) processes, changes in environmental conditions

select for taxa with specific response traits, which may be coupled with the effect trait of interest. Bacterial community succession in response to phytoplankton blooms (response trait), and subsequent increases in carbon remineralization rates (effect trait) (Teeling et al., 2012), represents a niche filtration process in which the response and effect traits are coupled. Alternatively, when communities are shaped by neutral (stochastic) processes, the response and effect traits are decoupled. Thus, changes in community composition can have varied impacts on ecosystem function.

In the oceans, water masses are characterized by hydrographic signatures that shape microbial communities (Agogue et al., 2011; Galand et al., 2010), but the extent to which compositional differences have significance for organic matter degradation capabilities are poorly characterized. We investigated the succession of distinct marine microbial communities—from four different North Atlantic water masses—in response to addition of high molecular weight particulate organic matter (HMW-POM). This HMW-POM was derived from *Thalassiosira weissflogii*, a globally widespread centric diatom (Hartley et al., 1996; Stoermer et al., 1999). We tested the hypothesis that distinct microbial communities would exhibit varying compositional succession in response to the HMW-POM. We also hypothesized that differences in community composition would parallel variations in the rates and spectrum of enzymatic activities, as the ability to associate with HMW-POM (response trait) is likely coupled with the effect trait of enzymatic breakdown of organic matter. Finally, as particulate matter hosts bacterial communities with a broad spectrum of enzymatic activities (Ziervogel and Arnosti, 2008), we hypothesized that microbial communities would secrete a broader spectrum of enzymes in the presence of HMW-POM than without. Inducing the same disturbance among distinct microbial communities through this mesocosm approach provides insight into the consequences of community differences.

4.2 Materials and Methods

Water collection and characteristics. Between April 28 and April 29, 2015, aboard R/V *Endeavor* (EN556), seawater was collected from the surface and near bottom at two stations: one within the continental shelf of the North Atlantic (Stn 4) and the other in the open North Atlantic (Stn 8) (Fig. 1). A 30L Niskin bottle rosette was used to collect the water. From each depth, 20L seawater from single Niskin bottles was dispensed using acid-cleaned silicon tubing into a single carboy. Prior to filling, carboys were rinsed 3x with water from the same Niskin bottle used to fill the carboy. Six carboys were filled at each depth. Surface water at Stn 4 (7.7°C , salinity of 33.4 PSU), was cooler and less saline than bottom water (199 m; 12°C and 35.6 PSU; Table 1). Based on water mass characteristics and previous physical oceanographic studies conducted in these waters, Stn 4 surface water is Mid Atlantic Bight shelf water, while Stn 4 bottom water is a Gulf Stream warm core ring (Hoarfrost et al., unpubl). At Stn 8, surface water (18.8°C and 36.3 PSU) was characteristic of Gulf Stream water. Bottom waters (4500 m) at Stn 8 measured at 2.2°C and 34.9 PSU, and is characteristic of North Atlantic Deep Water. Samples were stored either at 4°C or 20°C in polysterene (Nalgene) 20 L carboys.

Preparation of high molecular weight Thalassiosira particulate matter. *Thalassiosira weissflogii* (ReedMariculture) was frozen at -20°C, then thawed, homogenized with a tissue grinder, and dialyzed using a 10 kD membrane (SpectraPor) in order to remove low molecular weight compounds. The retentate was lyophilized, autoclaved, frozen and lyophilized again. The final C:N ratio of the prepared HMW *Thalassiosira* was 6.03:1. The total carbohydrate content was 6.15%.

Mesocosm setup and subsampling. Triplicate 20L carboys were amended with ca. 500 mg (exact mass was recorded for each addition) of HMW *Thalassiosira*; unamended triplicate carboys were used for controls. All mesocosms were incubated in the dark: Stn 8 surface water mesocosms were stored at room temperature (ca. 18°C), while the rest were

kept at 4°C. Mesocosms were sub-sampled at the start of incubation, and then after 2.5 d, 8d, 15d, 28d, and 69d for the following assays: bacterial production using ^{3}H-leucine, dissolved organic carbon (DOC), nutrients, bacterial cell counts, total carbohydrates (TCHO), peptidase and glucosidase activity measurements, and bacterial community composition analyses. At the 15d timepoint, sub-samples were also taken to measure polysaccharide hydrolase activities.

Bacterial production and cell counts. Bacterial production was measured in triplicate, plus a killed control. Each live replicate and killed control received 1.5 mL of mesocosm water and L-[3,4,5-3H(N)]-Leucine (PerkinElmer, NET460250UC); the killed control additionally received 100% (w/v) TCA. Samples were incubated between 4 and 24 hours in the dark, close to *in situ* temperature, and then killed using 89 µL of 100% TCA. Samples were processed following (Kirchman et al., 1985; Kirchman, 2001).

Bacterial cells were counted by flow cytometry (Gasol and Del Giorgio, 2000). At each subsampling timepoint, 1 mL water was fixed with 0.1% glutaraldehyde (final concentration) for 10 min at room temperature in the dark, and stored frozen at -80 °C. Prior to analysis, thawed samples were pipetted through a cell strainer (Flowmi, 70 µm porosity) and stained with SYBR Green I for 15 min on ice in the dark. Counts were performed with a FACSCalibur flow cytometer (Becton-Dickson) using fluorescent microspheres (Molecular Probes) of 1 µm in diameter as internal size standard. Cells were counted according to their right angle scatter and green fluorescence using the FloJo 7.6.1 software.

Dissolved Organic Carbon (DOC) concentration. Subamples were filtered through a combusted glass fiber filter (GFF, Whatman 1825-025 Glass Microfiber Binder Free Filter) in a polycarbonate filter holder attached to a 60 cc syringe. The filtrate was collected in 20 mL scintillation vials and acidified with 100 µL of 50% phosphoric acid. Acidified samples were frozen at -20°C until analysis via high temperature catalytic oxidation on a Shimadzu Total Organic Carbon analyzer (TOC-8000A/5050A).

Nutrient analyses. Subsamples (ca. 50 mL) were collected and filtered through a 0.2 µm pore-size surfactant-free cellulose acetate (SFCA, Sartorius Minisart) into 50 mL tubes, and frozen at -20°C. 15 mL subsamples were sent to the LSU College of the Coast and Environment, Wetland, Biogeochemistry, Analytical Services Facility (WBAS) for nutrient analyses. Concentrations of ammonia, nitrate, nitrite and soluble reactive phosphorus were determined using an OI Analytical Flow Solutions IV auto analyzer.

Peptidase and glucosidase activities. Activities of exo- (terminal-unit cleaving) and endo-acting (mid-chain cleaving) peptidases, and exo-acting glucosidases were measured using methylcoumarin-labelled (MCA) peptide and methylumbelliferyl-tagged (MUF) glucose substrates: leucine-MCA (Leu), alanine-alanine-phenylalanine-MCA (AAF-chym), alanine-alanine-proline-phenylalanine-MCA (AAPF-chym), glutamine-alanine-arginine-MCA (QAR-tryp), boc-phenylalanine-serine-arginine (FSR-tryp), α-D-glucopyranoside (α-glu), and β-D-glucopyranoside (β-glu). At each timepoint, from each amended and unamended mesocosm, live and autoclaved (killed control) seawater was added to 200 µL 96-well plates (black, “U” bottom, polystyrene). For each mesocosm, each enzyme activity was measured in triplicate. Peptide and glucose substrates were added to a final concentration of 125 µM, a concentration chosen following an initial saturation curve and kept constant for all enzymatic assays. Fluorescence was measured over a timecourse of 72h using a plate reader (Tecan SpectraFluor Plus). Fluorescence values were converted to concentration of hydrolyzed substrate by comparison with a standard curve made from the fluorescence response of free MCA and MUF.

Polysaccharide hydrolase activities. Activities of enzymes that hydrolyze six polysaccharides—pullulan, laminarin, xylan, fucoidan, arabinogalactan and chondroitin—were measured using fluorescently labeled (FLA-) polysaccharides in freshly collected seawater as well as in subsampled mesocosm waters at the 15d (t3) timepoint (Arnosti, 2003). Polysaccharide hydrolase activity was measured in the mesocosm water 15d post-

Thalassiosira addition in order to give the microbial community time to react—via changes in enzyme expression or community composition—to the addition of HMW substrates. Given the length of time required to measure polysaccharide hydrolase activities (incubation times of days to weeks) as well as the time-consuming nature of sample analysis, we did not measure polysaccharide hydrolase activities in the seawater initially added to the carboys. However, activities were measured in water collected from the same depths and stations in the same CTD cast (Hoarfrost et al., unpubl). Polysaccharide hydrolase incubations were stored at *in situ* temperature and subsampled immediately after FLA-polysaccharide addition, and at timepoints 2d, 5d, 10d, 17d, and 30d post-addition. The effect of treatment on enzymatic activities, as well as other bacterial parameters, including bacterial cell counts, bacterial production, enzymatic activities, and DOC was tested using Analysis of Variance (ANOVA). We report the maximum rate in the main text to focus on the maximum potentials of the community, but the rates measured at all timepoints are included in the supplementary materials (Fig. S7).

DNA extraction, sequencing, community composition, and statistical analyses. Samples were filtered using a vacuum pump through a 0.2 µm pore size Millipore filter for DNA extractions. The volumes filtered ranged from 300 mL to 1 L, depending on cell densities. Filters were stored at -80°C until DNA extraction. For community analysis, only a subset of all samples was sequenced. These included all timepoint samples from the first amended and unamended replicate mesocosms. For biological replication, samples from the second and third amended and unamended replicate mesocosms were also analyzed at 2.5d (t1) and 15d (t3). A Powersoil DNA extraction kit (Qiagen) was used to extract DNA following manufacturer protocol. The V1-V2 hypervariable region of the 16S rRNA gene was amplified and sequenced using Illumina MiSeq PE 2x250 and the following primer set at the UNC Core Microbiome Sequencing Facility: 8F (5'- AGA GTT TGA TCC TGG CTC AG -3') and 338R (5'- GCT GCC TCC CGT AGG AGT -3').

Sequenced amplicon pairs were merged using QIIME (Caporaso et al., 2010), and OTUs at the 97% sequence similarity cutoff were picked *de novo* using default parameters. Chimeric sequences—identified using *ChimeraSlayer* (Haas et al., 2011)—and singletons were excluded from further analyses. Greengenes was used for OTU taxonomic classification. The BIOM-formatted OTU table and phylogenetic tree of representative sequences were used as input for downstream analysis using *phyloseq* library on R Studio (McMurdie and Holmes, 2013). Data used for whole-community analyses were rarefied to 22,000 sequences per sample to enable comparison of relative proportions across treatments and locations.

To explore differences in bacterial community composition, Bray-Curtis dissimilarity indices were calculated for each community, and was ordinated using Non-metric multidimensional scaling (NMDS). Differences in community similarity using the Bray-Curtis index were then tested using Analysis of Similarity (ANOSIM; Table 3). Permutational multivariate analysis of variance (PerMANOVA) as implemented through ADONIS on the R package *vegan* (Oksanen et al., 2008) was used to quantify the variation in community dissimilarities (Bray-Curtis) as a function of water mass origin.

4.3 Results

Bacterial parameters and DOC. Initial cell counts ranged from $3.1 \times 10^4 \pm 1.3 \times 10^4$ cells/mL in Stn 8 surface water unamended mesocosms to $2.6 \times 10^5 \pm 6.0 \times 10^4$ cells/mL at Stn 8 bottom waters (Fig. 2A). Cell numbers for amended mesocosms generally increased, and were, in all cases, significantly higher than in the unamended mesocosms (Table 2A). The greatest change occurred in Stn 4 bottom water amended mesocosms, in which cell counts increased by two orders of magnitude by 8d, but decreased after this timepoint (Fig. 2A). Bacterial protein production was also significantly higher in amended mesocosms than in untreated controls (Fig. 2B; Table 2B). In amended mesocosms, bacterial production was highest in Stn 4 bottom water at the 28d time point. In contrast, bacterial production was

comparatively low at Stn 8 bottom water, reaching only half of the maximum bacterial production rate of Stn 4 bottom water (Fig. 2B). Addition of *Thalassiosira* biomass caused a significant increase in DOC concentrations at all stations and depths (Fig. 2C, Table 2C).

Bacterial community composition. Distinct bacterial communities populated the water masses sampled, evident as separate clusters based on Bray-Curtis dissimilarities of bacterial OTUs at 97% sequence dissimilarity (Fig. 3A). Differences between initial bacterial communities were statistically significant (ANOSIM, R = 0.915, p = 0.001; Table 3). This pattern was also evident when phylogenetic distances were considered using unweighted UniFrac (Fig. S1A,B). On broad taxonomic levels, surface water communities were characterized by large relative proportions of class *Alphaproteobacteria* and *Flavobacteria*, with lesser contributions of class *Gammaproteobacteria* and phylum *Actinobacteria* (Fig. 3C). Stn 4 bottom waters had a large relative contribution of class *Alphaproteobacteria*, followed by class *Gammaproteobacteria*, *Flavobacteria*, *Deltaproteobacteria* and class AB16 within the phylum SAR406. Stn 8 bottom waters contained many of the same bacterial groups in similar relative proportions as Stn 4 bottom waters, but with the additional contribution of SAR202 within phylum *Chloroflexi* (Fig. 3C).

Incubation with HMW *Thalassiosira* altered the composition of initially distinct bacterial assemblages (Fig. 3A; Table 3). Bacterial communities in amended mesocosms shifted towards some compositional (Fig. 3A) and phylogenetic similarity (Fig. S1A,B) to initial and unamended bacterial communities in Stn 4 surface waters; however, the nature and rate of compositional shifts varied substantially by station and depth (Fig. 3B, 3C). Whereas bacterial communities in amended Stn 4 surface waters exhibited incremental changes, those in other mesocosms showed more rapid shifts at varying timepoints (Fig. 3A,C, Fig. S1A,B). Amended mesocosms with Stn 4 bottom waters and Stn 8 surface waters exhibited robust changes by 2.5d (t1), while Stn 8 bottom waters only showed dramatic shifts at 8d (t2). Accordingly, changes in community diversity in response to HMW-POM

varied across water masses, ranging from significant reduction in diversity at Stn. 4 and 8 bottom waters, to no change in Stn 4 surface waters (Fig. 3B; Table 2A). Furthermore, water mass origin of microbial communities in amended and unamended mesocosms was the largest source of community dissimilarity (PerMANOVA, $R^2 = 0.314$, $p = 0.001$), evident in the ordination space as separate clusters by station and depth (Fig. 3A; Fig. S1A,B) that differ significantly from each other (Table 3).

The majority of taxa that increased in the amended and unamended mesocosms belonged to the three most relatively abundant classes—*Gammaproteobacteria*, *Flavobacteria*, and *Alphaproteobacteria*—but their relative proportions and temporal distribution varied across locations (Fig. 3C). In Stn 4 surface waters, members of the class *Gammaproteobacteria* gradually increased in relative abundances. Gammaproteobacterial taxa in the bottom waters of Stn 4 and Stn 8 dominated in response to the treatment, albeit at varying timescales. Taxa within the class *Flavobacteria* exhibited a rapid “boom and bust” in Stn 8 surface waters. Members of the class *Alphaproteobacteria* initially decreased in relative proportions, but returned to pre-disturbance relative proportions in later timepoints (Fig. 3C)

The identities and relative contributions of specific OTUs that responded to the organic matter addition showed variability by location and treatment. Within the *Gammaproteobacteria*, members of the families *Colwelliaceae*, *Moritellaceae*, *Oceanospirillaceae, Pseudoalteromonadaceae,* and *Vibrionaceae* were among the immediate and most relatively abundant responders to *Thalassiosira* addition (Fig. S5C). Within these bacterial families, one or few OTUs became proportionally dominant. For example, one *Colwelliaceae* OTU dominated the amendment mesocosms from the surface water of Stn 4 and the bottom waters of Stn 4 and 8. Two different, but closely-related OTUs of *Colwelliaceae* were proportionally abundant in the Stn 8 surface water amended mesocosms (Fig. S2). The dominant *Moritellaceae* OTU exhibited a similar distribution

pattern: abundant in the amended surface waters of Stn 4, and the amended mesocosms of Stn 4 and 8 bottom waters (Fig. S2). Within *Pseudoalteromonadaceae*, one OTU became highly represented in the bottom waters of Stn 4 and 8 (Fig. S2). In most of these cases, the OTUs that proliferated either represented a minor fraction of, or altogether undetected in, the initial bacterial community.

Temporal changes in the relative contribution of the class *Flavobacteria* were most rapid and robust in Stn 8 surface waters and gradual elsewhere, but compositional changes—usually a dominance of distinct members within the family *Flavobacteraceae*—were observed at all stations and depths. In Stn 8 surface waters, one OTU comprised the largest flavobacterial contribution; another closely-related OTU increased to a lesser extent in the amended mesocosms (Fig. S3). Consistent with gammaproteobacterial patterns, many of the OTUs that increase in representation in the amended mesocosms were detected minimally, if at all, in the initial community composition.

In response to *Thalassiosira* addition, members of the class *Alphaproteobacteria* decreased in relative abundance in the initial stages of the community development. In tandem with the decrease in relative abundance of *Alphaproteobacteria*, a compositional shift was observed (Fig. S4). Initially, the alphaproteobacterial communities in all water masses featured a nearly even representation of members of *Pelagibacteraceae*—dominated by an OTU most closely related to *P. ubique*—and *Rhodobacteraceae*; following the addition of HMW *Thalassiosira*, the alphaproteobacterial community became dominated by OTUs within *Rhodobacteraceae* (Fig. S4). The composition and temporal succession of *Rhodobacteraceae* OTUs, however, differed between the stations and depths. For example, in Stn 4 surface waters, an OTU detected in moderate proportions in the initial community increased in relative contribution and became the dominant *Rhodobacteraceae* OTU. In Stn 8 surface water amended mesocosms, OTUs within *Rhodobacteraceae* were nearly undetectable 2d after *Thalassiosira* addition (at t1); thereafter, a distinct set of OTUs within

Rhodobacteraceae that were undetected at the start of the incubation became dominant (Fig. S4).

Peptidase and glucosidase activities. Initial peptidase and glucosidase activities differed by station and depth. Stn 4 surface water was characterized initially by a large relative contribution of leucine-aminopeptidase, with lesser activities of AAPF-chymotrypsin, QAR-trypsin, FSR-trypsin and minimal contribution of β-glucosidase activities (Fig. S6A). In comparison, Stn 4 bottom water showed relatively higher proportions of AAPF-chymotrypsin, with some contribution of QAR-trypsin, FSR-trypsin, and little contribution of β-glucosidase (Fig. S6B). In Stn 8 surface water, enzymatic activities were relatively even (Fig. S6C), while in Stn 8 bottom waters, enzymatic activities were dominated by the contribution of AAF-chymotrypsin (Fig. S6D). Summed initial rates were highest in surface waters at both stations (data not shown). Over time, peptidase and glucosidase rates in unamended incubations remained low and generally showed a gradual decrease (Fig. S6A,B,C,D). The only exception to this general pattern were enzymatic activities in unamended mesocosms with Stn 8 surface waters, where activities of some enzymes peaked at 15d (t3) (Fig. S6C), and in amended Stn 8 bottom waters, where AAF-chym activities increased at 2.5d (t1) (Fig. S6D).

Changes in peptidase and glucosidase activities (Fig. 4) were concurrent with robust community composition shifts (Fig. 3). Within 2d (t1) of *Thalassiosira* addition, increased enzymatic activities were measured for all depths and stations, with the exception of Stn 8 bottom waters, for which a substantial increase in activity was first observed at the 8-day (t2) timepoint (Fig. 4). All peptidase and glucosidase rates were significantly higher in amended versus unamended mesocosms regardless of station and depth (Table 2B). Furthermore, the temporal succession and peak of enzymatic activities were also station and depth-dependent. For many of the enzyme activities—including α-glucosidase, β -glucosidase, AAPF-chymotrypsin, QAR-trypsin and FSR-trypsin—maximum rates were measured in Stn8

surface waters (Fig. 4). However, maximum rates of leucine aminopeptidase activities at Stn4 surface waters were similar to those at Stn 8 surface waters, although the former was measured at 8d (t2), while the latter was detected at 2.5d (t1). In contrast, maximum rates for AAF-chymotrypsin activities across all water masses was measured at Stn4 surface waters. Surprisingly, maximum activity rates for most of the enzymes in Stn 8 bottom waters were comparable to those in Stn4 bottom waters, despite differences in temperature and initial cell count.

Polysaccharide hydrolase activities. Addition of HMW-POM also induced changes in polysaccharide hydrolase activities in all locations to varying degrees. In amended mesocosms, all six substrates were eventually hydrolyzed, except for Stn 8 bottom water, in which only four substrates were hydrolyzed (Fig. 5). The corresponding unamended mesocosms showed either fewer (Stn 4 and 8 surface waters) or the same (Stn 4 and 8 bottom) substrates hydrolyzed. The maximum rates and temporal development of polysaccharide hydrolase activities in amended mesocosms also differ between each water mass (Fig. 5; Table 2C). For example, pullulan was hydrolyzed at all four locations, but the highest hydrolysis rates are at Stn 8 surface water (Fig. 5). The same pattern was evident for laminarin, but with less difference in maximum rates across the water masses. Xylan was hydrolyzed at all locations at comparable rates, except for Stn 8 surface water, but the timepoints at which maximum hydrolysis was detected varied across locations (Fig. S7). Fucoidan and arabinogalactan were not hydrolyzed in Stn 8 bottom waters, and were hydrolyzed only late and at low rates in Stn 4 surface and bottom waters, but were rapidly hydrolyzed in Stn 8 surface waters. Maximum rates of chondroitin hydrolysis were comparable across water masses, and in Stn. 4 surface and bottom waters, these rates did not vary between amended and unamended mesocosms. Thus, the addition of HMW *Thalassiosira* biomass affected microbial community enzymatic activities in ways unique to each water mass.

4.4 Discussion

The extent to which community composition has functional consequences reveals the nature of microbial structure-function relationships, and has implications on whether ecosystem process rates are altered following changes in environmental conditions (Allison and Martiny, 2008). Testing the functional significance of differences in community composition, we hypothesized that distinct microbial assemblages would exhibit varying compositional and functional succession in response to HMW-POM. Successional patterns showed both convergent and divergent features among different bacterial communities, illustrating the complexity in interpreting the functional consequences of compositional differences (Bier et al., 2015). Specifically, while several initially rare taxa showed similar patterns of proportional dominance across water masses, the overall community structure and diversity in response to the same HMW-POM differed substantially. Furthermore, whether differences in functionality were observed among microbial assemblages depended on the enzymatic function of interest. Thus, the resolution with which consequences of communities are described (e.g., individual taxa versus whole community, specific enzymatic activities versus enzymatic spectra) greatly influences the interpretation (Balser and Firestone, 2005; Langenheder et al., 2006). Factors that underlie these complex successional patterns and their ecological consequences are discussed below.

Convergent response: conditionally rare taxa, trait complexity, and microbial seed banks. Addition of HMW-POM in different water masses served as an ecological filter, likely selecting for microbial taxa with the ability to associate with and metabolize particulate matter. Few taxa within several families of bacterial classes *Gammaproteobacteria*, *Alphaproteobacteria*, and *Flavobacteria* dominated in the amended mesocosms. Consistent with their response to HMW-POM, specific members within these groups predominate in response to phytoplankton blooms and degrade organic matter (Teeling et al., 2012; Buchan et al., 2014; Teeling et al., 2016). Many of these taxa were closely related—even identical

on the OTU level (97% sequence similarity)—and initially rare or undetected. Referred to as *conditionally rare taxa* (Shade et al., 2014; Newton and Shade, 2016), these microbes are capable of responding readily to pulses of available resource (Campbell et al., 2011; Newton and Shade, 2016). The “boom and bust” patterns of these conditionally rare taxa in our amended mesocosms are congruent with temporal succession patterns exhibited by conditionally rare copiotrophs (Shade et al., 2014; Alonso-Sáez et al., 2015; Newton and Shade, 2016), as well as microbial adaptations in environments with substantial temporal fluctuations (Lennon and Jones, 2011). Additionally, members of the ‘rare biosphere’ (Sogin et al., 2006) have been shown to play a role in convergent community assembly among distinct freshwater microbial communities in response to the same environmental alteration (Pagaling et al., 2014).

The relatively narrow phylogenetic distribution of taxa that become proportionally dominant in response to the addition may be linked to the trait complexity of associating with and degrading HMW-POM. Trait complexity, in this context, is related to the repertoire of genes necessary to carry out specific processes (Martiny et al., 2013). The ability to associate with HMW-POM is contingent upon particle encounter rates, microbial chemotaxis, and perhapls also production of exopolysaccharides to attach to surfaces (Dang and Lovell, 2016; Datta et al., 2016). Accessing and metabolizing carbon sources from HMW-POM requires production of appropriate enzymes that initiate hydrolysis to smaller constituents, and transporters for product uptake (Weiss et al., 1991). Microbial taxa with these genetic potentials are limited to a fraction of the natural community (Berlemont and Martiny, 2015), consistent with the finding that trait complexity and its phylogenetic distribution are inversely correlated (Martiny et al., 2013). Accordingly, mesocosms in which low molecular weight substrates were provided to different communities exhibited markedly different bacterial succession overtime (Logue et al., 2016). The ability to degrade and metabolize HMW-POM may be an even more phylogenetically narrow trait, and hence a

stronger selective filter during community succession, than the ability to attach to particles (Datta et al., 2016). Thus, in the phase of community succession defined by increased abundances in genes associated with particulate matter metabolism, community diversity decreases (Datta et al., 2016). The timescale during which we observed decreases in community diversity, and significant shifts in enzymatic activities, correspond with this described successional phase.

The widespread detection and dominance of closely-related, even potentially identical taxa in response to HMW-POM highlights the interactions of environmental selection and geographic dispersal in determining community structure. For example, within *Gammaproteobacteria*, individual OTUs belonging to the families *Colwelliaceae* and *Moritellaceae* were consistently detected in high proportions at Stn 4 surface and bottom waters, as well as Stn 8 bottom water. The 'high dispersal' concept maintains that organisms are not geographically bound, but viable populations exist under favorable conditions (Darling et al., 2007; Sexton and Norris, 2008). Hence, that closely-related or potentially the same taxa became proportionally dominant in different water masses illustrates two important points: 1) microbial capabilities to utilize high molecular weight particulate matter exist in the deep sea, as they do in surface waters; and 2) microbial taxa may overcome dispersal limitation imposed by hydrographic or other physical barriers (Spencer-Cervato and Thiersten, 1997; Galand et al., 2010). Occasional pulses of particulate matter could possibly transport, and, at the same time, sustain heterotrophic microbes in the deep ocean (Boetius et al., 2013). Oceanic dispersal of diverse plankton has been shown (Sexton and Norris, 2008; Malviya et al., 2016; Whittaker and Rynearson, 2017), but such large vertical range for the same taxa is less frequently documented.

During times of unfavorable conditions microbial communities must employ competitive strategies, including dormancy, to maintain a population that can respond to pulses of available resources. The existence of these conditionally rare, copiotrophic taxa

below the detection limit or in low relative proportions prior to their bloom suggests population maintenance strategies under nutrient depleted conditions (Lennon and Jones, 2011; Shade et al., 2014). Moreover, delayed microbial response in amended 4500 m waters—relative to that in other mesocosms—may reflect the time period necessary to ramp up metabolism to exit dormancy (Lennon and Jones, 2011). Additionally, the observation that fewer OTUs within *Flavobacteriaceae* and *Rhodobacteraceae* responded in Stn 8 bottom water than at other depths and stations may indicate a limited niche for particulate matter breakdown that prohibits many closely-related OTUs from co-existing in deep waters. These findings shed light on the ecological importance of microbial seed banks in determining community succession in response to resource availability (Lennon and Jones, 2011)

Divergent response and consequences of compositional differences. In spite of convergent successional patterns driven by several conditionally rare taxa, the overarching response of the distinct communities markedly differed. Consistent with these divergent successional patterns, differing community succession patterns have been observed even among identical microbial communities subjected to the same environmental perturbation (Langenheder et al., 2006). In this study, bacterial diversity in amended mesocosms 1) dramatically changed in Stn 8 bottom waters, 2) were altered to a lesser extent in Stn 8 surface waters and Stn 4 bottom waters, and 3) remained similar in Stn 4 surface waters. Variations in the intensity of bacterial community diversity shifts between stations and depths likely reflect the differences in the number of taxa capable of occupying the HMW-OM enriched niche, as mentioned previously. Moreover, the extent of community shifts may be linked to the degree of similarity of the new, perturbed environment to the ambient environment. Stn 4 surface waters typically experience high levels of primary production (Kuring et al., 1990), whereas open ocean bottom waters receive a small fraction of organic matter exported from surface waters (Karl et al., 2012). Based on compositional shifts and

greatest diversity decrease observed in amended Stn 8 bottom water, HMW-OM enrichments may have consequently imposed a stronger community re-assembly on bacterial communities in Stn 8 bottom waters compared to Stn 4 surface waters.

Community succession in amended mesocosms correspond to changes in enzymatic activities (Fig. 4,5, S6A-D, S7), vividly demonstrating that community shifts can have robust functional consequences (Teeling et al., 2012; Pagaling et al., 2014; Datta et al., 2016). Peptidase and glucosidase activities generally increased in the amended treatments, and polysaccharide substrates that were not hydrolyzed in unamended mesocosms (e.g. fucoidan and arabinogalactan) were hydrolyzed in amended mesocosms at most locations. Increased enzyme activities in amended mesocosms are in accordance with findings that copiotrophs possess genetic repertoires that enable rapid exploitation of pulses of resource availability (Shade et al., 2014; Newton and Shade, 2016), including a wider range of exoenzymes (Lauro et al., 2009). Given their dominance in amended mesocosms, conditionally rare—and potentially copiotrophic—taxa likely play a major role in the degradation of sporadically-available HMW-OM. Many of these bacterial taxa possess extensive hydrolytic capabilities and membrane transporters necessary to access high molecular weight substrates (Teeling et al., 2012).

The spatial variability and temporal dynamics of a range of enzymatic activities illustrate the nuanced responses of distinct microbial communities. For example, high activities of α- and β-glucosidase in amended treatments were only observed in Stn 4 bottom waters and in Stn 8 surface waters. Enrichment with the same HMW-POM resulted in varied glucosidase responses between some communities; however, the similarity in glucosidase activities at Stn4 bottom waters and Stn 8 surface waters is notable, and may be related to their similar origin as Gulf Stream surface water (Hoarfrost et al., unpubl). The temporal development of leucine-aminopeptidase activities in amended mesocosms differed substantially. However, caution should be used, as patterns in leucine aminopeptidase

activities may be due to the abilities of broader classes of peptidases to hydrolyze the leucine-MCA substrate (Steen et al. 2015). Furthermore, while activity patterns of chymotrypsins and trypsins exhibit differences across amended treatments, the substrate specificities of these enzymes may have varying potential to further distinguish functional variations. In particular, the activity of the two chymotrypsins, which target different amino acid residues attached to alanine, vary considerably among microbial communities. In contrast, the activity patterns of the two trypsins do not vary significantly from each other. Using structurally diverse enzymes therefore enhances the resolution with which to examine functional differences among distinct communities.

The polysaccharide hydrolase activities that develop in amended mesocosms further demonstrate functional differences among communities. All polysaccharide hydrolase activities were stimulated following the HMW-OM amendment at all locations except for Stn 8 bottom water. Amended waters used for polysaccharide hydrolase activity measurements exhibited proportionally dominant conditionally rare taxa, indicating the involvement of these community members in polysaccharide degradation. The absence of detectable fucoidan and arabinogalactan hydrolysis in Stn 8 bottom water may be due to a lack of organisms enzymatically equipped to hydrolyze these substrates, related to the low community diversity observed in these waters. Alternatively, these taxa may have been present, but unable to produce the necessary hydrolytic enzymes. Incubation temperature alone is an unlikely reason for the difference, considering that fucoidan and arabinogalactan hydrolysis have been observed in low-temperature sediments of Svalbard fjords (Teske et al., 2011). Thus, community-related differences more likely drove the variations in polysaccharide hydrolase activities between water masses. Consistent with previous findings, these results illustrate the synergy of a broad suite of hydrolytic enzymes necessary to break down HMW-OM (Arnosti, 2011; Teeling et al., 2012; D'Ambrosio et al., 2014), likely produced by conditionally-rare microbial taxa.

Biological reproducibility and potential bottle effects. The remarkable reproducibility in community function (Fig. 5, S6A-D) as well as in community composition (Fig. S5) in the triplicate mesocosms strengthen the interpretation that these observed compositional and functional changes are due to the amendment, as opposed to shifts only due to bottle effects. Admittedly, bacterial communities in unamended controls exhibit compositional and functional shifts ("bottle effects") independent of any treatment effects (Stewart et al., 2012). These effects include the relative increase of a few OTUs within the classes *Gammaproteobacteria* and *Flavobacteria* in several mesocosms (Fig. 3B, S2, S3). Enzymatic activities also exhibited shifts over time in unamended mesocosms (Fig. S6A-D), although the extent to which these are related to community changes or a reflection of changing organic matter status (Bong et al., 2013) at present cannot be discerned. Nevertheless, the treatment effect is significant on both community composition and enzymatic potentials, and the identities of bacterial taxa that rise and fall in relative proportions in unamended mesocosms differ from those in amended incubations. The reproducibility among triplicates also suggests a stronger influence of species sorting—in response to the treatment—relative to neutral effects (Pagaling et al., 2014; Langenheder and Szekely, 2011). In addition, such high similarity across mesocosm triplicates—which contrast other studies that have found high inter-replicate variability in microbial community composition (Langenheder et al., 2006; Ofiteru et al., 2010)—supports observations that the strength of environmental perturbation results in highly predictable community development (Chase, 2007; Violle et al., 2010). In scenarios of predictable community assembly, members of the rare biosphere have been shown to play a major role (Pagaling et al., 2014), consistent with our observations.

4.5 Conclusion

The varying response of distinct microbial communities to high molecular weight organic matter yields a vivid picture of the functional consequences of community structure.

Addition of HMW-POM acted as an ecological filter, apparently selecting for microbial members with the ability to initiate organic matter breakdown. This niche-driven change in the community altered the structure-function relationship (Knelman and Nemergut, 2014), decreasing diversity in amended mesocosms, but increasing the overall enzymatic capabilities of the community to carry out organic matter degradation. Such a response is consistent with scenarios in which response traits (association with particles) and measured effect traits (metabolism of particulate matter) are coupled (Knelman and Nemergut, 2014). However, the manner in which distinct microbial communities responded to and degraded HMW-POM vastly differed, evident by varying temporal dynamics and activities of peptidases, glucosidases and polysaccharide hydrolases across water masses. Measuring enzymatic activities using a broad range of structurally diverse substrates provided multiple ways through which functional differences can be evaluated—a necessary effort, as examining the consequences of community compositional differences depends on the function of interest.

Yet, alongside divergent successional patterns, similar shifts in relative proportions of several closely-related taxa are observed, highlighting the complexity of interpreting consequences of community structural differences. These conditionally rare, putatively copiotrophic taxa exhibit metabolic adaptations similar to those of particle-associated microbes, and have been implicated in convergent community shifts in previous studies (Pagaling et al., 2014). Emergence and proportional dominance of these taxa provide support for the concept of microbial seed banks. Under similar environmental conditions, distinct communities can exhibit similar responses by recruiting low-population count or dormant taxa awaiting resource availability (Lennon and Jones, 2011). The conditionally rare copiotrophs that bloom in response to the amendment likely possess wide-ranging enzymatic activities. By restricting the size distribution of the added organic matter, we have shown a crucial role of these taxa in cycling high molecular weight compounds, as has been

observed in phytoplankton blooms (Teeling et al., 2012; Buchan et al., 2014). Finally, detecting a subset of these conditionally rare, copiotrophic taxa in bathypelagic waters point to their spatially widespread ecological role and the importance of pulses of particulate matter in maintaining these populations in deep waters.

4.6 Acknowledgements

We thank the crew and scientific party of R/V *Endeavor* (EN556) for their fieldwork support. Additionally, we thank Karylle Abella for assistance with sample processing. This project and JP Balmonte were funded by the NSF OCE-1332881 grant to Carol Arnosti. JP Balmonte was additionally funded by the UNC Dissertation Completion Fellowship.

4.7 Main Figures and Tables

Figure 1. Sampling stations in the North Atlantic, and mesocosm experimental setup. The green carboys indicate triplicate amended treatments, while the blue carboys represent unamended control triplicates. Colors in the map reflect sea surface temperatures: warm and cool colors indicate warmer and cooler temperatures. The map is modified from Scripps Institution of Oceanography.

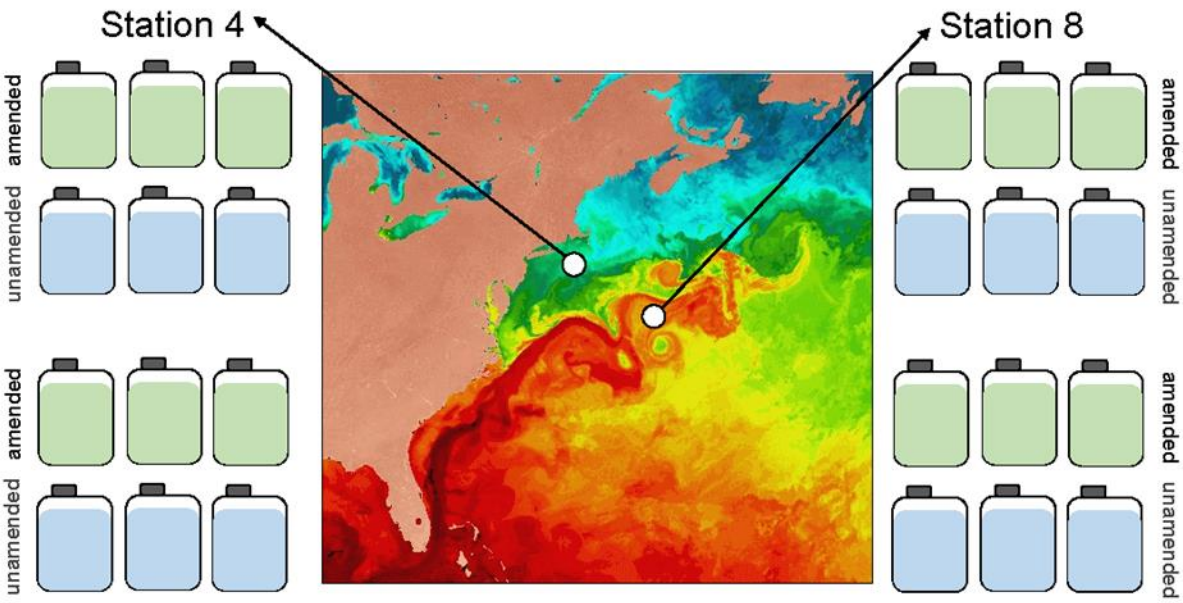

Figure 2. (A) Bacterial cell counts, (B) ^{3}H-Leucine bacterial production, and (C) dissolved organic carbon (DOC) concentrations. Note the differences in scale. Subsampling timepoints correspond to 0d, 2.5d, 8d, 15d, 28d, and 69d. Circle and triangle data points correspond to amended and unamended measurements.

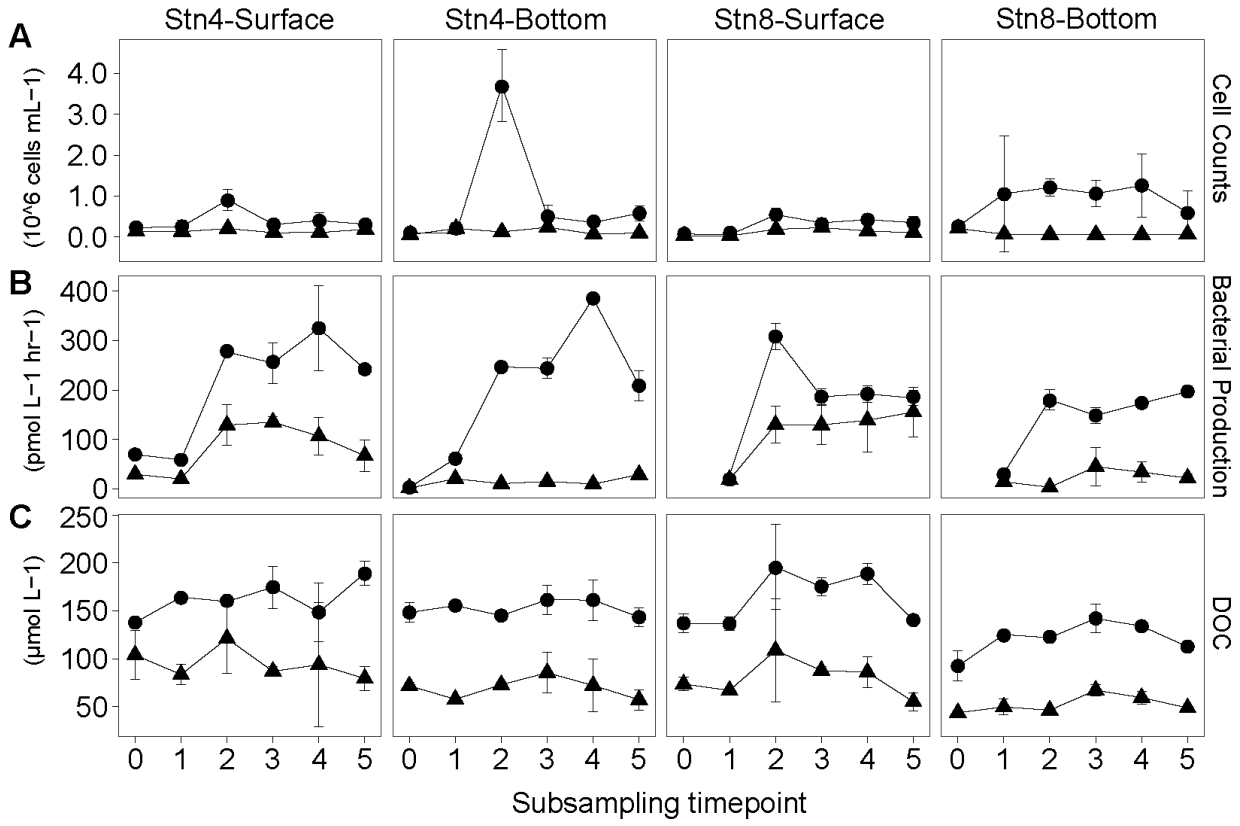

Figure 3. Non-metric multidimensional scaling (NMDS) of bacterial community compositional dissimilarity using Bray-Curtis index. The ordination was conducted on OTUs defined at 97% sequence similarity from all samples. (B) Comparison of Faith's Phylogenetic Diversity index across water masses. Diversity was calculated from bacterial communities from only one unamended and one amended mesocosm across all timepoints and at all locations. Circle and triangle data points correspond to amended and unamended measurements, respectively. (C) Class-level taxonomic breakdown of bacterial communities in amended and unamended treatments. The visualized data is based on one unamended and one amended mesocosm from each water mass across all timepoints, as in (B). To de-convolute the plot, only bacterial classes that are ≥1% in relative proportions were included in the visualization. Subsampling timepoints correspond to 0d, 2.5d, 8d, 15d, 28d, and 69d. [Figure in the next page]

Figure 3

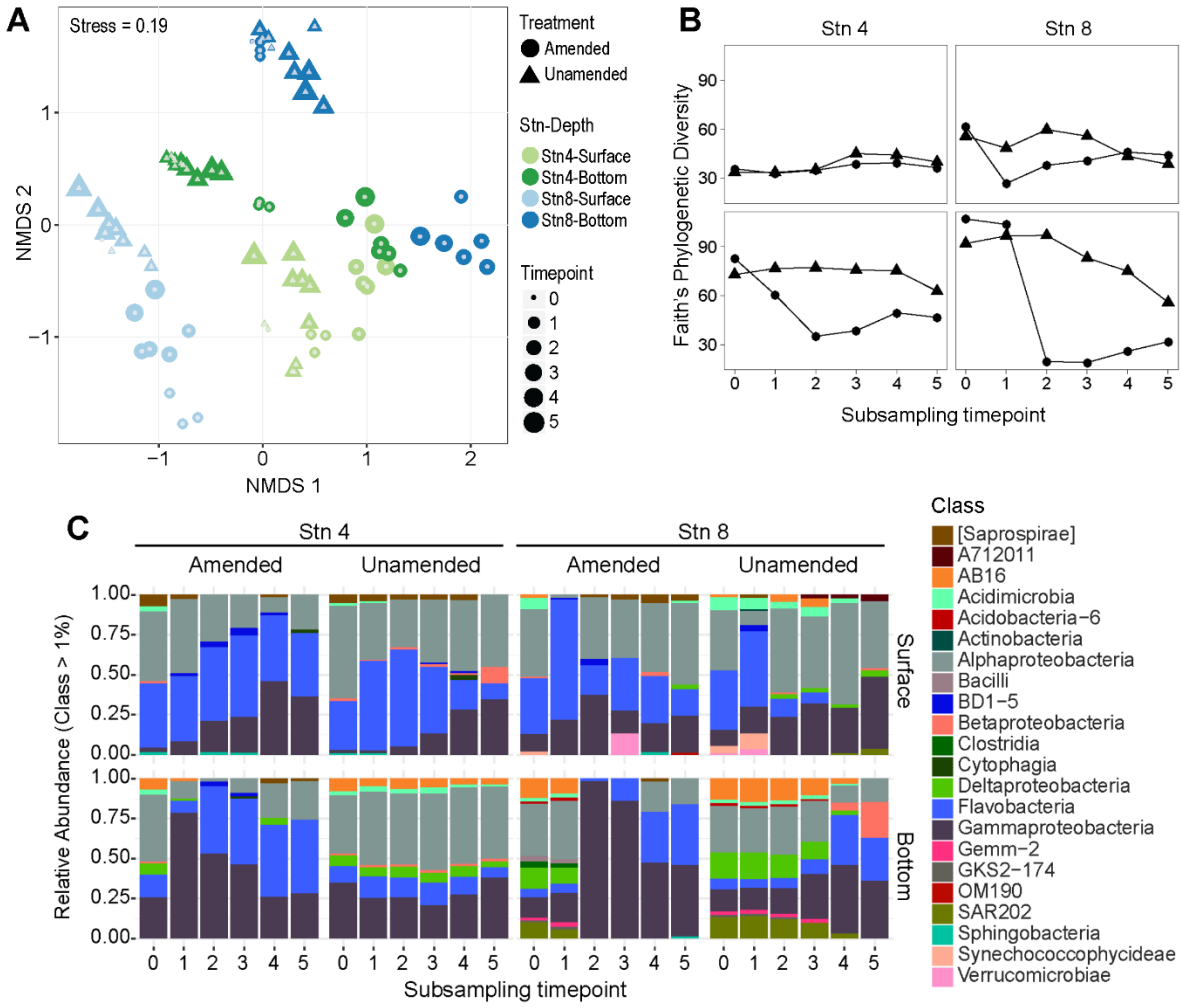
A
Stress = 0.19
NMDS 2
NMDS 1
Treatment
Amended
Unamended
Stn-Depth
Stn4-Surface
Stn4-Bottom
Stn8-Surface
Stn8-Bottom
Timepoint
B
Stn 4
Stn 8
Faith's Phylogenetic Diversity
Surface
Bottom
Subsampling timepoint
C
Stn 4
Stn 8
Amended
Unamended
Relative Abundance (Class > 1%)
Subsampling timepoint
Class
[Saprospirae]
A712011
AB16
Acidimicrobia
Acidobacteria−6
Actinobacteria
Alphaproteobacteria
Bacilli
BD1−5
Betaproteobacteria
Clostridia
Cytophagia
Deltaproteobacteria
Flavobacteria
Gammaproteobacteria
Gemm−2
GKS2−174
OM190
SAR202
Sphingobacteria
Synechococcophycideae
Verrucomicrobiae

Figure 4. Glucosidase (top two rows) and peptidase activities at all locations. Each data is the averaged rate across the mesocosm triplicates, separating amended and unamended treatments. The rate from each mesocosm triplicate is an average of all rates obtained throughout the plate incubation (see *Methods and Materials*). Error bars indicate the standard deviation of the rate across the mesocosm triplicates. Subsampling timepoints correspond to 0d, 2.5d, 8d, 15d, 28d, and 69d. Note the scale differences.

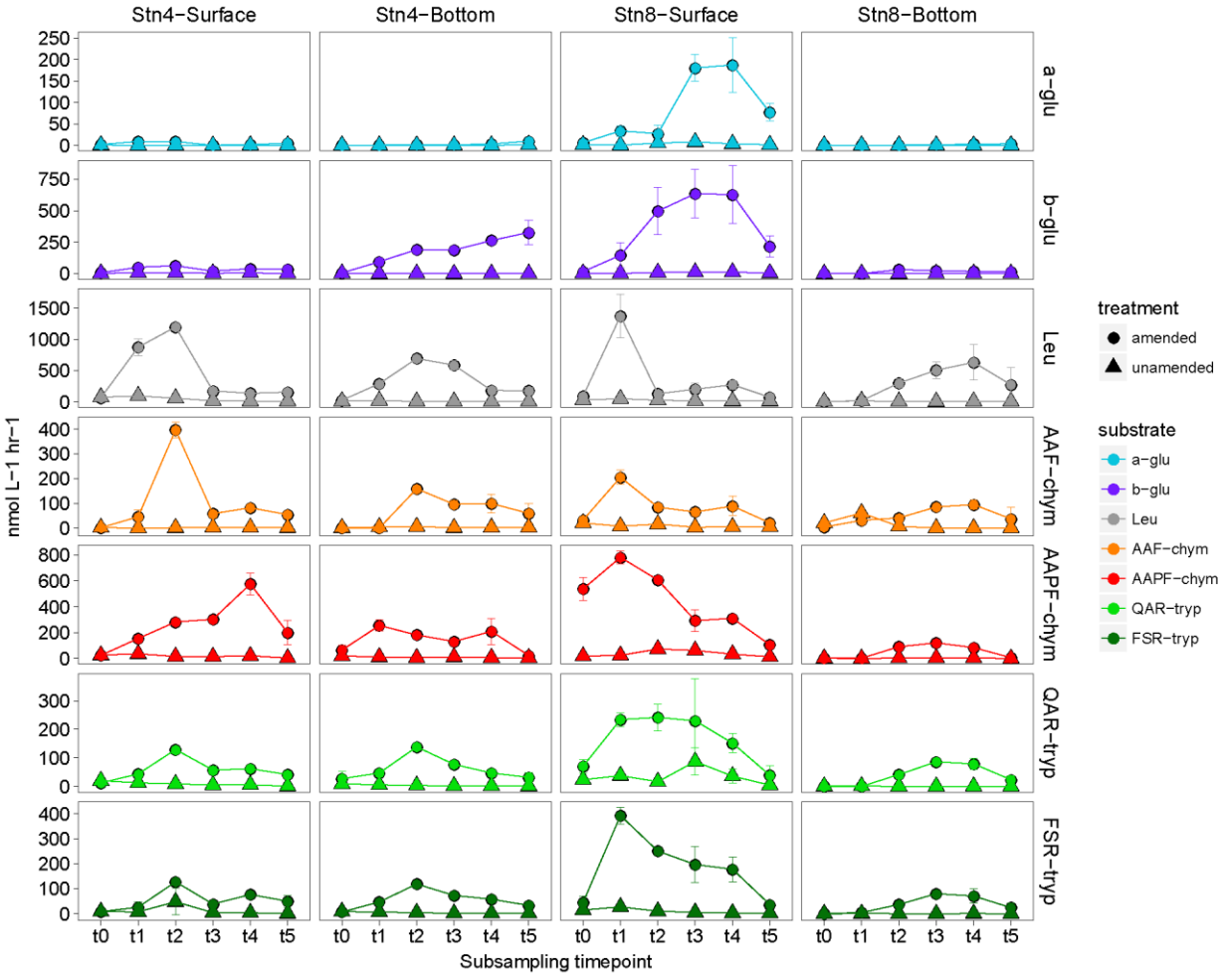

Figure 5. Maximum polysaccharide hydrolase rates for each mesocosm. These maximum rates were taken at varying timepoints (see Fig. S7). The plotted rates and error bars represent the average and standard deviation of rates obtained from triplicate incubations for each mesocosm incubation (carboy); see *Methods and Materials* for experimental setup. Samples used for these measurements were obtained at the 15d (t3) subsampling timepoint.

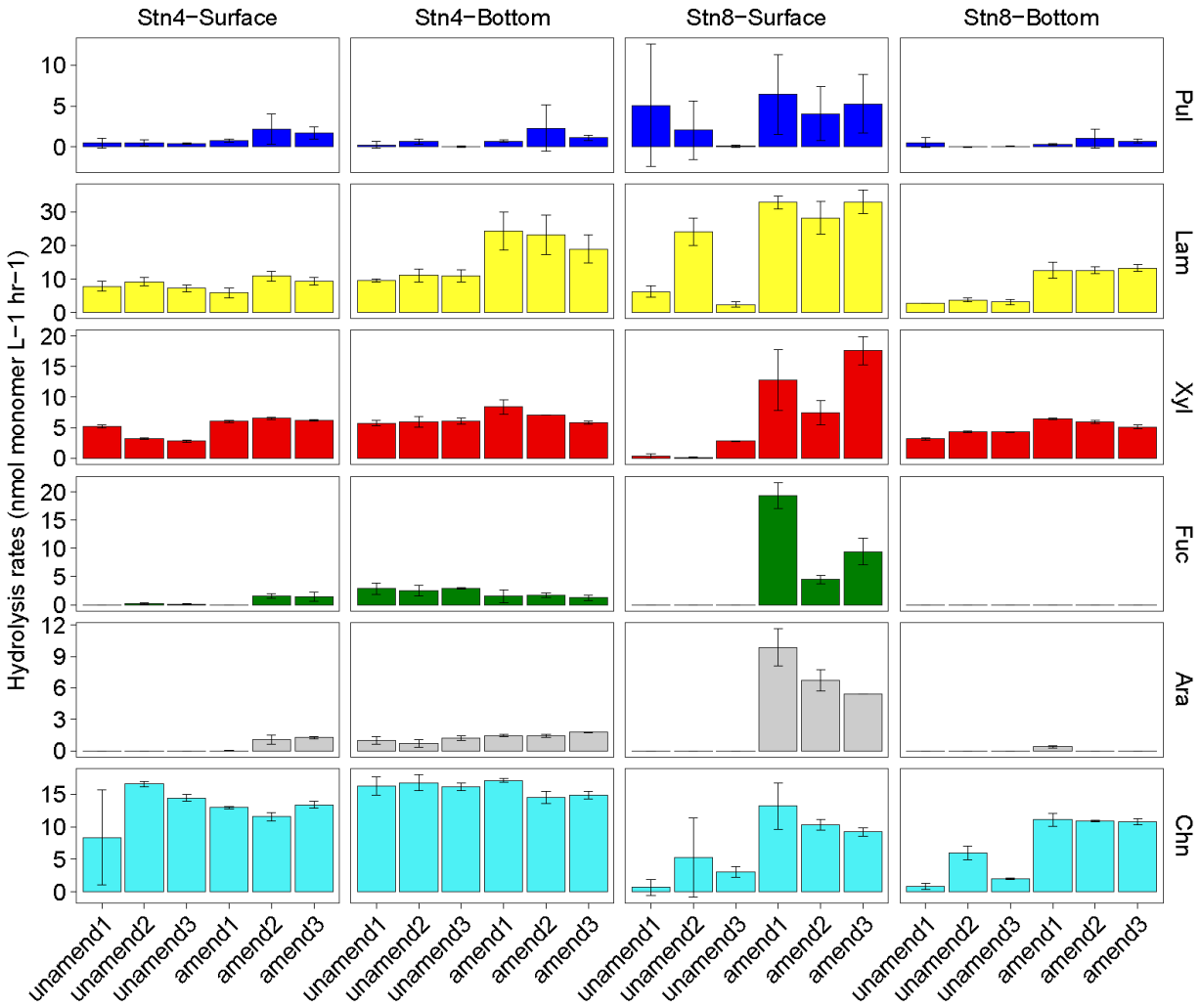

Table 1. Water mass physicochemical characteristics and experimental details. 'DOC' stands for dissolved organic carbon concentration. 'Meso. Incub. Temp.' stands for mesocosm incubation temperature. 'EEA Incub. Temp' stands for extracellular enzymatic activity assay incubation temperature.

	Stn4		**Stn8**	
	Surface	**Bottom**	**Surface**	**Bottom**
Sampling Date	28-Apr-15	28-Apr-15	29-Apr-15	29-Apr-15
Latitude (° N)	40.07	40.07	37.60	37.61
Longitude (° W)	71.00	71.01	68.40	68.41
Depth (m)	1	199	6	4574
Temperature (°C)	7.7	12.0	18.8	2.2
Salinity (PSU)	33.4	35.6	36.3	34.9
Oxygen (mL/L)	7.3	4.7	5.1	5.7
$NO_2 + NO_3$ (µM)	0.04	5.17	0.16	15.97
PO_4 (µM)	0.45	0.51	0.27	1.39
NH_4 (µM)	1.39	0.36	0.60	0.62
DOC (µM)	89.0	63.5	96.7	68.5
Meso. Incub. Temp. (°C)	4	4	21	4
EEA Incub. Temp. (°C)	8	14	21	4

Table 2. Analysis of variance (ANOVA) significance values, testing for treatment effects on (A) cell counts, bacterial production, dissolved organic carbon (DOC) and Faith's Phylogenetic Diversity; (B) glucosidase and peptidase rates; and (C) polysaccharide hydrolase rates. Values in bold are considered statistically significant (<0.05).

A

	Stn4-Surface	Stn4-Bottom	Stn8-Surface	Stn8-Bottom
Cell counts	**<0.001**	**0.028**	**<0.001**	**<0.001**
Bacterial production	**<0.001**	**<0.001**	**0.023**	**<0.001**
DOC	**<0.001**	**<0.001**	**<0.001**	**<0.001**
Faith's PD	0.257	**0.011**	0.246	**0.036**

B

	Stn4-Surface	Stn4-Bottom	Stn8-Surface	Stn8-Bottom
α-glucosidase	**<0.001**	**0.003**	**<0.001**	**0.007**
β-glucosidase	**<0.001**	**<0.001**	**<0.001**	**<0.001**
Leucine	**<0.001**	**<0.001**	**0.006**	**<0.001**
AAF-Chymotrypsin	**0.003**	**<0.001**	**<0.001**	**<0.001**
AAPF-Chymotrypsin	**<0.001**	**<0.001**	**<0.001**	**<0.001**
QAR-Trypsin	**<0.001**	**<0.001**	**<0.001**	**<0.001**
FSR-Trypsin	**<0.001**	**<0.001**	**<0.001**	**<0.001**

C

	Stn4-Surface	Stn4-Bottom	Stn8-Surface	Stn8-Bottom
Pullulan	0.059	0.105	0.151	0.145
Laminarin	0.727	**0.002**	**0.04**	**<0.001**
Xylan	**0.03**	0.202	**0.02**	**0.022**
Fucoidan	0.146	**0.002**	**0.065**	na
Arabinogalactan	0.117	**0.033**	**0.005**	0.374
Chondroitin	0.852	0.354	**0.012**	**0.007**

Table 3. Analysis of Similarity (ANOSIM) results, testing for the statistical significance of bacterial community dissimilarities in various groupings. Samples considered as 'unamended' in these analyses included all t0 samples (unamended and amended, not statistically significantly different at t0), and t1-t5 samples in unamended mesocosms. Consequently, samples considered as 'amended' only include those from t1-t5 of the amended mesocosms. 'R' is the ANOSIM statistic. P values in bold are considered statistically significant (<0.05).

ANOSIM Comparisons	R	p_{val}
All (unamended versus amended)	0.439	**0.001**
Stn 4 Surface (unamended versus amended)	0.764	**0.001**
Stn 4 Bottom (unamended versus amended)	0.958	**0.001**
Stn 8 Surface (unamended versus amended)	0.605	**0.001**
Stn 8 Bottom (unamended versus amended)	0.953	**0.001**
Amended (by water masses)	0.523	**0.001**
Unamended (by water masses)	0.915	**0.001**

4.8 Supplementary Materials

Figure S1A. Nonmetric multidimensional scaling (NMDS) on bacterial community composition using unweighted UniFrac dissimilarity index. The OTU cutoff was set at 97% sequence similarity cutoff. The NMDS is used in this analysis to emphasize the differences in the composition of bacterial communities in amended treatments.

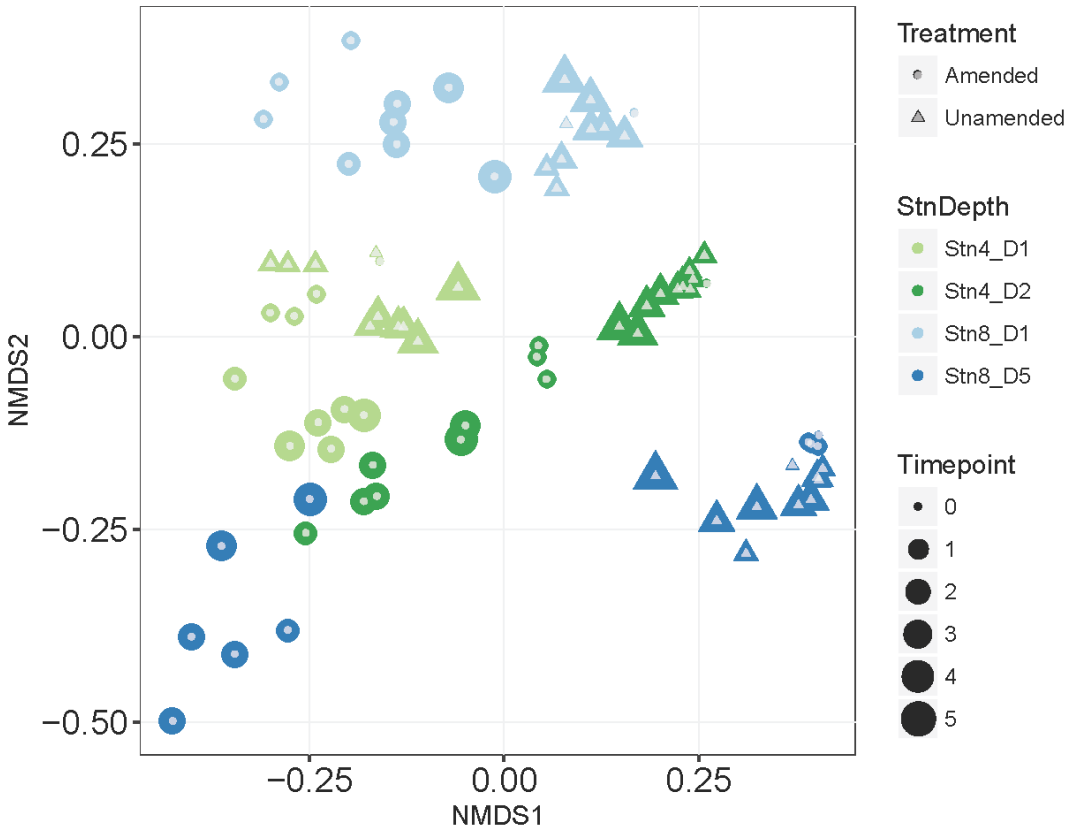

Figure S1B. Principal coordinates analysis (PCoA) on bacterial community composition using unweighted UniFrac dissimilarity index. The OTU cutoff was set at 97% sequence similarity cutoff. The percent variation explained for each axis is shown in the axis label. The PCoA ordination was used here to illustrate the similarity in the direction of the compositional succession of bacterial communities. However, the PCoA was not used for the main text because of the low explanatory power of the ordination, which only explains 20.% of the variation in the dataset.

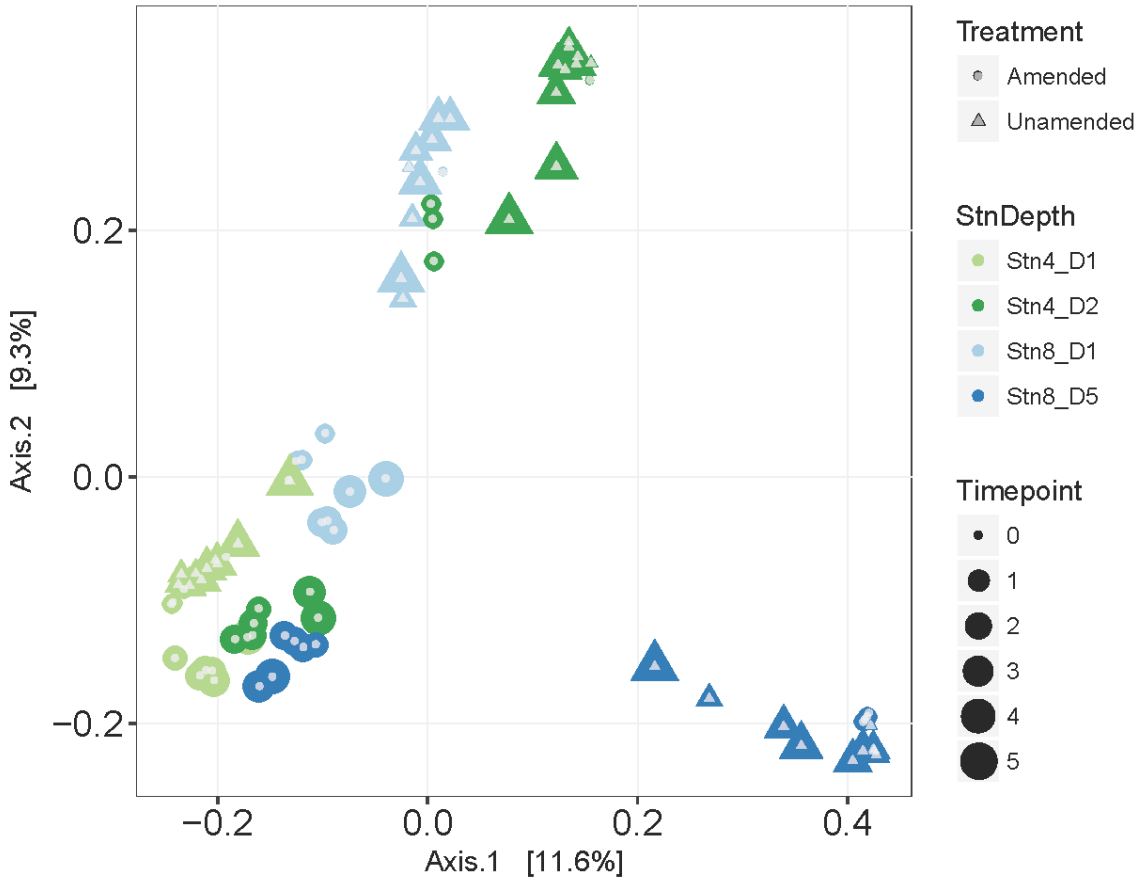

Figure S2. Top OTUs within five families of the bacterial class *Gammaproteobacteria*, including (A) *Collwelliaceae*, (B) *Moritellaceae*, (C) *Oceanospirillaceae*, (D) *Pseudoalteromonadaceae*, and (E) *Vibrionaceae*. Note the scale differences. The data plotted are the sequence count from a rarefied dataset of 22,000 sequences per sample.

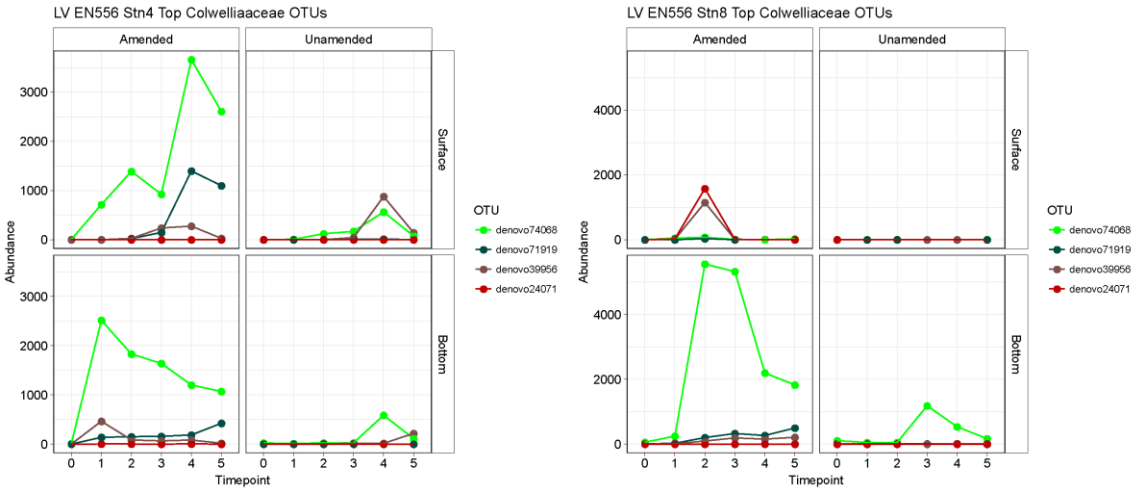

A

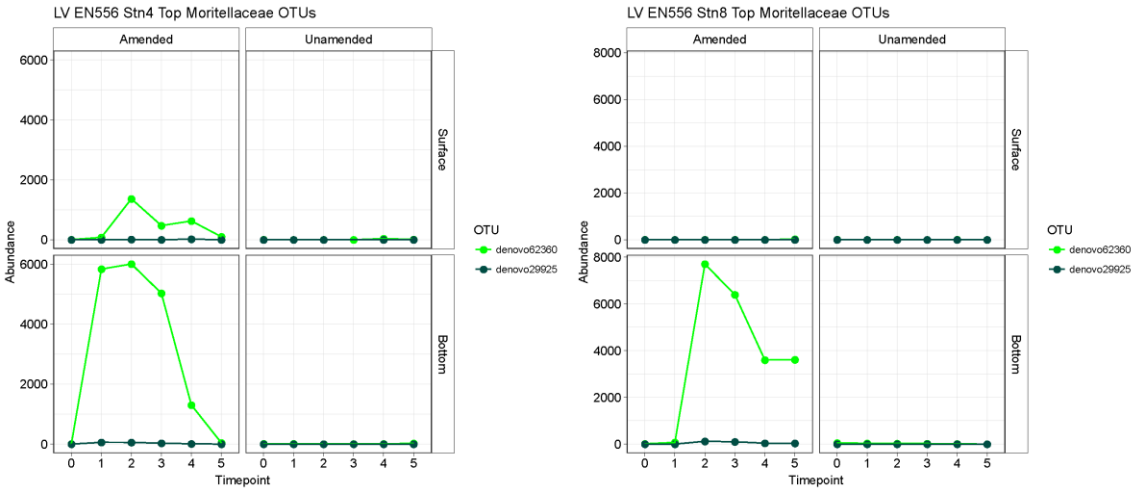

B

[Figures S2C, S2D and S2E are in the next pages]

Figure S2. Top OTUs within five families of the bacterial class *Gammaproteobacteria*, including (A) *Collwelliaceae*, (B) *Moritellaceae*, (C) *Oceanospirillaceae*, (D) *Pseudoalteromonadaceae*, and (E) *Vibrionaceae*. Note the scale differences. The data plotted are the sequence count from a rarefied dataset of 22,000 sequences per sample.

C

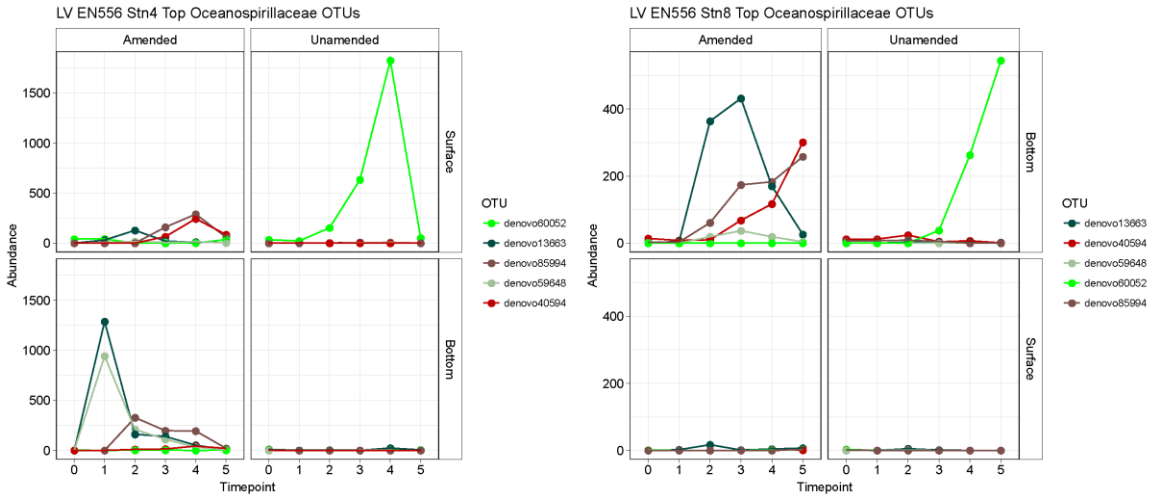

D

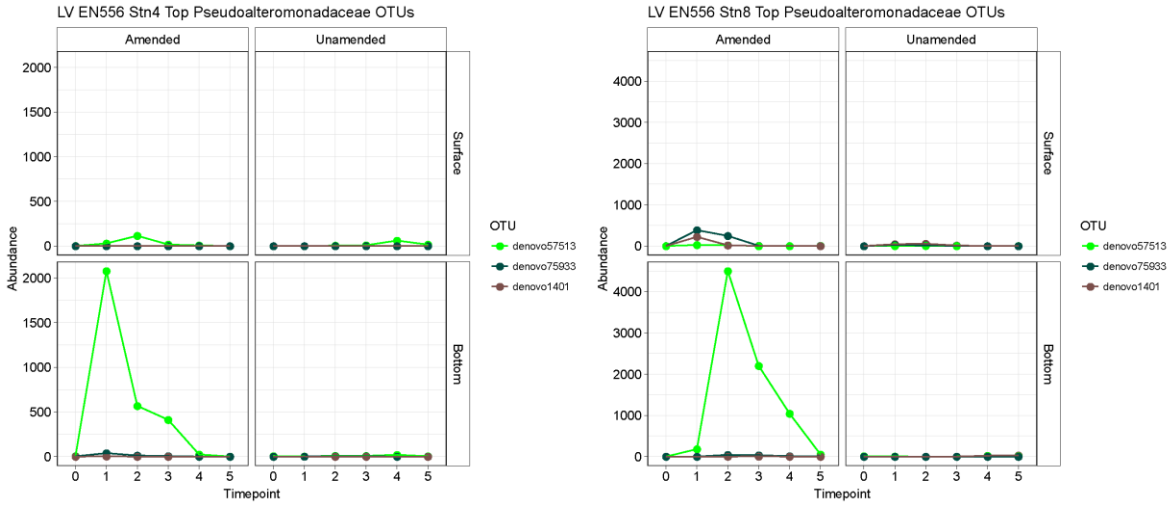

[Figure S2E is in the next page]

Figure S2. Top OTUs within five families of the bacterial class *Gammaproteobacteria*, including (A) *Collwelliaceae*, (B) *Moritellaceae*, (C) *Oceanospirillaceae*, (D) *Pseudoalteromonadaceae*, and (E) *Vibrionaceae*. Note the scale differences. The data plotted are the sequence count from a rarefied dataset of 22,000 sequences per sample.

E

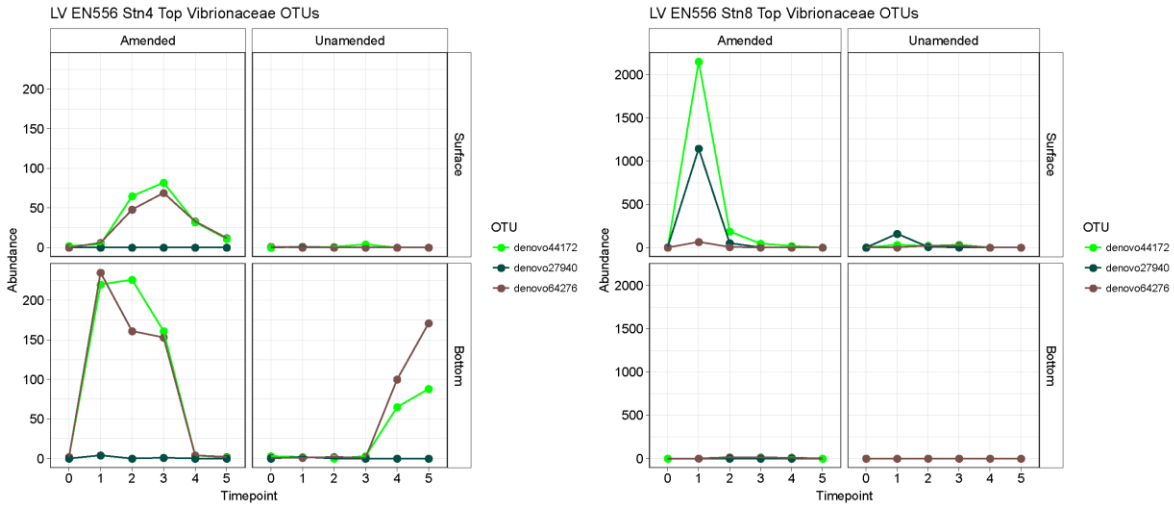

Figure S3. Top OTUs within the family *Flavobacteraceae* of the class *Flavobacteriia*. Note the scale differences. The data plotted are the sequence count from a rarefied dataset of 22,000 sequences per sample.

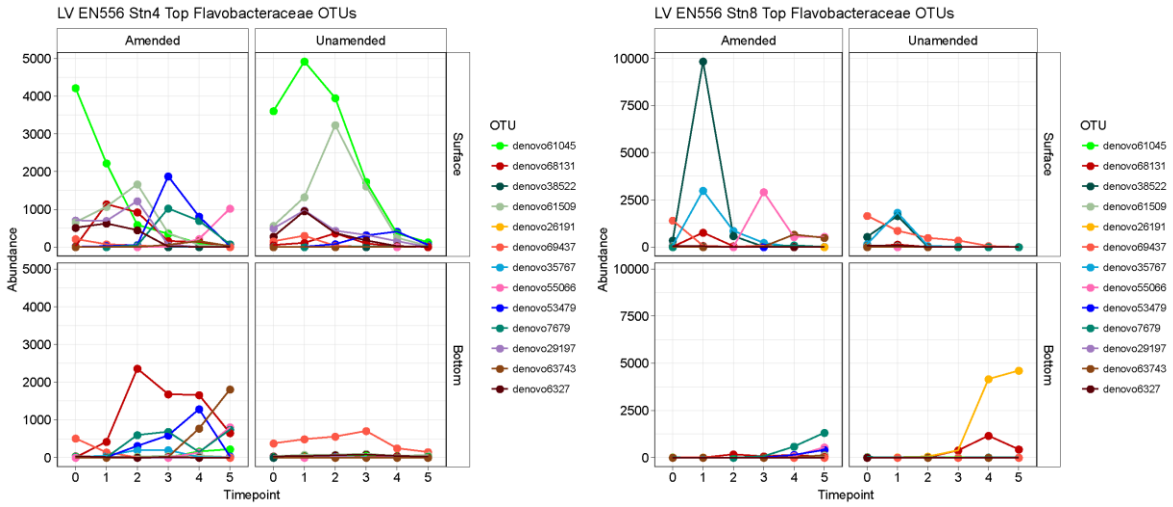

Figure S4. Top OTUs within the family *Rhodobacteraceae* of the class *Alphaproteobacteria*. Note the scale differences. The data plotted are the sequence count from a rarefied dataset of 22,000 sequences per sample.

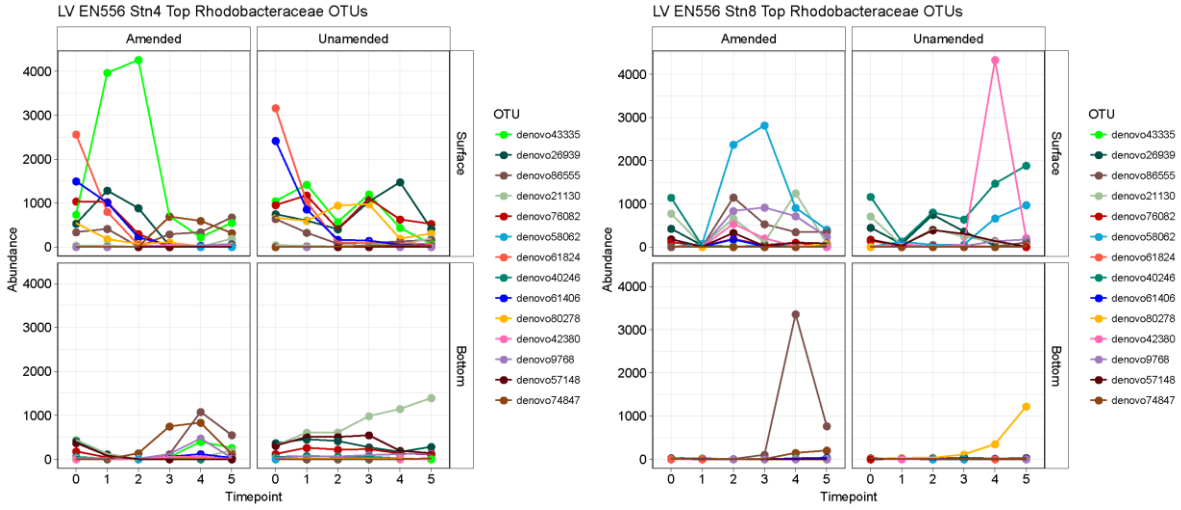

Figure S5. Reproducibility of bacterial community composition in amended (LV1, LV2, LV3) and unamended (LV4, LV5, LV6) mesocosm triplicates. Examples include (A) class-level taxonomic breakdown at 2.5d (t1); (B) class-level taxonomic breakdown at 15d (t3); (C) family-level breakdown for class *Gammaproteobacteria* at 2.5d (t1); (D) family-level taxonomic breakdown at 15d (t3). No sample is available for the unamended replicate LV4 at t1. The data shown are relative abundances of bacterial classes or families, but only include those with relative proportions of ≥1% of the entire community. Each sample was rarefied to 22,000 sequences for comparative purposes. Note the legend differences for each figure (A, B, C, D).

A

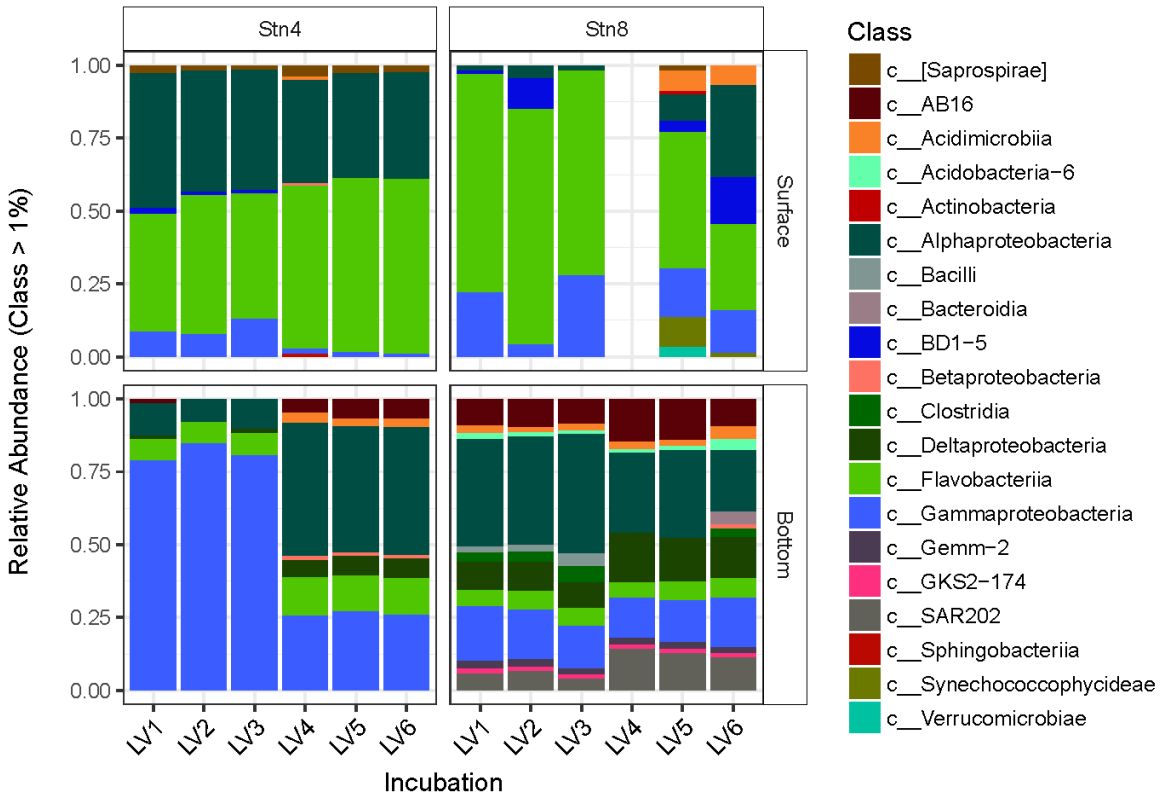

[Figures S5B, S5C, and S5D are in the next pages]

Figure S5. Reproducibility of bacterial community composition in amended (LV1, LV2, LV3) and unamended (LV4, LV5, LV6) mesocosm triplicates. Examples include (A) class-level taxonomic breakdown at 2.5d (t1); (B) class-level taxonomic breakdown at 15d (t3); (C) family-level breakdown for class *Gammaproteobacteria* at 2.5d (t1); (D) family-level taxonomic breakdown at 15d (t3). No sample is available for the unamended replicate LV4 at t1. The data shown are relative abundances of bacterial classes or families, but only include those with relative proportions of ≥1% of the entire community. Each sample was rarefied to 22,000 sequences for comparative purposes. Note the legend differences for each figure (A, B, C, D).

B

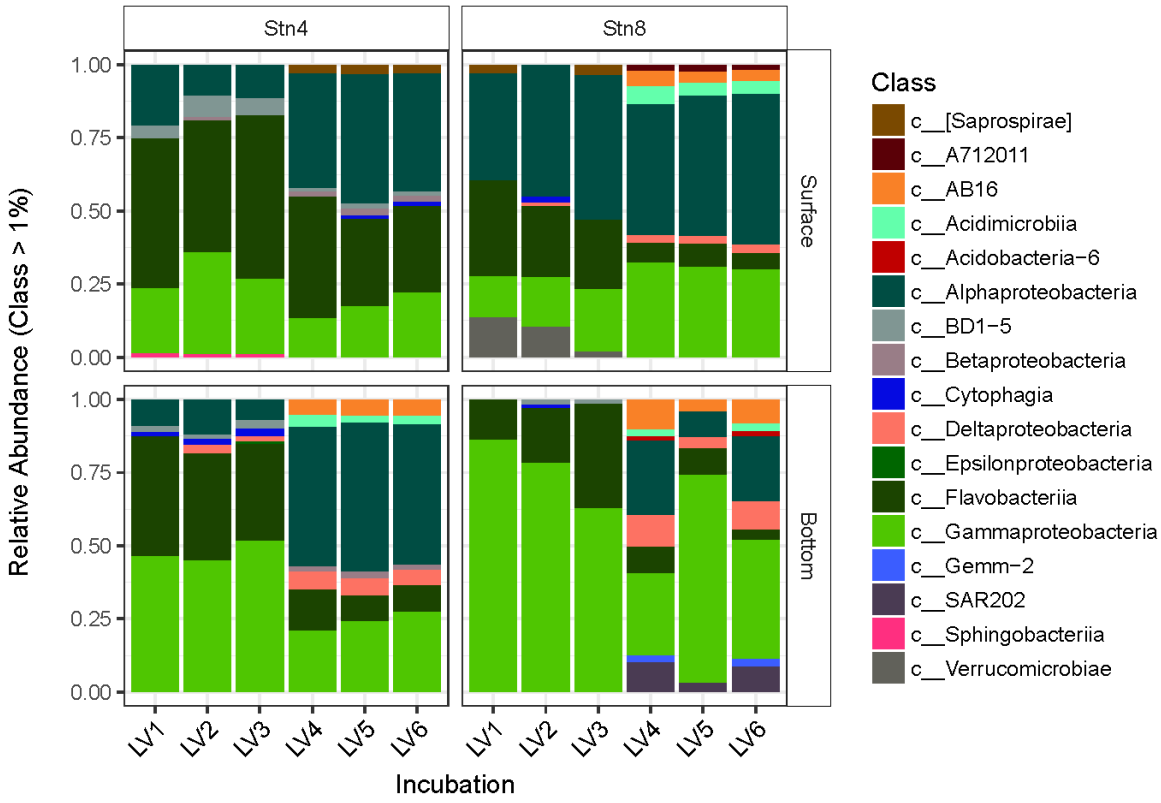

[Figures S5C, and S5D are in the next pages]

Figure S5. Reproducibility of bacterial community composition in amended (LV1, LV2, LV3) and unamended (LV4, LV5, LV6) mesocosm triplicates. Examples include (A) class-level taxonomic breakdown at 2.5d (t1); (B) class-level taxonomic breakdown at 15d (t3); (C) family-level breakdown for class *Gammaproteobacteria* at 2.5d (t1); (D) family-level taxonomic breakdown at 15d (t3). No sample is available for the unamended replicate LV4 at t1. The data shown are relative abundances of bacterial classes or families, but only include those with relative proportions of ≥1% of the entire community. Each sample was rarefied to 22,000 sequences for comparative purposes. Note the legend differences for each figure (A, B, C, D).

C

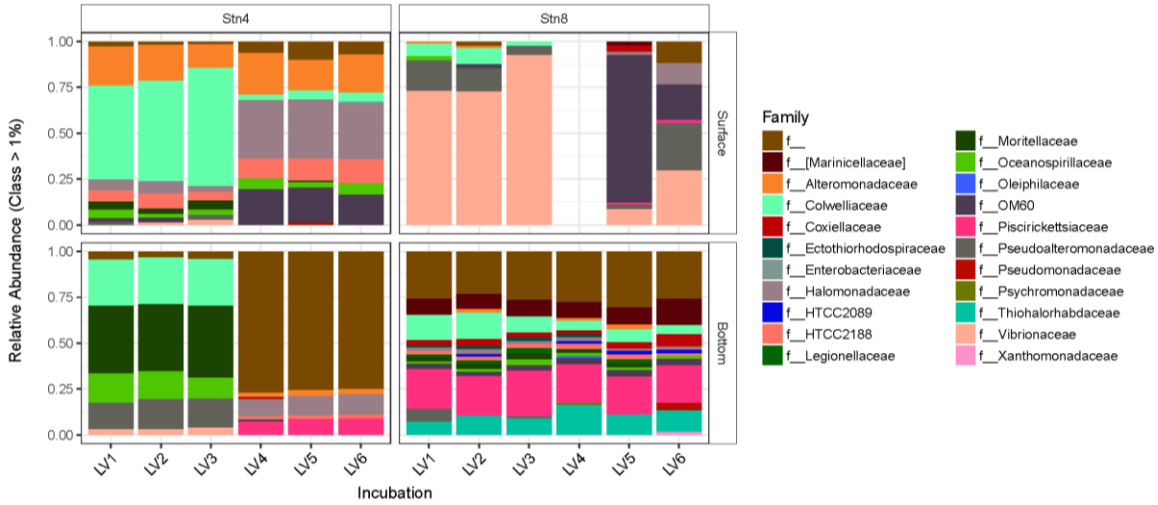

[Figure S5D is in the next page]

Figure S5. Reproducibility of bacterial community composition in amended (LV1, LV2, LV3) and unamended (LV4, LV5, LV6) mesocosm triplicates. Examples include (A) class-level taxonomic breakdown at 2.5d (t1); (B) class-level taxonomic breakdown at 15d (t3); (C) family-level breakdown for class *Gammaproteobacteria* at 2.5d (t1); (D) family-level taxonomic breakdown at 15d (t3). No sample is available for the unamended replicate LV4 at t1. The data shown are relative abundances of bacterial classes or families, but only include those with relative proportions of ≥1% of the entire community. Each sample was rarefied to 22,000 sequences for comparative purposes. Note the legend differences for each figure (A, B, C, D).

D

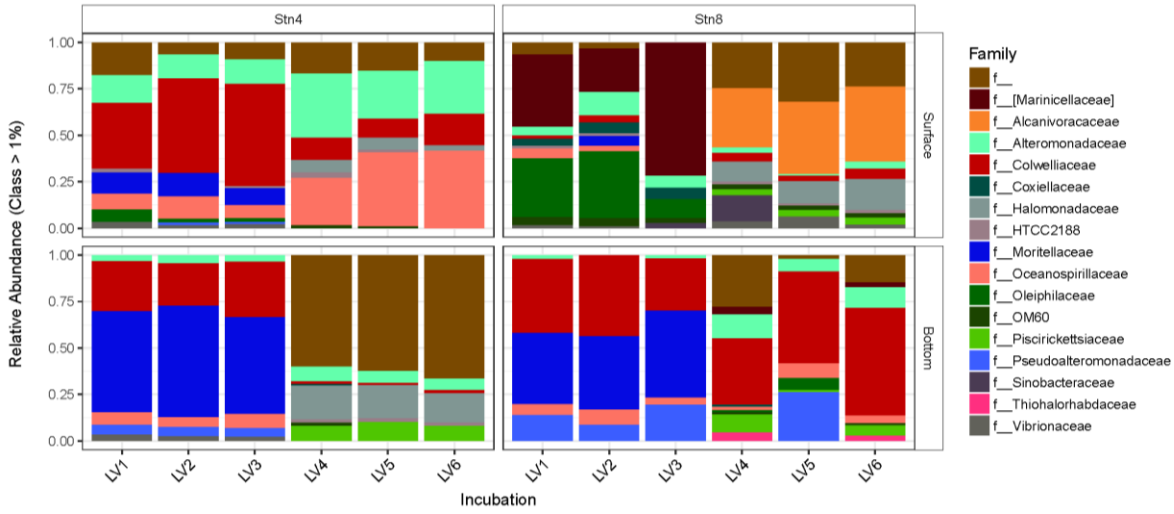

Figure S6A. Stn 4 surface water temporal development of peptidase and glucosidase activities, separated by mesocosm. Rates represented by each bar and error bars are the time-averaged rates —over a span of 72 hours—and standard deviation of each enzymatic activity measurement.

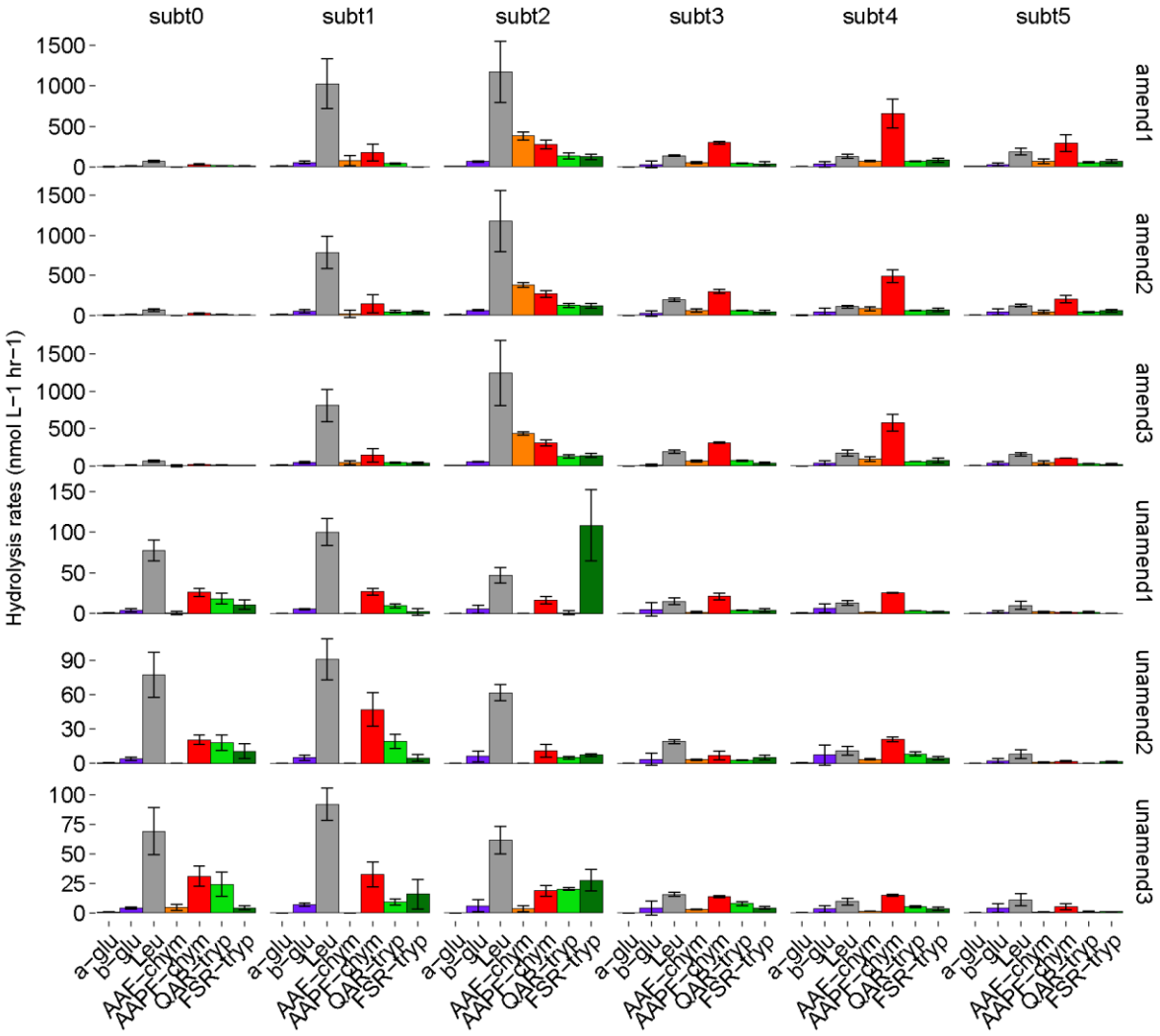

Figure S6B. Stn 4 bottom water temporal development of peptidase and glucosidase activities, separated by mesocosm. Rates represented by each bar and error bars are the time-averaged rates —over a span of 72 hours—and standard deviation of each enzymatic activity measurement.

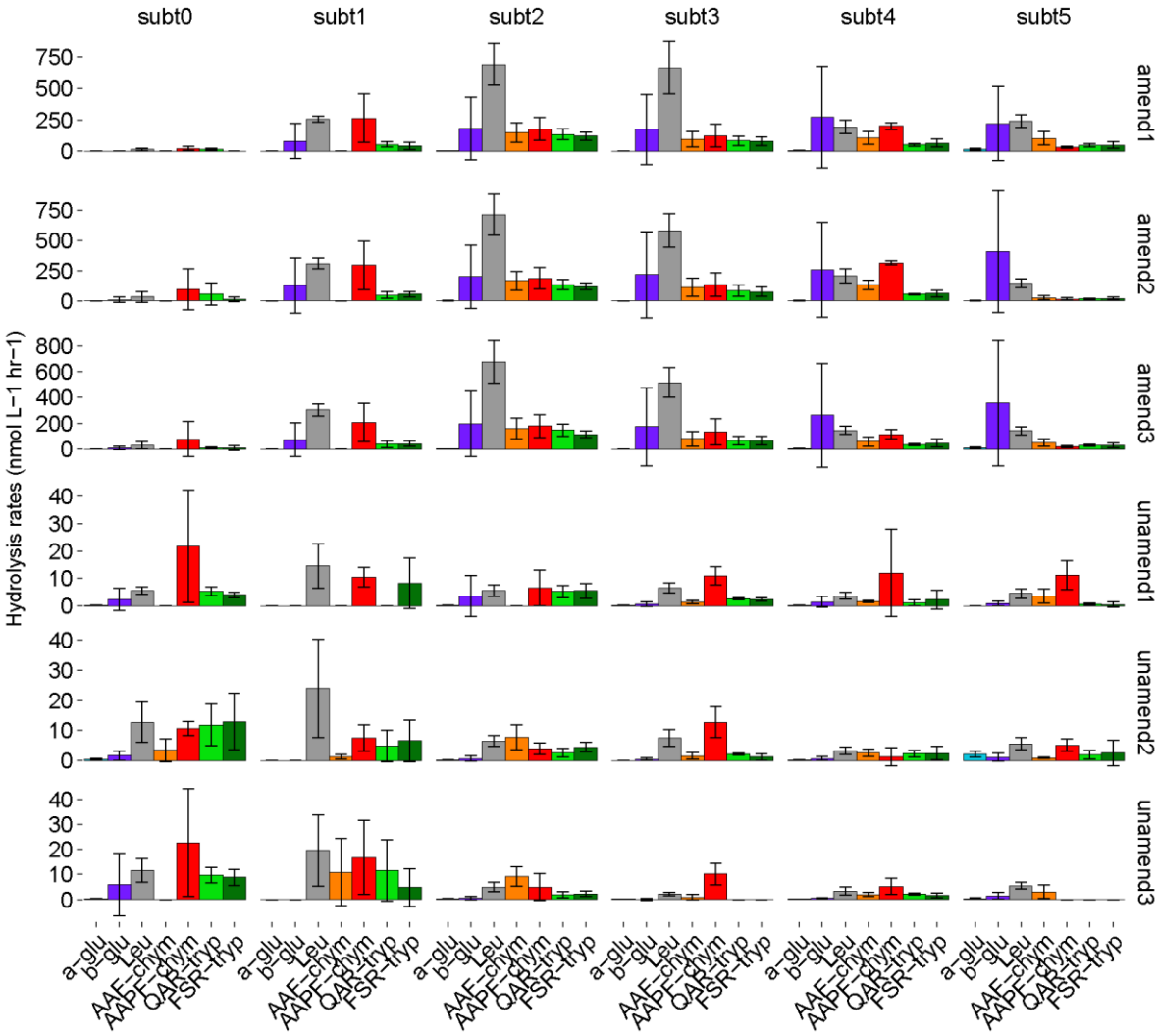

Figure S6C. Stn 8 surface water temporal development of peptidase and glucosidase activities, separated by mesocosm. Rates represented by each bar and error bars are the time-averaged rates —over a span of 72 hours—and standard deviation of each enzymatic activity measurement.

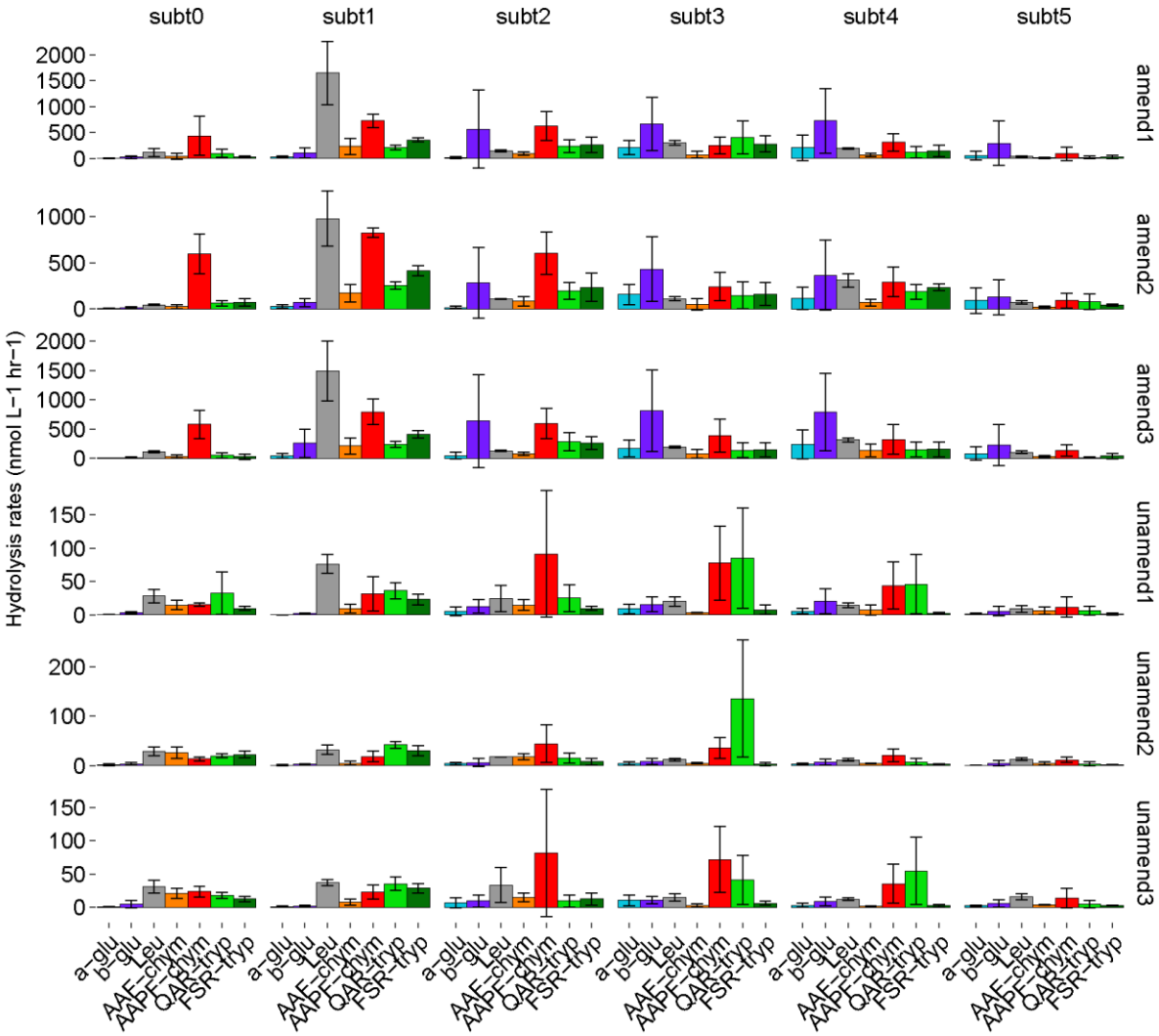

Figure S6D. Stn 8 bottom water temporal development of peptidase and glucosidase activities, separated by mesocosm. Rates represented by each bar and error bars are the time-averaged rates —over a span of 72 hours—and standard deviation of each enzymatic activity measurement.

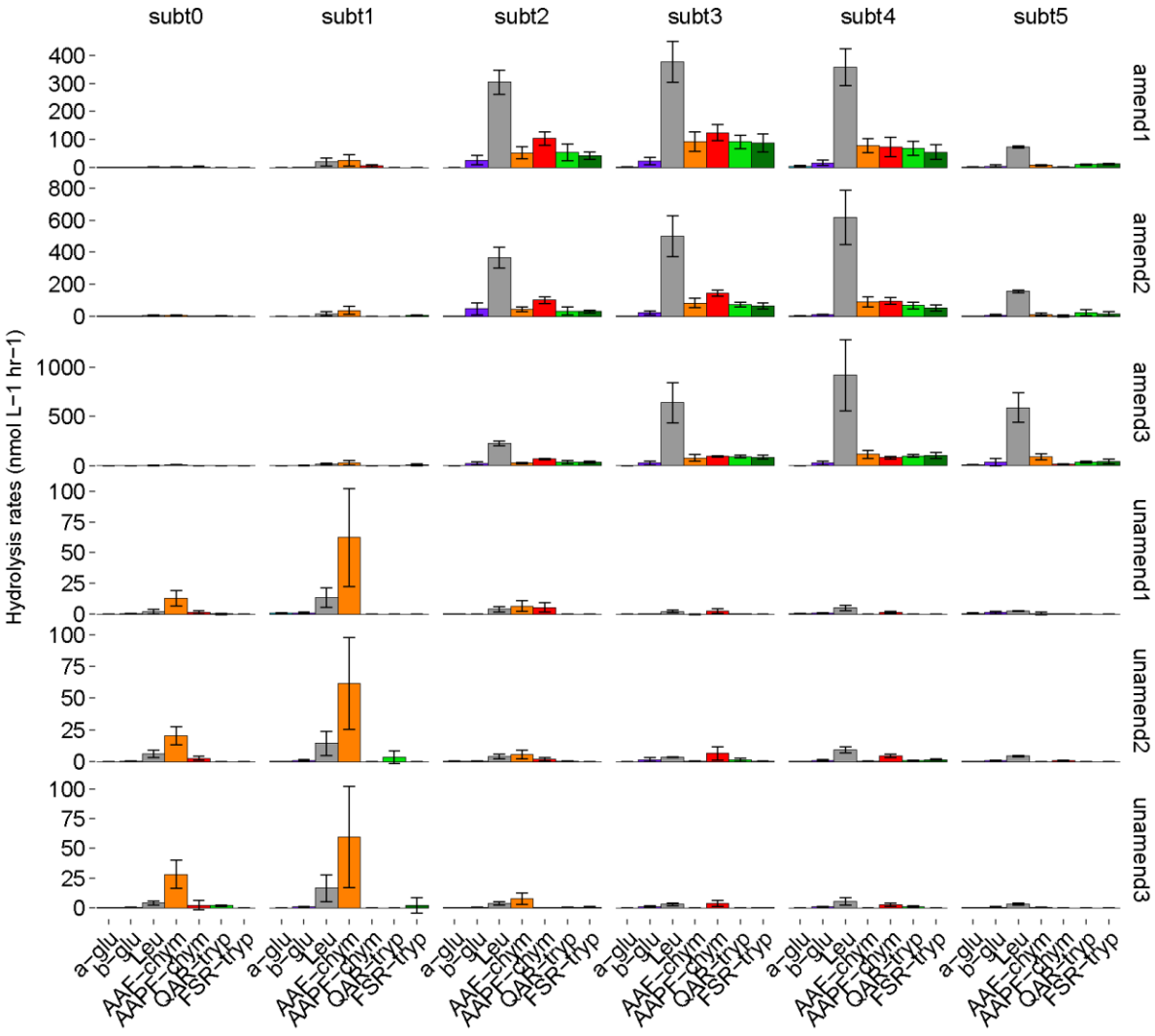

Figure S7. Temporal development of polysaccharide hydrolase activities for incubations using mesocosm waters sampled at the t3 timepoint. Each data point and error bar are the average and standard deviation of rates across triplicate enzymatic activity incubations for triplicate amended and unamended mesocosms.

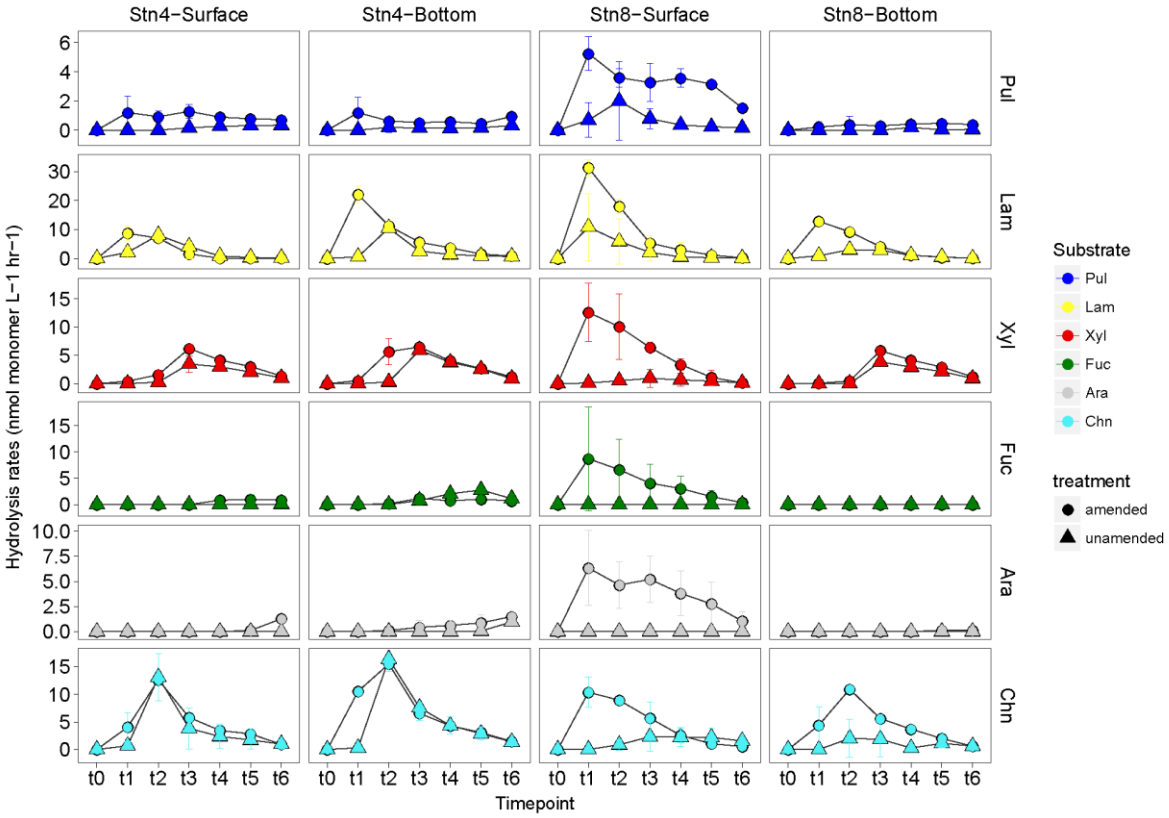

REFERENCES

Agogue H, Lamy D, Neal PR, Sogin ML, Herndl GJ. (2011). Water mass-specificity of bacterial communities in the North Atlantic revealed by massively parallel sequencing. *Molec Ecol* **20**: 258-274.

Allison SD, Martiny JBH. (2008). Resistance, resilience, and redundancy in microbial communities. *Proc Natl Acad Sci USA* **105**: 11512-11519.

Alonso-Sáez L, Díaz-Pérez L, Morán XAG. (2015). The hidden seasonality of the rare biosphere in coastal marine bacterioplankton. *Environ Microbiol* **17**: 3766-3780.

Arnosti C. (2003). Fluorescent derivatization of polysaccharides and carbohydrate-containing biopolymers for measurement of enzyme activities in complex media. *J Chromatogr* B **793**: 181-191.

Arnosti C. (2011). Microbial extracellular enzymes and the marine carbon cycle. *Annu Rev Mar Sci* **3**: 401-425.

Balser TC, Firestone MK. (2005). Linking microbial community composition and soil processes in a California annual grassland and mixed-conifer forest. *Biogeochemistry* **73**: 395-415.

Bell T, Newman JA, Silverman BW, Turner SL, Lilley AK. (2005). The contribution of species richness and composition to bacterial services. *Nature* **436**: 1157-1160.

Berlemont R, Martiny AC. (2015). Genomic potential for polysaccharide deconstruction in bacteria. *Appl Environ Microbiol* **81**: 1513-1519.

Bier RL, Bernhardt ES, Boot CM, Graham EB, Hall EK, Lennon JT *et al*. (2015). Linking microbial community structure and microbial processes: an empirical and conceptual overview. *FEMS Microbiol Ecol* **91**: fiv113.

Boetius A, Albrecht S, Bakker K, Bienhold C, Felden J, Fernandez-Mendez M *et al*. (2013). Export of algal biomass from the melting Arctic sea ice. *Science* **339**: 1430-1432.

Bong CW, Obayashi Y, Suzuki S. (2013). Succession of protease activity in seawater and bacterial isolates during starvation in a mesocosm experiment. *Aquat Microb Ecol* **69**: 33-46.

Buchan A, LeCleir GR, Gulvik CA, Gonzalez JM. (2014). Master recyclers: features and functions of bacteria associated with phytoplankton blooms. *Nat Rev Micro* **12**: 686-698.

Burke C, Thomas T, Lewis M, Steinberg P, Kjelleberg S. (2011). Composition, uniqueness and variability of the epiphytic bacterial community of the green alga *Ulva australis*. *ISME J* **5**: 590-600.

Campbell BJ, Yu L, Heidelberg JF, Kirchman DL. (2011). Activity of abundant and rare bacteria in a coastal ocean. *Proc Natl Acad Sci USA* **108**: 12776-12781.

Caporaso JG, Kuczynski J, Stombaugh J, Bittinger K, Bushman FD, Costello EK. (2010). QIIME allows analysis of high-throughput community sequencing data. *Nat Methods* **7**: 335-336.

Chase JM. (2007). Drought mediates the importance of stochastic community assembly. *Proc Natl Acad Sci USA* **104**: 17430-17434.

Comte J, Fauteux L, del Giorgio PA. (2013). Links between metabolic plasticity and functional redundancy in freshwater bacterioplankton communities. *Front Microbiol* **4**: 112.

D'Ambrosio L, Ziervogel K, MacGregor B, Teske A, Arnosti C. (2014). Composition and enzymatic function of particle-associated and free-living bacteria: a coastal/offshore comparison. *ISME J* **8**: 2167-2179.

Dang H, Lovell CR. (2016). Microbial surface colonization and biofilm development in marine environments. *Microbiol Mol Biol Rev* **80**: 91-138.

Darling KF, Kucera M, Wade CM (2007). Global molecular phylogeography reveals persistent Arctic circumpolar isolation in a marine planktonic protist. *Proc Natl Acad Sci USA* **104**: 5002-5007.

Datta MS, Sliwerska E, Gore J, Polz MF, Cordero OX. (2016). Microbial interactions lead to rapid micro-scale successions on model marine particles *Nat Commun* **7**: 11965.

Frossard A, Gerull L, Mutz M, Gessner MO. (2012). Disconnect of microbial structure and function: enzyme activities and bacterial communities in nascent stream corridors. *ISME J* **6**: 680-691.

Galand PE, Potvin M, Casamayor EO, Lovejoy C. (2010). Hydrography shapes bacterial biogeography of the deep Arctic Ocean. *ISME J* **4**: 564-576.

Gasol JM, del Giorgio PA. (2000). Using flow cytometry for counting natural planktonic bacteria and understanding the structure of planktonic bacterial communities. *Sci Mar* **64**: 28.

Haas BJ, Gevers D, Earl AM, Feldgarden M, Ward DV, Giannoukos G *et al.* (2011). Chimeric 16S rRNA sequence formation and detection in Sanger and 454-pyrosequenced PCR amplicons. *Genome Res* **21**: 494-504.

Hoarfrost A, Balmonte JP, Gawarkiewicz G, Ghobrial S, Ziervogel K, Arnosti C. Microbially-driven carbon cycling is influenced by ringwater intrusion on the Mid-Atlantic Bight shelf. Submitted to *J Geophys Res: Biogeosci*

Karl DM, Church MJ, Dore JE, Letelier RM, Mahaffey C. (2012). Predictable and efficient carbon sequestration in the North Pacific Ocean supported by symbiotic nitrogen fixation. *Proc Natl Acad Sci USA* **109**: 1842-1849.

Kirchman D, K'Nees E, Hodson R. (1985). Leucine incorporation and its potential as a measure of protein synthesis by bacteria in natural aquatic systems. *Appl Environ Microbiol* **49**: 599-607.

Kirchman D. (2001). Measuring bacterial biomass production and growth rates from leucine incorporation in natural aquatic environments. *Method Microbiol*. Academic Press. pp 227-237.

Knelman JE, Nemergut DR. (2014). Changes in community assembly may shift the relationship between biodiversity and ecosystem function. *Front Microbiol* **5**: 424.

Kuring N, Lewis MR, Platt T, O'Reilly JE. (1990). Satellite-derived estimates of primary production on the northwest Atlantic continental shelf. *Cont Shelf Res* **10**: 461-484.

Langenheder S, Lindström ES, Tranvik LJ. (2006). Structure and function of bacterial communities emerging from different sources under identical conditions. *Appl Environ Microbiol* **72**: 212-220.

Langenheder S, Székely AJ. (2011). Species sorting and neutral processes are both important during the initial assembly of bacterial communities. *ISME J* **5**: 1086-1094.

Lauro FM, McDougald D, Thomas T, Williams TJ, Egan S, Rice S *et al*. (2009). The genomic basis of trophic strategy in marine bacteria. *Proc Natl Acad Sci USA* **106**: 15527-15533.

Lennon JT, Jones SE. (2011). Microbial seed banks: the ecological and evolutionary implications of dormancy. *Nat Rev Microbiol* **9**: 119-130.

Logue JB, Stedmon CA, Kellerman AM, Nielsen NJ, Andersson AF, Laudon H *et al.* (2016). Experimental insights into the importance of aquatic bacterial community composition to the degradation of dissolved organic matter. *ISME J* **10**: 533-545.

Malviya S, Scalco E, Audic S, Vincent F, Veluchamy A, Poulain J *et al*. (2016). Insights into global diatom distribution and diversity in the world's ocean. *Proc Natl Acad Sci USA* **113**: E1516-E1525.

Martiny AC, Treseder K, Pusch G. (2013). Phylogenetic conservatism of functional traits in microorganisms. *ISME J* **7**: 830-838.

Martiny JBH, Bohannan BJM, Brown JH, Colwell RK, Fuhrman JA, Green JL *et al*. (2006). Microbial biogeography: putting microorganisms on the map. *Nat Rev Microbiol* **4**: 102-112.

McMurdie PJ, Holmes S. (2013). phyloseq: An R package for reproducible interactive analysis and graphics of microbiome census data. *PLoS One* **8:** e61217

Nemergut DR, Schmidt SK, Fukami T, O'Neill SP, Bilinski TM, Stanish LF *et al*. (2013). Patterns and Processes of Microbial Community Assembly. *Microbiol Mol Biol Rev* **77**: 342-356.

Newton RJ, Shade A. (2016). Lifestyles of rarity: understanding heterotrophic strategies to inform the ecology of the microbial rare biosphere. *Aquat Microb Ecol* **78**: 51-63.

Oksanen J, Blanchet FG, Kindt R, Legendre P, Minchin PR, O'Hara *et al*. (2008). vegan: Community Ecology Package. R package version 2.4-3.

Pagaling E, Strathdee F, Spears BM, Cates ME, Allen RJ, Free A. (2014). Community history affects the predictability of microbial ecosystem development. *ISME J* **8**: 19-30.

Ramette A, Tiedje JM. (2007). Multiscale responses of microbial life to spatial distance and environmental heterogeneity in a patchy ecosystem. *Proc Natl Acad Sci USA* **104**: 2761-2766.

Reed HE, Martiny JBH. (2007). Testing the functional significance of microbial composition in natural communities. *FEMS Microbiol Ecol* **62**: 161-170.

Sexton PF, Norris RD. (2008). Dispersal and biogeography of marine plankton: Long-distance dispersal of the foraminifer *Truncorotalia truncatulinoides*. *Geology* **36**: 899-902.

Shade A, Jones SE, Caporaso JG, Handelsman J, Knight R, Fierer N *et al*. (2014). Conditionally rare taxa disproportionately contribute to temporal changes in microbial diversity. *mBio* **5**.

Sogin ML, Morrison HG, Huber JA, Welch DA, Huse SM, Neal PR *et al*. (2006). Microbial diversity in the deep sea and the underexplored "rare biosphere". *Proc Natl Acad Sci USA* **103**: 12115-12120.

Spencer-Cervato C, Thierstein HR (1997). First appearance of *Globorotalia truncatulinoides*: cladogenesis and immigration. *Mar Micropaleontol* **30**: 267-291.

Steen AD, Vazin JP, Hagen SM, Mulligan KH, Wilhelm SW. (2015). Substrate specificity of aquatic extracellular peptidases assessed by competitive inhibition assays using synthetic substrates. *Aquat Microb Ecol* **75**: 271-281.

Stewart FJ, Dalsgaard T, Young CR, Thamdrup B, Revsbech NP, Ulloa O *et al*. (2012). Experimental incubations elicit profound changes in community transcription in OMZ bacterioplankton. *PLoS One* **7**: e37118.

Strickland MS, Lauber C, Fierer N, Bradford MA. (2009). Testing the functional significance of microbial community composition. *Ecology* **90**: 441-451.

Teeling H, Fuchs BM, Becher D, Klockow C, Gardebrecht A, Bennke CM *et al*. (2012). Substrate-controlled succession of marine bacterioplankton populations induced by a phytoplankton bloom. *Science* **336**: 608-611.

Teeling H, Fuchs BM, Bennke CM, Krüger K, Chafee M, Kappelmann L *et al*. (2016). Recurring patterns in bacterioplankton dynamics during coastal spring algae blooms. *eLife* **5**: e11888.

Teske A, Durbin A, Ziervogel K, Cox C, Arnosti C. (2011). Microbial community composition and function in permanently cold seawater and sediments from an Arctic fjord of Svalbard. *Appl Environ Microbiol* **77**: 2008-2018.

Violle C, Pu ZC, Jiang L. (2010). Experimental demonstration of the importance of competition under disturbance. *Proc Natl Acad Sci USA* **107**: 12925-12929.

Weiss MS, Abele U, Weckesser J, Welte W, Schiltz E, Schulz GE. (1991). Molecular architecture and electrostatic properties of a bacterial porin. *Science* **254**: 1627-1630.

Whittaker KA, Rynearson TA. (2017). Evidence for environmental and ecological selection in a microbe with no geographic limits to gene flow. *Proc Natl Acad Sci USA* **114**: 2651-2656.

CHAPTER 5: DISSERTATION SYNTHESIS AND CONCLUSIONS

Among the main goals of ecological research are to: 1) identify the members of biological communities; 2) understand the factors that shape the composition and diversity of these communities across habitats; and 3) evaluate the influence of biological communities on ecosystem processes (Vellend, 2010). These questions are relevant to organisms across the domains of life, and are of interest to ecologists and biogeochemists. Owing to recent technological advances, particularly in the past two decades, these questions have been applied to microbial systems. The recognition that bacteria are among the most abundant organisms on the planet, regulating the bulk of global biogeochemical cycles, has opened endless intriguing avenues for microbial ecological research.

5.1 Main Objectives

This dissertation explored fundamental concepts in marine microbial ecology using high-throughput sequencing (Ch.2, Ch.3, Ch.4), enzymatic activity measurements on a wide array of organic substrates (Ch.2, Ch.3, Ch.4) and, when available, metabolomics to analyze dissolved organic matter composition (Ch.3). The overall charge of this dissertation was to understand the composition and activities of microbial communities within the context of aquatic carbon cycling. In particular, the aims of this dissertation were to: 1) investigate the composition of bacterial communities from various aquatic habitats (both freshwater and marine), and along depth and environmental gradients; 2) determine the organic matter degrading capabilities of these microbial communities; and 3) understand the nature of bacterial structure and function relationships. Here, key findings and their contribution to oceanographic and microbial ecological concepts, as well as their implications on biogeochemical cycles, are reviewed.

5.2 Factors that Structure Microbial Community Composition

***Physicochemical parameters*.** Bacterial communities in the marine water column exhibit compositional dissimilarity as a function of hydrographically-distinct water masses (Galand et al., 2010; Agogue et al., 2011; Han et al., 2015). This observation can result from two differing forces. First, environmental conditions can select for the most adapted microbial taxa—a deterministic process (Nemergut et al., 2013). Alternatively, differences in physicochemical parameters can create strong density gradients that prevent the mixing of water masses, spatially isolating microbial communities (Martiny et al., 2006; Nemergut et al., 2013). When in isolation, stochastic processes, such as genetic drift may occur, and microbial communities can become compositionally dissimilar. Investigating the relative importance of determinism or stochasticity illuminates the strongest structuring forces of microbial community composition in nature. Notably, deterministic and stochastic forces can act on microbial communities simultaneously (Langenheder and Székely, 2011; Nemergut et al., 2013).

In the Arctic Ocean (Chapter 2), temperature and salinity, which differ among water masses, significantly correlated with pelagic bacterial community dissimilarity. This finding alone, however, cannot disentangle the relative importance of deterministic versus stochastic processes. Statistical analyses of the relationship between community dissimilarity and environmental conditions, holding for the effect of vertical (depth-related) distances, and vice versa—community dissimilarity versus vertical distances, holding for environmental conditions (distance-decay relationships)—reveal that bacterial community composition is strongly and positively related to the tested physicochemical parameters. Results from phylogenetic beta diversity analyses and null models (Stegen et al., 2012) were consistent with determinism among microbial communities, although this data was not included in the dissertation. However, correlations of community composition with environmental conditions do not preclude the possibility of stochastic processes concertedly

playing a more minor role in shaping community composition (Langenheder and Székely, 2011). In any case, while hydrography has been shown to shape microbial communities in the upper 1000 m of the central Arctic Ocean (Galand et al., 2010), findings from this dissertation extend this observation to the deepest water mass. Furthermore, environmental selection is likely a more important process—compared to spatial isolation—underlying observed water mass-related community dissimilarity patterns.

The importance of the relationship between environmental conditions and community composition is echoed in Chapter 3 and 4. In Chapter 3, however, the experimental setup enabled the investigation of microbial communities where water masses are more dynamic and actively mix (i.e., rivers that discharge into the fjord). In this chapter, the strong salinity differences—owing to the origin of the water masses (glacial and snow melt versus Greenland Sea inflow)—positively correlated with community compositional dissimilarity. Where river waters discharged into the fjord, microbial community composition had a primarily marine signature, which coincided with high salinity values with some freshwater influence. Salinity is known to influence community composition across various aquatic habitats (Crump et al., 1999; Lozupone and Knight, 2007). Salinity differences, in combination with physicochemical factors related to the origin of the water masses, may account for observed community dissimilarities in Tyrolerfjord-Young Sound. In Chapter 4, microbial communities from the surface and bottom waters at two stations in the North Atlantic Ocean—one on the continental shelf (Stn 4), and the other in the open ocean (Stn 8)—exhibited compositional differences also related to their water mass origin. Moreover, as Stn4 bottom water was likely of Gulf Stream (Stn 8 surface water) origin (Hoarfrost et al., *submitted*), the communities in these water masses showed significant compositional similarities. Altogether, these compositional patterns underscore the influence of water mass physicochemical parameters on microbial communities.

***Microbial association with particles*.** Particulate matter in aquatic environments can contain high concentrations of organic compounds, selecting for microbial taxa that are able to access these substrates for energy and metabolism (Simon et al., 2002). Surveys of microbial community composition have shown distinct particle-associated assemblages compared to their free-living counterparts (DeLong et al., 1993; Crump et al., 1999). Results from this dissertation present a relevant, but slightly different angle: differences in the composition of particle-associated bacterial communities versus that of the whole community (free-living + particle-associated). As discussed in succeeding sections, this approach was taken to compare functionality in bulk waters and, separately, on particles.

In Chapters 2 and 3, the effect of particle association on bacterial community composition was evident, although this varied by water mass or depth. For example, the composition of Arctic Ocean particle-associated bacterial communities only subtly diverged from that of the whole community, whereas this compositional difference was more prominent in deeper waters (Ch. 2). Microbial colonization and decolonization of particles in the upper water column—where a substantial portion of particulate matter is produced from primary production—may explain the compositional overlap observed in the upper water column (Thiele et al., 2015). Additionally, the lower concentration of particles in deep waters suggest that microbial colonization and decolonization likely occur less frequently, resulting in a more distinct particle-associated microbial assemblage. The low diversity of mesopelagic particle-associated bacterial communities highlights the ability of relatively few taxa to occupy this niche. In particular, members of *Gammaproteobacteria*, which dominate on deep water particles, likely play an important role in organic matter degradation. The low particle-associated community diversity, however, must be interpreted within the context of fewer particles in deep waters, which may contribute to apparently decreased diversity patterns at depth.

In the Tyrolerfjord-Young Sound system, snow- and glacial-fed rivers harbored particle-associated bacterial communities that were distinct from those in bulk river water (Ch. 3). These riverine particle-associated microbes persisted into the river transition zones—a freshwater signal in the otherwise mostly marine mixing sites. However, the bulk water and particle-associated bacterial community difference was not evident in waters within the fjord. One possible explanation is that the abundance of organic particles in the fjord promotes microbial colonization and decolonization (Pedrós-Alió and Brock, 1983), resulting in minimal compositional divergence between the bulk water and particle-associated communities. Alternatively, the large volumes of water filtered to analyze the particle-associated communities, and the possible retention of free-living assemblages on the filters, may have resulted in this similarity between the two communities (Padilla et al., 2015). In any case, the distinct composition of particle-associated bacterial communities in freshwaters highlight the importance of glacially- and terrestrially derived particles in shaping downstream fjord microbial systems, a topic that has been sparsely investigated.

Pulse of high molecular weight particulate organic matter. Addition of particulate organic matter (POM) induced a rapid succession of microbial communities (Ch. 4). Such a phenomenon is evident in nature during phytoplankton blooms (Teeling et al., 2012), and has also been observed using model organic particles (Datta et al., 2016). These successions are driven in part by microbial taxa capable of surface colonization (Dang and Lovell, 2016). Results from this dissertation expand on this topic by comparing the extent of community re-structuring in response to addition to high molecular weight particulate organic matter (HMW-POM) across various depths and locations in the North Atlantic. Microbial response to HMW-POM addition is comparatively less understood than that to organic compounds with a broad size spectrum and lability (Logue et al., 2016). Over time, initially-distinct microbial communities enriched with HMW-POM showed greater similarity in composition. In particular, out of initially distinct microbial communities emerged closely-

related taxa that became proportionally dominant. This observation suggests the importance of marine microbial seed banks across oceanic regions (Lennon and Jones, 2011), from which closely-related or even identical taxa can emerge in response to the same environmental fluctuation. Yet, in spite of similar successional patterns, robust differences in whole community composition and functionality (discussed below) persisted throughout the experiment. Furthermore, the intensity of community re-assembly was least in coastal surface waters, and greatest among bathypelagic microbial communities. Thus, the extent of community change is proportional to the change of environmental conditions relative to ambient conditions. Moreover, this pattern is consistent with the expectation that fewer microbial taxa can occupy the niche to degrade and transform HMW-POM in the deep ocean. Thus, organic matter supply, and the degree of environmental perturbation, may concertedly influence microbial community composition.

5.3 Enzymatic Activities Across Spatial and Environmental Gradients

Microbial enzymatic activities were measured across various habitats, water masses, and depths using a wide range of substrates, including glucose, peptides, and polysaccharides. With this methodological approach, important activity comparisons were possible: 1) peptidase (using low molecular weight substrates) versus polysaccharide hydrolases (using high molecular weight substrates); 2) exo- (terminal-cleaving) versus endo-acting (mid-chain-cleaving) peptidases; 3; pelagic versus benthic enzymatic activities; 4) freshwater versus marine enzymatic activities; 5) bulk versus particle-associated; 6) activities in waters under ambient versus enriched organic matter conditions.

***Depth gradients*.** Few studies to date have measured enzymatic activities in the deep ocean (Davey et al., 2001; Hoarfrost and Arnosti, 2017; Arnosti et al., unpublished-EN556/584; Balmonte et al., unpublished-SO248). Results from this dissertation (Ch. 2, Ch. 4) therefore contribute to the limited body of information on the extent to which organic matter degradation varies with depth in the marine water column, down to the bathypelagic.

Summed peptidase activity rates in the central Arctic decreased dramatically below the upper water column; however, summed polysaccharide hydrolase rates often peaked in the mesopelagic (Ch. 2). This pattern may reflect microbial adaptation and strategies in response to available substrates. Nitrogen-rich, proteinaceous compounds are preferentially removed, increasing the C:N ratio of particulate matter with depth (Lee et al., 2000). Furthermore, the finding that a narrower subset of peptidases were measurably active in bottom waters, both in the central Arctic (Ch. 2) and the North Atlantic (Ch. 4) may be related to the limited organic compounds available in the deep ocean. Accordingly, when organic matter concentrations were enriched, deep ocean microbial communities can evidently produce a broader range of enzymes to access the organic substrates (Ch. 4), as will be discussed in a following section.

***Pelagic-benthic activity contrasts*.** Differences in the ability of pelagic versus benthic microbial communities to access organic matter has also been of considerable interest (Teske et al., 2011; Arnosti, 2015). These studies have shown that benthic microbial communities a greater range of enzymatic potentials compared to their pelagic counterparts (Teske et al., 2011). These differing spectra may be related to community composition and/or organic matter supply. Measurements made in the water column and sediments of the central Arctic reflected these differing spectra and proportions of peptidase activities (Ch. 2). Furthermore, summed peptidase rates were greatest in sediments from seasonally ice-free regions compared to those beneath the ice edge and pack ice. Surprisingly, peptidase activity ratios showed less spatial variability in sediments than in the water column—a trend that paralleled the lower β-diversity of benthic versus pelagic microbial communities. Differences in the degree of spatial variation between the water column and sediments are a relatively unexplored dimension of pelagic-benthic activity comparisons.

***Enzymatic activities on particles*.** Particles are sites of intense enzymatic activities (Smith et al., 1992), and can host microbial communities with a broader spectrum of organic

matter degrading capabilities than those in ambient water (Ziervogel and Arnosti, 2008; D'Ambrosio et al., 2014). The particle-associated enzymatic spectra observed in this dissertation are consistent with previous findings, and further expand on this topic by employing a wider range of substrates to measure particle-associated enzymatic activities than previously used. Particle-associated peptidase activities showed differing proportions compared to measurements made in bulk water. Specifically, endo-acting peptidases were typically proportionally more active than exo-peptidases on particles than in bulk water (Ch. 2, Ch. 3). These peptidase ratios may be related to the role of these enzymes in hydrolyzing larger organic compounds mid-chain (Bong et al., 2013). Moreover, these trends are also evident in the North Pacific (Arnosti et al., unpublished-EN556/EN584), from South Pacific to North Pacific, and in the Bering Sea (Balmonte et al., unpublished-SO248). Additionally, polysaccharide hydrolase activities not measured in bulk water were frequently detected on particles (Ch. 2, Ch. 3). Altogether, these patterns signify that particle-associated microbial communities employ enzymatic strategies to access organic compounds that are distinct from those observed in bulk waters. The potential role of microbial cooperation and signaling through quorum sensing in shaping enzymatic activity patterns (Gram et al., 2002), especially those of polysaccharide hydrolases, should be examined.

Freshwater versus marine. The extent to which freshwater versus marine microbial communities differ in their abilities to hydrolyze organic matter is of fundamental interest to biogeochemists (Crump et al., 1999; Ghai et al., 2011; Eiler et al., 2014). The activities and substrate preferences of these microbial communities in part determine the fate of allochthonous and autochthonous organic matter in freshwater systems that are ultimately transported to the coast (Guillemette et al., 2013; Guillemette et al., 2016). Comparing the hydrolytic capabilities of microbial communities in rivers influenced by glacial and snow melt, and within Tyrolerfjord-Young Sound, revealed differing freshwater and marine enzymatic patterns (Ch. 3). These varying enzymatic activities were hypothesized as the basis for

differing percent bioavailable dissolved organic carbon measurements of microbial communities along a glacially-influenced salinity gradient (Fellman et al., 2010). Key features of the differing enzymatic spectra included: 1) more consistent and higher rates of hydrolysis of xylan and chondroitin in freshwater and marine sites, respectively; and 2) higher rates of glucosidase compared to peptidase activities in freshwater versus marine sites, respectively. Furthermore, activity rates of specific enzymes positively correlated with the relative concentrations of their putative hydrolysis products. This finding indicates that the differing enzymatic spectra, in part, reflects the responses of microbial communities to differing supply of organic matter in fresh and marine waters. Teasing apart the relative importance of organic matter supply versus community composition in shaping microbial activities is a challenge, but should be a focus of future efforts.

***Responses to organic matter enrichments*.** As organic matter supply may influence microbial activities, enrichment of carbon sources is likely to initiate a functional shift among microbial communities (Datta et al., 2016). However, the extent to which these functional responses vary between communities is poorly understood. By enriching microbial communities from distinct water masses in the North Atlantic with the same diatom-derived, high molecular weight particulate organic matter (HMW-POM), the functional consequences of community structural differences became apparent (Ch. 4). Peptidase, glucosidase, and polysaccharide hydrolases were stimulated in HMW-POM-amended treatments, but to varying degrees. For example, α- and β-glucosidases were most active in waters with Gulf-Stream influence, but their activities remained low in the other water masses. In contrast, leucine aminopeptidase activities were high at all sites, but maximal rates were observed at varying timepoints. Moreover, addition of HMW-POM stimulated the breakdown of several substrates that were not detectably hydrolyzed in the unamended treatments. Notably, these enzymatic activity differences were apparent in spite of large similarities in community composition—due to proliferation of initially rare, closely-

related taxa—in amended treatments at all sites. Similarly, findings from similar mesocosm experiments conducted in the South and North Pacific—but enriched with different organic matter sources—showed systematic differences in microbial enzymatic activity responses across water masses (M. Weitz et al., unpublished data). These results expand our understanding of functional consequences of differences in community structure, a widely-studied concept in microbial ecology (Reed and Martiny, 2007; Strickland et al., 2009).

5.4 Structure and Function Relationships

The concerted approach of characterizing bacterial community composition and measuring enzymatic activities enabled the evaluation of structure and function relationships across habitats. In the Arctic Ocean, the nature of structure and function relationships differed between the water column (bulk water and particle-associated) and sediments (Ch. 2). Specifically, pelagic microbial communities were characterized by functional redundancy and metabolic plasticity to initiate protein degradation, whereas benthic microbial communities exhibited functional dissimilarity. These results imply that the relative importance of environmental conditions in shaping ecosystem processes differ in pelagic and benthic realms. Varying microbial structure-function relationships complicate efforts to predict the influence of environmental fluctuations on ecosystem processes (Comte et al., 2013), but suggest that the impacts of environmental changes on specific processes may vary in the water column and in sediments.

In the Tyrolerfjord-Young Sound system (Ch. 3), a positive relationship between microbial community composition and enzymatic dissimilarity was observed, and was influenced by differing sources and mixing of water masses. Furthermore, microbial communities in rivers and in the fjord interact with different pools of organic matter. Thus, the relative influences of community differences and organic matter supply on enzymatic capabilities are difficult to disentangle. These findings nevertheless suggest that factors intrinsic (eg. composition) and extrinsic (eg. organic matter supply) to microbial communities

may influence their activities. Therefore, changes in these intrinsic and extrinsic factors due to increased freshwater and organic matter input (Mernild et al., 2007; Wassmann et al., 2015) can likely have major consequences on microbial carbon cycling in high latitude coastal systems. A long-term, seasonal study employing similar approaches used in Chapter 3—especially capturing the system before and after the start of increased glacial and snow melt (Paulsen et al., 2017)—could provide further insights into biogeochemical effects of increased freshwater runoff.

The enrichment of HMW-POM in Chapter 4 caused a compositional and functional succession, as discussed earlier, and a different structure-function relationship. In particular, bacterial community diversity decreased—potentially due to deterministic selection for bacterial taxa that can interact with HMW-POM—but enzymatic activities were enhanced. In addition, a stronger relationship was observed between community and enzymatic activity dissimilarity in amended compared to unamended treatments using the Mantel Test, although this data was not included in the dissertation. This stronger structure-function relationship is likely due to the coupling of response trait (i.e., ability to associate with HMW-POM) and the measured effect trait (i.e., ability to break down HMW-POM) (Knelman and Nemergut, 2014). These results therefore indicate that structure-function relationships are largely influenced by the assembly mechanism that shapes microbial communities (Nemergut et al., 2013; Knelman and Nemergut, 2014). Such deterministic community re-assembly processes among microbial communities are observed following phytoplankton blooms. These successions are marked by relative increases of genes involved in organic matter breakdown, internal transport, and utilization (Teeling et al., 2012). Results from this dissertation further illustrate that the nature of compositional and functional successions, in response to the same perturbation, can vary due to differences in initial microbial community composition (Langenheder et al., 2006).

5.5 Limitations

Methodological limitations bias experimental results, but their impacts can be constrained in part with cautious interpretation. Here, the most obvious and relevant methodological limitations are discussed—including their impact on results and data interpretation—and categorized by the three main topics of this research: 1) bacterial community composition, 2) enzymatic activities, and 3) structure-function relationships.

Bacterial community composition. Interpreting the composition of bacterial communities suffers from several methodological constraints. At the beginning of the community analysis process, the volume of water filtered may bias taxonomic composition results. This limitation holds especially true for analyses of particle-associated bacterial community: filtering large volumes of water can entrain free-living bacterial cells on the filters, and bias the diversity and taxonomic composition of particle-associated bacterial communities (Padilla et al., 2015). Similarly, the decision of filter pore size used to distinguish particle-associated versus free-living taxa is subjective, and varies among scientists and depending on the research question (Ch. 2, Ch. 3). Such decisions may result in conflicting interpretations of which taxa are or are not likely to be attached to particles. Subsequently, the choice of DNA extraction method may influence the observed microbial taxonomic composition (Martin-Laurent, 2001; Feinstein et al., 2009), as some gram-positive cells are difficult to lyse. Relic DNA may additionally be extracted and severely skew diversity estimates and community composition (Carini et al., 2016).

Technical constraints in various steps of the sequencing process affect diversity and taxonomic interpretations. As this methodological approach relies on polymerase chain reaction (PCR) amplification of 16S rRNA genes, several abundant taxa can be disproportionally amplified, and result in spurious taxonomic composition and species evenness observations. Hence, interpretations based on relative proportions should be made with caution, especially when sequence counts per sample are not even. Moreover,

the sequencing primers of choice—and, consequently, the sequenced hypervariable region—could bias results (Soergel et al., 2012; Guo et al., 2013). This is evident by differences in the taxonomic composition and proportions produced from Arctic samples sequenced using primers targeting the V1-V2 (Ch. 2) and V4-V6 (Balmonte et al., unpublished data) hypervariable regions of the 16S rRNA gene. The workaround for these primers is to sequence the entire marker gene, but the throughput (ie., sequences per sample) is sacrificed. Identification of the taxonomic affiliation of sequences is also sensitive to the quality of the database used. However, OTU-based analyses (ie., setting a sequence similarity cutoff), especially when OTUs are picked using *de novo* methods, avoid this issue. Finally, interpretations of environmental gradients underlying community compositional patterns are sensitive to the environmental parameters available. If, for example, an unmeasured environmental parameter—that co-varies with another variable—is important for community structuring, its influence on community patterns will be missed.

Enzymatic activity assays. The ability to empirically measure rates of enzymatic hydrolysis provides evidence that metabolic potentials uncovered through other approaches, such as metagenomics or metatranscriptomics, are actually at play. Yet, enzymatic activity assays used in this dissertation possess limitations. These include the extent to which the MUF/MCA substrate analogs and polysaccharide substrates represent the structural complexity or diversity, respectively, of natural organic matter (discussed in Ch. 1 and Ch. 2; Arnosti, 2011). Additionally, the length of incubation for both types of assays, especially ones that use polysaccharide substrates, makes it likely that microbial responses beyond those to the substrates (e.g., bottle effects/confinement, community shifts) may have occurred (Stewart et al., 2012). However, these pitfalls may partially be circumvented by only discussing patterns of enzymatic potentials of a community within a sample. Furthermore, while these enzymatic activity assays have been used for over a decade (Hoppe et al., 1983; Arnosti, 2003), these approaches have not been applied to much of the

world's oceans, in comparison to other analyses (eg., microbial community composition, bacterial production, cell counts, etc). This constraint also limits a global comparison, although recent progress in the laboratory is shedding light on enzymatic activity patterns in other regions and depths of the oceans not previously investigated (Arnosti et al., unpublished- EN556/EN584; Balmonte et al., unpublished- SO248). Finally, the detection limit of enzymatic activities should be considered. Enzymatic assays with polysaccharides, in particular, may not be sensitive to very minor enzyme-catalyzed hydrolysis by microbial communities.

Structure-function. While relatively few studies have integrated bacterial community composition analyses with empirical measurements of enzymatic activities, the correlation analyses used to assess structure-function relationships are sensitive to the pitfalls of community composition and enzymatic activity analytical techniques. In particular, the issue with relic DNA as previously described can obscure structure-function relationships. Similarly, bacterial taxa identified using the DNA for 16S rRNA gene (whole community) versus those characterized using the RNA (active community) may not be congruent (D'Ambrosio et al., 2014; Osterholz et al., 2016). Furthermore, within the active community, rare taxa—which comprise a minor fraction of the community—may disproportionately contribute to community activity (Campbell et al., 2011; Jousset et al., 2017). However, the approach in this dissertation cannot discriminate their contribution, or the specific contributions of any microbial taxon for that matter. Finally, caution should constantly be taken regarding the broader implications of structure-function relationships, considering that only a specific subset of microbial metabolism is measured.

5.6 Future Work

Efforts to link microbial community structure and function may benefit from employing other methodological approaches. Recent discovery of 'selfish uptake' by some marine bacteria provides the opportunity to directly observe and identify some of the organisms that

degrade specific polysaccharides (Reintjes et al., 2017). In addition, coupling enzyme activity assays with metagenomics and metatranscriptomics could provide insights into whether the absence of hydrolytic activities on certain substrates corresponds to the absence of the metabolic potential among the community, or may be due to environmental regulation of gene transcription. However, even this approach is constrained by: 1) the level of accuracy of functional annotations for genes, and 2) the sequencing depth employed. Nevertheless, using meta-'omics' techniques can also expand structure-function investigations beyond just several functions of interest, as diverse biogeochemical processes happen simultaneously and among microbial networks with equally diverse metabolic capabilities. The composition of bacterial communities can also be obtained from these meta-'omics' approaches, and, depending on the question at hand, may be sufficient to represent the taxonomic composition of communities of interest. Moreover, to more directly link structure and function by determining key players in a biogeochemical process, stable isotope probing techniques, such as Chip-SIP (Mayali et al., 2012), may be used.

Furthermore, using single-cell genomics to expand on the findings from Chapter 4 would illuminate the identity and similarity/differences in the closely-related taxa/OTUs that become proportionally dominant HMW-POM amended mesocosms. The concept of OTU suffers largely because it is 'operational': researchers choose to set the sequence similarity cutoff using any desired value, although this value typically ranges from 95 to 99%. Yet, even bacteria with completely identical 16S rRNA genes can exhibit drastic differences in physiology and genomic content (Jaspers and Overmann, 2004). Single-cell genomics would alleviate the issue of obscured differences in genomic repertoires of organisms classified within the same OTU. Evidence that the OTUs that emerged in amended mesocosms (Ch. 4) are identical based on genetic potentials would strongly support the concept of microbial seed banks (Lennon and Jones, 2011). Single-cell genomes would also provide insights into their potential niche, beyond that for degrading HMW-POM.

5.7 Concluding Remarks

By integrating community compositional analyses and empirical activity measurements, the identity, ecological roles, and environmental sensitivity of marine microbial communities in previously underexplored regions and depths of the ocean have been characterized. In summary, microbial communities respond to physicochemical gradients and environmental alterations. Patterns of microbial community composition may parallel differences in enzymatic activities, but the correlation of these factors varies substantially by habitat and environmental conditions. The structure-function relationships observed in this dissertation reveal the potential for changes observed in the oceans to alter microbial community composition and function. Precisely identifying the conditions under which communities will change, with and without direct consequences for functionality, should be a goal of future research. In addition to providing predictive biogeochemical models with empirical data, these studies will continue to unify oceanographic concepts and community ecology theories.

REFERENCES

Agogue H, Lamy D, Neal PR, Sogin ML, Herndl GJ. (2011). Water mass-specificity of bacterial communities in the North Atlantic revealed by massively parallel sequencing. *Molec Ecol* **20**: 258-274.

Arnosti C. (2003). Fluorescent derivatization of polysaccharides and carbohydrate-containing biopolymers for measurement of enzyme activities in complex media. *J Chromatogr* B **793**: 181-191.

Arnosti C. (2011). Microbial extracellular enzymes and the marine carbon cycle. *Annu Rev Mar Sci* **3**: 401-425.

Arnosti C, Steen AD, Ziervogel K, Ghobrial S, Jeffrey WH. (2011). Latitudinal gradients in degradation of marine dissolved organic carbon. *PLoS One* **6**: e28900.

Arnosti C. (2015). Contrasting patterns of peptidase activities in seawater and sediments: An example from Arctic fjords of Svalbard. *Mar Chem* **168**: 151-156.

Bong CW, Obayashi Y, Suzuki S. (2013). Succession of protease activity in seawater and bacterial isolates during starvation in a mesocosm experiment. *Aquat Microb Ecol* **69**: 33-46.

Campbell BJ, Yu L, Heidelberg JF, Kirchman DL. (2011). Activity of abundant and rare bacteria in a coastal ocean. *Proc Natl Acad Sci USA* **108**: 12776-12781.

Carini P, Marsden PJ, Leff JW, Morgan EE, Strickland MS, Fierer N. (2016). Relict DNA is abundant in soil and obscures estimates of soil microbial diversity *Nat Microbiol* **2**: 16242.

Comte J, Fauteux L, del Giorgio PA. (2013). Links between metabolic plasticity and functional redundancy in freshwater bacterioplankton communities. *Front Microbiol* **4**: 112.

Crump BC, Armbrust EV, Baross JA. (1999). Phylogenetic analysis of particle-attached and free-living bacterial communities in the Columbia river, its estuary, and the adjacent coastal ocean. *Appl Environ Microbiol* **65**: 3192-3204.

D'Ambrosio L, Ziervogel K, MacGregor B, Teske A, Arnosti C. (2014). Composition and enzymatic function of particle-associated and free-living bacteria: a coastal/offshore comparison. *ISME J* **8**: 2167-2179.

Dang H, Lovell CR. (2016). Microbial surface colonization and biofilm development in marine environments. *Microbiol Mol Biol Rev* **80**: 91-138.

Datta MS, Sliwerska E, Gore J, Polz MF, Cordero OX. (2016). Microbial interactions lead to rapid micro-scale successions on model marine particles. *Nat Commun* **7**: 11965.

Davey KE, Kirby RR, Turley CM, Weightman AJ, Fry JC. (2001). Depth variation of bacterial extracellular enzyme activity and population diversity in the northeastern North Atlantic Ocean. *Deep Sea Res Part II Top Stud Oceanogr* **48:** 1003-1017.

Delong EF, Franks DG, Alldredge AL. (1993). Phylogenetic diversity of diversity and aggregate-attached vs free-living marine bacterial assemblages. *Limnol Oceanogr* **38:** 924-934.

Eiler A, Zaremba-Niedzwiedzka K, Martínez-García M, McMahon KD, Stepanauskas R, Andersson SGE *et al*. (2014) Productivity and salinity structuring of the microplankton revealed by comparative freshwater metagenomics. *Environ Microbiol* **16**: 2682-2698.

Feinstein LM, Sul WJ, Blackwood CB. (2009). Assessment of bias associated with incomplete extraction of microbial DNA from soil. *Appl Environ Microbiol* **75**: 5428-5433.

Fellman JB, Spencer RGM, Hernes PJ, Edwards RT, D'Amore DV, Hood E. (2010). The impact of glacier runoff on the biodegradability and biochemical composition of terrigenous dissolved organic matter in near-shore marine ecosystems. *Mar Chem* **121**: 112-122.

Galand PE, Potvin M, Casamayor EO, Lovejoy C. (2010). Hydrography shapes bacterial biogeography of the deep Arctic Ocean. *ISME J* **4**: 564-576.

Ghai R, Rodríguez-Valera F, McMahon KD, Toyama D, Rinke R, de Oliveira TCS *et al*. (2011). Metagenomics of the water column in the pristine upper course of the Amazon River. *PloS One* **6**: e23785.

Gram L, Grossart H-P, Schlingloff A, Kiørboe T. (2002). Possible quorum sensing in marine snow bacteria: Production of acylated homoserine lactones by *Roseobacter* strains isolated from marine snow. *Appl Environ Microbiol* **68**: 4111-4116.

Guillemette F, McCallister SL, del Giorgio PA. (2013). Differentiating the degradation dynamics of algal and terrestrial carbon within complex natural dissolved organic carbon in temperate lakes. *J Geophys Res – Biogeosci* **118**: 963-973.

Guillemette F, McCallister SL, del Giorgio PA. (2016). Selective consumption and metabolic allocation of terrestrial and algal carbon determine allochthony in lake bacteria. *ISME J* **10**: 1373-1382.

Guo F, Ju F, Cai L, Zhang T. (2013). Taxonomic precision of different hypervariable regions of 16S rRNA gene and annotation methods for functional bacterial groups in biological wastewater treatment. *PLoS One* **8**: e76185.

Han D, Ha HK, Hwang CY, Lee BY, Hur HG, Lee YK. (2015). Bacterial communities along stratified water columns at the Chukchi Borderland in the western Arctic Ocean. *Deep Sea Res Part II Top Stud Oceanogr* **120**: 52-60.

Hoarfrost A, Arnosti C (2017). Heterotrophic extracellular enzymatic activities in the Atlantic Ocean follow patterns across spatial and depth regimes. *Front Mar Sci* **4**: 200.

Hoppe, HG. (1993). Use of fluorogenic model substrates for extracellular enzyme activity (EEA) measurement of bacteria, p. 423-431. *In* P. F. Kemp, B. F. Sherr, E. B. Sherr,

and J. J. Cole (ed.), Handbook of methods in aquatic microbial ecology. Lewis Publishers, Boca Raton, FL.

Jaspers E, Overmann J. (2004). Ecological significance of microdiversity: Identical 16S rRNA gene sequences can be found in bacteria with highly divergent genomes and ecophysiologies. *Appl Environ Microbiol* **70**: 4831-4839.

Jousset A, Bienhold C, Chatzinotas A, Gallien L, Gobet A, Kurm V *et al*. (2017). Where less may be more: how the rare biosphere pulls ecosystems strings. *ISME J* **11**: 853-862.

Knelman JE, Nemergut DR. (2014). Changes in community assembly may shift the relationship between biodiversity and ecosystem function. *Front Microbiol* **5**: 424.

Langenheder S, Lindström ES, Tranvik LJ. (2006). Structure and function of bacterial communities emerging from different sources under identical conditions. *Appl Environ Microbiol* **72**: 212-220.

Langenheder S, Szekely AJ. (2011). Species sorting and neutral processes are both important during the initial assembly of bacterial communities. *ISME J* **5**: 1086-1094.

Lee C, Wakeham SG, I. Hedges J. (2000). Composition and flux of particulate amino acids and chloropigments in equatorial Pacific seawater and sediments. *Deep Sea Res Part I: Oceanogr Res* **47**: 1535-1568.

Lennon JT, Jones SE. (2011). Microbial seed banks: the ecological and evolutionary implications of dormancy. *Nat Rev Microbiol* **9**: 119-130.

Logue JB, Stedmon CA, Kellerman AM, Nielsen NJ, Andersson AF, Laudon H *et al*. (2016). Experimental insights into the importance of aquatic bacterial community composition to the degradation of dissolved organic matter. *ISME J* **10**: 533-545.

Lozupone CA, Knight R. (2007). Global patterns in bacterial diversity. *Proc Natl Acad Sci USA* **104**: 11436-11440.

Martin-Laurent F, Philippot L, Hallet S, Chaussod R, Germon JC, Soulas G *et al*. (2001). DNA extraction from soils: Old bias for new microbial diversity analysis methods. *Appl Environ Microbiol* **67**: 2354-2359.

Mayali X, Weber PK, Brodie EL, Mabery S, Hoeprich PD, Pett-Ridge J. (2012). High-throughput isotopic analysis of RNA microarrays to quantify microbial resource use. *ISME J* **6**: 1210-1221.

Mernild SH, Sigsgaard C, Rasch M, Hasholt B, Hansen BU, Stjernholm M *et al*. (2007). Climate, river discharge and suspended sediment transport in the Zackenberg River drainage basin and Young Sound/Tyrolerfjord, Northeast Greenland. In: Rysgaard, S. & Glud, R. N. (Eds.), Carbon cycling in Arctic marine ecosystems: Case study Young Sound. Meddr. Grønland, Bioscience. **58**: 24-43

Nemergut DR, Schmidt SK, Fukami T, O'Neill SP, Bilinski TM, Stanish LF *et al.* (2013). Patterns and Processes of Microbial Community Assembly. *Microbiol Mol Biol Rev* **77:** 342-356.

Osterholz H, Singer G, Wemheuer B, Daniel R, Simon M, Niggemann J *et al*. (2016). Deciphering associations between dissolved organic molecules and bacterial communities in a pelagic marine system. *ISME J* **10**: 1717-1730.

Padilla CC, Ganesh S, Gantt S, Huhman A, Parris DJ, Sarode N *et al*. (2015). Standard filtration practices may significantly distort planktonic microbial diversity estimates. *Front Microbiol* **6**:547.

Paulsen ML, Nielsen SEB, Müller O, Møller EF, Stedmon CA, Juul-Pederson T *et al.* (2017). Carbon bioavailability in a high Arctic fjord influenced by glacial meltwater, NE Greenland. *Front Mar Sci* **4**: 176. doi: 10.3389/fmars.2017.00176

Pedrós-Alió C, Brock TD (1983). The importance of attachment to particles for planktonic bacteria. *Archiv fur Hydrobiol* **98:** 354-379.

Reed HE, Martiny JBH. (2007). Testing the functional significance of microbial composition in natural communities. *FEMS Microbiol Ecol* **62:** 161-170.

Reintjes G, Arnosti C, Fuchs BM, Amann R. (2017). An alternative polysaccharide uptake mechanism of marine bacteria. *ISME J* **11**: 1640-1650.

Simon H, Grossart H-P, Schweitzer B, Ploug H. (2002). Microbial ecology of organic aggregates in aquatic ecosystems. *Aquat Microb Ecol* **28**: 175-211.

Soergel DAW, Dey N, Knight R, Brenner SE. (2012). Selection of primers for optimal taxonomic classification of environmental 16S rRNA gene sequences. *ISME J* **6**: 1440-1444.

Stegen JC, Lin X, Konopka AE, Fredrickson JK. (2012). Stochastic and deterministic assembly processes in subsurface microbial communities. *ISME J* **6**: 1653-1664.

Stewart FJ, Dalsgaard T, Young CR, Thamdrup B, Revsbech NP, Ulloa O *et al.* (2012). Experimental incubations elicit profound changes in community transcription in OMZ bacterioplankton. *PLoS One* **7:** e37118.

Strickland MS, Lauber C, Fierer N, Bradford MA. (2009). Testing the functional significance of microbial community composition. *Ecology* **90:** 441-451.

Teeling H, Fuchs BM, Becher D, Klockow C, Gardebrecht A, Bennke CM *et al*. (2012). Substrate-controlled succession of marine bacterioplankton populations induced by a phytoplankton bloom. *Science* **336**: 608-611.

Teske A, Durbin A, Ziervogel K, Cox C, Arnosti C. (2011). Microbial community composition and function in permanently cold seawater and sediments from an Arctic fjord of Svalbard. *Appl Environ Microbiol* **77**: 2008-2018.

Thiele S, Fuchs BM, Amann R, Iversen MH. (2015). Colonization in the photic zone and subsequent changes during sinking determine bacterial community composition in marine snow. *Appl Environ Microbiol* **81**: 1463-1471.

Vellend BM. (2010). Conceptual synthesis in community ecology. *Q Rev Biol* **85**: 183-206.

Wassmann P. (2015). Overarching perspectives of contemporary and future ecosystems in the Arctic Ocean. *Prog Oceanogr* **139**: 1-12.

Ziervogel K, Arnosti C. (2008). Polysaccharide hydrolysis in aggregates and free enzyme activity in aggregate-free seawater from the north-eastern Gulf of Mexico. *Environ Microbiol* **10**: 289-299.